nagra.

Arbeitsbericht NAB 14-90

Feasibility evaluation study of candidate canister solutions for the disposal of spent nuclear fuel and high level waste

A status review

September 2014

S.R. Holdsworth, T. Graule, E. Mazza (EMPA)

**Nationale Genossenschaft
für die Lagerung
radioaktiver Abfälle**

Hardstrasse 73
CH-5430 Wettingen
Telefon 056-437 11 11

www.nagra.ch

nagra.

Arbeitsbericht NAB 14-90

Feasibility evaluation study of candidate canister solutions for the disposal of spent nuclear fuel and high level waste

A status review

September 2014

S.R. Holdsworth, T. Graule, E. Mazza (EMPA)

KEYWORDS

Disposal canister, canister material, feasibility, carbon steel, copper, ceramic, nickel alloy, titanium

**Nationale Genossenschaft
für die Lagerung
radioaktiver Abfälle**

Hardstrasse 73
CH-5430 Wettingen
Telefon 056-437 11 11

www.nagra.ch

Nagra Working Reports concern work in progress that may have had limited review. They are intended to provide rapid dissemination of information. The viewpoints presented and conclusions reached are those of the author(s) and do not necessarily represent those of Nagra.

thEmpa
Überlandstrasse 129
CH-8600 Dübendorf
T +41 58 765 11 11
F +41 58 765 11 22
www.empa.ch

EMPA
Materials Science & Technology

Report No. 5214001638 [HTIG-TR14-05]

FEASIBILITY EVALUATION STUDY OF CANDIDATE CANISTER SOLUTIONS FOR THE DISPOSAL OF NUCLEAR SPENT FUEL AND HIGH LEVEL WASTE

A STATUS REVIEW
for

NAGRA

SR Holdsworth, T Graule, E Mazza

Prepared as part of a NAGRA Working Group activity with: L Johnson and N Diomidis (NAGRA), and F King (Integrity Corrosion Consulting)

CONTENTS

0 SUMMARY

A feasibility evaluation study has been made of candidate canister solutions for the disposal of nuclear spent fuel and vitrified high level waste, respectively involving the consideration of nominally 5m long and 1.5 (or 3m) long thick walled containers. Assessment has been based on the consideration of a wide range of factors under four generic headings, i.e. ***mechanical integrity***, ***environmental damage*** (including impact on the geological barrier), ***fabrication***, and ***costs***. An integral part of the evaluations has been a due regard for the robustness of life time predictions.

The following observations are inevitably influenced by considerations such as: *i)* the legitimacy of the assumed load cases for the mechanical integrity assessments, *ii)* the reliability of the long-time environmental damage predictions based on almost no direct observations in relevant environmental conditions and the judgements of a relatively small number of specialists serving the nuclear waste disposal community, *iii)* the effectiveness of fabrication feasibility predictions for those concepts without direct practical experience and existing technology, and *iv)* the accuracy of investment and unit cost predictions, in particular for those cases for which the technology currently does not exist.

Carbon steel canisters with an appropriate thickness: *a)* for the required structural strength, with a corrosion allowance, and *b)* to ensure that the radiation level at the external surface is insufficient to influence corrosion resistance, provide a possible nuclear waste disposal solution. There is well established manufacturing and fabrication experience with parts of the required size, and the associated costs are well established. The main concern with this solution relates to the evolution of hydrogen as a by-product of the corrosion process, and the consequent potential impact on the surrounding geological barrier.

The KBS-3 outer thick walled copper container concept has been considered because of the vast experience gathered in Scandinavia during the past 30 years. As an alternative to the KBS-3 configuration, copper coated carbon steel canister solutions overcome uncertainties associated with creep of this corrosion barrier, although there are still manufacturing and fabrication details relating to this second copper-based concept to be optimised fit-for purpose.

Nuclear waste disposal canister solutions involving carbon steel clad with titanium or nickel alloy have been evaluated. While both are feasible with existing manufacturing and fabrication technology, there are uncertainties associated with long time environmental damage resistance (due to insufficient existing long time damage data). Moreover, material and fabrication costs are relatively high.

The mechanical integrity of solid titanium and nickel alloy solutions has also been evaluated.

There is a strong incentive to adopt a canister solution with negligible hydrogen production during corrosion, primarily driven by uncertainties relating to the impact of the gas on geological barrier integrity and repository performance. A number of possibilities exist, including the use of ceramics such as Al_2O_3/SiO_2 or SSiC. For such solutions, significant concerns associated with mechanical integrity, large-part manufacture and final-sealing feasibility could conceivably be overcome for the smaller VHLW canisters with appropriate development activity and financial investment. However, it is debatable if the very high level of funding which would be required is justifiable for the relatively low number of canister units ultimately needed, in particular when the successful outcome of such a research and development activity could be by no means assured, and if recommended further investigations confirm that there are already acceptable alternative solutions. In principle, other possibilities do exist, including coating or cladding a carbon steel sub-structure with a highly corrosive-resistant metal for which the long term rate of hydrogen evolution is so low that it remains dissolved in the pore water, and no gas phase is formed.

The evaluation of the ceramic canister concept is underpinned by the results of a recent comprehensive supplier review (App. **G**).

In terms of ***mechanical integrity***, ***fabrication*** and ***cost*** assessment categories, carbon steel canisters provide by far the most superior solution for nuclear waste disposal, but seriously suffer from the risk limitations associated with susceptibility to ***environmental damage***. The concerns associated with ***environmental damage*** may be overcome by the coating or cladding of a carbon steel sub-structure with a highly corrosion resistant material for which the long term rate of hydrogen evolution is so low

that any gas generated is dissolved in the pore water. Of the three solutions evaluated, copper is potentially the most promising (and advanced, in terms of state-of-the-art), but with future cost and supply uncertainties. Titanium and nickel alloy cladding could provide more effective solutions, but are expensive, and would require fabrication research and development investment to complement what is already known from the petro-chemical industry. A ceramic such as SSiC provides an interesting solution due to its very high resistance to ***environmental damage***, but the risks associated with ***mechanical integrity***, ***fabrication*** state-of-the-art, and (investment) ***costs*** are high.

A number of recommendations are made for further research and development activity relating to candidate canister solutions for the disposal of nuclear spent fuel and high level waste.

1 BACKGROUND AND INTRODUCTION

The purpose of the following review is to establish a project risk assessment matrix for spent fuel (SF) and vitrified high level waste (VHLW) candidate disposal canister solutions, specific to Swiss geological barrier conditions.[1] The outcome is a well-informed indication of the concepts with prospects for successful development in Switzerland, and a listing of recommendations concerning future research activity necessary to underpin their timely and effective implementation.

The canister provides the internal shell of a multi-barrier concept for the disposal of spent fuel (SF) and vitrified high level waste (VHLW). In Switzerland, the proposal is to place such canisters in an underground repository in Opalinus Clay, with a backfill of bentonite clay, at depths of up to ~900m (Fig. 1).

Spent fuel is uranium oxide fuel that has been used in a nuclear power reactor but can no longer be used to produce electricity in an efficient way. Uranium-235 (^{235}U) produces radioactive isotopes of several lighter elements such as cesium-137 (^{137}Cs) and strontium-90 (^{90}Sr) as a consequence of the fission process, and these account for most of the heat and penetrating radiation in HLW. Some uranium atoms also capture neutrons from nearby fissioning uranium atoms to form heavier atoms like plutonium. Such transuranic elements do not produce the same amount of heat or penetrating radiation as the fission products, but take much longer to decay, thereby accounting for most of the radioactive hazard remaining after 1000 years (e.g. Fig. 2). The disintegration of uranium over billions of years is responsible for the formation of so-called daughters such as ^{230}Th, ^{226}Ra, and radon daughters ^{210}Pb and ^{210}Po (Fig. 2). While there is a regulatory lifetime requirement of ≥ 1,000 years for SF and VHLW canisters, the NAGRA canister integrity requirement is ≥ 10,000 years to provide a suitable safety margin. Some of the canister concepts to be considered in the following report have a potential for much longer lifetimes.

Only γ radiation and neutron radiation emitted by the waste are sufficiently penetrating to produce a field at the outer surface of a thick walled nuclear waste canister, and even then at a low level [3]. The majority of SF/VHLW canister designs developed internationally provides significant shielding because of the use of thick walled metallic vessels (either for structural or corrosion purposes) [4]. Nevertheless, dose rates are typically well above levels acceptable for contact handling, and therefore external shielding is necessary for handling the canisters. The aim external surface radiation field is typically <1Gy/h (from both gamma and neutron radiation), this being the value found empirically to be the threshold below which radiation effects on corrosion processes are insignificant [5].

The evolution of environmental conditions at the container surface in bentonite, after canister emplacement, is envisaged to go through four phases (Fig. 3) [3]. Phase 1 is the initial dry-out period coinciding with the attainment of a peak surface temperature of 120 to 140°C after ~5-10 years. Phase 1 continues until the time when the canister surface is first wetted with liquid water after ~20-40 years of emplacement. During this period, oxygen is consumed by corrosion of the canister and corrosion of the steel mesh stabilising the repository tunnel wall. Dry conditions continue (in the aerobic unsaturated Phase 2) until the temperature falls below ~100°C and increasing aqueous bentonite saturation is responsible for the relative humidity to increase above the critical level for aqueous corrosion to become possible. Phase 3 (the anaerobic unsaturated phase) corresponds to the period between the onset of anaerobic conditions when all oxygen has been consumed and complete saturation of the bentonite (coinciding with complete development of the swelling pressure). The end of Phase 3 and commencement of the long-term anoxic Phase 4 typically occurs after ~100 years when the bentonite is completely saturated and all oxidised corrosion products formed at the canister surface and the rock support structures have been consumed.

Assuming the nuclear waste repository remains undisturbed, the only mechanism by which radionuclides could reach the biosphere is by the dissolution of waste in the groundwater, followed by migration of the radioactive solution to the surface. One of the major factors in selecting a canister solution for ultimate disposal underground is its resistance to corrosion by the repository environment. Following disposal, resistance to irradiation damage and other environmental damage processes are therefore important.

---

[1] *A Nomenclature listing is given in App.* ***A***

For some metallic waste disposal canister solutions, corrosion may not only lead to a loss of wall thickness but also to the evolution of gas (in particular H_2) which could in principle impact on the integrity of the geological barrier. This is an important consideration in the following report, and accounts for the interest shown in the adoption of a ceramics solution since such materials do not generate gaseous products as a consequence of any environmental damage process.

Critical weaknesses in most canister solutions are usually associated with joints, which are therefore kept to a minimum (ideally only one to facilitate final containment).

2 CANISTER CONCEPTS

2.1 OVERVIEW

There are a number of different nuclear waste disposal canister concepts proposed for adoption worldwide, their configuration depending mainly on the type of waste to be disposed, the surrounding geological structure, and the material solution adopted to minimise the risk of canister integrity breakdown due to environmental damage. Of principal interest in the present study was the disposal of spent fuel (SF) assemblies, which are typically up to 4.5m in length, and vitrified high level waste (VHLW) cylinders, which are typically 1.34m long. These require different canister configurations. General corrosion is typically combatted either by the addition of a corrosion allowance to the container wall thickness or by the adoption of a passive material forming the outer layer of the containment system. The adoption of a passive material solution may involve an additional internal canister structure to provide the necessary mechanical strength. Moreover mechanical strengthening may or may not integrate the internal structure used for example to separate the spent fuel assemblies, e.g. Fig. 4b.

2.2 MATERIAL SOLUTIONS

Five categories of material solution were evaluated in the present study, namely:
i) Carbon-steel (with a corrosion allowance)
ii) Copper shell (50mm thick) with internal cast iron support (KBS-3 concept)
iii) Copper coated (3-5mm thick) with carbon steel support
iv) Titanium or nickel-based alloy shell with carbon steel support, and
v) Ceramic with ceramic or carbon steel support

More background details concerning the materials of interest are given in a series of appendices, i.e. carbon steel (App. **B**), cast iron (App. **C**), copper (App. **D**), titanium and titanium alloys (App. **E**), nickel-base alloys (App. **F**), and ceramics (App. **G**). The Scandinavian KBS-3 concept is summarised in App. **H**.

Stainless steel was also a possibility, but was not considered further here because of the propensity to localised (pitting and/or crevice) corrosion and stress corrosion cracking by chloride ions [4].

2.3 CANISTER DIMENSIONS

The disposal of both SF and VHLW were considered in the evaluation. The respective requirements for SF and VHLW storage containers involved different size constraints which determined the manufacturing challenges associated with each material solution (e.g. [6]).

2.3.1 Spent Fuel (SF)

In Switzerland, there is an interest in the disposal of both BWR and PWR spent fuel assemblies. In practice, canister lengths for both sources of SF are nominally 5m.

BWR-SF assemblies are 4.48m long x 139x139mm in section. They are ideally stored in a cluster of nine (9) 145x145mm cavities (e.g. Fig. 4a). Typically, these require a container internal support structure within a cylinder with an effective ID of 760mm (and OD of ≤ 1050mm, depending upon canister material solution).

Conceivably, it would also be possible to contain BWR-SF assemblies in clusters of three (3), which would require a container internal support structure within cylinders with an effective ID of 460mm and OD of ~560mm. Adopting 3-cluster SF assembly disposal units would permit respective reductions in the BWR-SF disposal canister ODs (depending upon canister material solution).

PWR-SF assemblies are 3.52m long x 198x198mm in section, or 4.29m long x 215x215mm in section. They are ideally stored in a cluster of four (4) 235x235mm cavities (e.g. Fig. 5). These require a container internal support structure with the same dimensions as those for the BWR 9-cluster disposal unit (with an OD depending on canister material solution).

It is conceivable (albeit unlikely) that there could also be a single PWR-SF assembly disposal unit with an effective ID of 347mm (and an OD of ~500mm, depending on canister material solution).

Details of the KBS-3 copper shell with internal cast iron support canister concept are reviewed in App. **H**.

2.3.2 Vitrified High Level Waste

Vitrified high level waste is typically manufactured as cylinders 1.34m long x 430mm in diameter (e.g. Fig. 6). These are ideally placed in pairs or can be placed individually, therefore requiring canisters with an ID of 0.45m and lengths of ~3m or ~1.5m (and an OD depending on canister material solution), e.g. Fig. 6.

3 CANISTER RISK ASSESSMENT CATEGORIES

Six canister risk assessment categories were evaluated for the material solutions listed in Sect. 2.2, namely:
- Mechanical Integrity,
- Environmental Damage
- Impact on Geological Barrier,
- Robustness of Lifetime Prediction,
- Fabrication, and
- Costs

The following sections describe the categories and their significance, and summarise the overall results for the different materials and design concepts. The feasibilities for each concept are presented in Table 6a to Table 7e, and material property summaries are given in Apps. **B** to **G**.

3.1 MECHANICAL INTEGRITY

3.1.1 Overview

Initially, the risks associated with mechanical integrity were considered under two sub-categories, one concerned with handling, and the second concerned with disposal. Load cases concerned with disposal were relatively easy to formulate, whereas those concerned with handling were not, in particular since they depended on the specific canister handling and emplacement method and the characteristics of the required shielding overpack, all of which had still to be established for the Swiss cases. Consequently, while mechanical integrity risks could be based on specific disposal load cases, their consideration in terms of mechanical handling had to be more generic.

In the following, mechanical integrity is characterised with respect to the failure envelope in a failure assessment diagram (FAD). FADs comprise axes of K_r and L_r, where

$$K_r = K_{1a} / K_{1C} \quad (1)$$

$$L_r = \sigma_{ref} / R_{p0.2} \quad (2)$$

where for the component and defect geometries of interest, K_{1a} is the applied stress intensity factor (e.g. [87-89]) and σ_{ref} is the reference stress (e.g. [88-90]). The cut-off value of L_r to prevent plastic collapse is:

$$L_r^{max} = R_{pX} / R_{p0.2} \quad (3)$$

There are various options for defining the failure envelope. Option 1 [91] did not require stress-strain data, needing only a knowledge of the flow strength of the material, and was suitable for the purpose of this assessment, i.e.

$$K_r = \left(1+0.5.\left(L_r\right)^2\right)^{-0.5}.\left[0.3+0.7.\exp\left(-0.6.\left(L_r\right)^6\right)\right] \quad \text{for } L_r \le 1 \qquad (4a)$$

$$K_r = \left(1+0.5.\left(L_r\right)^2\right)^{-0.5}.\left[0.3+0.7.\exp\left(-0.6.\left(L_r\right)^6\right)\right].\left(L_r\right)^{(N-1)/2N} \quad \text{for } 1 < L_r < L_{r,max} \qquad (4b)$$

where $\mu = \min\left[0.001.E / R_{p0.2}, 0.6\right]$ and $N = 0.3\left[1 - R_{p0.2} / R_M\right]$

and where the flow strength, R_{pX} is usually taken to be $(R_{p0.2} + R_M)/2$. Eqn. 4 defined the failure assessment envelope (FAE) in the failure assessment diagram (FAD) adopted in this study. While it would be more appropriate to use Options 2 or 3 [91] in defect assessments relating to close-to-final canister designs, use of the Option 1 failure assessment envelope was reasonable for material comparison purposes. In this respect, the terms in Eqns. 1 to 4 may be rearranged to enable the mechanical integrity characteristics of candidate canister materials to be compared, e.g. Fig. 7 (using the material properties reviewed in Apps. **B** to **G**).

In the following evaluation, the likelihood of failure was indicated by the CO/CO^{FAE} ratio where in the failure assessment diagram, CO is the distance between the origin and the $K_r(L_r)$ assessment co-ordinate and CO^{FEA} is the corresponding distance between the origin and the failure assessment line defined by Eqn. 4 (Fig. 8).

3.1.2 Handling

To a significant extent, the mechanical property requirements for nuclear waste canisters were determined by forces likely to be encountered during handling, either during preparation and transportation to the disposal position or retrieval (if necessary) from the repository. In normal circumstances, the canister would be surrounded by a heavy thick-walled transfer/shielding cask while in the encapsulation facility and during transfer underground. Consequently, the most severe handling incident might involve a drop onto the operations tunnel floor/rail bed while the canister was being emplaced onto the bentonite blocks. An illustrative case was considered in the recent Nagra canister design study [10]. Handling load cases had also been considered in other repository studies, e.g. [41,92,93], but were not examined in this review.[2]

Potential handling incidents were judged to be repository concept specific, and it was regarded as premature to define load cases which could be representative of a Swiss scenario. Nonetheless, the FAD based diagram in Fig. 7 clearly illustrated the challenges associated with brittle material solutions such as those involving ceramics, in comparison to more ductile metal structures, in relation to probable response to handling load cases.

3.1.3 Disposal

After disposal, the external pressure was said to develop in the way shown schematically in Fig. 9 for a repository at a depth of 900m [10]. The full buffer swelling pressure of ~4MPa was expected to develop as a result of hydration after ~100 years (cf. Fig. 3). Two evolution scenarios are illustrated in Fig. 9, one for a strong (crystalline) rock, and one for a weaker rock such as Opalinus clay. The lower bound scenario was based on the long-term recovery of hydrostatic pressure in an emplacement borehole in crystalline rock, while the upper bound scenario considered the self-weight deformation of the clay rock and bentonite at a depth of 900m resulting in the generation of maximum conceivable compressive stresses of 22MPa (vertical) and 29MPa (horizontal) on the canister in a horizontal emplacement tunnel over a period of 10,000 years. The upper bound scenario formed the basis of a number of load case analyses based on carbon steel canister designs [10,94-98], the details of which are summarised in Table I1. Variable buffer swelling stresses were also considered for the early bentonite hydration stage based on NAGRA assumptions related to poor control of bentonite density during emplacement.

Stress Analysis. A significant outcome from the disposal load case stress analyses was that the maximum stresses arising from the short time loading (TWI-5 case, variable buffer swelling) of both SF and VHLW canisters were axial at the external surface, whereas those arising from long time (TWI-2

---

[2] *The fact that potential drop conditions (height/inclination) were so dependent on local handling/disposal arrangements made it difficult to define a realistic load case for this risk sub-category in this evaluation. Specific load cases would clearly have to be evaluated prior to final design assessment.*

case, 29-22MPa) were hoop at the internal surface (App. **I**). This meant that FAD constructions considering short time canister loading assessed a circumferential defect condition on the external surface, whereas those considering long time canister loading assessed an axial defect condition on the internal surface (App. **I**).

A simple von Mises limit stress analysis using the results of the elastic FEA indicated that carbon steel full size SF rod closed-end cylinders with a wall thickness of greater than ~90mm would be acceptable (Fig.I 10). For a VHLF configuration, a wall thickness of 50mm also appeared to be acceptable. In terms of this approach, the acceptability of other solutions is summarised in Tables I6 and I7.

Failure Assessment. Using the stress analysis results summarised in App. **I**, FADs for the following canister options are constructed in App. **J**:
For SF rod disposal:
- Carbon steel (770mm ID, 4.6m long, 140/120mm thick), Fig.J 2,
- Carbon steel (770mm ID, 4.6m long, 100mm thick), without and with copper coating (Fig.J 3), with titanium cladding (Fig.J 5) and with nickel alloy cladding (Fig.J 7),
- Carbon steel (770mm ID, 4.6m long, 80mm thick), without and with copper coating (Fig.J 4), with titanium cladding (Fig.J 6) and with nickel alloy cladding (Fig.J 8),
- Solid titanium (770mm ID, 4.6m long), with 100mm thickness (Fig.J 9), and with 80mm thickness (Fig.J 10),
- Solid nickel alloy C22 (770mm ID, 4.6m long), with 100mm thickness (Fig.J 11), and with 80mm thickness (Fig.J 12),
- Solid Al_2O_3/SiO_2 (770mm ID, 4.6m long, 80mm thick), Fig.J 13, and
- Solid SSiC (770mm ID, 4.6m long, 80mm thick), Fig.J 14)

For VHLW disposal:
- Carbon steel (440mm ID, 1.6m long, 50mm thick), without and with copper coating (Fig.J 15), and titanium cladding (Fig.J 16) and nickel alloy cladding (Fig.J 17),
- Solid titanium Gr.2/7 (440mm ID, 1.6m long, 50mm thick), Fig.J 18,
- Solid nickel alloy C22 (440mm ID, 1.6m long, 50mm thick), Fig.J 19,
- Solid Al_2O_3/SiO_2 (440mm ID, 1.6m long, 50mm thick), Fig.J 20, and
- Solid SSiC (440mm ID, 1.6m long, 50mm thick), Fig.J 21.

Defect assessment involved consideration of the integrity of semi-circular surface defects with depths of *i)* 2mm and *ii)* 0.25*t* (in line with common practice in the nuclear industry to assume a quarter wall thickness reference flaw). Such semi-circular surface defects were judged to be acceptable in all considered short and long-time SF rod disposal canister load case scenarios, apart from those involving Al_2O_3/SiO_2, and SSiC (and 50mm thick carbon steel), Table J1.

All the considered short and long-time VHLW disposal canister load case mechanical integrity scenarios were acceptable apart from Al_2O_3/SiO_2 (irrespective of initial defect size criterion) and SSiC with an existing 0.25*t* deep semi-circular surface defect, Table J2.

Importantly, this evaluation did not consider the mechanical integrity of canisters with a final sealing joint. In practice, this location was likely to be the most critical in terms of mechanical integrity.

3.2 Environmental Damage

3.2.1 Overview

Both active and passive outer barrier material solutions were considered, whereby containers constructed from active materials such as carbon steel required a corrosion allowance added to their wall thicknesses, and those with an external passive layer did not. Passive materials form a thin compact self-healing oxide film (of ~1-3nm), resulting in low rates of general corrosion, but which may be susceptible to localised corrosion under certain environmental conditions.

Based on studies relating to a number of repository conditions, there was a significant knowledge base relating to the environmental damage characteristics of a number of candidate nuclear waste disposal canister materials (e.g. [3,4,7,33,14,63]). However, the information had been collected for different repository environments (depending on country and local geological characteristics), and it was therefore necessary to consider the evidence with this in mind. Compositions of pore waters in

Opalinus and bentonite clays (relevant to Swiss conditions) are summarised in Table 1. Saturated bentonite has an ionic strength approximately equivalent to a solution of 0.3M NaCl.

Evidence relating to the important environmental damage mechanisms relevant for nuclear waste disposal conditions, in particular in Switzerland, is considered in the following section.

3.2.2 General Corrosion

The general corrosion characteristics of the materials under consideration are reviewed in Apps. **B** to **G**, and summarised in Table 2. This table acknowledges that there are two important periods during the evolution of the repository environment to consider with respect to corrosion activity, i.e. the relatively short initial period when conditions are likely to be aerobic and transition from dry to wet at an elevated temperature (Fig. 3), and the long-time period when conditions are likely to be anaerobic and wet.

For the short-time aerobic period, general corrosion is typically expressed as a depth accumulated (as there is a limited inventory of trapped oxygen available in the bentonite), whereas for the long-time anaerobic period, it is more usual to consider an annual rate (Table 2).

Of the materials considered in Table 2, carbon steel (cast iron) and copper are regarded as active materials and, as such, container external surfaces involving these materials have to be designed with a corrosion allowance, although the corrosion allowance for carbon steel (20mm for 10,000 years) greatly exceeds that of copper (2mm for 100,000 years).

Passive alloys (Ti and Ni-alloys) have extremely low general corrosion rates (1-10nm/a), and therefore a limited thickness of ~5mm may be sufficient.

Most ceramics exhibit negligible general corrosion rates, which are independent of redox conditions.

3.2.3 Localised Corrosion

Pitting, crevice corrosion and intergranular attack (IGA) are the main local corrosion processes of concern with regards to the integrity of nuclear waste disposal containers. Susceptibility to local corrosion is primarily a problem for passive materials. The active materials such as carbon steel and copper are prone to surface roughening rather than pitting corrosion [4].

While it is necessary to know if a material is susceptible to the initiation of a local corrosion process, it is equally important to understand subsequent propagation characteristics and, for example, if the development of the process becomes self-arresting, e.g. copper and Ti Gr.7 (Table 3).

In order to quantify and fairly rank initiation susceptibilities, a knowledge of the corrosion potential of the material/environment condition with respect to the appropriate pitting and crevice corrosion potentials is important. Unfortunately, this information is not available in a systematic way, and with these constraints, the situation is summarised in Table 3. For those materials which are prone to local corrosion, it would be desirable to know the limiting conditions for these mechanisms, but these are generally unknown.

None of the metallic materials reviewed are susceptible to IGA, Table 3. Those ceramics comprising intergranular glassy phase type infill are vulnerable to IGA (local dissolution associated with fluid intrusion).

3.2.4 Microbially Induced Corrosion

When considering the risk of microbially induced corrosion (MIC), it was usually necessary only to consider microbial activity at the canister surface [101]. MIC at the canister surface could involve the development of biofilms and the resultant separation of anodic and cathodic processes. Microbial activity further away from the canister only impacted on canister performance if aggressive metabolic by-products were transported through the backfill material. The baseline assumption was that microbial activity at the surface of a canister embedded in highly compacted bentonite would be low enough that species such as sulphide would not be produced in significant quantities at any time during the evolution of the local environment [102]. For example, a strong decrease in the flux of microbially produced sulphide to a copper surface had been observed as the density of bentonite was increased [101] (App. **D**).

Titanium and ceramics were in any case considered to be immune to MIC.

3.2.5 Stress Corrosion and Hydrogen Induced Cracking

Conventional parameters for characterising a material's threshold stress (R_{SCC}) or threshold stress intensity factor (K_{ISCC}) for stress corrosion cracking depended not only on material composition and strength, but also on environment and the adopted no-crack formation/development time (threshold) criterion. While such quantities existed for design relevant time life criteria for steam turbine steels in pure low oxygen condensing steam environments (e.g. [103]), they were not commonly available for other applications, and certainly not for long time nuclear waste disposal conditions.

Adoption of the most appropriate environmental cracking threshold criterion was particularly important. At low applied σ_1 and K_1 values, environmental crack incubation periods could be very long [103], and far in excess of realistically practical experimental test times for nuclear waste disposal conditions [18].

SCC. As a generality, for low strength steels (and other metallic materials) exposed to relatively benign environments, susceptibility to stress corrosion crack initiation is negligible at stresses below the yield strength [103]. The evidence relating to SCC susceptibility is summarised in Table 4. The risk of SCC can be reduced by minimising residual (welding) stresses and by the removal of surface breaking defects.

HIC. Of the materials under evaluation, carbon steel and titanium were potentially the most at risk to hydrogen induced cracking (Table 4). Allowances were made for this in the feasibility evaluations. While the possible effects of hydrogen on the lifetimes of carbon steel nuclear waste canisters had been comprehensively reviewed [19], this was not the case for titanium.

3.2.6 Influence of Radiation on Corrosion Properties

The evidence indicated that there was no influence of γ-radiation on the corrosion properties of metals for absorbed dose rates of ≤ 1Gy/h (which in magnitude related to the equivalent dose rate expressed in Sv/h (or 1000mSv/h)[3]) [104]. This absorbed dose rate was regarded as the limit above which more work related to the influence of corrosion on a candidate canister material would have to be conducted. An upper limit of 1Gy/h at the external canister surface during emplacement was therefore an additional criterion determining the choice of wall thickness.

Of the candidate materials under evaluation, empirical studies indicated that the titanium alloys were the least susceptible to γ-radiation effects, with nickel alloys being the most susceptible. The effect appeared to be inversely related to density, although there was no theoretical reason for this. Based on a consideration of both material characteristics and container thickness, canister external dose rates were likely to be highest for ceramics. However, in terms of the respective corrosion properties of the different potential canister materials, ceramics were likely to be the least affected by radiation induced phenomena.

3.3 Impact on Geological Barrier

Of all the candidate materials, carbon steel had potentially the greatest impact on the other barriers (compacted bentonite and low permeability host rock), i.e. due to H_2 and Fe(II) formation during anaerobic corrosion. Hydrogen is produced by the reduction of water. It can be transported through bentonite by pathway dilation when the pressure exceeds the bentonite swelling pressure. Hydrogen becomes a problem if the pressure in the rock rises to values that are a substantial fraction of the in-situ stress. It is not a problem when the gas production rate is sufficiently low for the hydrogen to simply dissolve in the pore water. A realistic gas production rate for steel is considered to be 1μm/a [3], and for copper to be possibly 1000 times lower. At such low rates, any hydrogen generated from Cu would dissolve in the pore water.

Fe(II) arising from anaerobic corrosion can react with bentonite, potentially reducing its swelling capacity. Corrosion products from other potential canister materials are considered to have negligible impact on the barrier system.

---

[3] *≤ 2mSv/h is regarded as the maximum permissible occupational exposure limit*

3.4 Robustness of Lifetime Prediction

The robustness of lifetime predictions depended on the assumptions and uncertainties associated with the adopted analytical approaches and assessment material property input data. While consideration of these was important for the evaluation of mechanical integrity, they were by far of most influence on the prediction of environmental damage development.

3.4.1 Mechanical Integrity

Analytical Approaches. The procedures for predicting the mechanical integrity of metallic structures were relatively mature after much development and effectiveness benchmark activity during the last 50 years. Probably the biggest uncertainties relating to the mechanical analysis of nuclear waste storage containers would be the magnitude and distribution of residual stresses associated with the final closure weld, in particular when complete PWHT was not possible.

The maturity of procedures for determining the mechanical integrity of large ceramic structures was significantly lower.

Assessment Boundary Conditions. The robustness of the mechanical integrity contribution to canister lifetime prediction depended on the validity and reliability of the adopted load case (input boundary) conditions, as well as the assessment material property input data.

Assessment Material Property Input Data. The most significant uncertainties were associated with assessment material property input data such as R_{pX}, R_M, K_{IC}, the main requirements being that: *i)* the datasets providing the minimum values used in analysis were fully representative of the specified material, and *ii)* the material of construction conformed with the material specification. It was likely that, in this regard, the uncertainties associated with these mechanical integrity parameters (in particular, fracture toughness) could be relatively high for certain of the considered materials at the present time. However, this situation could be readily rectified in advance of a formal design assessment, by taking appropriate action beforehand. The effort required for a ceramic material solution would be significantly greater than for a metallic solution (i.e. for the property characterisation of material in a representative product form).

The generation of an appropriate database for the formal design analysis of the selected material solution would have to fully consider the influence of relevant degradation mechanisms (e.g. hydrogen on K_{IC}), and the properties of the closure joint.

It was conceivable that there could be changes to material properties over very long time scales which were currently unknown. While this was most unlikely with the existing understanding of physical mechanics and mechanisms, the possibility could not be excluded.

3.4.2 Environmental Damage

The requirement to be able to predict canister integrity with respect to corrosion processes over many 1000s of years presented a significant technological and scientific challenge, with such predictions needing to be justifiable, mechanistically sound and conservative. Predicted lifetimes for this application were typically required to be >>x1000 the maximum experimentally observed times (compared with accepted observed to predicted lifetime extrapolations of x3 in power generation [105]). A number of approaches could be used to complement lifetime predictions [106], including:

- prediction reproducibility using alternative modelling approaches
- the use of analogues, and
- long term (*in situ*, full scale) testing.

Alternative Models. Improved confidence in corrosion predictions was gained when good agreement was achieved from results determined using different modelling approaches, e.g. *i)* the use of mass-balance and detailed reaction-transport models for prediction of the aerobic corrosion of copper, or *ii)* pitting corrosion predictions based on empirical pitting factors and the statistical analysis of pit-depth data. While this concept was used to provide supporting evidence in the US Yucca Mountain programme, it had not been widely adopted elsewhere.

Analogues. The use of archaeological analogues was more contentious, and in any case was really only applicable for underpinning aerobic and anaerobic corrosion rate predictions for copper and carbon steel (and possibly ceramics). Examples were observations made from naturally occurring

deposits, meteorites and historical artefacts (e.g. [107]). The main uncertainties of this approach were that material and environmental analogues and potential repository conditions were almost certainly inconsistent, but then even this type of long-time prediction benchmarking was better than nothing.

Long-Term Tests. Traditionally, long-term testing under controlled conditions was the accepted method of reducing uncertainty for long life-time predictions. However, for this application, this ideally meant laboratory and in-situ testing for tens of years. As a generality, this was approach was unusual for the corrosion community.

Mechanistic Understanding. The most important factor in the adoption of all these approaches was that the evidence provided and used in long term lifetime prediction was mechanistically consistent with the corrosion process(es) under evaluation.

3.5 FABRICATION

The risks associated with canister manufacture, final sealing and inspection were considered as part of the fabrication category.

3.5.1 Canister Manufacture

Carbon Steel. Of the different solutions evaluated, those based on large thick walled carbon steel were by far the most feasible on the basis of manufacturing considerations [10]. There were many engineering applications involving the adoption of large forgings or castings of the required sizes and properties, and so a number of technologies were proven and known to be implementable by a number of manufacturers, App. **B**.

Cu Corrosion Barrier Solutions. There were two copper based corrosion barrier solutions for nuclear waste disposal canisters. The first was the Scandinavian KBS-3 solution involving a 50mm thick copper canister reinforced by an SG cast iron insert (App. **H**). After a research and development activity lasting for more than 30 years, the manufacturing feasibility of this solution was now well demonstrated (e.g. [26,25]).

The second copper based canister solution was one involving copper coated carbon steel, App. **D**. With the main canister structure being carbon steel, the manufacturing challenges were mainly concerned with the homogeneous defect-free deposition of a (3-5mm) thick coating of pure copper [29]. The current concept was to electro deposit copper over the main body and top plate, and to then cold spray deposit over the final sealing weld. While the technology for this application was reasonably well advanced, significant development effort and proof of concept was still required [29].

Ti and Ni Alloy Clad Carbon Steel. In principle, there was well established expertise for Ti and Ni alloy cladding of thick section carbon steel pressure vessels, in particular relating to the petro-chemical industry (e.g. [43,54]), Apps. **E**,**F**. Common practices were processes such as hot roll-bonding, explosive bonding and weld overlay [65], although of these, only weld overlay could realistically be used on convex (external) surfaces. Thin sleeve solutions were an option, but would require fixation in the case of titanium, to avoid any risk of creep.

Ceramics. While the use of a ceramic material as the basis for a large thick walled nuclear waste disposal canister concept was very attractive, not least because of the absence of any corrosion related gas generation to ultimately impact on the surrounding geological barrier, existing manufacturing experience was mainly with the production of relatively small parts. As a generality, there had not traditionally been a demand for large parts with optimum density characteristics, and so no need for developing the necessary manufacturing procedures and investing in the appropriate infrastructure (for pressing, green-state handling and high temperature sintering).

While many of the challenges associated with the manufacture of ceramic VHLW disposal canisters were judged to be surmountable with appropriate investment and development activity, it was suggested that the adoption of materials such as Al_2O_3/SiO_2 and SiC to form the basis of a large SF rod disposal canister solution was not feasible, even with significant investment.

3.5.2 Sealing

In the context of nuclear waste disposal canisters, there were in principle two types of joint to consider, namely those which could be fabricated in a production workshop environment (under nominally ideal

conditions), and the final seal which must be made (and inspected) remotely in a hot cell, once the SF rods or VHLW had been placed in the canister. The focus here is with the final sealing joint.

Technologies for welding the metallic canister solutions were well developed, e.g. [10,43]. In particular, solutions for thick section carbon steel welds were routinely practised. Titanium and nickel alloys were also readily weldable, although care was required with titanium since the integrity of Ti weldments was severely affected by the presence of oil or grease leading to porosity, gases (O_2, N_2 or H_2) responsible for embrittlement, and to contamination from iron bearing species.

A major concern with welding thick section metallic parts was the associated consequential residual stresses which required post weld stress relief treatment at temperatures typically well in excess of the maximum permissible temperatures for nuclear waste (~400-450°C). The magnitude of such residual welding stresses could be minimised by moving the plane of the weld to a significant distance from the waste (e.g. ≥ ~0.5m), where a local heating solution could be acceptable (e.g. [10]).

Ceramics could not be welded in the conventional sense. So-called laser welding was being increasingly adopted for sealing/joining ceramics, although in practice the laser was being used to heat the substrate as part of a soldering process [83]. Heating high thermal conductivity non oxide ceramics such as SiC typically involved the absorption of CO_2 or diode laser radiation at the surface and through thickness heat transport by conduction. In contrast, diode laser radiation absorption through the section thickness was required to heat lower thermal conductivity oxide ceramics. Glass ceramic solders (e.g. Y_2O_3-Al_2O_3-SiO_2) were the most widely used because it was easy to tailor their composition to match the required sealing depth. In principle this was not a good solution for an SiC nuclear waste disposal canister, for which a matching filler was realistically the ultimate goal. Although laser welding SiC parts was an evolving technology, only production joints of ~5-10mm had been made to date [77]. Significant development activity was therefore required in this area.

3.5.3 Inspection

Thick section metallic canisters, including welded joints, could be reliably inspected by a range of surface and sub-surface inspection procedures (e.g. [10]). The non-destructive inspection of ceramics was also feasible using techniques such as ultrasonic testing, radiography, x-ray computed tomography and acoustic emission [85], although in practice the applicability and detection limits in thick wall sections had to be optimised and demonstrated (e.g. [7]).

3.6 Costs

Costs were considered under two sub-categories, namely development costs and production unit costs.

3.6.1 Development Costs

Development costs were those required to get the canister waste disposal concept to the point where it provided a feasible solution and could be implemented in a safe, reliable and acceptable way. The development costs for carbon steel solutions were likely to be relatively low [10] since the mechanical properties, manufacturing/welding/inspection possibilities and costs of large thick walled containers were already well known from other well developed engineering applications. This contrasted with the cost of development of the Scandinavian KBS-3 cast iron reinforced copper canister solution which already exceeded 100MCHF [26,25].

The development costs associated with the copper coated, and titanium and nickel alloy clad solutions were likely to be significant, but not of the same order as the KBS-3 concept. In principle, there was existing expertise with the three approaches involving cladding. For copper coating, a development activity for the specific application was already underway [29].

The required development and investment costs for a ceramic canister solution were likely to be of the same order if not in excess of those for the KBS-3 canister. It was estimated that the cost of an SiSiC canister development activity (not including joining/sealing research) could be ≥ ~45MCHF (Table G7). This was not inconsistent with the estimate of ≥ ~120MCHF for an SSiC total concept development activity [77].

3.6.2 Unit Costs

Quantifying the absolute and relative costs of candidate canister solutions was not a trivial activity. Even raw material costs were sensitive not only to market fluctuations, but also to the required product form and quantity of order. The relative material costs given in Table 5 were based on information received from suppliers and from the internet. Such were the uncertainties, that the values cited could only be regarded as indicative.

Table 5 gives relative costs by-volume as well as by-weight. This served to indicate that 'by-volume' the relative costs of titanium products were not as excessive as indicated by a 'by-weight' comparison. In these terms, the relative costs of copper (at the time of writing) and sintered ceramic parts were similar, but with the future raw material costs for ceramics unlikely to be as sensitive to external market influences as those of copper.

SF Rod Disposal. Some unit costs were available. The cost of a carbon steel SF rod disposal canister was estimated to be 150-190kCHF [10]. This compared with estimates of 200-250kCHF for a KBS-3 50mm thick copper container with cast iron insert, and 175-220kCHF for a copper coated (5mm) carbon steel SF canister.

An indicative cost estimate for a full size Ti Gr.7 clad carbon steel SF rod disposal canister without final sealing was 278kCHF. The indicative cost for a full size Alloy C22 clad carbon steel SF rod disposal canister without final sealing was estimated to be ~250kCHF (without final sealing).

The estimated cost of a full size forged and machined Ti Gr.2 canister (without final sealing) was ~338kCHF. Needless to say, that for a full size forged and machined palladium containing Ti Gr.7 canister (without final sealing) was prohibitive (~125,000kCHF).

VHLW Disposal. Indicative unit costs were only available for VHLW disposal canisters without final sealing. For example, for such a condition, the estimated unit cost of a 1.5m long SiC canister was ~25-80kCHF. This compared with that for a 3m long Ti Gr.7 clad carbon steel canister of ~112kCHF and a 3m long solid Ti Gr.2 canister of ~77kCHF.

4 DISCUSSION

Based on the evidence reviewed in this report, feasibility evaluation summaries for each material/canister concept are given in Table 6 and Table 7. These concern the risk assessment categories introduced in Sect. 3 and cross refer to the details contained in Apps. **B** to **J**.

Two types of canister were considered. These were for the disposal of: *i)* a number of spent fuel (SF) rods requiring a length in excess of 4.3m, and *ii)* one (or two) vitrified high level waste (VHLW) cylinders requiring a length in excess of 1.5m (3m), Fig. 4 to Fig. 6, Fig.I 1. The evaluation tables comprise feasibility rankings for a number of sub-categories to the main categories identified in Sect. 3. Where possible, feasibility ranking is quantitative, although in many cases it has had to be qualitative.

4.1 CANISTER CONCEPT FEASIBILITY EVALUATION

A number of canister feasibility evaluations are summarised in Table 6 for SF rod disposal, and in Table 7 for VHLW disposal.

4.1.1 Evaluation Summary

The evaluation summaries cover aspects of the principal canister risk assessment categories covered in the main text and appendices of the report.

4.1.2 SF Rod Disposal

Carbon Steel. The evaluated carbon steel SF rod disposal concept involved a 140m thick canister with an ID of 770mm and a length of 4.6m, Table 6a. The thickness included a 20mm corrosion allowance. This solution had been comprehensively evaluated [10], and shown to be feasible with respect to mechanical integrity (for the assumed load cases), fabrication and cost. The mechanical properties were widely known. The manufacturing, welding and inspection possibilities for large thick section pressure vessels were well established. As such, future development costs were judged to be

minimal, and the unit cost of ~150-190kCHF provided the benchmark against which other solutions could be compared.

The main concerns with the carbon steel concept related to the environmental damage characteristics of the material. Carbon steel was an active corrosion material requiring a significant ruling section allowance. While the corrosion behaviour of carbon steels was relatively well understood in the proposed Swiss repository environment, there were uncertainties associated with very long lifetime predictions, and these were examined in Sect. 3.4.2. By far the biggest concern was the impact on the geological barrier of the hydrogen produced as a by-product of corrosion processes. There was disagreement about the magnitude of the impact, with the main problem being the uncertainties associated with the detail presented by specialists on both sides of the debate.

Copper with Cast Iron Insert. The Scandinavian KBS-3 SF rod disposal concept had been well developed over a number of years (App. **H**, Table 6b), and was generally regarded as an acceptable solution. Nevertheless, there were inevitably uncertainties associated with the very long corrosion lifetime predictions for Cu-OFP, and significant concerns about the material's long time multi-axial creep ductility [41].

Copper Coated Carbon Steel. Two copper coated carbon steel SF rod disposal concepts were evaluated, involving 100mm and 80mm thick canisters with an ID of 770mm and a length of 4.6m (Table 6c). Of the two sizes considered, only the 100mm thick solution was regarded as feasible in terms of mechanical integrity (for the grade of carbon steel evaluated).

Carbon steel canisters and covers were to be electro-deposited with a 3-5mm thick coating, with the final sealing weld to be cold spray coated. The advantage of this canister copper outer layer solution was that there was no reason to consider the risk of creep deformation since complete intimate support was provided by the carbon steel sub-structure. Conceptually, the fabrication technology was proven, but to date had not been repeatably demonstrated on a full scale model. There was therefore still development activity required for proof-of-concept.

Titanium Clad Carbon Steel. Similarly, two titanium clad carbon steel SF rod disposal concepts were evaluated, involving 100mm and 80mm thick canisters with an ID of 770mm and a length of 4.6m (Table 6d). As for the copper coated carbon steel canister, only the 100mm thick solution was regarded as feasible in terms of mechanical integrity (for the grade of carbon steel evaluated).

Of the two main candidate grades of titanium considered for the 3-5mm thick clad solution, Gr.7 was by far the preferred solution in terms of environmental damage resistance, but with a big cost penalty (App. **E**). On the basis of available evidence, Gr.7 was highly resistant to environmental damage, although there were inevitable uncertainties associated with very long time properties.

Thick section titanium clad carbon steel pressure vessels were extensively constructed for petrochemical applications, albeit with the cladding mainly on internal surfaces. There was therefore existing expertise, although it would require further development for this specific application.

Nickel Alloy Clad Carbon Steel. Similarly, two nickel alloy clad carbon steel SF rod disposal concepts were evaluated, involving 100mm and 80mm thick canisters with an ID of 770mm and a length of 4.6m (Table 6e). As for the copper coated carbon steel canister, only the 100mm thick solution was regarded as feasible in terms of mechanical integrity (for the grade of carbon steel considered).

The preferred choice of nickel alloy cladding (3-5mm thickness) was Alloy C22 (App. **F**). This provided a good solution in terms of environmental damage resistance, but with similar very long time property uncertainties. The material cost was significantly lower than that for Ti Gr.7.

Similarly, thick section nickel alloy clad carbon steel pressure vessels were extensively constructed for petrochemical applications, albeit with the cladding mainly on internal surfaces. There was therefore existing expertise, although it would require further development for this specific application.

Ceramics. The strongest candidate ceramic solutions for nuclear waste disposal were Al_2O_3/SiO_2 and SiC. Despite the attraction of such materials in view of their high resistance to environmental damage and associated minimal impact on the geological barrier, it seemed unlikely that challenges relating to

mechanical integrity, and the fabrication of large thick section containers would be overcome in the foreseeable future, in particular with respect to the manufacture of SF rod disposal canisters.

4.1.3 VHLW Disposal

The evaluated VHLW disposal canister concepts were all based on a 50mm thick canister with an ID of 440mm and a length of 1.7m (Table 7).

Copper Coated Carbon Steel. From a fabrication and cost perspective, this copper coated VHLW disposal canister concept (companion to the SF rod disposal concept reviewed above) provided a good solution. The thickness of the carbon steel sub-structure was debatably too thin, not only from a mechanical integrity perspective (Table 7a), but also from the point of view that the dose rate at the outer surface of this container would be of a magnitude which could significantly influence corrosion properties of the copper. The feasibility of such a solution could therefore be enhanced simply by increasing the canister thickness. Indeed, for such a solution, it would make more sense to consider a thicker canister with a length of ~3m, to contain two VHLW cylinders.

The technology involving the deposition of 3-5mm thick defect free copper coatings to very large parts was relatively young, and significant research and development effort was still required for the effectiveness verification of this application.

Titanium Clad Carbon Steel. The issues relating to the feasibility of a titanium clad version of the VHLW disposal canister under consideration were similar to those of the copper coated solution, apart from the very high cost of Gr.7 relative to copper (Table 7b)). Feasibility in terms of environmental damage and fabrication were the same as those for the companion titanium clad SF rod disposal concept reviewed above.

Nickel Alloy Clad Carbon Steel. Similarly, the issues relating to the feasibility of an Alloy C22 clad version of the VHLW disposal canister under consideration were comparable to those of the copper coated solution (Table 7c). The cost of this solution was high compared with the copper coated concept but not compared with the Ti Gr.7 configuration. Feasibility in terms of environmental damage and fabrication were the same as those for the companion nickel alloy clad SF rod disposal concept reviewed above.

Solid Titanium. An alternative to the Gr.7 clad solution could be a solid Ti Gr.2 VHLW disposal canister (Table 7d). For a solid structure, the cost of Gr.2 was less prohibitive, and for thick sections there was an associated added corrosion allowance.

Solid Nickel Alloy. An alternative to the Alloy C22 clad solution could be a solid VHLW disposal canister (Table 7e). The adoption of IN625 (or IN617) could also be considered in standard pipe sections.

Al_2O_3/SiO_2. The main advantage of a ceramic VHLW disposal canister was the negligible risk of hydrogen generation and associated impact on the geological barrier. While manufacture of a 50mm thick canister was feasible [7], the associated mechanical integrity and final sealing viability was low (Table 7f). It had previously been concluded that this type of ceramic solution could be feasible in the future, but only with significant investment and development activity [70].

SiC. Of the ceramic candidates for a VHLW disposal canister material, silicon carbide had emerged as one of the strongest (App. **G**). The mechanical property characteristics of SSiC canisters were superior to those of Al_2O_3/SiO_2, and manufacture of the size of canister under consideration was thought to be just feasible with current technology (Table 7g). Nevertheless, significant investment would be required to produce high integrity canisters in a production environment, and the problem of sealing thick section vessels in a way which did not introduce mechanical integrity and environmental damage risks was far from solved.

There was a debate about which was the most appropriate grade of SiC to adopt for this application, i.e. SiSiC or SSiC (App. **G**). However, the consensus from those specialists who had considered the adoption of silicon carbide as a nuclear waste disposal canister material in detail was that SSiC was the most appropriate grade for the purpose.

4.2 EFFECT OF SECTION SIZE

For the Swiss concept, canister section size was important for a number of reasons. The section dimensions had to be sufficient to ensure the mechanical integrity of the structure, and for a given load case this may be examined in terms of a defect-free plastic-collapse analysis and/or a FAD defect assessment procedure (Apps. **I**,**J**). In terms of a plastic collapse criterion ($\sigma_{VMmax} \leq 1.5.R_{p0.2}$), a carbon steel SF disposal canister with a thickness of ≥ ~90mm would be acceptable (e.g. Fig.I 10), whereas for $\sigma_1/R_{p0.2}$ and CO/CO^{FEA} criteria a lower limiting thickness (≥ ~55mm) appeared to be permissible (e.g. Fig.I 6).

The available evidence indicated that there was no influence of γ-radiation on the corrosion properties of metals for absorbed dose rates of ≤ 1Gy/h [104]. For this reason, it was important that canister section thicknesses were sufficient to limit absorbed dose rate to this level. For carbon steel, this was said to be ~100mm, although the opinion was apparently without substantiation, and considered to be less by others (e.g. [108]). Of the other candidate materials, empirical studies indicated that titanium alloys were the least susceptible to γ-radiation effects, with nickel alloys being the most susceptible, the effect appearing to be inversely related to density. While canister external dose rates were likely to be highest for ceramics, this material class was likely to be the least affected by corrosion related radiation induced phenomena (because of the inherently high resistance of ceramics to environmental damage mechanisms).

At relatively low dose rates (~13-27Gy/h), γ-radiation was said to have a beneficial effect on corrosion rate, but could have a significantly deleterious influence at higher levels ≥~700Gy/h [38].

There appeared not to be a manufacturing size limitation for the metallic solutions considered. However, this was not the case for ceramics (App. **G**). Even the relatively low bending strength and fracture toughness properties associated with this class of materials were dependent on attainment of the highest through-section density. At the current time, ~50mm thickness appeared to be the practical limit to meet this requirement without invoking hot iso static pressing (hipping) as part of the sintering process.

4.3 RECOMMENDATIONS

The canister concept feasibility evaluation led to a number of recommendations.

4.3.1 Material Property Data

While every effort had been made to work with realistic material property characteristics in the study, it was acknowledged that the quantities used in the analyses did not always represent lower bound values for the specified pedigree and product form. It is recommended that once the strongest candidate solutions have been selected, a comprehensive data acquisition programme is established to determine representative property scatterbands for the specified materials in a relevant product form with specimens from multiple suppliers. This must include the characterisation of (welded) joints.

It will be important for such a material property characterisation programme to include a rigorous and focussed environmental damage evaluation study influenced by scientific expertise from both within and outside of the nuclear waste disposal community. There are acknowledged areas of uncertainty, in particular relating to long time property characterisation, and these should be re-examined in a systematic way.

4.3.2 Mechanical Integrity

The observations and conclusions from this report relating to mechanical integrity are very dependent on the details of the disposal load cases proposed by Nagra. It is recommended that the physical reality of these repository scenario boundary conditions are rigorously evaluated by appropriate specialists for Swiss conditions, prior to the execution of a formal design assessment.

Appropriate physically real emplacement and withdrawal handling load cases also need to be defined for Swiss conditions prior to the execution of a formal design assessment.

The mechanical integrity assessments conducted in this report were based on the results of elastic finite element studies of stress state. While this was acceptable for the purposes of this feasibility

evaluation study, it is recommended that a fully non linear elastic approach is adopted for the canister design assessment.

4.3.3 Coated and Clad Carbon Steel Solutions

A number of the considered concepts involved coating or cladding. While conceptually offering advantageous solutions, there were uncertainties associated with the detail for each. Prototype(s) of the strongest candidate solution(s) should be constructed at the earliest opportunity to verify concept viability and fabrication (manufacture/sealing/inspection) feasibility. These could then be used as a source of material in the appropriate product form, on which the basis for representative property characterisation could be established for design assessment.

The strongest candidate solutions appear to be those involving carbon steel, coated (or clad) with a highly corrosion resistant material. Of those evaluated in the report, the most advanced in terms of its state-of-the-art for nuclear waste disposal canister applications is OFP copper coated carbon steel, and this should continue to receive high priority research and development activity to resolve outstanding issues. Nevertheless, it is recommended that a back-up solution is also simultaneously pursued, not least to provide an alternative in the event of a future copper cost/supply crisis. For this, Ni Alloy C22 clad carbon steel is proposed.

4.3.4 Ceramics

Apart from the clear advantages of almost no susceptibility to environmental damage, and no gas generation as a by-product of corrosion (with no consequent impact on the surrounding geological structure), there is not a strong driving force to pursue a ceramic nuclear waste disposal solution. Improvements to the strength and fracture toughness properties, and the developments necessary to attain the required fabrication technology targets (relating to fully dense, larger section vessel manufacture (requiring pressing, green-state handleability and sintering developments), and sealing and inspection), will only happen with significant extermal financial investment. There appear not to be requirements from other industrial sectors for large ceramic parts, and thereby no incentive for the ceramic parts manufacturers to fund the necessary developments for a relatively small quantity of nuclear waste disposal canisters entirely themselves. If it is concluded that a ceramic such as SSiC is to become a strong candidate solution for this application, it is recommended that a significant investment in the necessary research and development is initiated as a matter of urgency. A significant period of time will be required for the necessary research and development.

As for coated and clad carbon steel solutions, if considered to be of interest, prototype canisters should be constructed at the earliest opportunity to verify concept viability and fabrication (manufacture/sealing/inspection) feasibility. However, in the case of a ceramic solution, a more fundamental research and development activity would first be needed. Existing manufacturing capability would have to be up-scaled, the conditions for achieving acceptable density levels in thick section (≥ 50mm thick) parts would have to be established, a technology for reliable and repeatable thick section sealing would have to be devised, and the capability to inspect to the required acceptable defect standard would have to be demonstrated. Following successful prototype construction, the canister could then be used as a source of material in the appropriate product form, on which the basis for representative property characterisation could be established.

5 CONCLUDING REMARKS

A feasibility evaluation study has been made of candidate canister solutions for the disposal of nuclear spent fuel and vitrified high level waste, respectively involving the consideration of nominally 5m long and 1.5 (or 3m) long thick walled containers. Assessment has been based on the consideration of a wide range of factors under four generic headings, i.e. ***mechanical integrity***, ***environmental damage*** (including impact on the geological barrier), ***fabrication***, and ***costs***.

The following observations are inevitably influenced by considerations such as: *i)* the legitimacy of the assumed load cases for the mechanical integrity assessments, *ii)* the reliability of the long-time environmental damage predictions based on almost no direct observations in relevant environmental conditions and the judgements of a relatively small number of specialists serving the nuclear waste disposal community, *iii)* the effectiveness of fabrication feasibility predictions for those concepts without direct practical experience and existing technology, and *iv)* the accuracy of investment and unit cost predictions, in particular for those cases for which the technology currently does not exist.

Carbon steel canisters with an appropriate thickness: *a)* for the required structural strength, with a corrosion allowance, and *b)* to ensure that the radiation level at the external surface is insufficient to influence corrosion resistance, provide a possible nuclear waste disposal solution. There is well established manufacturing and fabrication experience with parts of the required size, and the associated costs are well established. The main concern with this solution relates to the evolution of hydrogen as a by-product of the corrosion process, and the consequent potential impact on the surrounding geological barrier.

The KBS-3 outer thick walled copper container concept was considered because of the vast experience gathered in Scandinavia during the past 30 years. As an alternative to the KBS-3 configuration, copper coated carbon steel canister solutions overcome uncertainties associated with creep of this corrosion barrier, although there are still manufacturing and fabrication details relating to this second copper-based concept to be optimised fit-for purpose.

Nuclear waste disposal canister solutions involving carbon steel clad with titanium or nickel alloy have been evaluated. While both are feasible with existing manufacturing and fabrication technology, there are uncertainties associated with long time environmental damage resistance (due to insufficient existing long time damage data). Moreover, material and fabrication costs are relatively high.

There is a strong incentive to adopt a canister solution with negligible hydrogen production during corrosion, primarily driven by uncertainties relating to the impact of the gas on geological barrier integrity and repository performance. A number of possibilities exist, including the use of ceramics such as Al_2O_3/SiO_2 or SSiC. For such solutions, significant concerns associated with mechanical integrity, large-part manufacture and final-sealing feasibility could conceivably be overcome for the smaller VHLW canisters with appropriate development activity and financial investment. However, it is debatable if the very high level of funding which would be required is justifiable for the relatively low number of canister units ultimately needed, in particular when the successful outcome of such a research and development activity could be by no means assured, and if recommended further investigations (Sect. 4.3) confirm that there are already acceptable alternative solutions. In principle, other possibilities do exist, including coating or cladding a carbon steel sub-structure with a highly corrosive-resistant metal for which the long term rate of hydrogen evolution is so low that it remains dissolved in the pore water, and no gas phase is formed.

In terms of ***mechanical integrity***, ***fabrication*** and ***cost*** assessment categories, carbon steel canisters provide by far the most superior solution for nuclear waste disposal, but seriously suffer from the risk limitations associated with susceptibility to ***environmental damage***. The concerns associated with ***environmental damage*** may be overcome by the coating or cladding of a carbon steel sub-structure with a highly corrosion resistant material for which the long term rate of hydrogen evolution is so low that any gas generated is dissolved in the pore water. Of the three solutions evaluated, copper is potentially the most promising (and advanced, in terms of state-of-the-art), but with future cost and supply uncertainties. Titanium and nickel alloy cladding could provide more effective solutions, but are expensive, and would require fabrication research and development investment to complement what is already known from the petro-chemical industry. A ceramic such as SSiC provides an interesting solution due to its very high resistance to ***environmental damage***, but the risks associated with ***mechanical integrity***, ***fabrication*** state-of-the-art, and (investment) ***costs*** are high.

A number of recommendations are made for further research and development activity relating to candidate canister solutions for the disposal of nuclear spent fuel and high level waste (Sect. 4.3).

6 ACKNOWLEDGEMENTS

The review was conducted in collaboration with a working group involving L Johnson and N Diomidis of Nagra, and F King of Integrity Corrosion Consulting. This report would not have been possible without the invaluable input of these working group members.

The contributions of L Banfi (Loterios), L Hauber (Titan Metal Fabricators), G Coates (Nickel Institute), J Lippmann and M Herrmann (TU-Dresden), J Schmitt and M Rozumek (Haldenwanger), G Wötting and R Simolka (FCT Hartbearbeitungs), and A Kreber and J Knorr (SiCeram) are also gratefully acknowledged.

7 REFERENCES

1 Nagra, 2002, 'Project Opalinus Clay', Safety Report, *Nagra Technical Report 02-05*, Nagra, Wettingen, Switzerland.

2 Johnson, L.H., 2011, 'Development of canisters for disposal of SF and HLW - history, status and requirements', *Nagra presentation*, Nagra, Wettingen, Switzerland.

3 Landolt, D., Davenport, A., Payer, J. & Shoesmith, D.W., 2009, 'A review of materials and corrosion issues regarding canisters for disposal of spent fuel and high-level waste in Opalinus clay', *Nagra Technical Report 09-02*, Nagra, Wettingen, Switzerland.

4 King, F. & Watson, S., 2010, 'Review of the corrosion performance of selected metals as canister materials for UK spent fuel and/or HLW', *Quintessa, QRS-1384J-1, 2.1*.

5 Shoesmith, D.W. & King, F., 1999, 'The effects of gamma radiation on the corrosion of candidate materials for the fabrication of nuclear waste packages', *Atomic Energy of Canada Report AECL-11999*.

6 Johnson, L.H. & King, F., 2003, 'Canister options for the disposal of spent fuel', *Nagra Technical Report 02-11*.

7 Baroux, C., 2013, 'Summary report of the preliminary feasibility study for ceramic HLW overpacks; (2007-2012)', *Andra CG.NT.ASCM.13.0004*.

8 EN 20222-2, 'Steel forgings for pressure purposes. Ferritic and martensitic steels with specified elevated temperature properties', *European Standard*.

9 EN 10293, 'Steel castings for general engineering uses', *European Standard*.

10 Patel, R., Punshon, C., Nicholas, J., Bastid, P, Zhou, R., Schneider, C., Bagshaw, N., Howse, D., Hutchinson, E., Asano, R. & King, F., 2012, ' Canister design concepts for disposal of spent fuel and high level waste', *NAGRA Technical Report NTB 12-06*.

11 Humphries, M.J., McLaughlin, J.E. & Pargeter, R.J., 2009, 'Toughness characteristics of hydrogen charged pressure vessel steels', *Welding Research Council Bulletin, Toughness Fracture and Fitness for Hydrogen Service*, 535, 7-12. ISBN 1581455399 ISSN: 0043-2326.

12 Honda, A., Teshima, T., Tsurudome, K., Ishikawa, H., Yusa, Y. & Sasaki, N., 1991, 'Effect of compacted bentonite on the corrosion behaviour of carbon steel as geological isolation overpack material', Materials Research Society Symposium 212, Pittsburgh (PA), pp. 287-294.

13 Smart, N.R., Blackwood, D.J. & Werme, L.O., 2001, 'Anaerobic corrosion of carbon steel and cast iron in artificial groundwaters', *SKB Technical Report TR01-22.*

14 Kursten, B., Smailos, E., Azkarate, I., Werme, L., Smart, N.R. & Santarini, G., 2004, 'State-of-the-art document on the corrosion behaviour of container materials', EC 5th Euratom Framework Programme, COBECOMA, Contract No. FIKW-CT-20014-20128, Final Report.

15 Johnson, L.H. & King, F., 2008, 'The effect of the evolution of environmental conditions on the corrosion evolutionary path in a repository for spent fuel and high level waste in Opalinus clay', *J. Nucl. Mater.*, 379, 9-15.

16 Yoshikawa, H., Gunji, E., Tokuda, M., 2008, 'Long term stability of iron for more than 1500 years indicated by archaeological samples from the 6th Yamato tumulus', *J. Nucl. Mater.*, 379, 112-117.

17 JNC, 2000, 'H12 project to establish the scientific and technical basis for HLW disposal in Japan', *Japan Nuclear Cycle Development Institute, Supporting Report 2, Repository Design and Engineering Technology.*

18 Simpson, J.P., 1989, 'Experiments on container materials for Swiss high-level waste disposal products', Part IV, *Nagra/Cédra/Cisra Technical Report 89-19, December*.

19 Turnbull, A., 2009, 'A review of the possible effects of hydrogen on lifetime of carbon steel nuclear waste canisters', *Nagra Technical Report NTB 09-04*.

20 Nagra, 2004, 'Effects of post-disposal gas generation in a repository for spent fuel, high level waste, and long-lived intermediate level waste sited in Opalinus Clay', *Nagra Technical Report NTB 04-06.*

21 EN 1563, 'Founding. Spheroidal graphite cast irons', *European Standard*.

22 Werme, L., 2006, 'Current status of SKB's research development and demonstration programme on copper canisters for spent fuel', *Report SKB IC-121.*

23 Raiko, H., Sandström, R., Rydén, H. & Johansson, M., 2010, 'Design analysis report for the canister', *SKB Technical Report TR-10-28*.

24 Martinsson, A., Henrick, CM., Andersson-Östling, HCM., Seitislearn, F., Wu, R. & Sandström, R., 2010, 'Creep testing of nodular iron at ambient and elevated temperatures', *SKB Report R-10-64.*

25 Anderson, CG., Eriksson, P., Westman, M. & Emilsson, G., 2004, 'Status report: Canister fabrication', *Swedish Nuclear Fuel and Waste Management Company Report, SKB TR-04-23.*

26 Koivula, J., Mäkinen, P. & Raiko, H., 2004, 'Further development of the structure and fabrication of the final disposal canister: Fabrication and costs of the canister', *Posiva Working Report 2004-49.*

27 Maak, P., 1999, 'The selection of a corrosion-barrier primary material for used-fuel disposal containers', *Ontario Power Generation, Nuclear Waste Management Division Report 06819-REP-01200-10020-R00*.

28 SKB, 2006, 'Fuel and canister process report for the safety assessment of SR-Can', *Swedish Nuclear Fuel and Waste Management Company Report, SKB TR-06-22*.

29 Keech, P.G., Vo, P., Ramamurthy, S., Chen, J. Jacklin, R. & Shoesmith, D.W., 2014, Design and development of copper coatings for long term storage of used nuclear fuel', *in press*.

30 Li, M. & Zinkle, S.J., 2012, 'Physical and mechanical properties of copper and copper alloys', *Comprehensive Nuclear Materials*, 4, 667-690.

31 Andersson-Österling, HCM & Sandström, R., 2009, 'Survey of creep properties of copper intended for nuclear waste disposal', *SKB TR-09-32, Svensk Kärnbränslehantering AB.*

32 Pettersson, K., 2012, 'A review of the creep ductility of copper for nuclear waste canister application', *SSM TN 2012:13.*

33 King, F., Lilja, C.,Pederson, K., Pitkänen, P & Vähänen, M., 2011, 'An update of the state-of-the-art report on the corrosion of copper under expected conditions in a deep geologic repository', POSIVA 2011-01, also SKB TR 2010-67.

34 Szakalos, P. & Hultquist, G., 2013, 'Copper corrosion and its implications for the KBS-3 concept', *Proc. Symp. on New Insights into the Repository's Engineered Barriers*, Kärnavfallsradet, Stockholm, 20/21.11.13.

35 Hedin, A., Lilja, C. & Johansson, J., 2013, 'Long-term integrity of the KBS-3 canister', *Proc. Symp. on New Insights into the Repository's Engineered Barriers*, Kärnavfallsradet, Stockholm, 20/21.11.13.

36 Scully, J.R. & Edwards, M., 2013, 'Review of the NWMO copper allowance', *NWMO TR-2013-04*.

37 Johnson, A.B. & Francis, B., 1980, 'Durability of metals from archaeological objects, metal meteorites and native metals', *Battelle Pacific Northwest Laboratory, PNL-3198*.

38 King, F., 2002, 'Corrosion of copper in alkaline chloride environments', *Swedish Nuclear Fuel and Waste Management Company Report, SKB TR-02-25*.

39 Bresle, A., Saers, J. & Arrhenius, B., 1983, 'Studies in pitting corrosion on archaeological bronzes', *Swedish Nuclear Fuel and Waste Management Company Report, SKB TR83-05.*

40 Masurat, P., Erikson, S. & Pedersen, K., 2007, ' Microbial sulphide production in compacted Wyoming MX-80 bentonite under in-situ conditions relevant to a repository for high level radioactive waste', *in Proc. Workshop on Long-Term Performance of Smectitic Clays Embedding Canisters with Highly Radioactive Waste*, Lund, 26-28.11.2007.

41 Raiko, H., 2013, 'Canister design 2012', Posiva 2012-13.

42 Yagodzinskyy, Y., Malitckii, E., Saukkonen, T. & Hänninen, H., 2012, 'Hydrogen-enhanced creep and cracking of oxygen-free phosphorus-doped copper', *Scripta Materialia*, 67(12), 931-934.

43 Holdsworth, S.R., 2013, 'Potential material options for nuclear waste disposal containers', *Notes of meeting with Loterios (Banfi. L. & Corti, M.)*, Gerenzano, 8.11.2013.

44 Johnson, L.H., Tait, J.C., Shoesmith, D.W., Crossthwaite, J.L. & Gray, M.N., 1994, 'The disposal of Canada's nuclear fuel waste: Engineered barrier alternatives', *AECL Report. 10718, COG-93-8*, Manitoba, Canada.

45 Gordan, GM., 2006, 'Update on titanium drip shield', *Proc. Nickel Institute Workshop 6*, Los Vegas, 5-6.4.2006.

46 Hegedues, F., Brütsch, R., Oliver, B. & Marmy, P., 2004, 'Fracture toughness and tensile properties of the titanium alloys Ti6Al4V and Ti5Al2.5Sn before and after proton and neutron irradiations at 150°C', *EFDA Task TWI-TVV/Titan & TW3-TVM-TICRFA Report*, Centre de

Recherche en Physique des Plasmas, Technologie de la Fusion, Association Euratom-Confédération Suisse, EPFL, 5232 Villigen, PSI Switzerland.

47 Anon, 2000, 'Titanium alloy guide', RMITitanium Company Data Sheet, *www.RMITitanium.com.*

48 Hua, F., Mon, K., Pasupathi, P., Gordon, G. & Shoesmith, D., 2005, 'A review of corrosion of titanium grade 7 and other titanium alloys in nuclear waste repository environments', Corrosion, 61, 987-1003.

49 Mattsson, H. & Olefjord, I., 1990, 'Analysis of oxide formed on Ti during exposure in bentonite clay, I The oxide growth', *Werk. Korros.*, 41, 383-390.

50 Little, B.,Wagner, P. & Mansfeld, F., 1991, 'Microbiologically influenced corrosion of metals and alloys', *Int. Mater. Rev.*, 36, 253-272.

51 DOE, 2008, 'Yucca mountain repository license application', *US Dept. of Energy, DOE/RW-0573.*

52 Toyota, M. and McKinley, I., 1998, 'Optimisation of the engineered barrier systems for vitrified HLW: Fabrication and emplacement', *in Proc. 8th Intern. Conf. on High Level Radioactive Waste* Management, American Nuclear Society, Las Vegas, 11-14.May-1998, pp.648-652.

53 Coates, G., 2013, 'Overview of Nickel Institute perspective on DOE Contract DE-AC28-01RW12101', *Private communication*, 21.11.2013.

54 Holdsworth, S.R, 2013, 'Potential material options for nuclear waste disposal containers', Unpublished *notes of meeting with Titan Metal Fabricators (Haubner. L.)*, Mannheim, 11.11.2013.

55 Holdsworth, S.R. & Cunnane, D.J., 2008, 'High temperature fracture toughness properties of Alloy-625', *OMMI*, 5(1), 1-13.

56 Anon, 'Hastelloy C-22 alloy', *Haynes Corrosion Resistant Alloys Data Sheet*, Haynes International.

57 San Marchi, C. & Somerday, B.P., 2008, 'Technical reference on hydrogen compatibility of materials', *Sandia National Laboratory Report SAND2008-1163*.

58 Smailos, E., Fiehn, B., Gago, J.A. & Azkarate, I., 1994, 'Corrosion studies on selected metallic materials for application in nuclear waste disposal containers', *Kernforschungszentrum Karlsruhe, Institut für Nukleare Entsorgungstechnik, KfK 5309*.

59 Dunn, D.S., Pan, Y.M., Chiang, K.T, Yang, L., Cragnolino, G.A. & He, X., 2005, 'The localised corrosion resistance of Alloy 22 waste package outer containers', *JOM*, January, 49-55.

60 Marcus, P., 1995, 'Sulfur-assisted corrosion mechanisms and the role of alloyed elements', in Corrosion Mechanisms in Theory and Practice, eds. Marcus, P. & Oudar, J., Marcel Decker (New York), pp. 239-263.

61 Cragnolino, G. et al, 1999, 'Assessment of performance issues related to alternate engineered barrier system materials and design options', *Centre for Nuclear Waste Regulatory Analysis Report, CNWRA 1999-03*.

62 Brossia, S., Browning, L., Dunn, D.S., Moghissi, O.C., Pensado, O. & Yang, L., 2001, 'Effect of environment on the corrosion of waste package and drip shield materials', *Centre for Nuclear Waste Regulatory Analysis Report CNWRA 1999-003*.

63 Farmer, J. et al., 2000, 'General and localised corrosion of outer barrier of high level waste container in Yucca mountain', *Proc. Transportation, Storage & Disposal of Radioactive Materials - 2000*, PVP-Vol 408 (ASME, New York), pp. 53-69.

64 Gordon, G.M., 2006, 'Update on waste package materials selection, heat treatment and degradation modes', *Proc. Nickel Institute Workshop 6*, Los Vegas, 5-6.4.2006.

65 Smith, L., 2012, 'Engineering with clad steel', Nickel Institute Technical Series No. 0064

66 Mattson, E., 1980, 'Aluminium oxide as the encapsulation material for unreprocessed nuclear fuel waste-evaluation from the viewpoint of corrosion', *Swedish Corrosion Institute, Final Report KBS 80-15*.

67 Anon., 1980, 'Comparison of the various alternative shielding methods and evaluation of their practicability', *KfK 3000*, Nuclear Research Centre, Karlsruhe Sept-1980.

68 Bienek, H., Finkbeiner, R. & Wick, W., 1984, 'Container closure means for storage of radioactive material', *US Patent 4,437,578*, March-1984.

69 Adams, J., Cowgill, M., Moskowitz, P. & Rokhvarger, A.E., 2000, 'Effect of radiation on spinel ceramics for permanent containers for nuclear waste transportation and storage', *BNL Report BNL-67518*, Brookhaven National Laboratory, Upton NY.

70 Holdsworth, S.R., 2013, 'Ceramic material solutions for nuclear waste disposal canisters', *Nagra Arbeitsbericht NAB 12-45.*

71 Wötting, G. & Martin, W., 2007, 'Large sized, complex shaped sintered silicon carbide components with excellent mechanical properties', *Proc. 10th ECerS Conf.*, Baden-Baden, 1067-1070.

72 Kerber, A. & Knorr, J., 2013, 'SiC encapsulation of high level waste for long-term immobilization', *atw 58. Jg Heft 1*, January, 8-13.

73 Wilfinger, KR., 1994, 'Ceramic package fabrication for YMP nuclear waste disposal', *Report No. UCRL-ID-118660*, Lawrence Livermore National Laboratory.

74 Linsmeier, K-D., 2011, 'Technical ceramics: The material of choice for the most demanding applications', *Süddeutscher Verlag onpact GmbH*, Munich.

75 Knorr, J., Lippmann, W., Reinecke, A-M., Wolf, R., Kerber, A. & Wolter, A., 2008, 'SiC encapsulation of (V)HTR components and waste by laser beam joining of ceramics', *Nuclear Engineering & Design*, 238, 3129-3135.

76 Martin, W. & Wötting, G., 2014, 'Company profile of FCT Hartbearbeitungs GmbH', Presentation, 3.6.2014, Movenpick, Nürnberg.

77 Holdsworth, SR., 2014, 'SiC canister sealing and manufacturing feasibility', Unpublished *notes of meetings with TU Dresden (Lippmann, W & Herrmann, M) and SiCeram, Jena (Kerber, A & Knorr, J)*, 18-19/6/2014.

78 Wötting, G., 2014, 'Ceramic container enquiry', FCT Hartbearbeirungs, *private communication*.

79 Onofrei, M., Raine, D.K., Brown, L. & Stanchell, F., 1985, 'Leaching studies of non-metallic materials for nuclear fuel immobilisation containers', *Proc. Mat. Res. Soc. Symp.*, Materials Research Society, pp. 395-404.

80 Kübler, J. & Berroth, K., 1996, 'Bestimmung unterkritischer Risswachstums-Parameter', EMPA, Abt.123 Bericht-Nr. 150960.

81 Andrews, A., Herrmann, M., Sephton, M., Machio, Chr. & Michaelis, A., 2007, 'Electrochemical corrosion of solid and liquid phase sintered silicon carbide in acidic and alkaline environments', *J. European Ceramics Society*, 27, pp. 2127-2135.

82 Schneider, M., Kremmer, K., Lämmel, C., Sempf, K. & Herrmann, M., 2014, 'Galvanic corrosion of metal/ceramic coupling', *Corrosion Science*, 80, pp. 191-196.

83 Lippmann, W., 2014, 'Laser based joining of ceramic materials, TU Dresden', AN 14-063 *Notes of 4th Nagra-Empa Project meeting*, Empa, 24.Jan.

84 Haslam, J.J., Farmer, J.C., Hopper, R.W. & Wilfinger, K.R., 2005, 'Ceramic coatings for corrosion resistant nuclear waste container evaluated in simulated ground water at 90ºC', *Metallurgical and Materials Transactions A,* 36A, May, 1085-1095.

85 Kim, J. & Liaw, P.K, 1998, 'The nondestructive evaluation of advanced ceramics and ceramic-matrix composites', *JOM*, 50(11).

86 Schmitt, J. & Rozumek, M., 2014, 'SiC container enquiry', Technical Ceramics - Haldenwanger, Morgan Advanced Materials, 20.5.2014.

87 Murakami, Y., *Stress Intensity Handbook*, a) Vols 1 & 2, Pergamon Press, Oxford (1987), b) Vol 3, Japan Soc. Mat. Sci., Kyoto, (1992).

88 Al Laham, S., 1998, 'Stress intensity factor and limit load handbook', *British Energy Generation Ltd SINTAP Report*, Issue 2.

89 BS 7910, 2013, 'Guide on methods for assessing the acceptability of flaws in metallic structures', *British Standards Institution*.

90 Miller, AG., 1988, 'Review of limit loads of structures containing defects', *Pressure Vessels & Piping*, 32, 191-327.

91 R6 Panel, 2001, *Assessment of the Integrity of Structures Containing Defects*, Revision 4 (as amended), EDF Energy.

92 Izatt, C., 2012, 'Development of standardized disposal canister designs for legacy spent fuel and HLW', Final Design Report, *Arup Rep. 218762-01-03*, 13.June.

93 Ho, Y.H., 2012, 'Extraction of stress analysis results of carbon steel HLW/SF disposal canister to support long-term evolution evaluation', *Arup Rep. 218762-08-01*, 6.December.

94 Bastid, P. & Blackwell, S., 2014, 'Finite element stress analysis of a 140mm wall thickness spent fuel canister under variable self-balancing swelling pressure', unpublished *TWI Report 23705/3/14, March*.

95 Bastid, P. & Blackwell, S., 2014, 'Finite element stress analysis of a 100mm wall thickness spent fuel canister under variable self-balancing swelling pressure', unpublished *TWI Report 23705/4/14, December*.

96 Bastid, P. & Blackwell, S., 2014, 'Finite element stress analyses of a copper coated 3 BWR spent fuel canister under circumferentially and longitudinally variable swelling pressure', unpublished *TWI Report 23705/1/14, January*.

97 Bastid, P. & Blackwell, S., 2014, 'Finite element analyses of nuclear waste canister under non-uniform self-balanced swelling pressure', unpublished *TWI Report 23705/2/14*, *February.*

98 Bastid, P. & Blackwell, S., 2014, 'Finite element analyses of a copper-coated 3 BWR spent fuel canister under variable self-balanced swelling pressure', unpublished *TWI Report 23707/5/14, April*.

99 Mazza, E., 2014, 'Simple analytical expression relating nuclear waste disposal container axial stress to wall thickness', *private communication*.

100 ASME VIII Boiler and Pressure Vessel Code, Division 2: Alternative Rules for Pressure Vessels.

101 King, F., 2009, 'Microbiologically influenced corrosion of nuclear waste containers', *Corrosion NACE*, 65(4), 233-251.

102 Stroes-Gascoyne, S., Hamon, C.J., Dixon, D.A., Kohle, C. & Maak, P., 2007, 'The effects of dry density and porewater salinity on the physical and microbiological characteristics of highly compacted bentonite', *in Scientific Basis for Nuclear Waste Management XXX*, Dunn, D., Poinssot, C. & Begg, B. (eds), Material Research Society Symposium Proceedings 985, Warrendale (PA), paper 0985-NN13-02.

103 Holdsworth, S.R., 2002, 'Status of prediction and prevention of corrosion fatigue and stress corrosion cracking in LP steam turbines', *Power Plant Chemistry,* 4(4), pp. 197-208.

104 King, F., 2014, 'Review of radiation effects on container materials', AN 14-063 *Notes of 4th Nagra-Empa Project meeting*, Empa, 24.Jan.

105 ISO 6303, 1981, 'Pressure vessel steels not included in ISO 2604, Parts 1 to 6 - Derivation of long time stress rupture properties', Annex, *International Standards Organisation*.

106 King, F., 2014, 'Predicting the lifetimes of nuclear waste containers', *JOM*, 66(3), 526-537.

107 Miller, B., Hooker, P., Smellie, J., Dalton, J., Degnan, P., Knight, L., Nosek, U., Ahonen, L., Laciok, A., Trotignon, L., Wooters, L., Hernan, P. & Vela, A., 2006, 'Network to review natural analogue studies and their application to repository safety assessment and public communication (NAnet)', *European Community Report EUR 21919*.

108 Smart, N.R., Rance, A.P. & Werme, L.O., 2008, 'The effect of radiation on the anaerobic corrosion of steel', *J. Nuclear Materials*, 379, 97-104.

8 TABLES

Table 1 Compositions of Opalinus Clay and Bentonite Pore Waters [3]

			Maximum expected variation	
	Opalinus Clay reference water	**Bentonite reference water**	**Bentonite low pH**	**Bentonite high pH**
pH log pCO_2 [bar]	7.24 -2.2	7.25 -2.2	6.90 -1.5	7.89 -3.5
Ionic strength [eq/L]	2.28×10^{-1}	3.23×10^{-1}	3.65×10^{-1}	2.63×10^{-1}
CO_3	2.70×10^{-3}	2.83×10^{-3}	6.99×10^{-3}	5.86×10^{-4}
Na	1.69×10^{-1}	2.74×10^{-1}	2.91×10^{-1}	2.49×10^{-1}
Ca	1.05×10^{-2}	1.32×10^{-2}	1.33×10^{-2}	1.34×10^{-2}
Mg	7.48×10^{-3}	7.64×10^{-3}	8.91×10^{-3}	6.15×10^{-3}
K	5.65×10^{-3}	1.55×10^{-3}	1.67×10^{-3}	1.38×10^{-3}
SO_4	2.40×10^{-2}	6.16×10^{-2}	6.39×10^{-2}	5.59×10^{-2}
Cl	1.60×10^{-1}	1.66×10^{-1}	2.06×10^{-1}	8.61×10^{-2}
Fe	4.33×10^{-5}	4.33×10^{-5}	7.74×10^{-5}	8.00×10^{-6}
Al	2.17×10^{-8}	1.92×10^{-8}	1.53×10^{-8}	7.55×10^{-8}
Si	1.78×10^{-4}	1.80×10^{-4}	1.80×10^{-4}	1.84×10^{-4}

Table 2 Summary of General Corrosion Properties

	Short Time (aerobic)	Long Time (anaerobic)	Comments
Carbon Steel	150μm [3] ~100μm [4] 10μm/a [12]	1-2μm/a [3,4] 0.1-1.0μm/a [14]	*Short-time aerobic corrosion judged to occur at a rate of 10μm/a to a maximum of 150μm*
Copper (OFP)	100μm [4] 0.1-1mm [33]	~0 [4] <0.001μm/a [33]	*In absence of sulphide* *More in presence of sulphide*
Titanium Gr.2, Gr.7	<0.02μm/a [48] ~0 [44]	~0.001μm/a [49]	
Nickel Alloy C22 IN625 (IN617)	~0 ~0	<0.02μm/a [14,51] ~0.2μm/a [58] ~0.2μm/a [58]	*$MgCl_2$ rich brine* *$MgCl_2$ rich brine*
Ceramics Al_2O_3/SiO_2 SiC	~0 ~0	~0 ~0	*Does not corrode, but vulnerable to leaching of SiO_2 [7]* *Negligible general corrosion rate for SSiC, but SiSiC vulnerable to leaching*

Table 3 Summary of Localised Corrosion Properties (pitting, crevice corrosion, intergranular attack)

	E_{CORR}/E_{PIT}	E_{CORR}/E_{CREV}	IGA	Comments
Carbon Steel	<1	<1	N [4]	*Likely to undergo surface roughening rather than discrete pitting or crevice corrosion [4]*
Copper (OFP)	<1	<1 [33]	N [4]	*Likely to undergo surface roughening rather than discrete pitting or crevice corrosion. Crevice corrosion self-limiting [4]*
Titanium Gr.2 Gr.7	<1 [14,44] <1	>1 <1	N [4] N [4]	*Gr.2 not immune to crevice corrosion, but self-limiting [4]* *Immune to pitting and crevice corrosion [4]*
Nickel Alloy C22 IN625 (IN617)	<1 <1	<1 <1	N [4] N [4]	*Immune to pitting and crevice corrosion [4]*
Ceramics Al_2O_3/SiO_2 SiC			Y Y	*IGA: ~0.1μm/a [58]* *Severe IGA [58]*

Table 4 Environmental Cracking Properties

	STRESS CORROSION CRACKING	HYDROGEN INDUCED CRACKING
Carbon Steel	*Not susceptible in repository conditions except at stresses of yield point magnitude [4,18]*	*Potentially susceptible, but unlikely under repository conditions, in particular for low $R_{p0.2}$ grades [19].* *Could be a risk for non PWHT HAZ microstructures; assume $K/K_{1HIC} < 0.8$ [19]*
Copper (OFP)	*Susceptible in certain environments, but unlikely in repository conditions [4]*	*Generally regarded as not susceptible in repository conditions [4], but with reservations [42]*
Titanium Gr.2 Gr.7	 *Unlikely in repository conditions [14]* *Immune*	 *May be susceptible* *Not susceptible [48]*
Nickel Alloy C22 IN625 (IN617)	 *Immune under repository conditions [14]* *Immune under repository conditions [14]*	 *Relatively immune[64]* *Relatively immune[64]*
Ceramics Al_2O_3/SiO_2 SiC	 *Can be susceptible [80].* *Not susceptible to SCC*	 *Immune to HIC* *Immune to HIC*

In Table 6 and Table 7, the likelihoods of SCC and HIC are respectively indicated by $\sigma_{1,max}/R_{SCC}$ and $K_{1,max}/K_{1HIC}$ ratios. For low strength metallic solutions, it is assumed that $R_{SCC} \cong R_{p0.2min}$ when R_{SCC} is not known. Similarly, it is assumed that $K_{1HIC} \cong K_{1Cmin}$ when K_{1HIC} is not known

Table 5 Indicative Material Costs

Material	Indicative Cost¥ CHF/kg	*Relative Cost (by-weight) 1/(CHF/kg)^{CS}*	*Density g/cc*	*Relative Cost (by-volume) 1/(CHF/cc)^{CS}*
Carbon Steel (cs)	0.7	*1*	7.9	*1*
Cast Iron	1.5	*2*	7.1	*2*
Copper (OFP)	8	*11*	8.9	*13*
Titanium				
Ti Gr.2	30	*43*	4.5	*24*
Ti Gr.7	115	*164*	4.5	*94*
Ti Gr.12	50	*71*	4.5	*41*
Ti Gr.5	60	*86*	4.4	*48*
Nickel	24	*34*	8.9	*39*
Alloy C22	46	*66*	8.6	*72*
IN625 (IN617)	30	*43*	8.4	*46*
Ceramic				
Al_2O_3	10-20	*14-28*	3.8	*7-14*
SiC	10-20	*14-28*	3.1	*6-12*

¥ *Indicative (very) for simple plate product form (like-with-like comparison not possible)*

Table 6a Feasibilty Evaluation Summary for Carbon Steel SF Canister Concept for a Repository in Opalinus Clay (4.6m long, 770mm ID, 140/120mm thick)

Assessment Category	Sub-Category	Condition(s)	Desirable Features	Indicator(s)	Criteria	Quantities	Sect. in report	Feasibility
Mechanical Integrity	Handling	*tbd*	Damage tolerance (deformation/fracture)	$CO/CO^{FAE}(2mm)$	≤ 1.00			
	Disposal (short time)	P ≤ 6/1MPa (TWI-5 load case)	Acceptable structural integrity during aerobic phases	$\sigma_{VM,max}/R_{p0.2,min}$	≤ 1.50	0.29	App. **I**	High
				$CO/CO^{FAE}(2mm)_{max}$	≤ 1.00	0.21	App. **J**	High
	Disposal (long time)	P ≤ 29/22MPa (TWI-2 load case)	Acceptable structural integrity during anaerobic phase	$\sigma_{VM,max}/R_{p0.2,min}$	≤ 1.50	0.98	App. **I**	High
				$CO/CO^{FAE}(2mm)_{max}$	≤ 1.00	0.00	App. **J**	High
	Creep	*n/a*		$\varepsilon_C/\varepsilon_R$	< 1.00	-		High
Environmental Damage	General corrosion	Active material	Low and/or predictable rate of general corrosion	Anaerobic d*x*/d*t*	≤ 2μm/a	1-2μm/a [4]	App. **B**	High
		Passive material		Anaerobic d*x*/d*t*	≤ 0.02μm/a	*n/a*		
	Local/crevice/IG corrosion		Low susceptibility to:					
			- pitting	Y/N	Y	Y	App. **B**	High
			- crevice corrosion	Y/N	Y	Y	App. **B**	High
			- IGA	Y/N	Y	Y	App. **B**	High
	MIC		Low susceptibility to MIC	Y/N	Y	Y	App. **B**	High
	SCC/HIC		Low susceptibility to					
			- SCC	$\sigma_{1,max}/R_{SCC}$	≤ 0.80	≤~0.30	App. **B**	High
			- HIC	$K_{1a,max}/K_{1HIC}$	≤ 0.80	≤~0.15	App. **B**	Medium
Impact on geological barrier	Gas production		Low rate of H_2 production	Equivalent anaerobic CS corrosion rate	≤ 10μm/a	< 10μm	App. **B**	Medium
	Effect on buffer,		Effect on Bentonite buffer	Y/N	N	?	App. **B**	Medium/low
	host rock		Effect on host rock	Y/N	N	?	App. **B**	Medium/low

Assessment Category	Sub-Category	Condition(s)	Desirable Features	Indicator(s)	Criteria	Quantities	Sect. in report	Feasibility
Fabrication	Manufacture of canister body	SF	Involves current proven technology	Y/N	Y	Y	App. **B**	High
	Sealing		Involves current proven technology	Y/N	Y	Y	App. **B**	High
			Procedure can be performed remotely	Y/N	Y	Y	App. **B**	High
			- in radiation field	Y/N	Y	Y	App. **B**	High
			Sealing and PSHT temperatures do not exceed SF limit	T/400°C	≤ 1	Y	App. **B**	Medium
	Inspectability		Procedures can be performed remotely	Y/N	Y	Y	App. **B**	High
			- in radiation field	Y/N	Y	Y	App. **B**	High
			Material amenable to inspection	Y/N	Y	Y	App. **B**	High
Costs	Development costs		Involves currently available technology	Y/N	Y	Y	App. **B**	High
	Unit costs		Inexpensive raw materials	$(CHF/cc)^{mat}/(CHF/cc)^{cs}$	≤ 2	1	App. **B**	High
			Estimated unit cost	$kCHF/(kCHF)^{cs}$	≤ 1.3	1	App. **B**	High
			Multiple potential suppliers	N_{sup}	≥ 2xN_{sup}	Y	App. **B**	High

Table 6b Feasibilty Evaluation Summary for Copper (with cast iron insert) KBS-3 SF Canister Concept for a Repository in Opalinus Clay

Assessment Category	Sub-Category	Condition(s)	Desirable Features	Indicator(s)	Criteria	Quantities	Sect. in report	Feasibility
Mechanical Integrity	Handling	*tbd*	Damage tolerance (deformation/fracture)	$CO/CO^{FAE}(2mm)$	≤ 1.00			
	Disposal (short time)	P ≤ 6/1MPa (TWI-5 load case)	Acceptable structural integrity during aerobic phases	$\sigma_{VM,max}/R_{p0.2,min}$	≤ 1.50		App. **H**	High
				$CO/CO^{FAE}(2mm)_{max}$	≤ 1.00		App. **H**	High
	Disposal (long time)	P ≤ 29/22MPa (TWI-2 load case)	Acceptable structural integrity during anaerobic phase	$\sigma_{VM,max}/R_{p0.2,min}$	≤ 1.50		App. **H**	High
				$CO/CO^{FAE}(2mm)_{max}$	≤ 1.00		App. **H**	High
	Creep			$\varepsilon_C/\varepsilon_R$	< 1.00		App. **H**	Medium
Environmental Damage	General corrosion	Active material	Low and/or predictable rate of general corrosion	Anaerobic dx/dt	≤ 0.02μm/a	≤ 0.002μm/a	App. **D** App. **H**	High
		Passive material		Anaerobic dx/dt	≤ 0.02μm/a	*n/a*		
	Local/crevice/IG corrosion		Low susceptibility to:					
			- pitting	Y/N	Y	Y	App. **D**	High
			- crevice corrosion	Y/N	Y	Y	App. **D**	High
			- IGA	Y/N	Y	Y	App. **D**	High
	MIC		Low susceptibility to MIC	Y/N	Y	Y	App. **D**	High
	SCC/HIC		Low susceptibility to					
			- SCC	$\sigma_{1,max}/R_{SCC}$	≤ 0.80	~0	App. **D**	High
			- HIC	$K_{1a,max}/K_{1HIC}$	≤ 0.80	~0	App. **D**	High
Impact on geological barrier	Gas production		Low rate of H_2 production	Equivalent anaerobic CS corrosion rate	≤ 10μm/a	~0	App. **D**	High
	Effect on buffer,		Effect on Bentonite buffer	Y/N	N	N	App. **D**	High
	host rock		Effect on host rock	Y/N	N	N	App. **D**	High

This feasibility evaluation summary relies on the existing evidence provided by a number of SKB and Posiva reports

Assessment Category	Sub-Category	Condition(s)	Desirable Features	Indicator(s)	Criteria	Quantities	Sect. in report	Feasibility
Fabrication	Manufacture of canister body	SF	Involves current proven technology	Y/N	Y	Y	App. **H**	High
	Sealing		Involves current proven technology	Y/N	Y	Y	App. **H**	High
			Procedure can be performed remotely	Y/N	Y	Y	App. **H**	High
			- in radiation field	Y/N	Y	Y	App. **H**	High
			Sealing and PSHT temperatures do not exceed SF limit	*T*/400°C	≤ 1	*n/a*	App. **H**	High
	Inspectability		Procedures can be performed remotely	Y/N	Y	Y	App. **H**	High
			- in radiation field	Y/N	Y	Y	App. **H**	High
			Material amenable to inspection	Y/N	Y	Y	App. **H**	High
Costs	Development costs		Involves currently available technology	Y/N	Y	Y	App. **H**	High
	Unit costs		Inexpensive raw materials	$(CHF/cc)^{mat}/(CHF/cc)^{cs}$	≤ 2	13		Medium
			Estimated unit cost	$kCHF/(kCHF)^{cs}$	≤ 1.3	~1.3	App. **H**	High/medium
			Multiple potential suppliers	N_{sup}	≥ $2N_{sup}$	Y	App. **H**	High/medium

This feasibility evaluation summary relies on the existing evidence provided by a number of SKB and Posiva reports

Table 6c Feasibilty Evaluation Summary for Copper Coated Carbon Steel SF Canister Concept for a Repository in Opalinus Clay (4.6m long, 770mm ID, 100mm/5mm-Cu thick)

Assessment Category	Sub-Category	Condition(s)	Desirable Features	Indicator(s)	Criteria	Quantities	Sect. in report	Feasibility
Mechanical Integrity	Handling	*tbd*	Damage tolerance (deformation/fracture)	CO/CO^{FAE}(2mm)	≤ 1.00			
	Disposal (short time)	P ≤ 6/1MPa (TWI-5 load case)	Acceptable structural integrity during aerobic phases	$\sigma_{VM,max}/R_{p0.2,min}$ *100mm* $\sigma_{VM,max}/R_{p0.2,min}$ *80mm*	≤ 1.50	0.40 0.54	App. **I**	High High
				$CO/CO^{FAE}(2)_{max}$ *100mm* $CO/CO^{FAE}(2)_{max}$ *80mm*	≤ 1.00	0.14 0.14	App. **J**	High High
	Disposal (long time)	P ≤ 29/22MPa (TWI-2 load case)	Acceptable structural integrity during anaerobic phase	$\sigma_{VM,max}/R_{p0.2,min}$ *100mm* $\sigma_{VM,max}/R_{p0.2,min}$ *80mm*	≤ 1.50	1.20 1.69	App. **I**	High Medium/low
				$CO/CO^{FAE}(2)_{max}$ *100mm* $CO/CO^{FAE}(2)_{max}$ *80mm*	≤ 1.00	0.28 0.44	App. **J**	High High
	Creep	*n/a*		$\varepsilon_C/\varepsilon_R$	< 1.00		App. **D**	High
Environmental Damage	General corrosion	Active material Passive material	Low and/or predictable rate of general corrosion	Anaerobic d*x*/d*t* Anaerobic d*x*/d*t*	≤ 0.02μm/a ≤ 0.02μm/a	≤ 0.002μm *n/a*	App. **D**	High/medium
	Local/crevice/IG corrosion		Low susceptibility to: - pitting - crevice corrosion - IGA	 Y/N Y/N Y/N	 Y Y Y	 Y Y Y	 App. **D** App. **D** App. **D**	 Medium High High
	MIC		Low susceptibility to MIC	Y/N	Y	Y	App. **D**	High
	SCC/HIC		Low susceptibility to: - SCC - HIC	 $\sigma_{1,max}/R_{SCC}$ $K_{1a,max}/K_{1HIC}$	 ≤ 0.80 ≤ 0.80	 <<0.6 ≤~0.01	 App. **D** App. **D**	 High High
Impact on geological barrier	Gas production		Low rate of H_2 production	Equivalent anaerobic CS corrosion rate	≤ 10μm/a	~0	App. **D**	High
	Effect on buffer,		Effect on Bentonite buffer	Y/N	N	N	App. **D**	High
	host rock		Effect on host rock	Y/N	N	N	App. **D**	High

Mechanical integrity data for 80mm thick carbon steel sub-structure also included for information

Assessment Category	Sub-Category	Condition(s)	Desirable Features	Indicator(s)	Criteria	Quantities	Sect. in report	Feasibility
Fabrication	Manufacture of canister body	SF	Involves current proven technology	Y/N	Y	Y	App. **D**	High/medium
	Sealing		Involves current proven technology	Y/N	Y	Y	App. **D**	High/medium
			Procedure can be performed remotely	Y/N	Y	Y	App. **D**	High
			- in radiation field	Y/N	Y	Y	App. **D**	High
			Sealing and PSHT temperatures do not exceed SF limit	T/400°C	≤ 1	Y	App. **D**	High
	Inspectability		Procedures can be performed remotely	Y/N	Y	Y	App. **D**	High
			- in radiation field	Y/N	Y	Y	App. **D**	High
			Material amenable to inspection	Y/N	Y	Y	App. **D**	High
Costs	Development costs		Involves currently available technology	Y/N	Y	Y	App. **D**	High/medium
	Unit costs		Inexpensive raw materials	$(CHF/cc)^{mat}/(CHF/cc)^{cs}$	≤ 2	13	App. **D**	Medium
			Estimated unit cost	$kCHF/(kCHF)^{cs}$	≤ 1.3	~1.3	App. **D**	High/medium
			Multiple potential suppliers	N_{sup}	≥ $2N_{sup}$	Y	App. **D**	Medium

Table 6d Feasibilty Evaluation Summary for Ti (Gr.7) Clad Carbon Steel SF Canister Concept for a Repository in Opalinus Clay (4.6m long, 770mm ID, 100mm/5mm-Ti thick)

Assessment Category	Sub-Category	Condition(s)	Desirable Features	Indicator(s)	Criteria	Quantities	Sect. in report	Feasibility
Mechanical Integrity	Handling	*tbd*	Damage tolerance (deformation/fracture)	CO/CO^{FAE}(2mm)	≤ 1.00			
	Disposal (short time)	P ≤ 6/1MPa (TWI-5 load case)	Acceptable structural integrity during aerobic phases	$\sigma_{VM,max}/R_{p0.2,min}$ *100mm* $\sigma_{VM,max}/R_{p0.2,min}$ *80mm*	≤ 1.50	0.40 0.54	App. **I**	High High
				$CO/CO^{FAE}(2)_{max}$ *100mm* $CO/CO^{FAE}(2)_{max}$ *80mm*	≤ 1.00	0.30 0.39	App. **J**	High High
	Disposal (long time)	P ≤ 29/22MPa (TWI-2 load case)	Acceptable structural integrity during anaerobic phase	$\sigma_{VM,max}/R_{p0.2,min}$ *100mm* $\sigma_{VM,max}/R_{p0.2,min}$ *80mm*	≤ 1.50	1.20 1.69	App. **I**	High Medium/low
				$CO/CO^{FAE}(2)_{max}$ *100mm* $CO/CO^{FAE}(2)_{max}$ *80mm*	≤ 1.00	0.10 0.37	App. **J**	High High
	Creep	*n/a*		$\varepsilon_C/\varepsilon_R$	< 1.00			
Environmental Damage	General corrosion	Active material Passive material	Low and/or predictable rate of general corrosion	Anaerobic d*x*/d*t* Anaerobic d*x*/d*t*	≤ 0.02μm/a ≤ 0.02μm/a	*n/a* ~0.001μm/y	App. **E**	High
	Local/crevice/IG corrosion		Low susceptibility to: - pitting - crevice corrosion - IGA	 Y/N Y/N Y/N	 Y Y Y	 Y Y Y	 App. **E** App. **E** App. **F**	 High High High
	MIC		Low susceptibility to MIC	Y/N	Y	Y	App. **E**	High
	SCC/HIC		Low susceptibility to: - SCC - HIC	 $\sigma_{1,max}/R_{SCC}$ $K_{1a,max}/K_{1HIC}$	 ≤ 0.80 ≤ 0.80	 ≤~0.34 ≤~0.21	 App. **E** App. **E**	 High/medium High/medium
Impact on geological barrier	Gas production		Low rate of H_2 production	Equivalent anaerobic CS corrosion rate	≤ 10μm/a	~0	App. **E**	High
	Effect on buffer,		Effect on Bentonite buffer	Y/N	N	N	App. **E**	High
	host rock		Effect on host rock	Y/N	N	N	App. **E**	High

Mechanical integrity data for 80mm thick carbon steel sub-structure also included for information

Assessment Category	Sub-Category	Condition(s)	Desirable Features	Indicator(s)	Criteria	Quantities	Sect. in report	Feasibility
Fabrication	Manufacture of canister body	SF	Involves current proven technology	Y/N	Y	Y	App. **E**	High
	Sealing		Involves current proven technology	Y/N	Y	Y	App. **E**	High
			Procedure can be performed remotely	Y/N	Y	Y	App. **E**	High
			- in radiation field	Y/N	Y	Y	App. **E**	High
			Sealing and PSHT temperatures do not exceed SF limit	*T*/400°C	≤ 1	Y	App. **E**	High
	Inspectability		Procedures can be performed remotely	Y/N	Y	Y	App. **E**	High
			- in radiation field	Y/N	Y	Y	App. **E**	High
			Material amenable to inspection	Y/N	Y	Y	App. **E**	High
Costs	Development costs		Involves currently available technology	Y/N	Y	Y	App. **E**	High/medium
	Unit costs		Inexpensive raw materials	$(CHF/cc)^{mat}/(CHF/cc)^{cs}$	≤ 2	94	App.**E**	Medium/low
			Estimated unit cost	$kCHF/(kCHF)^{cs}$	≤ 1.3	*>>1.7*	App.**E**	Medium/low
			Multiple potential suppliers	N_{sup}	≥ $2N_{sup}$	Y	App.**E**	Medium

Table 6e Feasibilty Evaluation Summary for Ni-Alloy Clad Carbon Steel SF Canister Concept for a Repository in Opalinus Clay (4.6m long, 770mm ID, 100mm/5mm-C22 thick)

Assessment Category	Sub-Category	Condition(s)	Desirable Features	Indicator(s)	Criteria	Quantities	Sect. in report	Feasibility
Mechanical Integrity	Handling	*tbd*	Damage tolerance (deformation/fracture)	$CO/CO^{FAE}(2mm)$	≤ 1.00			
	Disposal (short time)	P ≤ 6/1MPa (TWI-5 load case)	Acceptable structural integrity during aerobic phases	$\sigma_{VM,max}/R_{p0.2,min}$ *100mm* $\sigma_{VM,max}/R_{p0.2,min}$ *80mm*	≤ 1.50	0.40 0.54	App. **I**	High High
				$CO/CO^{FAE}(2)_{max}$ *100mm* $CO/CO^{FAE}(2)_{max}$ *80mm*	≤ 1.00	0.16 0.21	App. **J**	High High
	Disposal (long time)	P ≤ 29/22MPa (TWI-2 load case)	Acceptable structural integrity during anaerobic phase	$\sigma_{VM,max}/R_{p0.2,min}$ *100mm* $\sigma_{VM,max}/R_{p0.2,min}$ *80mm*	≤ 1.50	1.20 1.69	App. **I**	High Medium/low
				$CO/CO^{FAE}(2)_{max}$ *100mm* $CO/CO^{FAE}(2)_{max}$ *80mm*	≤ 1.00	0.06 0.23	App. **J**	High High
	Creep	*n/a*		$\varepsilon_C/\varepsilon_R$	< 1.00			High
Environmental Damage	General corrosion	Active material Passive material	Low and/or predictable rate of general corrosion	Anaerobic d*x*/d*t* Anaerobic d*x*/d*t*	≤ 0.02μm/a ≤ 0.02μm/a	*n/a* <0.02μm/a	App. **F**	High
	Local/crevice/IG corrosion		Low susceptibility to: - pitting - crevice corrosion - IGA	 Y/N Y/N Y/N	 Y Y Y	 Y Y Y	 App. **F** App. **F** App. **F**	 High High High
	MIC		Low susceptibility to MIC	Y/N	Y	Y	App. **F**	High
	SCC/HIC		Low susceptibility to: - SCC - HIC	 $\sigma_{1,max}/R_{SCC}$ $K_{1a,max}/K_{1HIC}$	 ≤ 0.80 ≤ 0.80	 ≤~0.28 ≤~0.04	 App. **F** App. **F**	 High/medium High
Impact on geological barrier	Gas production		Low rate of H_2 production	Equivalent anaerobic CS corrosion rate	≤ 10μm/a	~0	App. **F**	High
	Effect on buffer,		Effect on Bentonite buffer	Y/N	N	N	App. **F**	High
	host rock		Effect on host rock	Y/N	N	N	App. **F**	High

Mechanical integrity data for 80mm thick carbon steel sub-structure also included for information

Assessment Category	Sub-Category	Condition(s)	Desirable Features	Indicator(s)	Criteria	Quantities	Sect. in report	Feasibility
Fabrication	Manufacture of canister body	SF	Involves current proven technology	Y/N	Y	Y	App. **F**	High
	Sealing		Involves current proven technology	Y/N	Y	Y	App. **F**	High
			Procedure can be performed remotely	Y/N	Y	Y	App. **F**	High
			- in radiation field	Y/N	Y	Y	App. **F**	High
			Sealing and PSHT temperatures do not exceed SF limit	*T*/400°C	≤ 1	Y	App. **F**	High
	Inspectability		Procedures can be performed remotely	Y/N	Y	Y	App. **F**	High
			- in radiation field	Y/N	Y	Y	App. **F**	High
			Material amenable to inspection	Y/N	Y	Y	App. **F**	High
Costs	Development costs		Involves currently available technology	Y/N	Y	Y	App. **F**	High/medium
	Unit costs		Inexpensive raw materials	$(CHF/cc)^{mat}/(CHF/cc)^{cs}$	≤ 2	72	App. **F**	Medium/low
			Estimated unit cost	$kCHF/(kCHF)^{cs}$	≤ 1.3	*>>1.5*		Medium/low
			Multiple potential suppliers	N_{sup}	≥ $2N_{sup}$	Y	App. **F**	Medium

Table 7a Feasibilty Evaluation Summary for Copper Coated Carbon Steel VHLW Canister Concept for a Repository in Opalinus Clay (1.6m long, 440mm ID, 50mm/5mm-Cu thick)

Assessment Category	Sub-Category	Condition(s)	Desirable Features	Indicator(s)	Criteria	Quantities	Sect. in report	Feasibility
Mechanical Integrity	Handling	*tbd*	Damage tolerance (deformation/fracture)	$CO/CO^{FAE}(2mm)$	≤ 1.00			
	Disposal (short time)	P ≤ 6/1MPa (TWI-5 load case)	Acceptable structural integrity during aerobic phases	$\sigma_{VM,max}/R_{p0.2,min}$ *50mm*	≤ 1.50	0.24	App. **I**	High
				$CO/CO^{FAE}(2)_{max}$ *50mm*	≤ 1.00	0.14	App. **J**	High
	Disposal (long time)	P ≤ 29/22MPa (TWI-2 load case)	Acceptable structural integrity during anaerobic phase	$\sigma_{VM,max}/R_{p0.2,min}$ *50mm*	≤ 1.50	1.40	App. **I**	Medium
				$CO/CO^{FAE}(2)_{max}$ *50mm*	≤ 1.00	0.44	App. **J**	High
	Creep	*n/a*		$\varepsilon_C/\varepsilon_R$	< 1.00		App. **D**	High
Environmental Damage	General corrosion	Active material	Low and/or predictable rate of general corrosion	Anaerobic dx/dt	≤ 0.02μm/a	≤ 0.002μm/a	App. **D**	High/medium
		Passive material		Anaerobic dx/dt	≤ 0.02μm/a	*n/a*		
	Local/crevice/IG corrosion		Low susceptibility to:					
			- pitting	Y/N	Y	Y	App. **D**	Medium
			- crevice corrosion	Y/N	Y	Y	App. **D**	High
			- IGA	Y/N	Y	Y	App. **D**	High
	MIC		Low susceptibility to MIC	Y/N	Y	Y	App. **D**	High
	SCC/HIC		Low susceptibility to:					
			- SCC	$\sigma_{1a,max}/R_{SCC}$	≤ 0.80	<<0.6	App. **D**	High
			- HIC	$K_{1,max}/K_{1HIC}$	≤ 0.80	≤~0.01	App. **D**	High
Impact on geological barrier	Gas production		Low rate of H_2 production	Equivalent anaerobic CS corrosion rate	≤ 10μm/a	~0	App. **D**	High
	Effect on buffer,		Effect on Bentonite buffer	Y/N	N	N	App. **D**	High
	host rock		Effect on host rock	Y/N	N	N	App. **D**	High

Assessment Category	Sub-Category	Condition(s)	Desirable Features	Indicator(s)	Criteria	Quantities	Sect. in report	Feasibility
Fabrication	Manufacture of canister body	VHLW	Involves current proven technology	Y/N	Y	Y	App. **D**	High
	Sealing		Involves current proven technology	Y/N	Y	Y	App. **D**	High
			Procedure can be performed remotely	Y/N	Y	Y	App. **D**	High
			- in radiation field	Y/N	Y	Y	App. **D**	High
			Sealing and PSHT temperatures do not exceed VHLW limit	T/450°C	≤ 1	Y	App. **D**	High
	Inspectability		Procedures can be performed remotely	Y/N	Y	Y	App. **D**	High
			- in radiation field	Y/N	Y	Y	App. **D**	High
			Material amenable to inspection	Y/N	Y	Y	App. **D**	High
Costs	Development costs		Involves currently available technology	Y/N	Y	Y	App. **D**	High/medium
	Unit costs		Inexpensive raw materials	$(CHF/cc)^{mat}/(CHF/cc)^{cs}$	≤ 2	13	App. **D**	Medium
			Estimated unit cost	$kCHF/(kCHF)^{cu\text{-}cs}$	≤ 1.3	1		High
			Multiple potential suppliers	N_{sup}	≥ $2N_{sup}$	Y	App. **D**	Medium

Table 7b Feasibilty Evaluation Summary for Ti (Gr.7) Clad Carbon Steel VHLW Canister Concept for a Repository in Opalinus Clay (1.6m long, 440mm ID, 50mm/5mm-Ti thick)

Assessment Category	Sub-Category	Condition(s)	Desirable Features	Indicator(s)	Criteria	Quantities	Sect. in report	Feasibility
Mechanical Integrity	Handling	*tbd*	Damage tolerance (deformation/fracture)	$CO/CO^{FAE}(2mm)$	≤ 1.00			
	Disposal (short time)	P ≤ 6/1MPa (TWI-5 load case)	Acceptable structural integrity during aerobic phases	$\sigma_{VM,max}/R_{p0.2,min}$ *50mm*	≤ 1.50	0.24	App. **I**	High
				$CO/CO^{FAE}(2)_{max}$ *50mm*	≤ 1.00	0.16	App. **J**	High
	Disposal (long time)	P ≤ 29/22MPa (TWI-2 load case)	Acceptable structural integrity during anaerobic phase	$\sigma_{VM,max}/R_{p0.2,min}$ *50mm*	≤ 1.50	1.40	App. **I**	Medium
				$CO/CO^{FAE}(2)_{max}$ *50mm*	≤ 1.00	0.20	App. **J**	High
	Creep	*n/a*		$\varepsilon_C/\varepsilon_R$	< 1.00			
Environmental Damage	General corrosion	Active material	Low and/or predictable rate of general corrosion	Anaerobic d*x*/d*t*	≤ 0.02μm/a	*n/a*		
		Passive material		Anaerobic d*x*/d*t*	≤ 0.02μm/a	~0.001μm/a	App. **E**	High
	Local/crevice/IG corrosion		Low susceptibility to:					
			- pitting	Y/N	Y	Y	App. **E**	High
			- crevice corrosion	Y/N	Y	Y	App. **E**	High
			- IGA	Y/N	Y	Y	App. **E**	High
	MIC		Low susceptibility to MIC	Y/N	Y	Y	App. **E**	High
	SCC/HIC		Low susceptibility to:					
			- SCC	$\sigma_{1,max}/R_{SCC}$	≤ 0.80	≤~0.19	App. **E**	High/medium
			- HIC	$K_{1a,max}/K_{1HIC}$	≤ 0.80	≤~0.03	App. **E**	High/medium
Impact on geological barrier	Gas production		Low rate of H_2 production	Equivalent anaerobic CS corrosion rate	≤ 10μm/a	~0	App. **E**	High
	Effect on buffer,		Effect on Bentonite buffer	Y/N	N	N	App. **E**	High
	host rock		Effect on host rock	Y/N	N	N	App. **E**	High

Assessment Category	Sub-Category	Condition(s)	Desirable Features	Indicator(s)	Criteria	Quantities	Sect. in report	Feasibility
Fabrication	Manufacture of canister body	VHLW	Involves current proven technology	Y/N	Y	Y	App. **E**	High
	Sealing		Involves current proven technology	Y/N	Y	Y	App. **E**	High
			Procedure can be performed remotely	Y/N	Y	Y	App. **E**	High
			- in radiation field	Y/N	Y	Y	App. **E**	High
			Sealing and PSHT temperatures do not exceed VHLW limit	*T*/450°C	≤ 1	Y	App. **E**	High
	Inspectability		Procedures can be performed remotely	Y/N	Y	Y	App. **E**	High
			- in radiation field	Y/N	Y	Y	App. **E**	High
			Material amenable to inspection	Y/N	Y	Y	App. **E**	High
Costs	Development costs		Involves currently available technology	Y/N	Y	Y	App. **E**	High/medium
	Unit costs		Inexpensive raw materials	$(CHF/cc)^{mat}/(CHF/cc)^{cs}$	≤ 2	94	App. **E**	Medium/low
			Estimated unit cost	$kCHF/(kCHF)^{cu\text{-}cs}$	≤ 1.3	*>>1.6*	App. **E**	Medium/low
			Multiple potential suppliers	N_{sup}	≥ $2N_{sup}$	Y	App. **E**	Medium

Table 7c Feasibilty Evaluation Summary for Ni-Alloy Clad Carbon Steel VHLW Canister Concept for a Repository in Opalinus Clay (1.6m long, 440mm ID, 50mm/5mm-C22 thick)

Assessment Category	Sub-Category	Condition(s)	Desirable Features	Indicator(s)	Criteria	Quantities	Sect. in report	Feasibility
Mechanical Integrity	Handling	*tbd*	Damage tolerance (deformation/fracture)	$CO/CO^{FAE}_{(2)}$	≤ 1.00			
	Disposal (short time)	P ≤ 6/1MPa (TWI-5 load case)	Acceptable structural integrity during aerobic phases	$\sigma_{VM,max}/R_{p0.2,min}$ *50mm*	≤ 1.50	0.24	App. **I**	High
				$CO/CO^{FAE}_{(2)max}$ *50mm*	≤ 1.00	0.09	App. **J**	High
	Disposal (long time)	P ≤ 29/22MPa (TWI-2 load case)	Acceptable structural integrity during anaerobic phase	$\sigma_{VM,max}/R_{p0.2,min}$ *50mm*	≤ 1.50	1.40	App. **I**	Medium
				$CO/CO^{FAE}_{(2)max}$ *50mm*	≤ 1.00	0.12	App. **J**	High
	Creep	*n/a*		$\varepsilon_C/\varepsilon_R$	< 1.00			
Environmental Damage	General corrosion	Active material	Low and/or predictable rate of general corrosion	Anaerobic d*x*/d*t*	≤ 0.02μm/a	*n/a*		
		Passive material		Anaerobic d*x*/d*t*	≤ 0.02μm/a	≤ 0.02μm/a	App. **F**	High
	Local/crevice/IG corrosion		Low susceptibility to:					
			- pitting	Y/N	Y	Y	App. **F**	High
			- crevice corrosion	Y/N	Y	Y	App. **F**	High
			- IGA	Y/N	Y	Y	App. **F**	High
	MIC		Low susceptibility to MIC	Y/N	Y	Y	App. **F**	High
	SCC/HIC		Low susceptibility to:					
			- SCC	$\sigma_{1,max}/R_{SCC}$	≤ 0.80	≤~0.15	App. **F**	High/medium
			- HIC	$K_{1a,max}/K_{1HIC}$	≤ 0.80	≤~0.01	App. **F**	High/medium
Impact on geological barrier	Gas production		Low rate of H_2 production	Equivalent anaerobic CS corrosion rate	≤ 10μm/a	~0	App. **F**	High
	Effect on buffer,		Effect on Bentonite buffer	Y/N	N	N	App. **F**	High
	host rock		Effect on host rock	Y/N	N	N	App. **F**	High

Assessment Category	Sub-Category	Condition(s)	Desirable Features	Indicator(s)	Criteria	Quantities	Sect. in report	Feasibility
Fabrication	Manufacture of canister body	VHLW	Involves current proven technology	Y/N	Y	Y	App. **F**	High
	Sealing		Involves current proven technology	Y/N	Y	Y	App. **F**	High
			Procedure can be performed remotely	Y/N	Y	Y	App. **F**	High
			- in radiation field	Y/N	Y	Y	App. **F**	High
			Sealing and PSHT temperatures do not exceed VHLW limit	*T*/450°C	≤ 1	Y	App. **F**	High
	Inspectability		Procedures can be performed remotely	Y/N	Y	Y	App. **F**	High
			- in radiation field	Y/N	Y	Y	App. **F**	High
			Material amenable to inspection	Y/N	Y	Y	App. **F**	High
Costs	Development costs		Involves currently available technology	Y/N	Y	Y	App. **F**	High/medium
	Unit costs		Inexpensive raw materials	$(CHF/cc)^{mat}/(CHF/cc)^{cs}$	≤ 2	72	App. **F**	Medium/low
			Estimated unit cost	$kCHF/(kCHF)^{cu\text{-}cs}$	≤ 1.3	*>>1.1*		High/medium
			Multiple potential suppliers	N_{sup}	≥ $2N_{sup}$	Y	App. **F**	Medium

Table 7d Feasibilty Evaluation Summary for a solid Ti (Gr.2) VHLW Canister Concept for a Repository in Opalinus Clay (1.6m long, 440mm ID, 50mm thick)

Assessment Category	Sub-Category	Condition(s)	Desirable Features	Indicator(s)	Criteria	Quantities	Sect. in report	Feasibility
Mechanical Integrity	Handling	*tbd*	Damage tolerance (deformation/fracture)	$CO/CO^{FAE}(2)$	≤ 1.00			
	Disposal (short time)	P ≤ 6/1MPa (TWI-5 load case)	Acceptable structural integrity during aerobic phases	$\sigma_{VM,max}/R_{p0.2,min}$ *50mm*	≤ 1.50	0.19	App. **I**	High
				$CO/CO^{FAE}(2)_{max}$ *50mm*	≤ 1.00	0.16	App. **J**	High
	Disposal (long time)	P ≤ 29/22MPa (TWI-2 load case)	Acceptable structural integrity during anaerobic phase	$\sigma_{VM,max}/R_{p0.2,min}$ *50mm*	≤ 1.50	1.15	App. **I**	High
				$CO/CO^{FAE}(2)_{max}$ *50mm*	≤ 1.00	0.20	App. **J**	High
	Creep	*n/a*		$\varepsilon_C/\varepsilon_R$	< 1.00			
Environmental Damage	General corrosion	Active material	Low and/or predictable rate of general corrosion	Anaerobic d*x*/d*t*	≤ 0.02μm/a	*n/a*		
		Passive material		Anaerobic d*x*/d*t*	≤ 0.02μm/a	~0.001μm/a	App. **E**	High
	Local/crevice/IG corrosion		Low susceptibility to:					
			- pitting	Y/N	Y	Y	App. **E**	High
			- crevice corrosion	Y/N	Y	Y	App. **E**	High
			- IGA	Y/N	Y	Y	App. **F**	High
	MIC		Low susceptibility to MIC	Y/N	Y	Y	App. **E**	High
	SCC/HIC		Low susceptibility to:					
			- SCC	$\sigma_{1,max}/R_{SCC}$	≤ 0.80	≤~0.19	App. **E**	High/medium
			- HIC	$K_{1a,max}/K_{1HIC}$	≤ 0.80	≤~0.08	App. **E**	High/medium
Impact on geological barrier	Gas production		Low rate of H_2 production	Equivalent anaerobic CS corrosion rate	≤ 10μm/a	~0	App. **E**	High
	Effect on buffer,		Effect on Bentonite buffer	Y/N	N	N	App. **E**	High
	host rock		Effect on host rock	Y/N	N	N	App. **E**	High

Assessment Category	Sub-Category	Condition(s)	Desirable Features	Indicator(s)	Criteria	Quantities	Sect. in report	Feasibility
Fabrication	Manufacture of canister body	VHLW	Involves current proven technology	Y/N	Y	Y	App. **E**	High
	Sealing		Involves current proven technology	Y/N	Y	Y	App. **E**	High
			Procedure can be performed remotely	Y/N	Y	Y	App. **E**	High
			- in radiation field	Y/N	Y	Y	App. **E**	High
			Sealing and PSHT temperatures do not exceed VHLW limit	*T*/450°C	≤ 1	Y	App. **E**	High
	Inspectability		Procedures can be performed remotely	Y/N	Y	Y	App. **E**	High
			- in radiation field	Y/N	Y	Y	App. **E**	High
			Material amenable to inspection	Y/N	Y	Y	App. **E**	High
Costs	Development costs		Involves currently available technology	Y/N	Y	Y	App. **E**	High/medium
	Unit costs		Inexpensive raw materials	$(CHF/cc)^{mat}/(CHF/cc)^{cs}$	≤ 2	24	App.**E**	Medium
			Estimated unit cost	$kCHF/(kCHF)^{cu\text{-}cs}$	≤ 1.3	*>>1.1*	App.**E**	High/medium
			Multiple potential suppliers	N_{sup}	≥ $2N_{sup}$	Y	App.**E**	Medium

Table 7e Feasibilty Evaluation Summary for a solid Ni-Alloy (C22) VHLW Canister Concept for a Repository in Opalinus Clay (1.6m long, 440mm ID, 50mm thick)

Assessment Category	Sub-Category	Condition(s)	Desirable Features	Indicator(s)	Criteria	Quantities	Sect. in report	Feasibility
Mechanical Integrity	Handling	*tbd*	Damage tolerance (deformation/fracture)	$CO/CO^{FAE}(2)$	≤ 1.00			
	Disposal (short time)	P ≤ 6/1MPa (TWI-5 load case)	Acceptable structural integrity during aerobic phases	$\sigma_{VM,max}/R_{p0.2,min}$ *50mm*	≤ 1.50	0.15	App. **I**	High
				$CO/CO^{FAE}(2)_{max}$ *50mm*	≤ 1.00	0.09	App. **J**	High
	Disposal (long time)	P ≤ 29/22MPa (TWI-2 load case)	Acceptable structural integrity during anaerobic phase	$\sigma_{VM,max}/R_{p0.2,min}$ *50mm*	≤ 1.50	1.02	App. **I**	High
				$CO/CO^{FAE}(2)_{max}$ *50mm*	≤ 1.00	0.12	App. **J**	High
	Creep	*n/a*		$\varepsilon_C/\varepsilon_R$	< 1.00			
Environmental Damage	General corrosion	Active material	Low and/or predictable rate of general corrosion	Anaerobic d*x*/d*t*	≤ 0.02μm/a	*n/a*		
		Passive material		Anaerobic d*x*/d*t*	≤ 0.02μm/a	<0.02μm/a	App. **F**	High
	Local/crevice/IG corrosion		Low susceptibility to:					
			- pitting	Y/N	Y	Y	App. **F**	High
			- crevice corrosion	Y/N	Y	Y	App. **F**	High
			- IGA	Y/N	Y	Y	App. **F**	High
	MIC		Low susceptibility to MIC	Y/N	Y	Y	App. **F**	High
	SCC/HIC		Low susceptibility to:					
			- SCC	$\sigma_{1,max}/R_{SCC}$	≤ 0.80	≤~0.15	App. **F**	High/medium
			- HIC	$K_{1a,max}/K_{1HIC}$	≤ 0.80	≤~0.01	App. **F**	High/medium
Impact on geological barrier	Gas production		Low rate of H_2 production	Equivalent anaerobic CS corrosion rate	≤ 10μm/a	~0	App. **F**	High
	Effect on buffer,		Effect on Bentonite buffer	Y/N	N	N	App. **F**	High
	host rock		Effect on host rock	Y/N	N	N	App. **F**	High

Assessment Category	Sub-Category	Condition(s)	Desirable Features	Indicator(s)	Criteria	Quantities	Sect. in report	Feasibility
Fabrication	Manufacture of canister body	VHLW	Involves current proven technology	Y/N	Y	Y	App. **F**	High
	Sealing		Involves current proven technology	Y/N	Y	Y	App. **F**	High
			Procedure can be performed remotely	Y/N	Y	Y	App. **F**	High
			- in radiation field	Y/N	Y	Y	App. **F**	High
			Sealing and PSHT temperatures do not exceed VHLW limit	*T*/450°C	≤ 1	Y	App. **F**	High
	Inspectability		Procedures can be performed remotely	Y/N	Y	Y	App. **F**	High
			- in radiation field	Y/N	Y	Y	App. **F**	High
			Material amenable to inspection	Y/N	Y	Y	App. **F**	High
Costs	Development costs		Involves currently available technology	Y/N	Y	Y	App. **F**	High/medium
	Unit costs		Inexpensive raw materials	$(CHF/cc)^{mat}/(CHF/cc)^{cs}$	≤ 2	72 (46)[¥]	App. **F**	Medium/low
			Estimated unit cost	$kCHF/(kCHF)^{cu\text{-}cs}$	≤ 1.3	*>>1.1 (>> 1)*		Medium
			Multiple potential suppliers	N_{sup}	≥ $2N_{sup}$	Y	App. **F**	Medium

[¥] *IN625 (IN617)*

Table 7f Feasibilty Evaluation Summary for Andra Type (Al_2O_3/SiO_2) Ceramic VHLW Canister Concept for a Repository in Opalinus Clay (1.6m long, 440mm ID, 50mm thick)

Assessment Category	Sub-Category	Condition(s)	Desirable Features	Indicator(s)	Criteria	Quantities	Sect. in report	Feasibility
Mechanical Integrity	Handling	*tbd*	Damage tolerance (deformation/fracture)	$CO/CO^{FAE}(2)$	≤ 1.00			
	Disposal (short time)	P ≤ 6/1MPa (TWI-5 load case)	Acceptable structural integrity during aerobic phases	$\sigma_{VM,max}/R_{p0.2,min}$ *50mm*	*n/a*			
				$CO/CO^{FAE}(2)_{max}$ *50mm*	≤ 1.00	1.23	App. **J**	Low
	Disposal (long time)	P ≤ 29/22MPa (TWI-2 load case)	Acceptable structural integrity during anaerobic phase	$\sigma_{VM,max}/R_{p0.2,min}$ *50mm*	*n/a*			
				$CO/CO^{FAE}(2)_{max}$ *50mm*	≤ 1.00	1.20	App. **J**	Low
	Creep	*n/a*		$\varepsilon_C/\varepsilon_R$	< 1.00			
Environmental Damage	General corrosion	Active material	Low and/or predictable rate of general corrosion	Anaerobic d*x*/d*t*	≤ 0.02μm/a			
		Passive material		Anaerobic d*x*/d*t*	≤ 0.02μm/a	~0	App. **G**	High
	Local/crevice/IG corrosion		Low susceptibility to:					
			- pitting	Y/N	Y	Y	App. **G**	High
			- crevice corrosion	Y/N	Y	Y	App. **G**	High
			- IGA	Y/N	Y	?	App. **G**	Medium
	MIC		Low susceptibility to MIC	Y/N	Y	Y	App. **G**	High
	SCC/HIC		Low susceptibility to:					
			- SCC	$\sigma_{1,max}/R_{SCC}$	≤ 0.80	~0	App. **G**	High
			- HIC	$K_{1a,max}/K_{1HIC}$	≤ 0.80	~0	App. **G**	High
Impact on geological barrier	Gas production		Low rate of H_2 production	Equivalent anaerobic CS corrosion rate	≤ 10μm/a	0	App. **G**	High
	Effect on buffer,		Effect on Bentonite buffer	Y/N	N	N	App. **G**	High
	host rock		Effect on host rock	Y/N	N	N	App. **G**	High

Assessment Category	Sub-Category	Condition(s)	Desirable Features	Indicator(s)	Criteria	Quantities	Sect. in report	Feasibility
Fabrication	Manufacture of canister body	VHLW	Involves current proven technology	Y/N	Y	N	App. **G**	Low
	Sealing		Involves current proven technology	Y/N	Y	N	App. **G**	Low
			Procedure can be performed remotely	Y/N	Y	N	App. **G**	Low
			- in radiation field	Y/N	Y	N	App. **G**	Low
			Sealing and PSHT temperatures do not exceed VHLW limit	*T*/450°C	≤ 1	?	App. **G**	Low
	Inspectability		Procedures can be performed remotely	Y/N	Y	?	App. **G**	Low
			- in radiation field	Y/N	Y	?	App. **G**	Low
			Material amenable to inspection	Y/N	Y	?	App. **G**	Low
Costs	Development costs		Involves currently available technology	Y/N	Y	N	App. **G**	Low
	Unit costs		Inexpensive raw materials	$(CHF/cc)^{mat}/(CHF/cc)^{cs}$	≤ 2	7-14	App. **G**	Medium
			Estimated unit cost	$kCHF/(kCHF)^{cu\text{-}cs}$	≤ 1.3	*>>~1*		Medium
			Multiple potential suppliers	N_{sup}	≥ $2N_{sup}$	N	App. **G**	Low

Table 7g Feasibilty Evaluation Summary for Ceramic (SSiC) VHLW Canister Concept for a Repository in Opalinus Clay (1.6m long, 440mm ID, 50mm thick)

Assessment Category	Sub-Category	Condition(s)	Desirable Features	Indicator(s)	Criteria	Quantities	Sect. in report	Feasibility
Mechanical Integrity	Handling	*tbd*	Damage tolerance (deformation/fracture)	$CO/CO^{FAE}(2)$	≤ 1.00			
	Disposal (short time)	P ≤ 6/1MPa (TWI-5 load case)	Acceptable structural integrity during aerobic phases	$\sigma_{VM,max}/R_{p0.2,min}$ *50mm*	*n/a*			
				$CO/CO^{FAE}(2)_{max}$ *50mm*	≤ 1.00	0.70	App. **J**	Medium/low
	Disposal (long time)	P ≤ 29/22MPa (TWI-2 load case)	Acceptable structural integrity during anaerobic phase	$\sigma_{VM,max}/R_{p0.2,min}$ *50mm*	*n/a*			
				$CO/CO^{FAE}(2)$ *50mm*	≤ 1.00	0.77	App. **J**	Low
	Creep	*n/a*		$\varepsilon_C/\varepsilon_R$	< 1.00			
Environmental Damage	General corrosion	Active material	Low and/or predictable rate of general corrosion	Anaerobic d*x*/d*t*	≤ 0.02μm/a			
		Passive material		Anaerobic d*x*/d*t*	≤ 0.02μm/a	~0	App. **G**	High
	Local/crevice/IG corrosion		Low susceptibility to:					
			- pitting	Y/N	Y	Y	App. **G**	High
			- crevice corrosion	Y/N	Y	Y	App. **G**	High
			- IGA	Y/N	Y	?	App. **G**	High/medium
	MIC		Low susceptibility to MIC	Y/N	Y	Y	App. **G**	High
	SCC/HIC		Low susceptibility to:					
			- SCC	$\sigma_{1,max}/R_{SCC}$	≤ 0.80	~0	App. **G**	
			- HIC	$K_{1a,max}/K_{1HIC}$	≤ 0.80	~0	App. **G**	
Impact on geological barrier	Gas production		Low rate of H_2 production	Equivalent anaerobic CS corrosion rate	≤ 10μm/a	0	App. **G**	High
	Effect on buffer,		Effect on Bentonite buffer	Y/N	N	N	App. **G**	High
	host rock		Effect on host rock	Y/N	N	N	App. **G**	High

Assessment Category	Sub-Category	Condition(s)	Desirable Features	Indicator(s)	Criteria	Quantities	Sect. in report	Feasibility
Fabrication	Manufacture of canister body	VHLW	Involves current proven technology	Y/N	Y	N	App. **G**	Low
	Sealing		Involves current proven technology	Y/N	Y	N	App. **G**	Low
			Procedure can be performed remotely	Y/N	Y	N	App. **G**	Low
			- in radiation field	Y/N	Y	N	App. **G**	Low
			Sealing and PSHT temperatures do not exceed VHLW limit	*T*/450°C	≤ 1	N	App. **G**	Low
	Inspectability		Procedures can be performed remotely	Y/N	Y	?	App. **G**	Low
			- in radiation field	Y/N	Y	?	App. **G**	Low
			Material amenable to inspection	Y/N	Y	?	App. **G**	Low
Costs	Development costs		Involves currently available technology	Y/N	Y	N	App. **G**	Low
	Unit costs		Inexpensive raw materials	$(CHF/cc)^{mat}/(CHF/cc)^{cs}$	≤ 2	6-12	App. **G**	Medium
			Estimated unit cost	$kCHF/(kCHF)^{cu\text{-}cs}$	≤ 1.3	*>>~1*	App. **G**	High/medium
			Multiple potential suppliers	N_{sup}	≥ $2N_{sup}$	N	App. **G**	Low

9 FIGURES

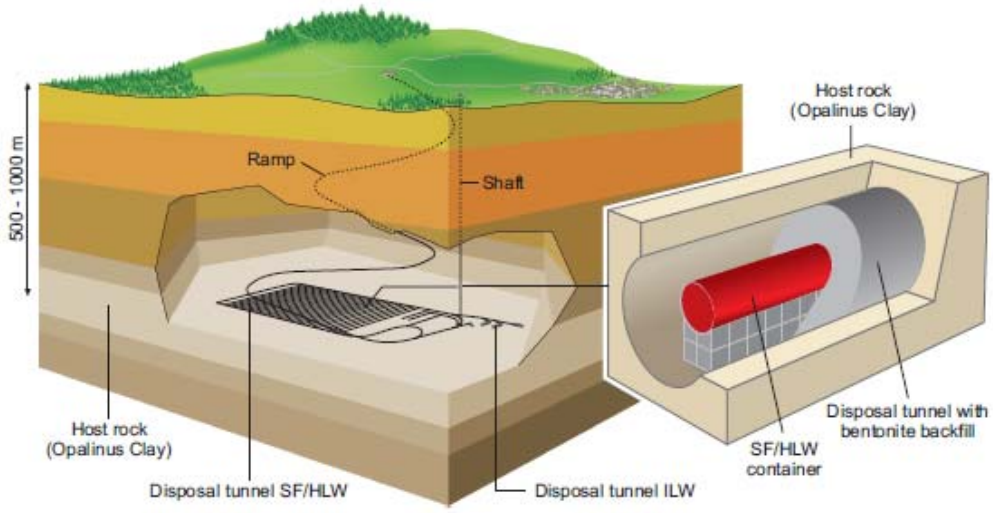

Fig. 1 Schematic of the multi-barrier concept for nuclear waste disposal in canisters placed in an underground repository in Opalinus Clay, with a bentonite clay backfill [1]

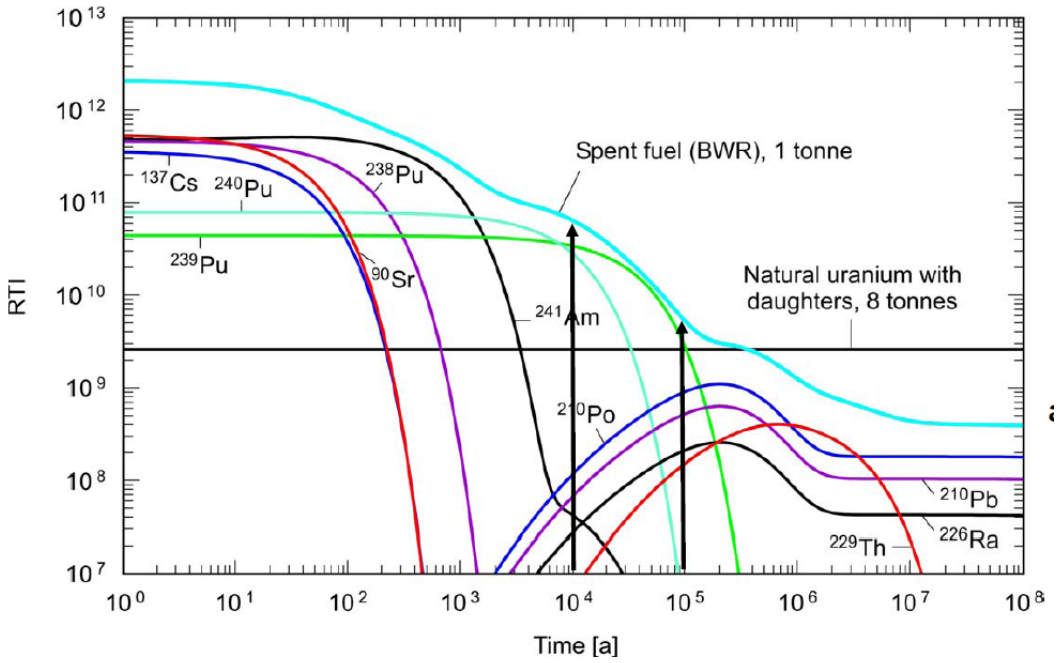

Fig. 2 Canister lifetime expressed as a function of radiotoxity index (RTI) (Nagra [2])

RTI is the radiological hazard potential due to ingestion of an activity A divided by the annual dose limit (0.1mSv)

Carbon steel canister: >10,000 years - 96% of inventory present at repository closure decayed

CuFe canister: >100,000 years - 99.5% of inventory present at repository closure decayed

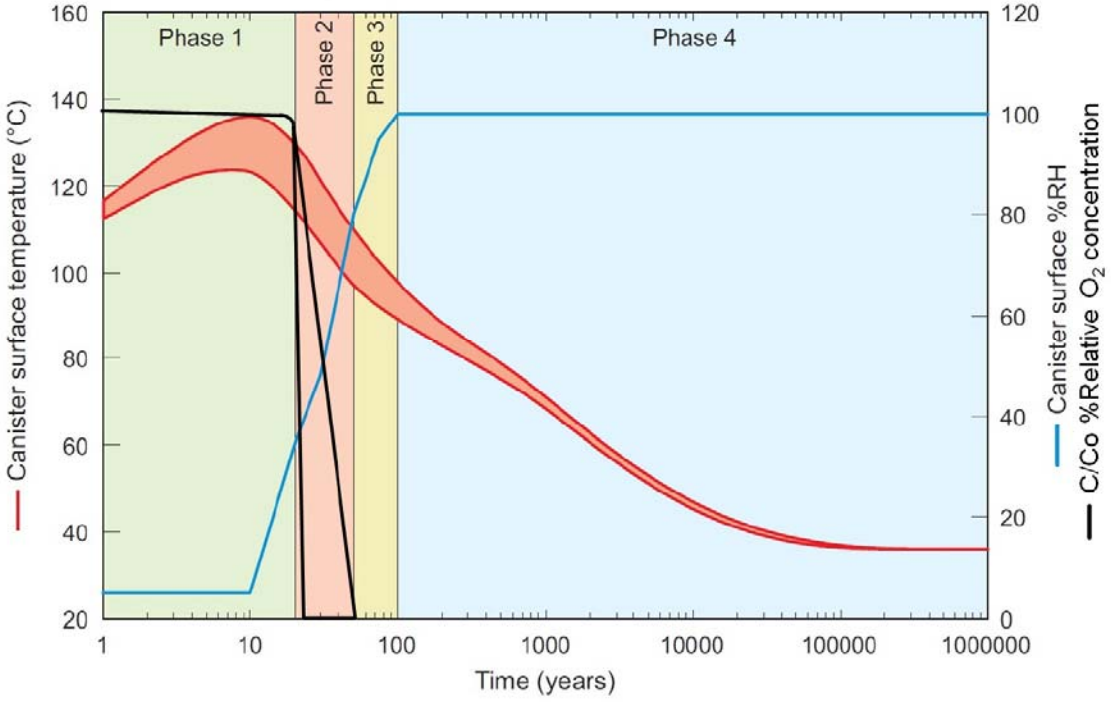

Fig. 3 Evolution of temperature, relative humidity (RH) and relative oxygen concentration (C/C_o) at the surface of a canister surrounded by bentonite in a repository in Opalinus Clay [3]

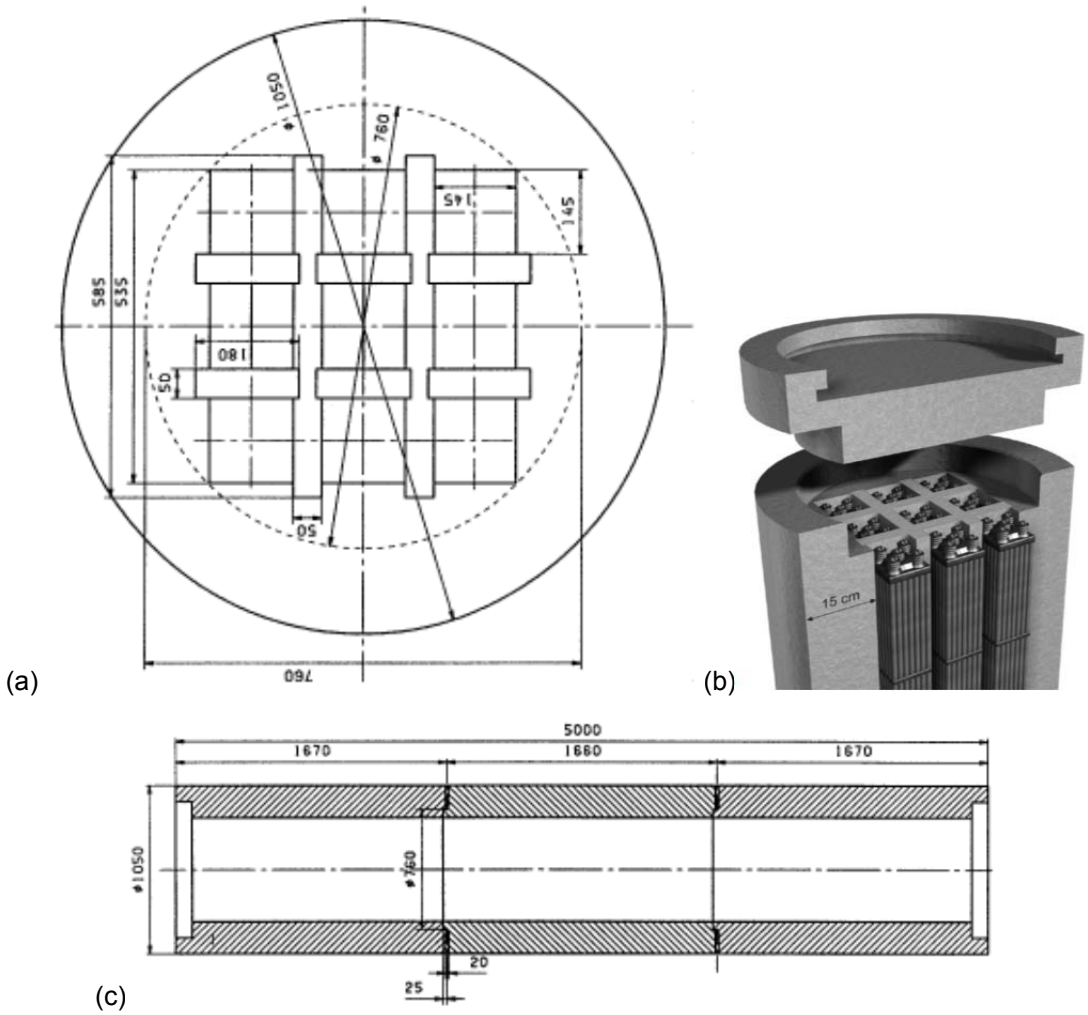

Fig. 4 Arrangement for BWR spent fuel rod disposal, with (a) example of internal detail for 9-cluster arrangement, (b) example of implementation in SKB canister concept solution, and (c) example of axial cross-section [6]

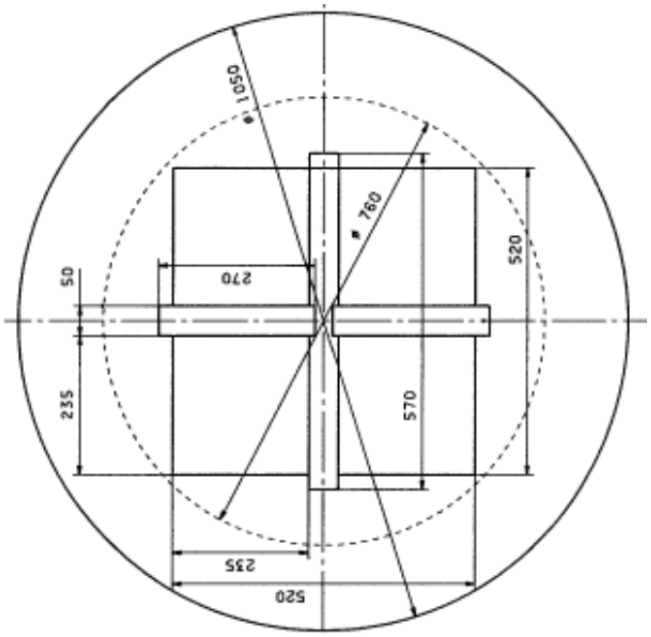

Fig. 5 Arrangement for PWR spent fuel rod disposal, with example of internal detail for 4-cluster arrangement [6]

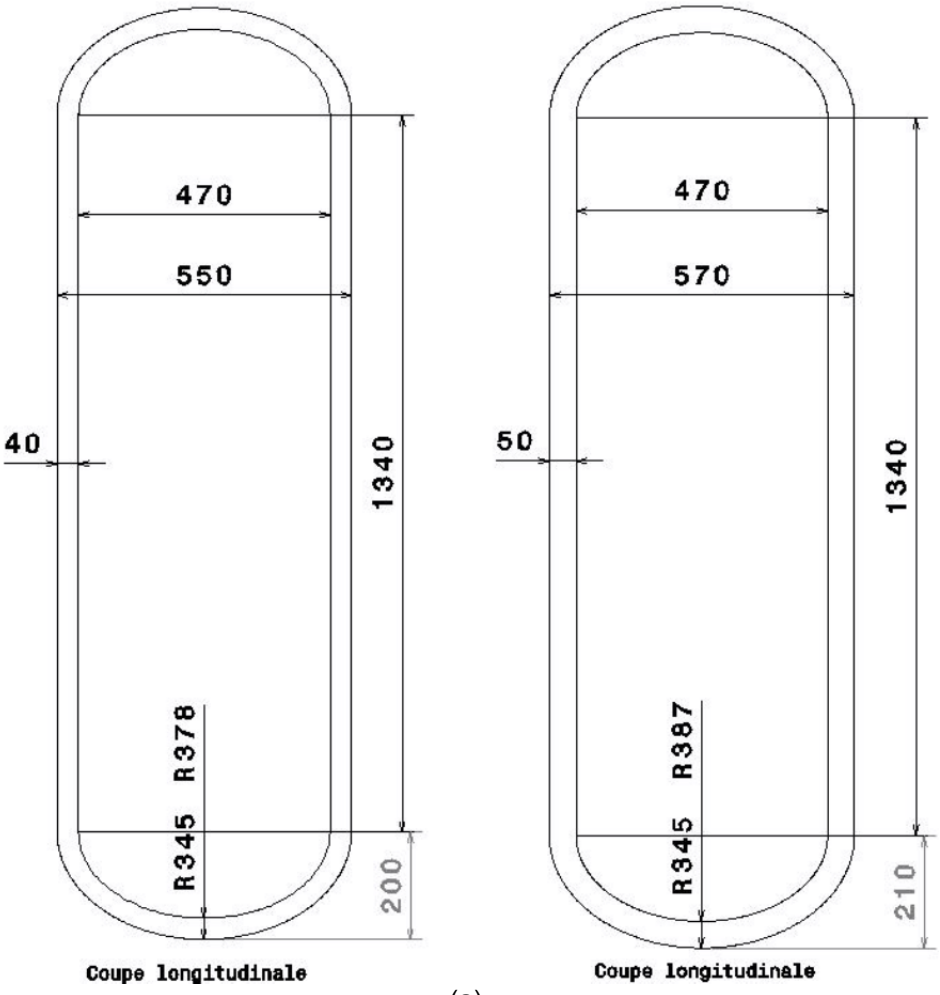

(a)

(b)

Fig. 6 Example of arrangement for vitrified high level waste disposal in a ceramic container, (a) schematic details, and (b) view of Andra prototype [7]

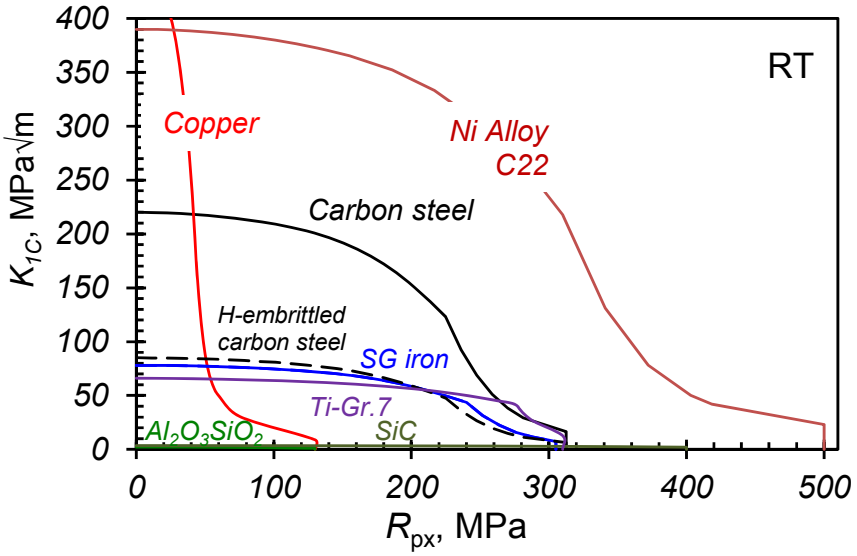

Fig. 7 Comparison of mechanical integrity characteristics of candidate canister materials

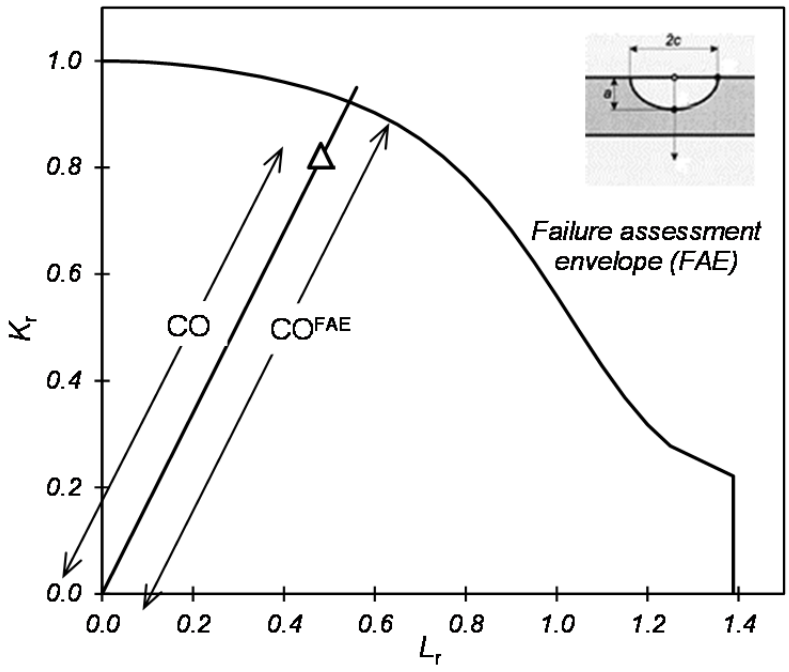

Fig. 8 Definition of the CO and CO^{FEA} quantities determined from the Option 1 failure assessment diagram

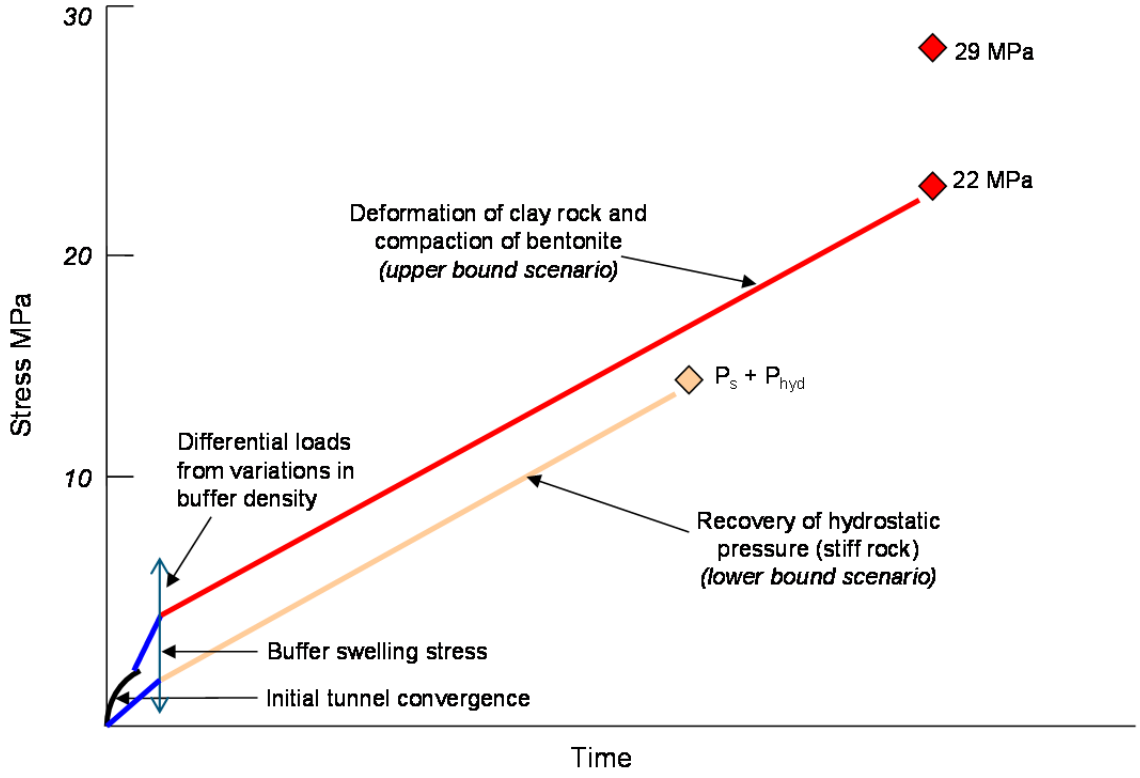

Fig. 9 Possible evolution of stresses experienced by a canister contained within bentonite backfill in an Opalinus clay repository at a depth of 900m

The two stress evolution paths represent two alternative possibilities, depending on the mechanical properties of the rock, with the maximum conceivable stresses at 900m being 29MPa horizontal and 22MPa vertical

10 APPENDICES

APPENDIX A: NOMENCLATURE

a	Crack depth
A	Tensile elongation at fracture
AOD	Argon oxygen decarburisation
BWR	Boiling water reactor
c	Half crack length
C_{VRT}	Room temperature impact energy
CO	Distance between the origin and the $K_r(L_r)$ assessment co-ordinate in FAD (Fig. 8)
CP	Commercially pure
CO^{FAE}	Distance between the origin and the FAE corresponding to CO in FAD (Fig. 8)
CS	Carbon steel
CTE	Coefficient of thermal expansion
d	Axial distance from centre span of canister
E	Elastic modulus
E_{CORR}	Corrosion potential
E_{CREV}	Crevice corrosion potential
E_{RCREV}	Re-passivation crevice corrosion potential
E_{PIT}	Pitting potential
EB	Electron beam (weld)
ESR	Electroslag refining
ET	Eddy current testing
FAD	Failure assessment diagram
FAE	Failure assessment envelope
FSW	Friction stir welding
HAZ	Heat affected zone (of welded joint)
HIC	Hydrogen induced cracking
HIP	Hot isostatic pressing
HLW	High level waste
ID	Inner diameter
IGA	Intergranular attack
K, K_{1C}	Stress intensity factor, Critical stress intensity factor
K_{1a}	Applied stress intensity factor
K_r	Fracture ratio of applied linear elastic stress intensity factor to the material's fracture toughness
K_{1HIC}	Threshold stress intensity factor for hydrogen induced cracking
K_{1SCC}	Threshold stress intensity factor for stress corrosion cracking
KfK	Kernforschungszentrum Karhlsruhe GmbH (Institut für Nukleare Entsorgungstechnik)
L	Length of canister
L_r	Ratio of total applied load giving rise to primary stresses, to the plastic limit load of the defective structure
m	Weibull modulus
MIC	Microbially induced corrosion
OD	Outer diameter
OFP	Oxygen free, phosphorous doped (copper)
N_{sup}	Number of suppliers
NG-GTAW	Narrow gap gas tungsten arc weld
P_e	External pressure
P_{end}, P_{mid}	Pressure at the end and mid length of the canister (Fig.I 3)
P_{max}, P_{min}	Maximum and minimum pressure values in the distribution (Fig.I 3)
PREN	Pitting resistance equivalent number (Eqn. F1)

PSHT	Post seal heat treat
PSZ	Partially stabilised zirconia
PWHT	Post weld heat treat
PWR	Pressurised water reactor
R_F	Fracture strength (defined separately for specimen and part in App. **G**)
R_{HIC}	Threshold stress for hydrogen induced cracking
R_M, $R_{p0.2}$	Tensile (ultimate) strength; 0.2% proof strength
R_{pX}	Flow strength (usually taken to be ($R_{p0.2}$ + R_M)/2)
R_{SCC}	Threshold stress for stress corrosion cracking
RH	Relative humidity
RTI	Radiotoxity index (radiological hazard potential due to ingestion of an activity *A* divided by the annual dose limit (0.1mSv)
SCC	Stress corrosion cracking
SF	Spent fuel
SG	Spheroidal graphite (cast iron)
SSiC	Sintered silicon carbide
SiSiC	Silicon infiltrated silicon carbide
t, t_o	Thickness (after time), initial thickness
TWE	Through wall extent
UT	Ultrasonic testing
V_{part}, V_{spec}	Tensile stress bearing volume of part, Tensile stress bearing volume of specimen
VHLW	Vitrified high level waste
x	Corrosion depth
z	Position along the canister length (from mid length), Fig.I 3
Z	Tensile reduction of area at fracture
ZTA	Zirconia toughened alumina

α	Angular position (from horizontal), Fig.I 3
ρ	Density
ε	Strain
ε_C, ε_R	Creep strain, Creep-rupture strain
ε_y	Yield strain
λ	Thermal conductivity
μ	Poissons ratio
σ	Stress, applied stress
σ_a, σ_h	Axial stress, Hoop stress
σ_{max}	Maximum stress
σ_{ref}	Reference stress
σ_{VM}	von Mises stress
σ_1	Maximum principal stress

APPENDIX B: CARBON STEEL

B1 Background and Introduction

Carbon steels could be produced with a range of metallurgical pedigree characteristics to meet specific application requirements. The NAGRA focus was currently on low carbon variants with low $R_{p0.2}$ strength and low $R_{p0.2}/R_M$, to ensure good weldability, high environmental cracking resistance, and significant plastic deformation prior to fracture, e.g. EN 10222 P245GH [8]. The steel could be supplied as forgings [8] or castings [9], with the focus here being on forged product forms.

Carbon steels were widely used in large product forms, and there was vast existing experience in manufacturing and fabrication (e.g. [10]). The following overview indicated that the metallurgical, mechanical and physical properties of the material were well characterised. Moreover, fabrication and inspection technologies were well established.

B2 Material Characteristics

Recommended limits for chemical composition for this application are summarised in Table B1 [10]. Vacuum degassing was recommended to keep oxygen and nitrogen concentrations as low as possible (e.g. <20ppm O) to maximise internal cleanliness. Low sulphur and oxygen concentrations limited the size and number of sulphide and oxide inclusions, and the susceptibility to environmental crack initiation.

B3 Mechanical Properties

The tensile mechanical properties given in Table B1 were recommended to provide the lowest strength possible to meet reasonable structural requirements for nuclear waste disposal canister applications [10], although there were many potentially suitable grades available for adoption. Low strength was preferred to limit susceptibility to environmental cracking, while a low $R_{p0.2}/R_M$ ratio (≤ 0.8) was recommended to ensure sufficient plastic strain accumulation prior to fracture. Consistent with [10], $R_{p0.2}$ (R_m) strength values of 220MPa (400MPa) and 175MPa (311MPa) were respectively used for the mechanical integrity calculations at ambient temperature and 150°C in Apps. **I** and **J**.

Low strength carbon steels characteristically exhibited high fracture toughness. However, hydrogen arising from canister manufacture, closure welding and corrosion during the disposal period could diffuse into carbon steel and cause embrittlement (e.g. [11]). The consequence of the reduction in CTOD shown in Fig.B 1 was equivalent to a reduction in K_{1C} fracture toughness from 220MPa$\sqrt{m}$ to 85MPa$\sqrt{m}$ [10].

B4 Environmental Damage

Carbon steels tended to corrode uniformly, especially at near neutral pH. When localised corrosion attack occured, it tended to do so only in the form of surface roughening.

B4.1 General Corrosion

The general corrosion behaviour of carbon steel was characteristically different under aerobic and anaerobic conditions, and the transition between the two could be important for localised corrosion [4]. Under aerobic conditions, corrosion rates for carbon steel in compacted bentonite were taken to be ~10μm/a [12], although the total depth of corrosion was limited by the amount of oxygen trapped in the bentonite backfill during emplacement. A ~0.2mm reduction of the wall thickness was normally estimated for the first 10 to100 years aerobic period [13].

For anaerobic conditions, the evidence indicated that corrosion rates for carbon steel in ground water were in the range 0.1 to 1μm/a (Fig.B 2, Fig.B 3), with a tendency to the higher rate in compacted bentonite [15]. These rates appeared to be supported by the evidence from archaeological analogues [4], e.g. Fig.B 4.

The effect of γ-radiation on corrosion rate was negligible below ~3Gy/h [5], but could be significant at higher dose rates (≥ 1000Gy/h) [14].

B4.2 Localised Corrosion

In bentonite back-filled repositories, there was evidence to indicate that carbon steel was not passive in the near neutral pH pore water [17]. In these circumstances, the localised corrosion of carbon steel canisters was unlikely to occur. Nevertheless, localised corrosion could be possible during the aerobic phase if the canister surface wetted non-uniformly during saturation [4].

B4.3 Microbially Induced Corrosion

Carbon steel was susceptible to MIC, especially in the presence of biofilms, but this could be prevented in repository environments through the use of highly compacted bentonite [4]. If microbial activity occured further away from the canister, aggressive metabolic by-products (such as HS^- produced by the reduction of sulphates) could result in higher rates of general corrosion and/or increased rates of hydrogen absorption. However, in the case of a highly compacted bentonite buffer, the rate of supply of remotely produced HS^- to the carbon steel canister would be slow and the impact of this form of MIC limited [4].

B4.4 Stress Corrosion and Hydrogen Induced Cracking

SCC was most likely to occur during the early aerobic phase when a suitable environment and relatively oxidising conditions could exist [18]. Of the environments potentially responsible for SCC in carbon steels, only a HCO_3^-/CO_3^{2-} solution was likely in repository conditions, and then at high stresses (of yield point magnitude in the presence of superimposed vibratory stresses. K_{1SCC} was said to be of the order of 20MPa$\sqrt{m}$ in concentrated carbonate solution [4].

While carbon steels were susceptible to HIC, the risk was minimal for low strength carbon steels in repository environments [19], and then only during the long term anaerobic period. K_{1HIC} was estimated to be in the range <70 to 100MPa$\sqrt{m}$ under these conditions [19], although this could be a non-conservative estimate for non-PWHTed HAZ microstructures.

B5 Impact on Geological Barrier

The corrosion of carbon steel under anoxic conditions was accompanied by the generation of hydrogen gas which could move away from the canister surface by mass transport processes through the bentonite backfill and the Opalinus Clay geological barrier, the transport through the latter being rate-limiting. There was therefore a risk of irreversible damage (geological structural cracking) permitting the escape of radioactive products from the repository site to the surface.

Gas generation and transport had been addressed in some detail by Nagra for Swiss disposal conditions [20]. The study provided gas transport rate predictions for various mechanisms as a function of gas pressure, Fig.B 5. Gas transport capacity could be converted to an equivalent anaerobic corrosion rate for carbon steels, with a H_2 flux of $10^{-5}mol_{STP}/m^2/a$ being equivalent to a corrosion rate of 0.003μm/a. For the corrosion rates observed in compacted bentonite, gas transport would be via two-phase flow (the higher rate mechanism in Fig.B 5), although some form of dilatancy-controlled transport might occur at higher pressures (the horizontal grey bar in Fig.B 5 represented a range of anaerobic corrosion rates of 1-10μm/a). Dilatancy-controlled gas flow was associated with rock deformation leading to enhanced porosity and permeability by micro-fracturing. There were uncertainties associated with the impact of H_2 on the geological barrier, and further work had been recommended [3].

Ferrous ions produced by the anaerobic corrosion of cast iron may also influence the properties of the surrounding bentonite in a deleterious way [4].

B6 Fabrication and Inspectability

B6.1 Canister Body and Lid Manufacture

The feasibility of four manufacturing practices were considered in [10], namely: casting, forging, pierce-and-draw, and welded plates. The outcome is summarised in Table B2. The TWI study concluded that a long forging with welded base option was the most desirable manufacturing route due to the inherent high integrity of hollow forgings. The pierce-and-draw process was also attractive, but there was only a single candidate supplier and there were concerns relating to the microstructural condition in the integral base. There were also concerns relating to the defect integrity of cast canisters and those fabricated from pressed and welded plates.

B6.2 Welding

Both EB and NG-GTAW welding processes were possible options for the closure welding of carbon steel canisters [10], as both were suitable for remote operation and weld parameters could be selected to achieve the required properties.

The main difficulty associated with closure welding related to the consequential residual stress state. In order to reduce the magnitude of tensile residual stresses in particular, full PWHT (~600-650°C) would be preferable, but the temperature of spent fuel assemblies should not exceed 400°C, and that of VHLW should not exceed 450°C. Local PWHT could be possible at a temperature in the range 550-600°C to give reduced levels of residual stress of an acceptable level. Other mitigation methods could be possible if the main concern was the presence of tensile residual stresses within 1-2mm of the weld surface, e.g. laser peening.

B6.3 Inspection

The inspection methodologies available for welded thick walled carbon steel containers were comprehensively reviewed in [10]. It was concluded that existing UT procedures could be designed to reliably detect a high proportion of foreseeable flaws of through wall extent (TWE) of 2mm. UT procedures could be readily complemented by ET, remotely deployable at temperatures above ~50°C, and capable of detecting TWE 1mm x 5mm long surface flaws on ground surfaces.

B7 Costs

Investment/Development Costs. It was likely that development costs for a carbon steel canister solution would be relatively small.

Unit Costs. Forgemaster quotations for 140mm wall thickness carbon steel canisters were in the range 150 to 190kCHF (see also Table B2).

B8 Summary

While carbon steel offered many advantages as a nuclear waste disposal canister material in terms of mechanical integrity, well established fabrication and inspectability technology, and cost, there were important concerns relating to environmental damage. Carbon steel was highly susceptible to corrosion, but in a way that could be managed, e.g. by the adoption of an appropriate corrosion allowance. There were uncertainties associated with the prediction of very long time corrosion behaviour which to some extent could be minimised by the availability of archaeological analogues. By far the biggest concern was the potentially adverse effect that corrosion products such as H_2 and Fe(II) could have on the properties of the bentonite buffer and low permeability host rock.

Table B1: Recommended Metallurgical Pedigree Characteristics

PROPERTY	EN 10222 P245GH		
	min	*max*	*Indicative*
Chemical Composition			
C, wt%	-	0.12	
Si, wt%	-	0.3	
Mn, wt%	-	0.8	
P, wt%	-	0.015	
S, wt%	-	0.025	
Cr, wt%	-	0.2	
Ni, wt%	-	0.2	
Cu, wt%	-	0.02	
Mechanical Properties			
$R_{p0.2}$, MPa	220	-	
R_M, MPa	410	530	
A, %	17	-	
Z, %	15	-	
C_{VRT}, J	27	-	
K_{IC}, MPa$\sqrt{m}$ (as-received)		-	220
K_{IC}, MPa$\sqrt{m}$ (H-embrittled)		-	85
Physical Properties			
ρ, g/cc			7.85
CTE, μm/m/°C			11.7

Table B2: Comparison of Carbon Steel Manufacturing Options [10]

METHOD	ADVANTAGES	DISADVANTAGES	BUDGETARY COSTS
Cast steel	*Ease of manufacture, low cost, minimal welding, can readily incorporate design features*	*Porosity/density and limits of height that can be cast in one piece*	*Not available*
Long forging with welded base	*One fabrication weld, machined first*	*Limited supplier base*	*~160kCHF*
Pierce and draw (with or without integrated base)	*Proven concept (in the case of copper, SKB), minimal welding, machined finish*	*Very limited supplier base*	*~150kCHF*
Pressed and welded plates	*Plates readily available*	*Significant welding effort required*	*~240kCHF*

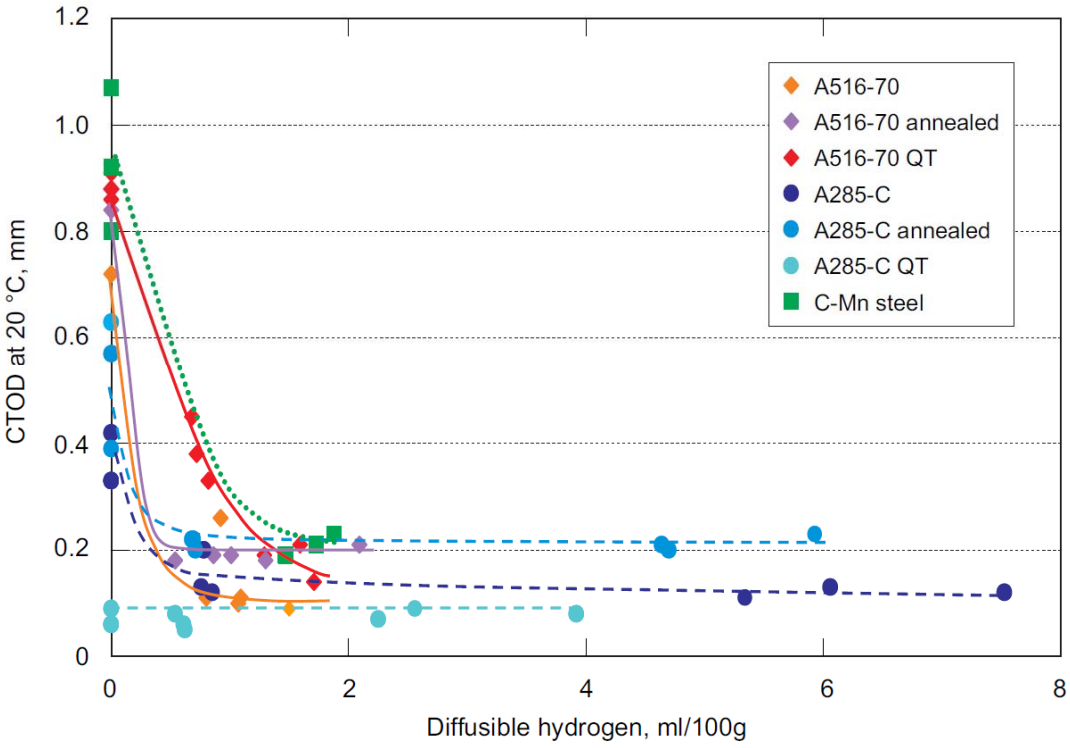

Fig.B 1 Effect of hydrogen on the toughness of a number of steels at 20°C [10]

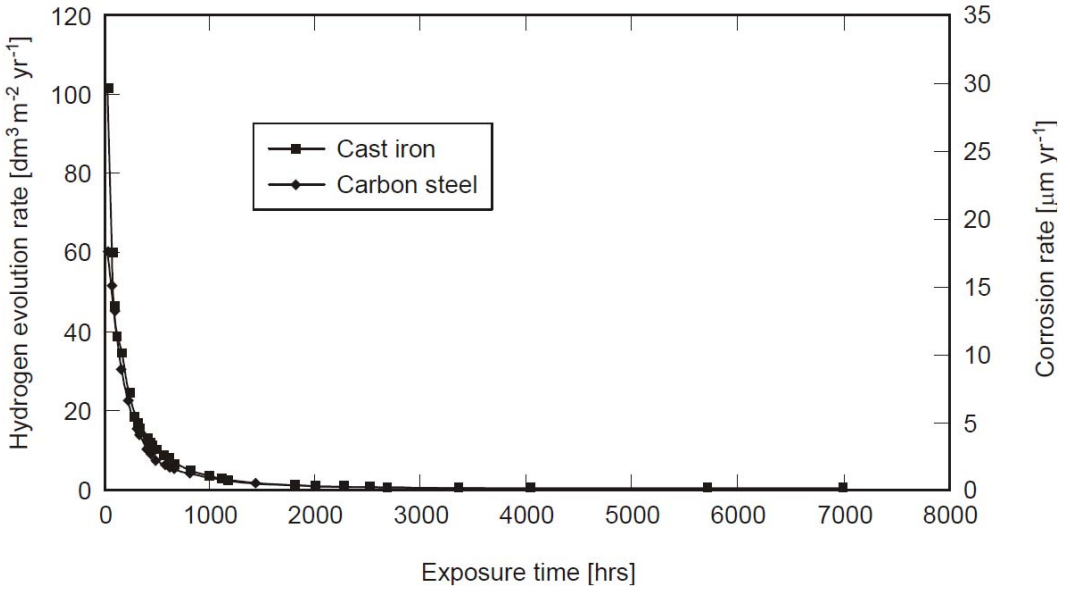

Fig.B 2 Time dependence of the corrosion rate of carbon steel and cast iron in deaerated granitic groundwater [13]

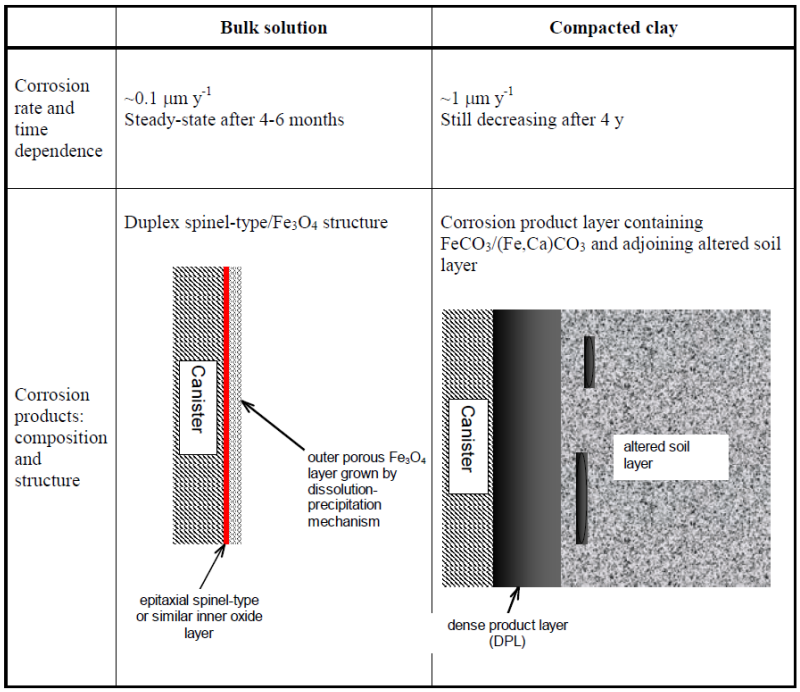

Fig.B 3 Comparison of the corrosion behaviour of carbon steel in bulk solution and in compacted bentonite [15]

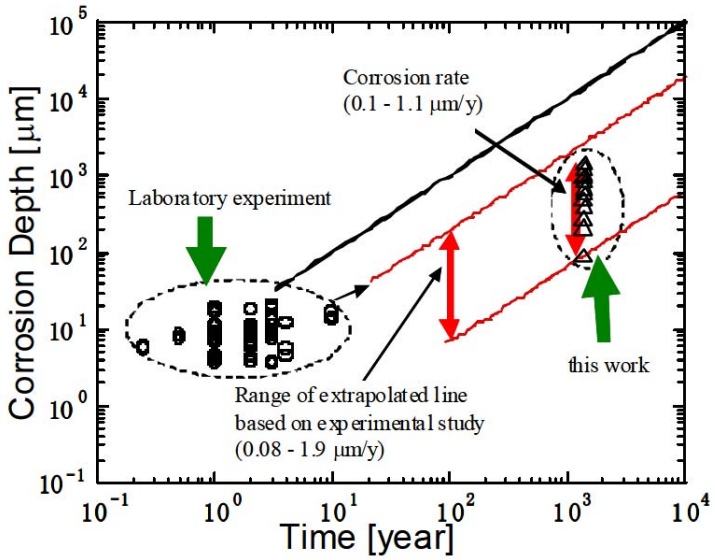

Fig.B 4 Comparison of extrapolated experimental corrosion rates and rates determined from artifacts from the Yamato ancient tomb (after [16])

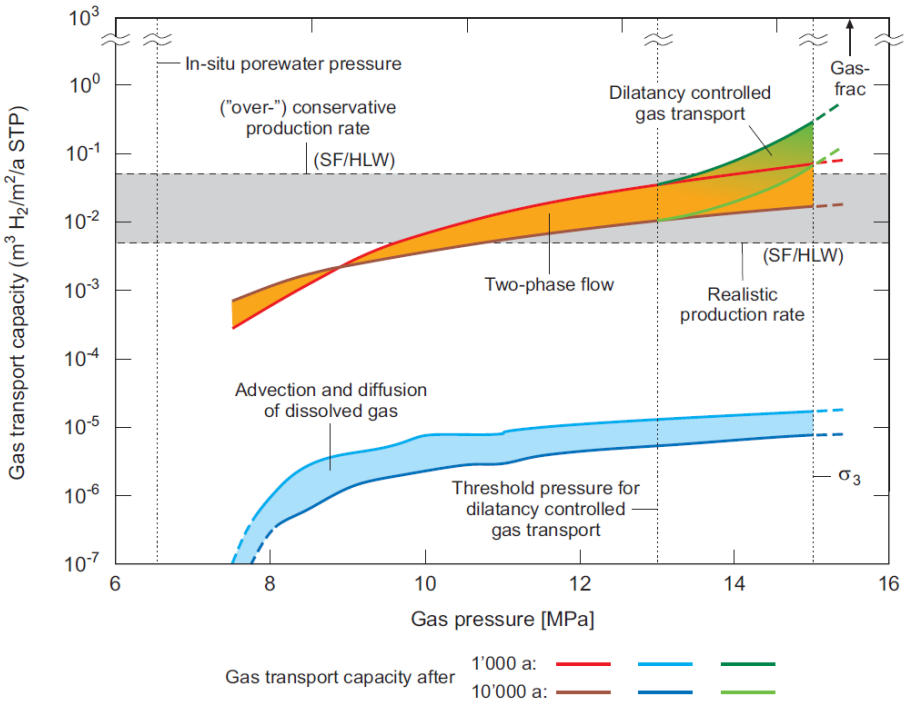

Fig.B 5 Gas transport capacity for various gas transport mechanisms in Opalinus Clay as a function of total pressure [20]

APPENDIX C: CAST IRON

C1 Background and Introduction

Cast irons were iron-carbon based alloys containing more than 2% carbon. There were a number of forms of cast iron, but the variant of most interest for nuclear waste disposal applications was spheroidal graphite (SG) iron, as adopted by SKB and Posiva. There were a number of variants of SG or ductile iron [21], with the grade of interest for this application being GJS-400-15U [22]. Cast iron was considered here in the context of its use as an internal structure for the KBS-3 canister (App. **H**), Fig.C 1.

Cast iron was selected over a steel insert for the KBS-3 application because it eliminated the need for a stabilising filler in the canister, and was judged by SKB to lead to lower development and investment costs, and to increased mechanical strength by a factor 2-3. An acknowledged disadvantage was that the weight of a canister with a cast iron insert was significantly higher.

C2 Material Characteristics

The material properties of SG iron tended to vary with thickness, and those relevant to cast iron insert applications are summarised in Table C1. For the KBS-3 insert, the SG iron was procured to EN1563 Grade GJS-400-15U, for which the nominal chemical composition is given in Table C1. The main requirement for this grade was the tensile strength.

A survey of inserts cast by Swedish manufacturers indicated that there could be significant variability in chemical composition, nodularity and mechanical properties within a single insert, and from insert to insert (trial data in Table C1).

C3 Mechanical Properties

An indication of the tensile properties of GJS-400 irons is given in Table C1. There could be a wide variability, and the ways to improve material quality control for this application were being examined.

Fracture Toughness. The fracture toughness of SG irons was mainly determined by the spheroidal graphite distribution and the microstructure of the iron matrix, which in turn was mainly determined by the cooling rate from the normalising temperature (i.e. by the ruling section size). The fracture toughness assumed in the KBS-3 design was 78MPa$\sqrt{m}$ [23].

Creep. The long-time creep response of SG iron (41kh) had been investigated for temperatures in the range 20 to 125°C, and shown to be almost negligible and logarithmic at stresses up to x1.15 of the yield strength [23]. The maximum creep strain recorded was 0.025% after >40kh at 125°C [24]. On the basis of this evidence, it was estimated that even at stresses above yield at 125°C, the accumulation of creep strains of $\leq$ 0.1% during repository lifetimes was unlikely.

C4 Environmental Damage

While cast iron was likely to have similar corrosion properties to carbon steel (App. **B**), they had not been studied extensively for this application because of the intention to always use the material with an overpack, usually of copper.

SKB had adopted what was postulated to be a conservative estimate of 10μm as the maximum depth of corrosion due to water being present in voids left by defective fuel assemblies. Experimental measurements had led to the conclusion that the corrosion rate of cast iron in Swedish groundwaters was <0.1μm/a, with an associated hydrogen production rate of 0.2L/m^2/a [13].

C5 Fabrication

C5.1 Manufacture

There were widely applied and well established practices for pouring large heavy section and complex SG iron castings in particular for automotive, petro-chemical and power generation industrial sectors. The feasibility of manufacturing nuclear waste disposal canister inserts from GJS-400 had specifically been well established by a number of Swedish foundries.

C5.2 Welding

SG cast iron was not an easy material to weld, but this posed no problems since there was not a requirement for this form of sealing in the KBS-3 design. It was proposed to fit the steel lid to the cast iron insert by mechanical fixation.

C5.3 Inspection

For the KBS-3 development, focus had been on the use of ultrasonic testing and radiography, and in particular pulsed echo ultrasound for inspection of the GJS-400 insert [25]. The geometry of the cast iron insert was complex, and refinement to the adopted procedures was ongoing.

C6 Costs

SG iron was a relatively low cost engineering material. The cost of BWR type cast iron inserts for the KBS-3 canister was said to be ~36k€ (44kCHF) per unit [26].

C7 Summary

SG cast iron was a widely used, well established structural material about which much was known. As a generality, material requirements were not tightly specified, properties were section size dependent, and so there was acknowledged cast-to-cast (piece-to-piece) variability. For application as a structural strengthening insert for nuclear waste disposal canisters, this variability was acceptable, providing the minimum strength requirements were met.

Table C1: Indicative Material Characteristics of EN1563 Grade GJS-400-15U

PROPERTY	*Indicative*	*GJS-400-15U*	*Trial I24*	*Trial I25*	*Trial I26*
Chemical Composition					
C, wt%	3.35-3.44	3.25-3.70	3.66	3.78	3.56
Si, wt%	<2.26	2.40-3.00	2.31	2.08	2.39
Mn, wt%	<0.24	0.10-0.30	0.15	0.21	0.52
P, wt%	<0.03	0.015-0.080	0.026	0.006	0.03
S, wt%	<0.007	0.005-0.020	0.009	0.008	0.010
Mg, wt%		0.04-0.07	0.050	0.035	0.063
Cr, wt%			0.03		
Ni, wt%			0.27	0.50	0.73
Mo, wt%			0.01		
Cu, wt%			0.11		
Nodules/mm^2	>100		35-415		
Mechanical Properties					
$R_{p0.2}$, MPa	>240	>240	257-289		
R_M, MPa	>370	>370-	299-408		
A, %	>11	>11	3.5-22.2		
E, GPa	103-118				
K_{IC}, MPa$\sqrt{m}$					
Physical Properties					
ρ, g/cc	7.3				
CTE, μm/m/°C	11.7				

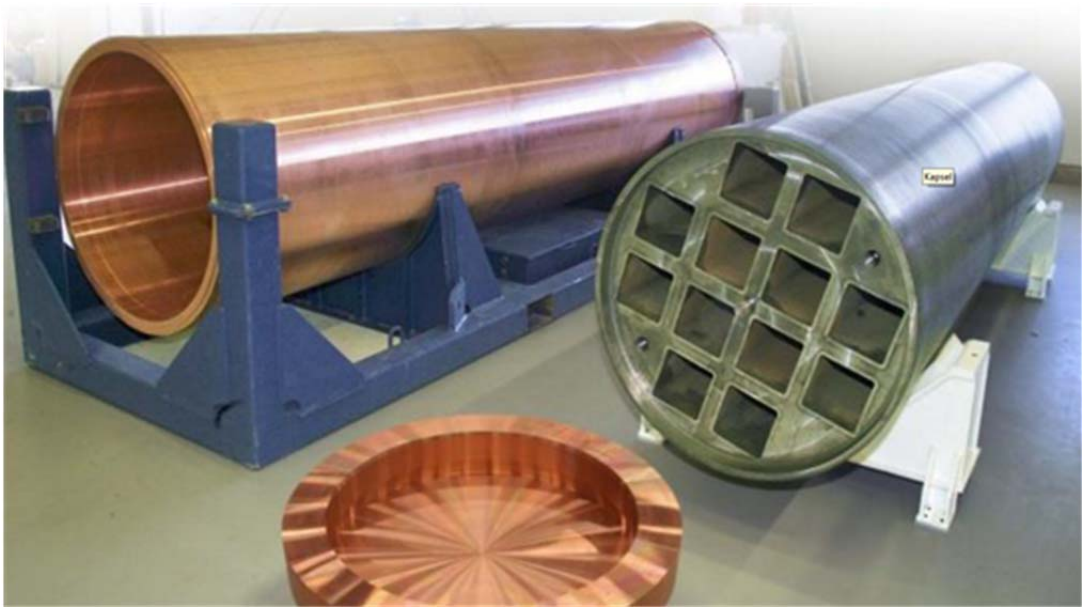

Fig.C 1 KBS-3 canister components, including: 50mm thick copper canister, SG cast iron internal support and copper lid [25]

APPENDIX D: COPPER

D1 Background and Introduction

Copper had a long history as a potential canister material for the disposal of radioactive waste, first being proposed for the disposal of spent fuel in Sweden in 1978, more recently by Finland and Canada, and as a candidate in Switzerland and Japan. Copper canisters were invariably at least considered, for use in conjunction with a bentonite based sealing material in an environment that would become anoxic and saturated when the repository was sealed and closed.

As a consequence of its low strength, copper was only considered for this application in conjunction with an internal structure to provide the necessary mechanical strength, e.g. cast iron in Sweden/Finland (App. **H**, Fig.C 1), and forged carbon steel in Canada. In these circumstances, where the outer copper container was maybe 25 to 50mm thick [27,28], minimum required insert wall thicknesses were 50-60mm [25]. More recently, outer copper barriers of the order of 3-5mm were being considered, whereby the copper was directly coated onto a carbon steel container [29].

D2 Material Characteristics

The copper of interest was oxygen free and phosphorus doped (i.e. OFP copper), typically meeting the requirements of EN1976:88 (also UNS C10100), with the added requirements of <5ppm oxygen, 30-70ppm phosphorus, <0.6ppm hydrogen and <8ppm sulphur, [22,25], Table D1. Copper alloys had not been considered because the thermodynamic stability of pure copper was lost by alloying it with less noble metals.

Details relating to both the copper shell and copper coated solutions are reviewed below.

D2.1 Copper Shell

A large number of copper outer shells had been produced by SKB and Posiva by pierce-and-draw, backward extrusion or open forging processes [26,25]. While the first solution had the advantage of offering an integral bottom, the required metallurgical characteristics were more consistently obtained by extrusion. The three forming routes all provided containers with a wall thickness of ≥ ~75mm, which meant that significant metal removal was required to achieve the target thickness of 50mm. Bottoms and tops were forged from the same OFP copper, with joints being made by welding (typically electron beam welding).

D2.2 Copper Coated Solution

While bulk copper canisters were considered to be a good alternative to steel in terms of corrosion resistance and safety at a time when copper resources were substantial, there were questions regarding the uncertainty in future costs, in particular if demand in developing nations approached that of already developed countries. Using copper-cladding on steel minimised these problems, but puts much more stringent demands on the specification of an acceptable corrosion allowance.

A number of copper coating techniques had been (were being) explored for nuclear waste disposal canister applications (e.g. [29]), including:

i) Laser cladding,
ii) Low pressure cold spray,
iii) Cold spray,
iv) Electro-deposition, and
v) Laser-weld cladding

Current experience suggested that processes *i)* and *ii)* did not provide practical solutions for this application, with laser cladding being too slow, and low pressure cold spray being prone to delamination depths of ~1mm. In contrast, conventional cold spray and electro-deposition processes were proving to be very successful. The evaluation of laser weld cladding for this application was at an early stage.

Good coating adhesion was achieved with both cold spray and electro-deposition processes, this being achieved through substrate surface roughening in the case of cold spray deposition. In practice, application of the cold spray process would only be to coat the closure weld in the underlying

structure. The remainder of the structure would be coated by electro-deposition prior to encapsulation of the spent fuel.

D3 Mechanical Properties

Yield strength properties in the range 40 to 75MPa had been gathered by SKB for their specified grade of P-doped copper [23]. With increasing temperature, yield strength reduced to a minimum of ~20MPa at ~100°C [30]. As-received, the $R_{p0.2}/R_M$ ratio was very low, although this changed significantly with increasing irradiation, Fig.D 1. While these $R_{p0.2}$ values were used in the mechanical integrity calculations in Apps. **I** and **J**, it was acknowledged that the elevated temperature strength values appeared to be lower than those adopted in the KBS-3 design analysis [23].

Fracture Toughness. The ductility of OFP copper was so high that the material did not exhibit a K_{IC} type fracture toughness [30]. Loaded cracks simply opened and did not extend.

Creep. Of the materials considered as candidates for nuclear waste disposal canister solutions, the consideration of creep was only important for those involving copper as the outer corrosion barrier, at least initially when in the form of a separate container to an inner load bearing structural member (e.g. [23]). There remained some debate about the adequacy of existing creep data. The limiting property was the creep ductility. While it was claimed that the creep ductility of OFP copper was sufficient to the necessary long times for this application [31], Fig.D 2, there was an alternative view that the evidence presented to justify this position was insufficient [32]. The creep of copper in these circumstances therefore continued to be a source of uncertainty.

D4 Environmental Damage

The main risk of environmental damage to copper canisters in a bentonite buffered Opalinus clay geological structure came from general corrosion. The possibility of localised (pitting) attack, microbiologically influenced corrosion, and stress corrosion cracking was conceivable, but most unlikely in such a host environment [33].

Copper tended to corrode uniformly with surface roughening but no localised corrosion. The element was susceptible to MIC if microbes were active, and also to SCC in a few specific environments (and then only under aerobic/oxidising conditions[4]). Copper was effectively thermodynamically stable in water and Cl^- solutions at neutral-alkaline pH, but would corrode with the evolution of H_2 in the presence of sulphide.

It had been claimed that under anoxic conditions copper could corrode with the evolution of hydrogen, and that the corrosion rate was high enough to impact on the lifetime of the SKB canister [34], although the findings of hydrogen generation had not been confirmed in other studies [35]. The absence of hydrogen generation (in the absence of sulphide) provided a significant advantage of copper barrier based solutions due to the associated minimal impact on the condition of the surrounding bentonite and geological barrier.

D4.1 General Corrosion

Significant general corrosion of copper was judged only likely to occur in the short time when aerated conditions prevailed. Corrosion to depths of 0.1 to 1mm could be possible during the initially moisture unsaturated aerated period [33]. However, during the long-time phase when moisture saturated anoxic and reducing conditions prevailed, corrosion rates reduced significantly, varying only between ~0 and ~0.001μ/a, with the higher values being associated with the presence of sulphides [33]. Copper was thermodynamically stable in water in the absence of sulphide.

This information compares with the NWMO overall one million year copper corrosion allowance of 1.27mm [36].

Evidence from archaeological analogues was available for copper samples, e.g. Fig.D 3. However, the relevance of this type of information could be limited due often to variations in chemical composition and environmental conditions which were unlikely to have been constant during the artefact's buriel. Nevertheless, the results of the study shown indicated a range of corrosion rates

[4] *SCC is possible in copper in anaerobic sulphide solutions with high HS^-*

between 0.025 to 1.27μm/a [37] which, due to the harsh conditions, could be considered to be an upper limit to that expected in a repository.

At relatively low dose rates (~13-27Gy/h), γ-radiation may have a beneficial effect on corrosion rate, but could have a significantly deleterious influence at dose rates ≥~700Gy/h [38].

D4.2 Localised Corrosion

Localised corrosion (pitting) was considered to be improbable in a bentonite buffered environment [33]. This was primarily because at higher pH, copper passivated (Fig.D 4). Pure copper tended to surface roughen rather than discretely pit under simulated repository conditions, and undulations of ±50μm are assumed in the KBS-3 safety case analysis.

What is now regarded as an extremely unrealistic prediction (and a highly unlikely event) is that by an early Swedish study which indicated that there was an effectively negligible probability that any pit on any one of 10,000 canisters could reach a depth of <8mm in 10^6 years [39].

D4.3 Microbially Induced Corrosion

While MIC of copper is possible in the presence of active microbes and biofilms, the potential rates of 0.2-8nm/a in compacted bentonite (inversely related to density) [40] appeared to be too small to severely limit the lifetime of the canister.

D4.4 Stress Corrosion and Hydrogen Induced Cracking

SCC was considered feasible (but unlikely) during the initial part of the aerobic phase, although the evidence suggested it to become unlikely in long times [4]. In these circumstances, in water saturated anoxic conditions, the maximum concentrations of critical species (such as oxygen, acetates, nitrates, ammonia and sulphides), and the corrosion potential, lay below the respective threshold conditions for SCC [41]. While SCC of copper could be feasible (but unlikely in repository conditions), HIC was generally regarded as not being possible [4], but with reservations [42].

D5 Fabrication

D5.1 Manufacture

Copper Shell. Copper canisters were made from cylindrical copper ingots which were then formed by extrusion, pierce-and-draw processing or forging [25]. Pierce-and-draw processing offered the advantage of canister manufacture with an integral bottom, as an alternative to the manufacture of cylinders requiring both bottoms and lids to be welded.

Copper-Coated Solution. Possible copper coating techniques for this application have already been reviewed in Sect. D2.2. While the feasibility of copper electro-deposition to depths in excess of 5mm on full size BWR type SF rod canisters had already been demonstrated, as had the concept of final cold spray coverage of the sealing weld, production development activity was still required [29].

D5.2 Welding

Copper Shell. Electron beam welding was currently the first choice sealing weld procedure for the KBS-3 copper shell, with friction-stir welding as the back-up solution [26]. The full penetration welding of 50mm thick copper sections (greater in the case of the shell bottoms prior to final machining) was challenging, but high integrity welds by both techniques were now possible.

Copper-Coated Solution. Welding was not an issue for the copper-coated carbon steel canister solution. The final weld would be between the carbon steel container and lid, with the joint covered by a layer of cold sprayed copper.

D5.3 Inspection

Prior to the KBS-3 development, there was little non-destructive testing inspection experience for large thick section copper structures. Copper canister manufacturers such as Wyman Gordon and Vallourec & Mannesmann Tubes employed ultrasonic testing, but only for defect detection, and not sizing [25]. With development activities focussing on time of flight diffraction (TOFD) and phased array, it was now possible to also size defects to the required acceptance standard.

D6 Costs

Investment/Development Costs. Significant costs had already been accumulated for the development of the 50mm thick KBS-3 outer copper shell (App. **H**), and it was not known how much more was required. Nevertheless, it must be reasonable to assume that the remaining effort was now likely to be relatively low compared with the current KBS-3 overall development budget of >100MCHF (App. **H**).

Similarly, the outstanding development costs required for the copper-coated carbon steel canister solution were not known with certainty. However, a significant investment had already been made, and the remaining required development activity was therefore likely to be relatively low.

Unit Costs. Predictably, the unit cost of a canister with a 50mm thick copper outer container was significantly more expensive than one involving a 5mm thick deposit of copper. The respective costs were 200-250kCHF compared to 175-220kCHF

D7 Summary

Copper provided a good solution for the outer corrosion resistant barrier of nuclear waste disposal canisters. Although susceptible to repository environmental damage during the initial dry aerobic disposal phase, it was almost immune to general and local corrosion processes, and to SCC and HIC during the long-time moist anoxic period (in particular in the absence of sulphide). Importantly, a copper outer skin posed insignificant risk to the integrity of the surrounding geological barrier. The material was low strength and high ductility, and entirely reliant on an appropriate sub-structure for mechanical integrity, which could be a cast iron insert as in the case of KBS-3 or a complete carbon steel container for a copper coated container solution.

Copper crept at room temperature, and this provided a potential problem for the KBS-3 canister as the clearance gap to the cast iron insert was closed due to external pressure resulting in the possible exhaustion of multi-axial ductility at stress concentrating features. This uncertainty did not exist for copper coated steel container solutions.

Copper-based solutions were relatively well advanced, and would involve relatively low future development costs. While currently the price of copper was at an acceptable level, there was no guarantee that this would remain the case in future as demand begins to outstrip supply.

Table D1: Indicative Material Characteristics of the EN1976 Modified OFP Copper for KBS-3 Canisters

PROPERTY	EN1976		KBS-3
	Cu-OFE	Cu-OFI	[22,25]
Chemical Composition			
Cu, wt%	99.99[a)]	*Rem*	
Ag, ppm	≤ 25	≤25	
As, ppm	≤ 5	5[b)]	
Fe, ppm	≤ 10	10[c)]	
S, ppm	≤ 15	≤15	≤ 8
Sb, ppm	≤ 4	≤ 4	
Se, ppm	≤ 3	2[d)]	
Te, ppm	≤ 2	2[e)]	
Pb, ppm	≤ 5	≤ 5	
P, ppm	≤ 3		30-70
Bi, ppm	≤ 1		
Cd, ppm	≤ 1		
Mn, ppm	≤ 0.5		
Hg, ppm	≤ 1		
Ni, ppm	≤ 10		
O, ppm	≤ 5		≤ 5
Sn, ppm	≤ 2		
Zn, ppm	≤ 1		
H, ppm			≤ 0.6
Mechanical Properties			
$R_{p0.2}$, MPa			
R_M, MPa			
A, %			≥ 40
E, GPa			
K_{IC}, MPa√m			
ε_R, %			≥ 10
Physical Properties			
ρ, g/cc			
CTE, μm/m/°C			

[a)] *Including Ag,* [b)] Σ*(As+Cd+Cr+Mn+Sb)* $\leq$ *15ppm,*
[c)] Σ*(Co+Fe+Ni+Si+Sn+Zn)* $\leq$ *20ppm,* [d)] Σ*(Bi+Se+Te)* $\leq$ *3ppm,*
[e)] Σ*(Se+Te)* $\leq$ *3.0ppm [22,25]*

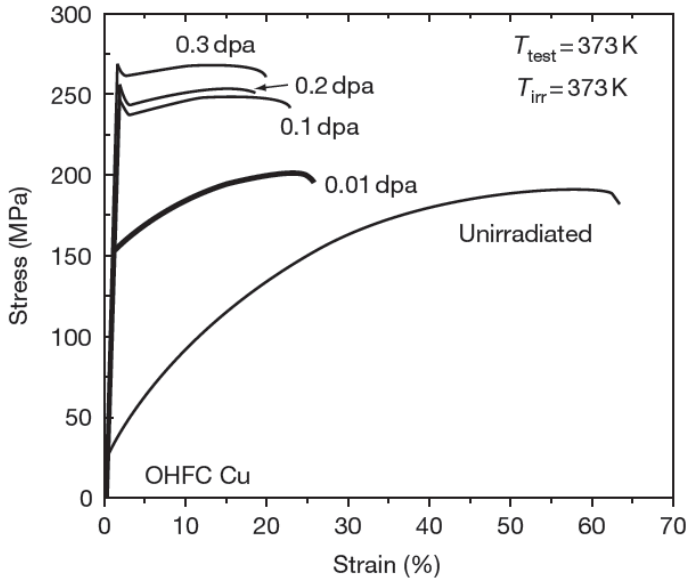

Fig.D 1 Influence of neutron irradiation on engineering stress strain characteristics for OFHC copper at 100°C [30]

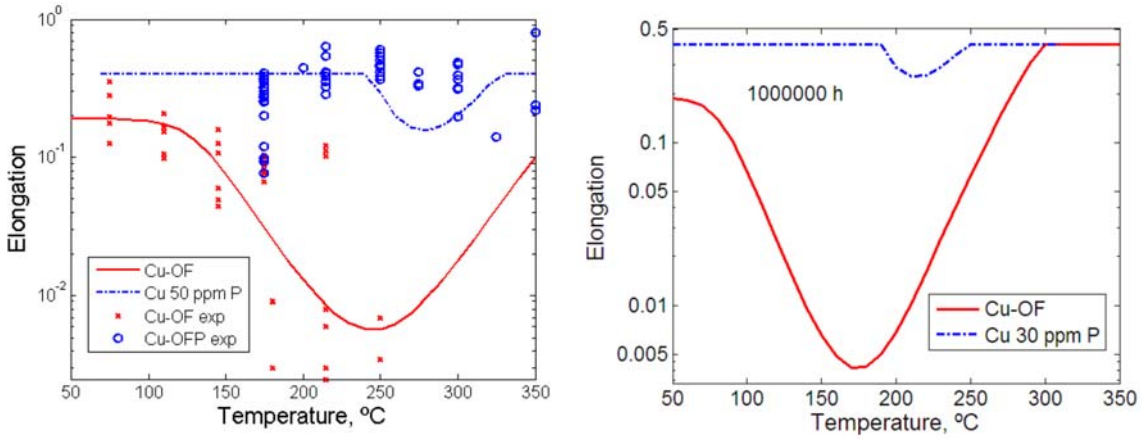

Fig.D 2 (a) Comparison of predicted and experimental 10kh creep-rupture elongations as a function of temperature for Cu-OF (0ppm P) and Cu-OFP (30ppm P), and (b) Predicted 1,000kh creep-rupture elongations for Cu-OF and Cu-OFP [31]

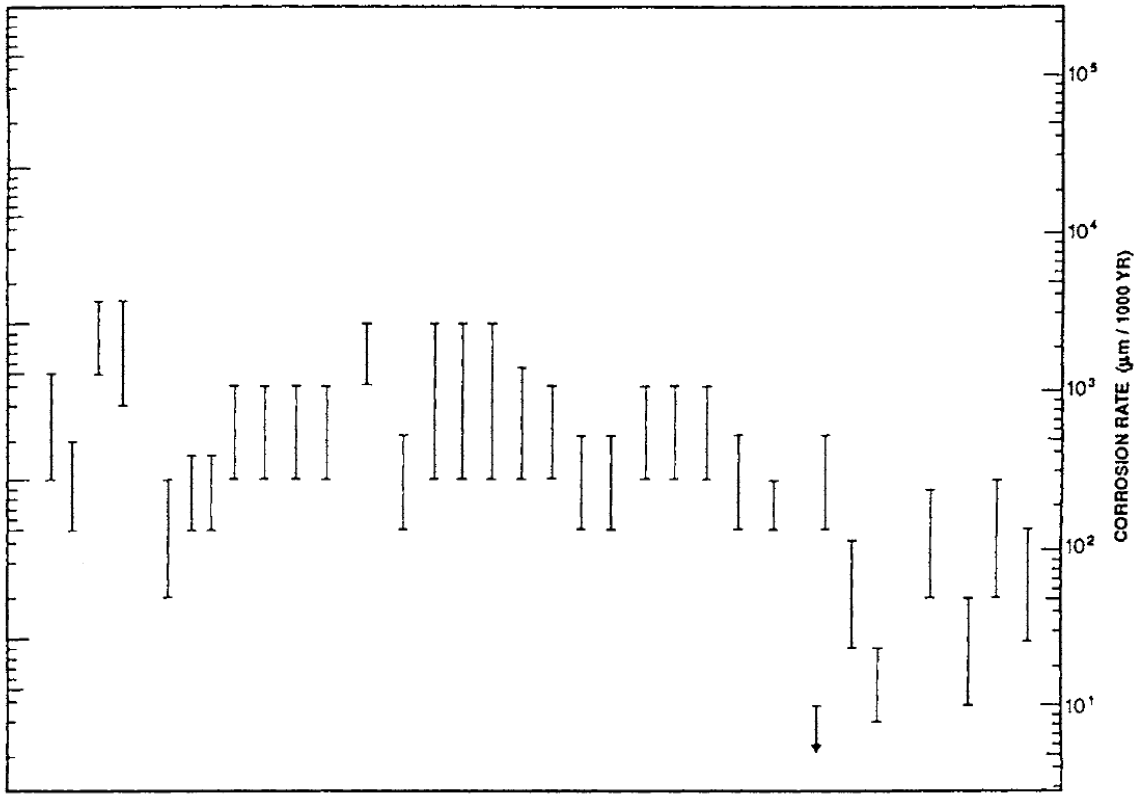

Fig.D 3 Corrosion rate data for 33 archaeological artefacts composed of copper or copper alloys [37]

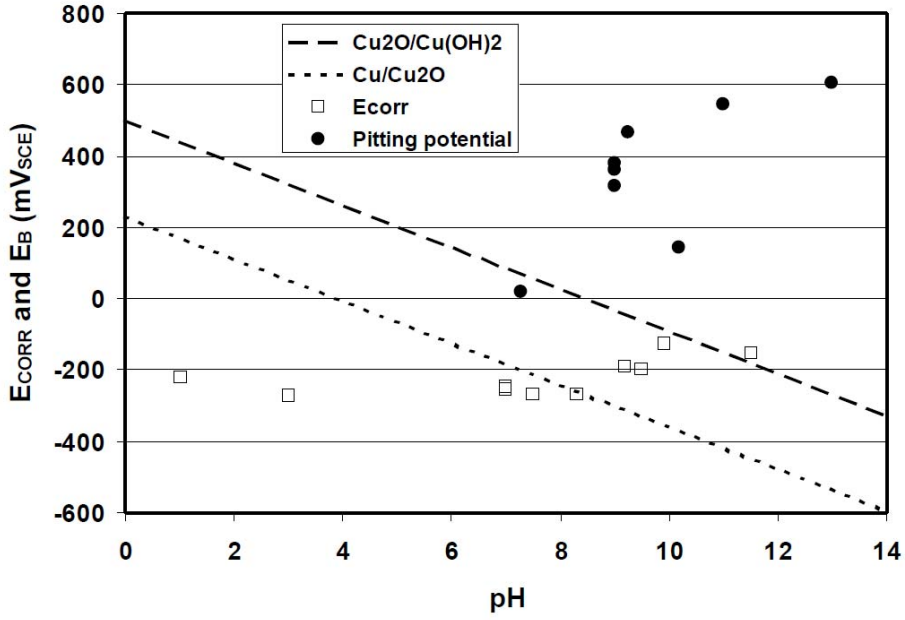

Fig.D 4 Dependence of the pitting and corrosion potentials of copper in 0.5mol/l chloride solution as a function of pH [38]

The dashed and dotted lines represent the equilibrium potentials for the $Cu_2O/Cu(OH)_2$ and Cu/Cu_2O couples respectively

APPENDIX E: TITANIUM AND TITANIUM ALLOYS

E1 Background and Introduction

Titanium and titanium alloys were widely used as full body and cladding materials for a variety of petro-chemical and aerospace pressure vessel applications [43], Fig.E 1. The combination of strength and toughness properties, superior corrosion resistance and low density made this class of materials very attractive for a variety of uses but, in practice, the high cost limited the scope of application. The use of titanium had been considered by a number of countries as a material for SF or VHLW disposal containers [44], either as the primary canister material or as a thinner layer surrounding a steel/iron-based support structure. The grades evaluated were those summarised in Table E1, with the main focus being on the single alpha -phase grades (i.e. ASTM Grades 2 and 7), but also with an interest in two of the alpha-beta grades (i.e. ASTM Grades 5 and 12). While Grade 7 had been the most widely evaluated for this application, Grade 12 had been regarded as a cheaper alternative. In practice, to date, the actual feasibility evaluation of a Ti Grade for this application had been limited to use as drip shields [45].

Titanium alloys ccould be susceptible to: general corrosion, crevice corrosion, and hydrogen induced cracking. However, they formed an extremely stable TiO_2 passive film, and were considered to be immune to MIC. Titanium alloys were immune to pitting under repository conditions.

Titanium alloys could be susceptible to rapid hydrogen pick-up in crevice conditions, and in such circumstances it was advisable to use crevice corrosion resistant grades. A main advantage of titanium alloys was that crevice-corrosion resistant grades could potentially survive very long canister lifetimes with minimal impact on other barriers. The disadvantages were that there was no long term corrosion data, and that a titanium alloy shell would require internal support.

E2 Material Characteristics

Material details of candidate Ti-Grades are summarised in Table E1. The most commonly used titanium was commercially pure (CP, e.g. Gr.2). For resistance to crevice corrosion, additions of palladium (e.g. Gr.7) or of molybdenum and nickel (e.g. Gr.12) were made to the CP grade. Increased strength was achieved by the addition of aluminium and vanadium to produce α+β alloys such as Gr.5.

As-clad Gr.7 was widely used for petro-chemical applications, and there was well-established experience of fabricating (e.g. Fig.E 1) and explosive bonding formed sheet of titanium grades [43].

E3 Mechanical Properties

Nominal mechanical properties for a number of Ti-Grades are reviewed in Table E1. There was evidence to show that these could be influenced by irradiation at temperatures of 21 and 150°C, most notably by a reduction in ductility, Fig.E 2 [46]. Evidence for the influence of temperature on the tensile strengths of Gr.2 and Gr.7 were determined from [47]. Minimum $R_{p0.2}$ and R_M values of 220MPa and 300MPa respectively were assumed for the mechanical integrity calculations for 150°C in Apps **I** and **J**.

The reduction in ductility associated with irradiation was also reflected by a significant reduction in fracture toughness, Fig.E 3, e.g. for Gr.5, from ~80 to ~40MPa$\sqrt{m}$ at 22°C [46]. There was a relatively small influence of hydrogen on the fracture toughness of Gr.7. A fracture toughness of 66MPa$\sqrt{m}$ was assumed for Gr.2 and Gr.7 in the mechanical integrity calculations conducted in App. **J** (Table E1).

Titanium and titanium alloys were susceptible to creep at room temperature at stresses of yield point magnitude. While creep rates were very slow compared with those of copper, they could not be ignored in the design assessment of a nuclear waste disposal canister.

E4 Environmental Damage

The excellent corrosion resistance of titanium alloys resulted from the formation of very stable, continuous, highly adherent and protective oxide films (e.g. TiO_2) on the metal surface which readily repaired, when damaged, in the presence of oxygen or moisture [14].

E4.1 General Corrosion

As a result of the stability of the passive oxide films formed on the surface of titanium and its alloys, general corrosion rates were of the order of nm/a, and relatively insensitive to the presence of chloride ions and temperature. Only under very acidic conditions (pH < 1) in concentrated Cl^- solutions was there a possibility of de-passivation. Rates of up to 0.02μm/a had been observed under aerobic conditions [48]. Rates of ~0.001μm/a had been reported for Ti Gr.2 and Gr.7 in a dilute synthetic groundwater, and in contact with compacted bentonite [49].

Coupling with dissimilar metals did not accelerate the corrosion of titanium [14].

No detrimental effects on corrosion properties of γ-radiation had been reported for Gr.2, Gr.7 or Gr.12 for dose rates below ~100Gy/h at temperatures up to 250°C [14].

E4.2 Localised Corrosion

Ti alloys were extremely resistant to pitting due to the stability of the passive film. However, commercially pure grades of Ti alloys were susceptible to crevice corrosion (Fig.E 4). Palladium containing grades (e.g. Gr.7) were resistant to crevice corrosion.

E4.3 Microbially Induced Corrosion

Ti alloys were immune to MIC [50].

E4.4 Stress Corrosion and Hydrogen Induced Cracking

Titanium alloys were generally very resistant to SCC, and in particular in repository related environments [14,51]. Incidences of SCC had been reported at stress levels in excess of yield and with superimposed vibratory stresses, but this mechanism in Ti alloys for this application could be avoided with adequate post weld stress relief.

Titanium alloys were susceptible to HIC due to the formation of brittle hydride phases [48], with the higher strength α+β alloys being the most susceptible. Hydrogen was a by-product of crevice corrosion which was avoided through the adoption of Gr.7, but the long term vulnerability of this Ti grade to HIC needed to be assessed.

E5 Fabrication

E5.1 Manufacture

Practices for the manufacture and fabrication of solid and clad titanium parts were well established for a variety of petro-chemical and aerospace pressure vessel applications [43]. However, while processes such as hot-roll and explosive bonding were commonplace for flat and internal curved (concave) surfaces, they were not feasible for external curved (convex) surfaces. Weld over-laying steels was not an alternative for Ti-Grades because of problems associated with Fe contamination. The solutions for nuclear waste disposal canisters were therefore solid Gr.2 or Gr.5, or the adoption of a Gr.7 welded sleeve over a carbon steel structure. For the sleeve solution, a screw-based mechanical fixation had been proposed to avoid potential problems associated with cold creep of the titanium [43].

The feasibility of Ti plating had been demonstrated [52], but the technology had not since been exploited.

E5.2 Welding

Techniques for welding Ti-Grades were well developed, and involved very clean conditions. Without appropriate precautions, Ti weldments were vulnerable to contamination. In particular, the integrity of Ti weldments was severely affected by the presence of grease or oil leading to porosity, gases (O_2, N_2 or H_2) responsible for embrittlement, and to iron bearing species. Normally, TIG or plasma processes were adopted. The problems associated with iron contamination posed difficulties when welding Ti-clad steel structures, but could readily be overcome by experienced specialist fabricators [43].

E5.3 Inspection

Solid and clad Ti grade pressure vessel technology was well developed, and the inspection capability for surface and sub-surface defect detection and sizing to the required Standards was available [43].

E6 Costs

While the properties and applicability of titanium grades were very attractive, the cost of these materials was very high. Compared with a price of ~0.7CHF/kg for carbon steel, the respective material costs of Ti Gr.2, Gr.7, Gr.12 and Gr.5 at the time of reporting were ~30, ~, ~115, ~50 and ~60 CHF/kg. These figures were also summarised in Table 5, in which costs relative to carbon steel are given by volume (as well as by weight) in order to reflect the lower densities of titanium grades.

The cost of large solid titanium canisters were prohibitively high. Estimated costs for 100mm thick 9-BWR SF rod canisters (without internals and welding) were estimated by one fabricator to be in excess of 338kCHF and 125,000kCHF for Gr.2 and Gr.7 respectively. The cost of a Gr.7 clad version was estimated to be >280kCHF.

Similar indicative costs for 3m long, 50mm thick VHLW canisters were also available. The cost of a solid Gr.2 canister was estimated to be ~77kCHF, while that of a Gr.7 clad carbon steel container was estimated to be ~112kCHF.

E7 Summary

Titanium and titanium clad carbon steel containers provided attractive solutions for consideration for nuclear waste disposal canister applications. The resistance to environmental damage of titanium in repository environments was very high, although there were concerns about uncertainties associated with the prediction of very long term corrosion behaviour of passive materials. There was good experience of fabricating large section pressure containing parts out of titanium, and the development costs of such a concept would be relatively low, but material costs were high.

Table E1: Characteristics of Candidate Titanium Grades for Nuclear Waste Disposal Application

PROPERTY	Grade 2		Grade 7		Grade 12		Grade 5		Grade 6	
	min	*max*	*min*	*max*	*min*	*max*	*min*	*max*	*min*	*max*
Chemical Composition										
N, wt.%	-	0.03	-	0.03	-	0.03	-	0.05	-	0.05
C, wt.%	-	0.08	-	0.08	-	0.08	-	0.08	-	0.08
H, wt.%	-	0.015	-	0.015		0.015	-	0.015	0.017	0.020
Fe, wt.%	-	0.30	-	0.30	-	0.30	-	0.40	-	0.50
O, wt.%	-	0.25	-	0.25	-	0.25	-	0.20	-	0.20
Pd, wt.%			0.12	0.25						
Mo, wt.%					0.20	0.40				
Ni, wt.%					0.60	0.90				
Al, wt.%							5.50	6.75	4.0	6.0
V, wt.%							3.50	4.50		
Sn, wt.%									2.0	3.0
Mechanical Properties										
$R_{p0.2}$, MPa	275	450	275	450	345	-	828	-	793	-
R_M, MPa	345	-	345	-	483	-	895	-	827	-
A, %	20	-	20	-	18	-	10	-	10	-
E, GPa	105(110)		105(110)		103		110		110	
K_{IC}, MPa√m	66	-					80			
μ	0.37		0.37							
Physical Properties										
ρ, g/cc	4.51		4.51		4.51		4.43		4.48	
CTE, μm/m/°C	8.70		8.70		9.50		9.30		9.5	

Requirements according to ASTM B265

(a) (b)

Fig.E 1 Examples of seam welded titanium fabrications (courtesy Loterios SpA) [43]

The submersible in (b) is 45mm thick and 800mm in diameter

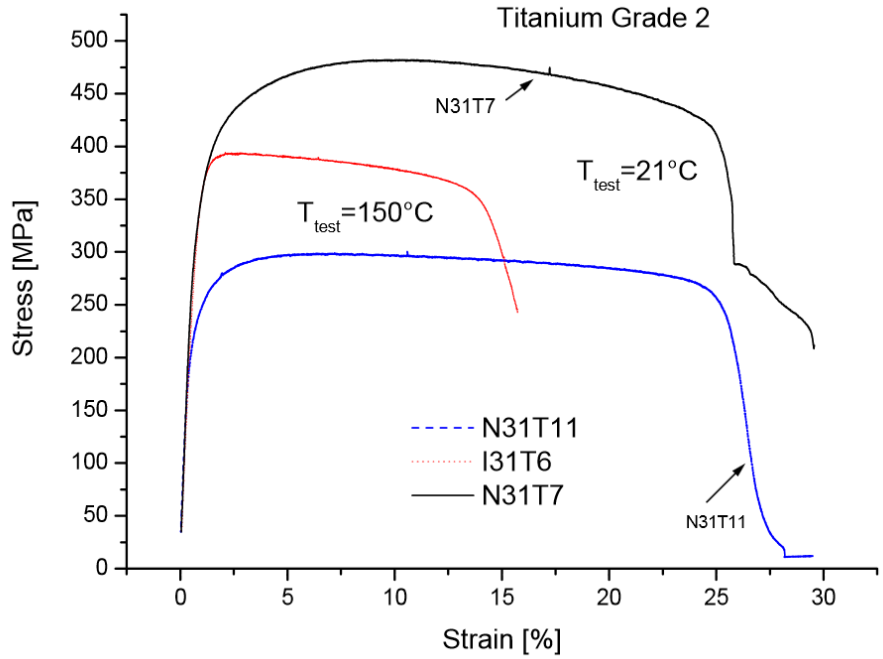

(a)

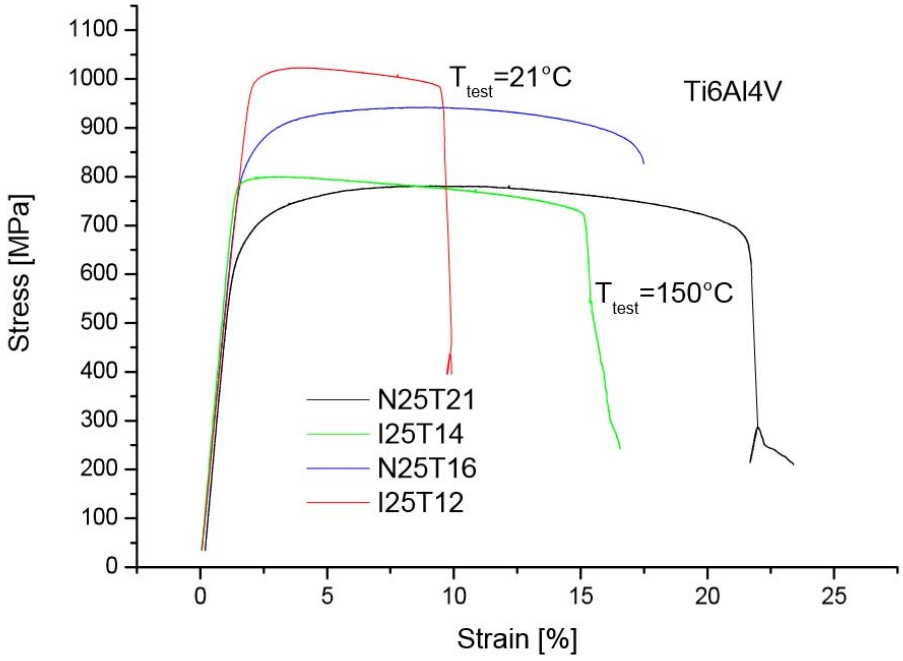

(b)

Fig.E 2 Influence of irradiation on tensile properties for (a) Ti-Grade 2 (I3IT6 was irradiated with high energy protons at 150°C, to 0.1dpa), and (b) Ti-Grade 5 (I25T12 tested at 21°C had a dose of 0.13dpa and I25T14 tested at 150°C had a dose of 0.04dpa) of this material[46]

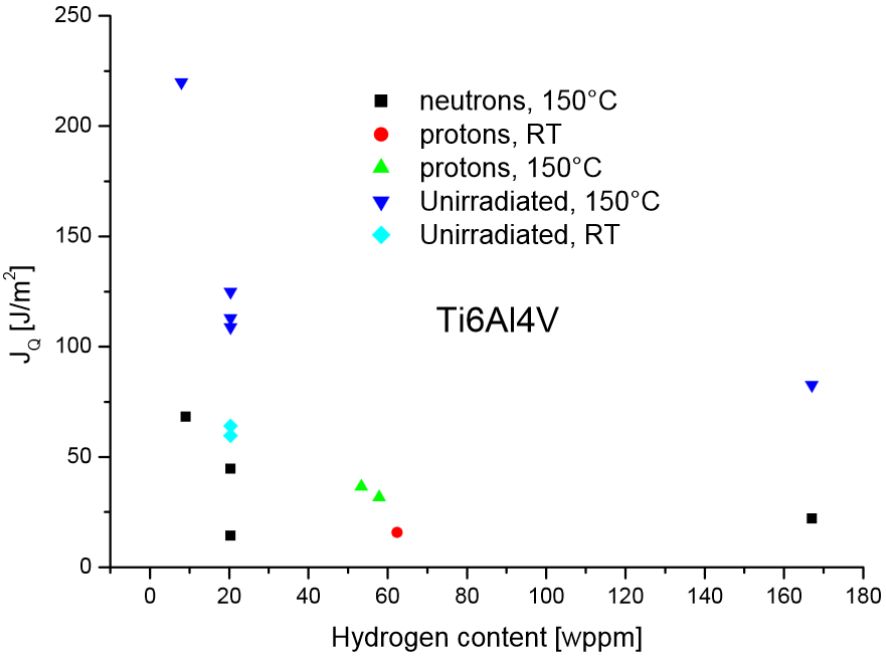

Fig.E 3 Influence of hydrogen on fracture toughness of Ti6Al4V alloy, unirradiated, irradiated at 150°C with protons to 0.163dpa and neutrons to 0.154dpa [46]

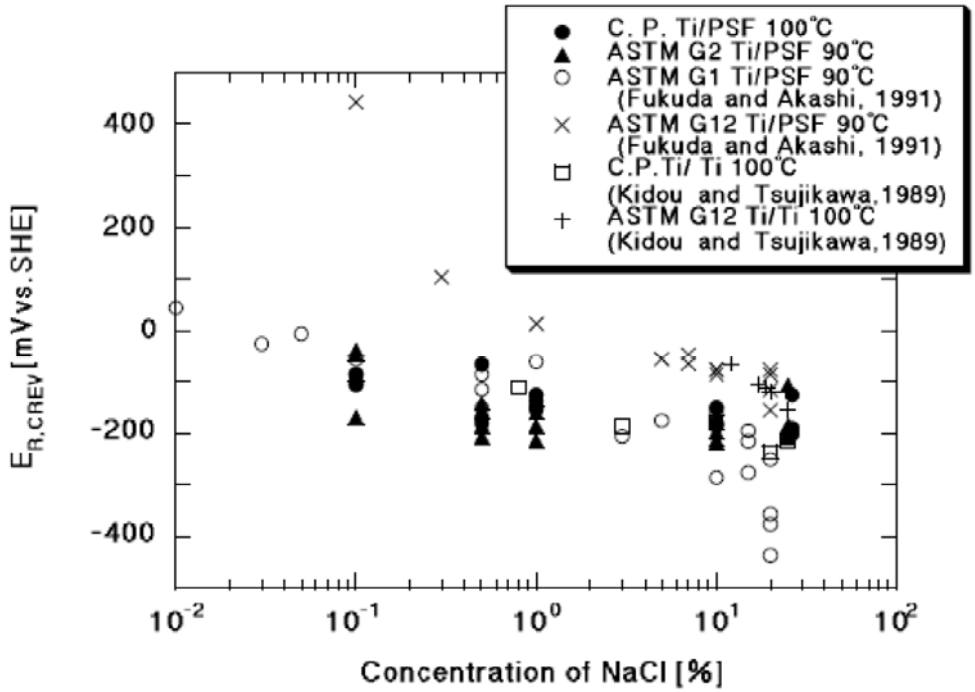

Fig.E 4 Dependence of the crevice re-passivation potential on chloride concentration for various titanium alloys [17]

APPENDIX F: NICKEL BASE ALLOYS

F1 Background and Introduction

Various nickel alloys had been considered for use as materials for SF or VHLW disposal canisters, either as the primary canister material or as a thinner layer surrounding a steel/iron-based support structure. The nominal compositions of these are summarised in Table F1.

A major attribute of Ni alloys is their formability and weldability, there being extensive experience in the manufacture and joining of such materials in a wide range of environments. Two solutions were considered in the following appendix. Complete containers could be constructed from Alloys 617 or 625. Alloy 617 in particular was not a traditional choice for this application, but both of these solution treated alloys were readily weldable without PWHT (apart from in very thick sections), were now being widely adopted for ultra super critical steam pipework, and were thereby readily available in standard pipe sizes.

Of the Ni-base alloys regarded suitable for the provision of an outer corrosion resistant barrier, Hastelloy C22 was the most widely considered, being adopted as the solution for the Yucca Mountain Project. Even though subsequent alloy development led to Alloys 59 (VDM), 685 (Special Metals) and C2000 (Haynes), focus in the US remained with C22 as a result of the significant prior investment [53,54]. Because of the theoretical potential for localised corrosion of C22 under conditions involving dripping chloride solution and consequent concentration over many years, Gr.7 titanium drip shields were introduced to eliminate the problem [45].

F2 Material Characteristics

The chemical compositions, and mechanical and physical properties for a number of nickel alloys, including Alloys 617/625 and C22 are summarised in Table F1.

Initially, C22 was only used in the ESR condition to reduce the impurity level, improve weldability and increase corrosion resistance, but the material could also be used in the AOD condition to reduce costs [53]. For nuclear waste storage container applications, it was usually considered for adoption as a 3-4 to 10-12mm thick cladding on steel (20mm thickness for Yucca mountain). It was claimed that integral cladding could be achieved by explosive bonding, although the viability of this practice when applied to convex surfaces was questioned. Other possibilities were rolling or roll bonding, but such processes would require development activity for external curved surface applications. Weld overlay was also possible, but rarely considered for this application because of difficulties in achieving uniformly acceptable quality requirements.

F3 Mechanical Properties

Nominal mechanical properties for a number of nickel alloys are summarised in Table F1. As a generality the fracture toughness of such alloys, which were mostly in the solution treated (solid solution strengthened) condition, was very high (e.g. [55]) as indicated in Table F1. However, there was evidence to indicate that the fracture toughness of such alloys could be influenced by hydrogen, with values as low as ~60MPa$\sqrt{m}$ being reported for Alloy 625 weldments under a H_2 pressure of 34.5MPa [57]. The significance of this evidence for Swiss nuclear waste repository conditions was questionable.

Evidence for the influence of temperature on the tensile strength of Alloy C22 was determined from [56]. Minimum $R_{p0.2}$ and R_M values of 270MPa and 650MPa respectively were assumed for the mechanical integrity calculations for 150°C in Apps **I** and **J**.

F4 Environmental Damage

The candidate nickel base alloys contained high Cr concentrations, and were relatively immune to general corrosion under aerobic condition due to the presence of a thin layer of Cr_2O_3 or $Cr(OH)_3$. In circumstances responsible for the breakdown of the passive film, the alloys became vulnerable to local corrosion processes such as pitting and crevice corrosion.

F4.1 General Corrosion

NiCrMo alloys were protected from corrosion by a Cr-based passive film. Of this alloy class, Inconel 625 and Hastelloy C22 were expected to have lower corrosion rates due to their higher Cr levels. The

mean corrosion rate of C22 in a range of simulated concentrated Yucca Mountain pore waters at a temperature of 60°C was 5-10nm/a, based on 5 and 10 year exposure tests [51]. Faster rates were observed under the more aggressive 'Q-brines' studied in the German programme [58], in which in 3 year tests corrosion rates ranged from 0.2μm/a at 90°C to 0.9μm/a at 200°C.

It was conceivable that the integrity of the passive layer responsible for such low corrosion rates could be compromised by the anodic segregation of sulphur at the metal film interface [60]. This risk was minimised by specifying high Cr and low S contents.

Nickel alloys were relatively sensitive to the influence of γ-radiation on corrosion properties. While no effect had been observed for dose rates up to ~1Gy/h, increases in corrosion rates and susceptibility to pitting had been reported for Alloy C4 for dose rates between 10 and 1000Gy/h [14].

F4.2 Localised Corrosion

NiCrMo alloys could be susceptible to film breakdown and transpassive dissolution.

A useful guide to the relative corrosion resistance (with respect to pitting and crevice corrosion) of stainless steels and nickel base alloys was the pitting resistance equivalent number (PREN), i.e.

$$PREN = \%Cr + 3.3\%Mo + 16\%N \qquad (F1)$$

Alloy C22 scored particularly highly in terms of such a parameter (Table F1),[5] although changes in metallurgical condition due to fabrication processes could influence crevice corrosion resistance [59].

The susceptibility of SF/VHLW materials to crevice corrosion was typically assessed by comparing the corrosion potential (E_{CORR}) with the re-passivation potential (E_{RCREV}). When:

$$E_{CORR} < E_{RCREV} \qquad (F2)$$

crevice corrosion would not develop. Chloride promoted film breakdown in nickel base alloys (e.g. Fig.F 1, Fig.F 2), whereas other anions such as nitrate, sulphate and carbonate were known to inhibit initiation (and possibly the propagation) of localised corrosion. Crevice corrosion in nickel base alloys could be related to Cr and Mo content (Fig.F 2). In the absence of localised film breakdown, NiCrMo alloys were resistant to corrosion over the practical range of redox potentials for this application. However, in the presence of Cl^-, pitting and crevice corrosion were possible under aerobic conditions. Under anaerobic conditions, pits or crevices would cease to grow.

F4.4 Microbially Induced Corrosion

Although not immune to MIC, the susceptibility of Ni-alloys to this corrosion mechanism was limited. Even in the presence of large quantities of nutrients, only a doubling of the general corrosion rate was reported [63].

F4.3 Stress Corrosion and Hydrogen Induced Cracking

The evidence of Speidel in Fig.F 3 suggested that the Ni-alloys listed in Table F1 were likely to be immune to SCC, whereas the evidence of Fleming and McCright was indicative of not complete immunity. Results generated in repository related environments were consistent with the evidence of Speidel [14,51].

Ni-base alloys were said to be immune to HIC in repository environments [64].

F5 Fabrication

F5.1 Manufacture

Practices for the manufacture and fabrication of solid and clad (overlay) nickel-based pressure vessels were well established for a variety of petro-chemical and aerospace pressure vessel applications [54]. The adoption of solid Ni-based canisters based on a standard pipe form was an attractive option, in particular from solid solution strengthened variants such as Alloys 617/625, which were now widely adopted for power generation applications with consequent lower costs due to higher production demand.

---

[5] *An alternative relationship is given as PREN = %Cr + 3.3.(%Mo + 0.5%W). This gives a similar ranking to Eqn. (F1)*

The use of corrosion resistant nickel alloys for cladding large steel pressure vessels had been well established for many years, in particular in petro-chemical industries [65]. Processes such as hot roll-bonding, explosive bonding and weld overlay were widely used, although of these, only weld overlay could realistically be used on convex surfaces. Sleeve solutions were an option without the same risk of creep as encountered with copper outer containers.

F5.2 Welding

There was much industry experience with the welding of nickel-based alloys such as Alloys 617/625 and C22, although it took x2-3 longer to weld C22 than, for example, Type 316 steel [53,54]. Solution treated alloys such as Alloys 617/625 had the advantage that they were readily weldable in large sizes and did not require post weld heat treatment except for thicker sections.

F5.3 Inspection

Solid and clad nickel-based pressure vessel technology was well developed, and the inspection capability for surface and sub-surface defect detection and sizing to the required Standards was available [54].

F6 Costs

Nickel-based alloys were expensive but not to the same extent as the most corrosion resistant titanium grades. For example, compared with a price of ~0.7CHF/kg for carbon steel, the respective material costs of Alloys 617/625 and C22 were ~30CHF/kg and ~46CHF/kg.

F7 Summary

Solid solution strengthened nickel alloy clad carbon steel containers provided attractive solutions for consideration for nuclear waste disposal canister applications. The resistance to environmental damage in repository environments was high, although there were concerns about uncertainties associated with the prediction of very long term corrosion behaviour of passive materials. There was wide experience of fabricating large section pressure containing parts out of nickel alloys, and the development costs of such a concept would be relatively low. Nevertheless, material costs were relatively high.

Table F1: Candidate Nickel Alloys for Nuclear Waste Disposal Application

PROPERTY	Nickel 200	Inconel 600	Inconel 617	Inconel 625	Inconel 800	Inconel 825	Hastelloy C4	Hastelloy C22	Hastelloy 276
Chemical Composition									
Ni, wt.%	≥ 99.0	≥ 72.0	≥ 44.5	≥ 58.0	30.0-35.0	38.0-46..0	65	56	57
Cr, wt.%		14.0-17.0	20.0-24.0	20.0-23.0	19.0-23.0	19.5-23.5	14.0-18.0	20.0-22.0	16
Fe, wt.%	≤ 0.40	6.00-10.0	≤ 3.0	≥ 5.0	≥ 39.5	≤ 22.0	≤ 3.0	2.0-6.0	5
Mo, wt.%			8.0-10.0	8.0-10.0		2.5-3.5	14.0-17.0	12.5-14.5	16
C, wt.%	≤ 0.15	≤ 0.15	0.05-0.15	≤ 0.10	≤ 0.10	≤ 0.05	≤ 0.01	≤ 0.015	≤ 0.01
Mn, wt.%	≤ 0.35	≤ 1.00	≤ 1.0	≤ 0.50	≤ 1.50	≤ 1.0	≤ 1.0	≤ 0.50	≤ 1
Si, wt.%	≤ 0.35	≤ 0.50	≤ 1.0	≤ 0.50		≤ 0.5	≤ 0.08	≤ 0.08	≤ 0.08
Cu, wt.%	≤ 0.25	≤ 0.50	≤ 0.5		≤ 0.75	1.5-3.0			
P, wt.%				≤ 0.015			≤0.025	≤ 0.020	
S, wt.%	≤ 0.010	≤ 0.015	≤ 0.015	≤ 0.015	≤ 0.015	≤ 0.030	≤ 0.010	≤ 0.020	
Al, wt.%			0.8-1.5	≤ 0.40	0.15-0.60	≤ 0.2			
Ti, wt.%			≤ 0.6	≤ 0.40	0.15-0.60	0.6-1.2	≤ 0.70		
Nb, wt.%				3.15-4.15					
V, wt.%								≤ 0.35	≤ 0.35
W. wt.%								2.5-3.5	4
Co, wt.%			10.0-15.0	≤ 1.0			≤ 2.0	≤ 2.5	≤ 2.5
B, wt.%			≤ 0.006						
PREN	-	16	52	51	21	31	35	66	69
Mechanical Properties									
$R_{p0.2}$, MPa	275-620	170-345	383	276-414	183	(324)	(335)	≥ 310	(364)
R_M, MPa	452-650	550-690	758	689-827	524	(690)	(805)	≥ 690	(783)
A, %	35-15	55-35	56	60-40	60	(45)	(63)	≥ 45	(59)
E, GPa	205	210	211	205	196.5	196	211	209	205
K_{IC}, MPa√m				(300)				(390)	
μ		0.26-0.33	0.26-0.33	0.26-0.33	0.26-0.33	0.26-0.33	0.26-0.33	0.26-0.33	0.26-0.33
Physical Properties									
ρ, g/cc	8.89	8.47	8.36	8.44	7.94	8.14	8.64	8.61	8.89
CTE, μm/m/°C	13.3	13.3	11.6	12.8	14.4	14.1	10.8	12.4	11.2

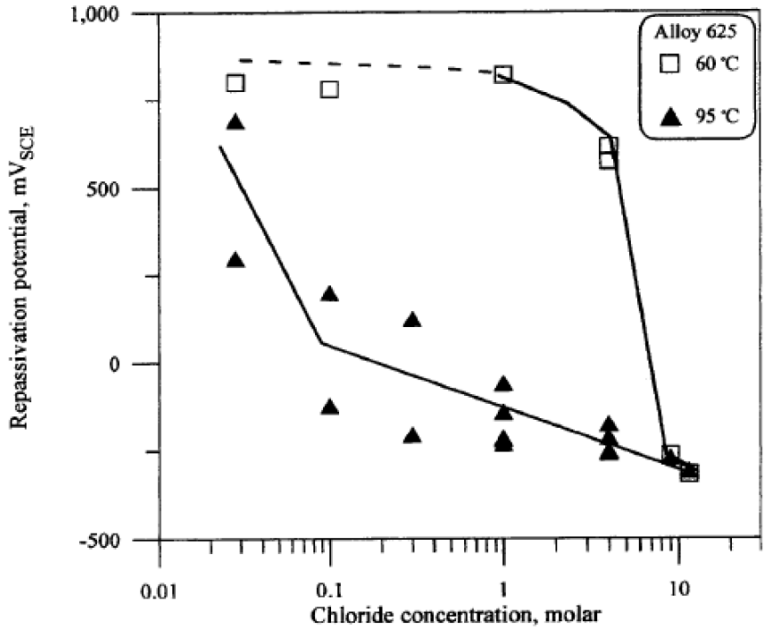

Fig.F 1 Influence of chloride concentration on crevice re-passivation potentials for Alloy 625 at 60 and 95°C [61]

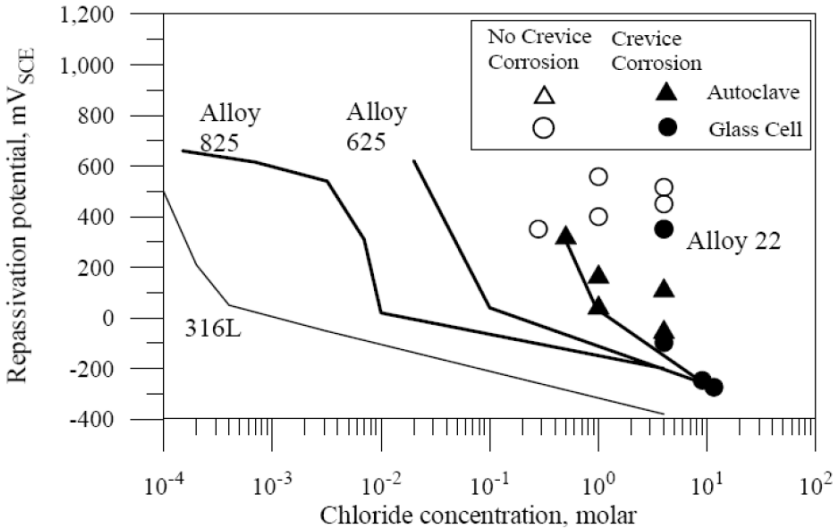

Fig.F 2 Comparison of crevice re-passivation potentials for a number of nickel-base alloys, as a function of chloride concentration [62]

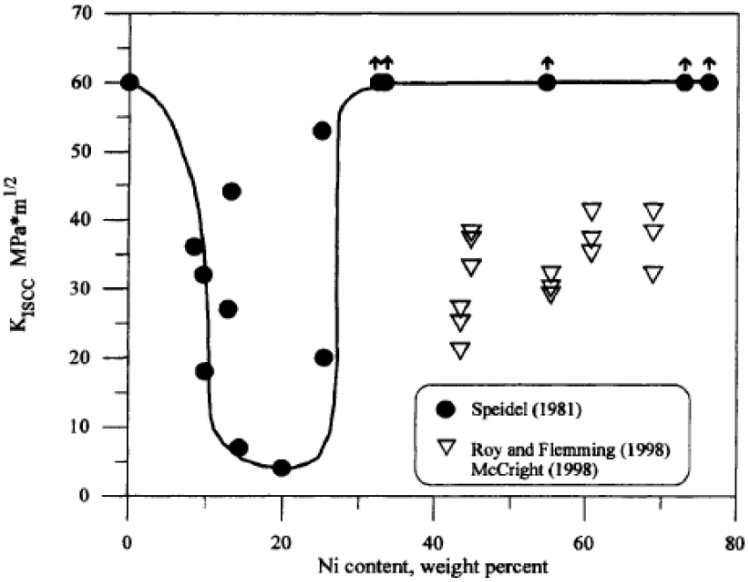

Fig.F 3 Influence of Ni content on K_{ISCC} of Ni-alloys in 5-22% wt% NaCl solutions at 90-120°C [61]

APPENDIX G: CERAMICS

G1 Background and Introduction

The use of ceramics for nuclear waste disposal containers was first seriously considered in the 1970s [66-68], and had continued to be an option [7,69-72], albeit apparently without a high level of commitment since the early-2000s. It seemed that there was insufficient motivation to invest in the research which would be necessary to overcome known difficulties, when there were already acknowledged feasible metallic canister solutions [70]. The reluctance of the ceramic parts manufacturers to invest without external support was almost certainly due in part to insufficient customer demand in the near future for large ceramic pieces.

Nevertheless, there had been significant developments relating to the consideration of ceramics as a candidate nuclear waste disposal canister material even since the last Nagra review in 2012 [70], and the comprehensive review of these is an integral part of the following appendix.

An indication of the engineering properties of materials from the main groups of technical ceramics is given in Table G1. Potential ceramics candidates for over-pack nuclear waste disposal canister applications were alumina (Al_2O_3), pure or in combination with silicon oxide (SiO_2) [7,67], silicon carbide (SiC) [71,72], silicon nitride (Si_3N_4), partially stabilised zirconia (PSZ), and titania (TiO_2), because of their chemical stability, reasonable mechanical properties, and ready availability [73]. The potentially less durable vitreous silicate ceramics were even more available, and more easily fabricated as monoliths due to lower processing temperatures. They could also be considered as candidates, although they suffered from low thermal conductivities (e.g. Table G1). Other non-oxide ceramics could be suitable, but they tended to be significantly more expensive to process than alumina. A characteristic feature of ceramics was their very low fracture toughness compared with metals. As a generality, the toughest ceramics had higher sintering temperatures, and were thereby harder to manufacture (in particular in large pieces), and harder to bond (join or seal) by thermally activated processes.

Up to the time of reporting, the main focus had been on the consideration of containers manufactured from Al_2O_3 [66,67] or Al_2O_3/SiO_2 [7]. Silicon carbide was also a realistic possibility [70,75]. Until recently, it was only feasible to manufacture large pieces out of SiSiC (silicon impregnated silicon carbide) and RSiC (recrystallised silicon carbide). However, now there was a possibility to make larger pieces from conventional SSiC (sintered silicon carbide) [72], and even high strength grades of SSiC [71]. Realising the potential of SiC for this application had been an important finding of the present project.

Despite these advances, maximum wall thicknesses were in the range of a few cms, and structural analysis calculations suggested that this could be insufficient for mechanical integrity under repository conditions (App. **J**). The limitations of even advanced SiC ceramics for disposal canister applications appeared to be acknowledged by the advocates of their use for this purpose invoking combination with structural strengthening by steel containment (e.g. Fig.G 1). The proposal with external structural support of course negated the main advantage of adopting a ceramic overpack solution to avoid the problems with hydrogen generation associated with steels (App. **B**).

G2 Material Characteristics

The characteristics of a range of ceramic materials are reviewed in Table G1. However, in the remainder of the following appendix, the focus is on Al_2O_3/SiO_2 and SiC grades.

Al_2O_3/SiO_2. Most recently, the feasibility of an Al_2O_3/SiO_2 canister solution was evaluated by Andra [7]. The characteristics of a range of compositions was systematically evaluated (Table G2), with a final focus being on the commercial P72 grade.

SiC. There were a number of variants of silicon carbide, namely sintered (SSIC), liquid phase sintered (LPSSiC), silicon infiltrated (SiSiC), recrystallised (RSiC) and SiC fibre reinforced (SiC_f/SiC), the latter being at a very early stage of development (and very expensive). Where available, properties for these grades are summarised in Table G3. SSiC is regarded as having the better properties, but like most ceramics (apart notably from SiSiC) was prone to significant shrinkage (up to 20%). SiSiC was regarded by many (but not all [71-77]) as currently the most appropriate grade for large structure

construction, but there were significant concerns about the material's corrosion resistance because of the relatively high proportion of infiltrated silicon contained in the microstructure. There was a view that the mechanical properties of SSiC were superior to those of SiSiC, but the apparent scarcity of reliable data for material in appropriate larger section size product forms made this opinion difficult to substantiate.

Si_3N_4. In principle, it was possible to fabricate large thick section silicon nitride parts, but there were several drawbacks to this being a candidate canister material compared with SSiC [78]. In contrast to Al_2O_3 and SSiC for which densification was achieved by diffusion-controlled 'solid-state sintering', the process for Si_3N_4 involved liquid phase sintering (LPS). In LP sintered materials, there always remained an amorphous glassy (or partially crystalline) grain boundary phase, notably responsible for increasing corrosion susceptibility. There was evidence to indicate that the strength of LP sintered materials (such as LPSSiC, Si_3N_4, YTZPE and ATZ) was significantly influenced by 100h exposures to water vapour, unlike materials such as Al_2O_3 and SSiC [78].

A significant drawback for Si_3N_4 could be that sintering was conducted under N_2 at 10bar pressure, and the maximum size of currently available gas tight furnaces with the required temperature capability was rather limited.

ZrO_2 had the advantage of high fracture toughness, but with the associated high sintering temperature. While the size of parts being manufactured in this ceramic was progressively increasing, it was not possible to manufacture a relatively small VHLW canister with the current state-of-the-art [76].

G3 Mechanical Properties

Elastic Modulus. Elastic modulus was an important mechanical analysis property, in particular for ceramics, since most types obeyed Hooke's law up to the point of fracture. There could be significant differences in the *E* values exhibited by different ceramics with values for oxide grades exhibiting lower values than non-oxide variants (Table G1a).

Fracture Strength. Nominal strength values for a number of ceramic grades are summarised in Table G1, but it was important to recognise that these would have been determined using relatively small specimens, and that there was a significant V_{spec}/V_{part} ratio strength effect which must be acknowledged in structural assessment [70], with the magnitude of this effect being determined by the Weibull modulus (*m*), i.e.

$$R_F^{part} = R_F^{spec} \cdot \left(V_{spec}/V_{part}\right)^{1/m} \qquad \text{(G1)}$$

In such a relationship, *V* is the volume of the specimen, or part, in which the stresses are tensile.

Following the Andra evaluation [7], an R_F^{spec} for Al_2O_3/SiO_2 of 131MPa was assumed to be representative. Then, adopting the Andra *m* value of 15, led to a long-time disposal load case scenario R_F^{part} of 97.3MPa, although a breaking stress value of 50.1MPa with a failure probability of 1:21,000 was ultimately adopted for assessment.

R_F^{spec} strength values for SiC were higher than those for Al_2O_3/SiO_2, and a representative value of 400MPa [72,71] was adopted for assessment purposes in this study. Assuming $m = 12$ [71] and similar specimen statistical strength distribution characteristics to those considered by Andra, respectively led to short and long-time load case specific R_F^{part} values of 144 and 304MPa, and ultimately assessment 1:21,000 failure probability breaking stresses of 90 and 250MPa.

Fracture Toughness. Published K_{IC} values for Al_2O_3/SiO_2 and SiC were typically ~1-3MPa√m [7]. In principle, K_{1C} should be determined by the same statistical approach standardised for flexural strength, and when adopting such an approach, ~2MPa√m may therefore be optimistic for alumina based grades. Fracture toughness values for SSiC and SiSiC appeared to be a little higher (e.g. Table G3). A value of 3.5MPa√m was assumed in the assessments conducted in App. **J**.

The highest toughness ceramics were typically the most refractory, and thereby the most difficult to sinter.

G4 Environmental Damage

Al_2O_3 and ZrO_2 were originally believed to be corrosion resistant in $MgCl_2$-rich brine, at high temperature and pressure [66]. However, the results of autoclave tests conducted by KfK under conditions aimed specifically at simulating a German repository environment appeared to show that Al_2O_3, ZrO_2, SiC and TiO_2 could be unsuitable for long duration VHLW packaging because of their susceptibility to IGA in salt brines [58]. Only steatite porcelain appeared to be resistant to general and local corrosion under these conditions. The results from the KfK screening and long term studies are reproduced in Tables G4 and G5 respectively. In these tables, weight gains represented brine intrusion into the ceramic specimens. Weight loss values were also influenced by brine intrusion effects, and were therefore indicative and should not be used in a quantitative way. It was now speculated that the form of silicon carbide evaluated was SiSiC which was in principle significantly more vulnerable to intergranular attack than SSiC because of its microstructural construction. At the time of reporting, it had not been possible to confirm this.

Porcelain comprising a high alumina content, but with Al_2O_3 grains surrounded by a glass mullite (Al_2O_3:SiO_2) matrix, exhibited the highest leaching rates due to preferential dissolution of the glassy phase in Canadian tests involving synthetic ground water without and with added Na-bentonite [79].

Chemical characterisation of a candidate alumina-silica ceramic container material had been determined using pure water Soxhlet tests at 100°C and column tests in Callovian-Oxfordian deep groundwater at temperatures between 50 and 90°C [7]. Although it was concluded that the chemical durability of the examined ceramic was suitable for purpose, an effective thickness reduction of ~3-4mm over a period of 1000 years was apparently predicted from the results of the groundwater tests.

There was evidence to show that Al_2O_3 was susceptible to stress corrosion cracking in deionised water at 20°C [80].

SSiC and LPSSiC grades had been shown to be susceptible to electrochemical corrosion in acid and alkaline solutions [81], although the practical significance of these observations in Swiss repository environmental conditions was not clear and needed to be quantified by investigation. Similarly, a small susceptibility to galvanic corrosion associated with SSiC/Ni and SSiC/steel couples had been identified [82].

There was little published information concerning the influence of γ-radiation on the corrosion behaviour of ceramics. For a given wall thickness, external surface dose rates were expected to be relatively low due to their low density, a view shared by [3].

G5 Fabrication

G5.1 Manufacture

Al_2O_3. As part of the Andra project [7], the feasibility of producing 40-50mm thick Al_2O_3/SiO_2 half-scale VHLW canisters was evaluated. With some technical difficulties, the concept was demonstrated at the half scale (Fig.G 2).

Silicon Carbide. Evaluating the potential of using SiC for the manufacture of nuclear waste disposal containers had been based on a review of manufacturers (Table G6).

Discussions with FCT Hartbearbeitungs [76] indicated that it was already potentially feasible to manufacture a half size VHLW canister (e.g. Fig.G 2), although verification was strongly recommended. Adequate press and sintering furnace capacities were already available [76]. Handling the large pieces necessary for such a structure, in the 'green' state, would be challenging but could conceivably be overcome, although attainment of acceptable density (porosity) levels may be a problem at 50mm thickness. In principle, this difficulty could be overcome by hipping (hot isostatic pressing). The cost of producing a prototype small VHLW container, without sealing, was estimated by FCT to be ~120kCHF.

SiCeram were more ambitious, suggesting that with an appropriate investment/development programme, the manufacture of full-size SF rod disposal canisters could be achieved, using for

example a hard sponge-like SiC based potting medium for added structural strength [72,77]. Details of the composition of this potting medium which could only be formed at T<400°C after SF rod insertion were not available. Samples had the appearance of SiC infiltrated Araldite.

G5.2 Coating

The ceramic coating of a carbon steel canister was a potential solution which had received limited attention because of the difficulties encountered so far in achieving a defect free deposit of the appropriate density and thickness [70]. While some progress had been made with the evaluation of up to 1mm thick alumina, spinel ($MgAl_2O_4$) and alumina/titania (Al_2O_3/TiO_2) coatings applied to steel by plasma, high velocity oxy-fuel, and detonation-gun spray processes [84], it had been concluded that thicker deposits would be required [70]. If this was the case, evaluation of the feasibility of thick, steel matching CTE coating applications would be necessary to minimise the risk of differential thermal strain induced cracking.

G5.3 Joining/Sealing

Sealing of ceramics remained a major challenge. Typically temperatures of at least 1200°C were needed to bond ceramic pieces together. Welding methods were generally not applicable, although there had recently been some progress in laser bonding SiC ceramic pieces, in particular using $Y_2O_3/Al_2O_3/SiO_2$ glass ceramic solders [83]. With this process, joint strength was currently reduced to less than half of the bending strength of the SiC substrate. Nothing was known of the resistance to environmental damage of such joints, although there was due cause for concern because of the significant glass content of the $Y_2O_3/Al_2O_3/SiO_2$ composition evaluated to date. With the current state-of-the-art, it was said to be possible to laser weld to a depth of 20-25mm, although in practice only 5-10mm thicknesses had actually been produced [77]. The limitation was not laser capacity but material heat flux characteristics. It may only be possible to achieve 50mm joint penetration depths using $Y_2O_3/Al_2O_3/SiO_2$ by increasing the glass content of the solder which would be unacceptable in terms of corrosion resistance [77]. Alternatively, a multi-step joining procedure could be feasible. It was proposed that the most appropriate form of sealing SiC nuclear waste canisters would be with a matching filler, rather than with a glassy based filler, but to the time of reporting, no work had been addressed to this topic.

G5.4 Inspection.

The feasibility of ultrasonic inspection was also evaluated as part of the Andra Al_2O_3/SiO_2 study [7]. It was shown to be possible to size 0.2 to 1mm defects in a 30mm wall thickness mould. These compared with the 0.12 to 0.39mm critical defect sizes identified in the mechanical integrity assessment forming part of the same investigation.

In principle, it was possible to characterise the defect condition in Al_2O_3/SiO_2 and SiC components using non-destructive inspection techniques such as ultrasonic testing, radiography, x-ray computed tomography and acoustic emission [85]. In practice, the feasibility of using such techniques for qualitative defect sizing in thick section (≤ ~50mm) had yet to be demonstrated for SiC. As mentioned above, the feasibility of using ultrasonic inspection for thick section Al_2O_3/SiO_2 had been demonstrated [7].

G6 Costs

G6.1 Investment/Development Costs

No information was available for an Al_2O_3/SiO_2 VHLW canister solution.

For SiSiC canister development, costs (not including those for joining/sealing) could be ≥ ~45MCHF [86] (Table G7). This was not inconsistent with the estimate of ≥ ~120MCHF for an SSiC total concept development activity [77].

G6.2 Unit Costs

No information was available for an Al_2O_3/SiO_2 solution. Powder costs appeared to be ~2-5CHF/kg.

While SiC powder costs were relatively low (5-10CHF/kg), the anticipated unit cost of a small VHLW container (Fig.G 2), after the appropriate investment would be in the range ~25-80kCHF, depending on the manufacturer consulted [76,86].

G7 Summary

While ceramics provided an attractive option in terms of their high corrosion resistance and the absence of gas (e.g. H_2) generation during long time emplacement, their mechanical strength and toughness property characteristics were low. While current press and sintering furnace capacities worldwide limited the size of canister sections which could be manufactured, such limitations could be overcome with the appropriate investment. Nevertheless major manufacturing challenges to be overcome with a systematic development activity included: *i)* effective handling of very large pieces in the green state, and *ii)* achieving adequate density (porosity levels) in section thicknesses of ≥ 50mm. Moreover, achieving effective sealing of thick section ceramics was never going to be possible without significant research and development activity. In the absence of a demand for large thick section ceramic pressure vessels from any other industrial sector, the funding of such R&D could only come from the nuclear waste disposal community.

There had been significant developments relating to the consideration of ceramics as a candidate nuclear waste disposal canister material since the last Nagra assessment in 2012 [70], and these had been comprehensively reviewed.

Table G1a: Engineering Properties of Some Ceramic Materials

	SiO_2-MgO	Al_2O_3 (96-99.1%)	Al_2O_3 (99.8%)	ZrO_2-MgO	ZrO_2-Y_2O_3	TiO_2	SiC	Si_3N_4-Y_2O_3
Gross density (g/cm^3)	2.2-2.8	3.80-3.82	3.96	5.74	6.08	4.26	3.10	3.21
Flexural strength (MPa)	110-180	280-350	500	500	1000	69-103	350	750
Compressive strength (MPa)		2000	4000	1600	2200		2000	3000
Fracture toughness (MPa√m)		4.0	4.3	8.1	10.0	2.5	3.8	7.0
Elastic modulus, dynamic (GPa)	70-120	270-340	380	210	210	283	350	305
Vickers hardness (GPa)		14-17	18	13	13		25	16
Thermal conductivity (W/mK)	2-5	24-28	30	3	2.5	8.8	100	21
Thermal expansion, CTE (10^{-6}/ºC)	4-7	7.1-7.3	7.5	10.2	10.4	9.4	3.5	3.2
Maximum operating temperature (ºC)	1000	1400	1500	850	1000		1800	1600
Melting point (ºC)		2015		2700		1840	2700	
	High insulating properties, low thermal conductivity	*High hardness, good wear resistance under abrasion, low electrical conductivity, relatively low cost.*		*Similar mechanical properties (Young's modulus, thermal longitudinal direction) to steel, making it especially suitable for composite steel/ ceramic components; harder than steel, low thermal conductivity, good tribology*			*Extremely hard, relatively light, good heat conducting properties, good tribology, resistant to thermal shock*	*Maximum mechanical strength, extremely fracture resistant, high hardness, relatively light, resistant to thermal shock*

Note: Based on information from [73,74]

Table G1b: Engineering Properties of Some Alumina-Zirconia (ZTA and ATZ) Composite Ceramics

	ZTA-950	ZTA-96	ATZ
Gross density (g/cm^3)	4.40	4.10	5.40
Flexural strength (MPa)	680	760	1600
Compressive strength (MPa)	2890		
Fracture toughness (MPa√m)	6.00	6.00	4.70
Elastic modulus, dynamic (GPa)	289	310	260
Vickers hardness (GPa)	1500	1750	1500
Thermal conductivity (W/mK)	15.0	21.6	
Thermal expansion, CTE (10^{-6}/ºC)	6.90	8.10	
Maximum operating temperature (ºC)	1500	1650	
Melting point (ºC)			
		15% ZrO_2	*18-22% Al_2O_3, 1-2% HfO_2, 3.6-4.1% Y_2O_3, 71-74% ZrO_2*

Table G2: Summary of Properties of Andra Evaluated Al_2O_3/SiO_2 Grades

Grade	P60	P72	E60	E72	E80
Al_2O_3	59.98	72.09	60.36	72.51	80.61
CaO	0.22	0.20	0.23	0.23	0.23
Fe_2O_3	0.25	0.26	0.35	0.27	0.22
K_2O	1.79	1.29	3.49	2.20	1.34
MgO	1.22	1.61	0.45	1.23	1.75
Na_2O	0.76	0.78	0.87	1.03	1.13
SiO_2	35.69	23.67	34.20	22.43	14.58
TiO_2	0.07	0.08	0.07	0.06	0.06
ρ_{bulk} (g/cm^3)	2.84	2.98	2.93	3.10	3.05
ρ_{solid} (g/cm^3)	3.07	3.17	3.04	3.30	3.47
Open porosity (%)	0.0	0.2	0.1	0.2	0.5
Closed porosity (%)	7.6	5.8	3.5	5.9	11.6
Breaking strength, (MPa)	106±9%	136±3%	102±8%	142±10%	136±8%
m		15			
K_{1C} (MPa√m)		1 - 3			
E, GPa	129	146	130	156	154
λ (W/mk)	3.4	5.3	3.5	5.8	7.4
μ	0.21	0.19	0.20	0.20	0.20

P grades were commercial grades (with quartz), E grades were specially prepared (without quartz)

Table G3: Summary of Properties of Silicon Carbide Grades

Grade	SSiC	LPSSiC	SiSiC
ρ (g/cm^3)	3.1 - 3.15	3.25	3.15 - 3.25
Porosity (%)	3	0	
Bending strength, (MPa)	400	450	
m	>12		
K_{1C} (MPa$\sqrt{m}$)	3 - 4	6.5	4 - 5
E, GPa	410	380	280 - 390
λ (W/mk)	100	80	
CTE (10^{-6}/°C)	4.0	4.9	
μ	0.16		

Table G4: Summary of Results of Corrosion Screening Tests on Ceramic Materials in Q-Brine[1),2)] [58]

MATERIAL	WEIGHT CHANGE (g/cm^2)	INTERGRANULAR CORROSION
Al_2O_3 *(>99.7% Al_2O_3)*	-1.9x10^{-4}	- [3)]
Steatite porcelain *(63% SiO_2; 30% MgO; Rest: Al_2O_3, Fe_2O_3, CaO, K_2O)*	-6.4x10^{-4}	- [3)]
ZrO_2 *(97% ZrO_2)*	-7.9x10^{-4}	- [3)]
SiC *(98%SiC)*	+5.5x10^{-5}	x [4)]
Zirconium-mullite *(18% SiO_2, 47% Al_2O_3, 33% ZrO_2)*	+5.5x10^{-3}	x [4)]
Zirconium-silicate *(65% ZrO_2, 33% SiO_2)*	+4.1x10^{-3}	x [4)]
Al_2O_3/ZrO_2 (ZTA) *(75% Al_2O_3, 25% ZrO_2)*	+6.2x10^{-3}	x [4)]
TiO_2 *(98% TiO_2)*	+3.3x10^{-3}	x [4)]
Si_3N_4	+1.6x10^{-2}	x [4)]
MgO *(>99% MgO)*	destroyed	x [4)]

1) *Q-brine composition at 55ºC was: 26.8% $MgCl_2$, 4.8% KCl, 1.4% $MgSO_4$, 1.4% NaCl, 65.7% H_2O. At this temperature, pH and O_2 values were 4.6 and 0.8mg/l*

2) *Tests were performed for 850h at 200ºC and a pressure of 13MPa*

3) *No inter-granular attack*

4) *Severe inter-granular attack*

Table G5: Summary of Long Term Corrosion Studies in Q-Brine[1)] [58]

MATERIAL	WEIGHT CHANGE (g/cm^2)			INTERGRANULAR CORROSION DEPTH
	80ºC	160ºC	200ºC	(mm)
Steatite porcelain	$-7x10^{-5}$	$-3x10^{-3}$	$-8x10^{-3}$	- [2)]
Al_2O_3 (coarse grained)	$-8x10^{-5}$	$-1x10^{-4}$	$+7x10^{-5}$	≥1.5
Al_2O_3 (fine grained)	$-6x10^{-5}$	$+8x10^{-5}$	$+6x10^{-4}$	≥2.0
ZrO_2	$+7x10^{-4}$	$-1x10^{-6}$	$+8x10^{-5}$	≥2.0

1) *Tested for 17,500h at the temperatures shown and a pressure of 13MPa;*
2) *No intergranular attack*

Table G6: Summary of Feedback from Manufacturers of Silicon Carbide

COMPANY	COMMENTS
CeramTec (Czech Republik) *Correspondence and meeting*	• *Product development essential* • *SiSiC could be joined during firing process to bigger/longer parts (Furnace capacity determines size limit)* • *Furnace sintered joints have higher free Si than surrounding material* • *SSiC has sintering shrinkage of circa. 20%, and so final dimensions are difficult to control* • *SSiC joints always require binders (e.g. glues, solders, …)* • *Manufacture of a small VHLW canister body is feasible with current capacity*
ESK Ceramics GmbH *Correspondence*	• *Do not see possibility to produce required parts based on existing capacity (of Company)*
FCT Hartbearbeitungs GmbH [76] *Correspondence and meeting*	• *Can only offer SSiC, although section thicknesses are high (concerns about target sinter density)* • *Length limited to 1.2m* • *Concern about 0.5wt.% B in their SSiC composition which could be activated by irradiation?* • *SiSiC parts of the required size are difficult to fabricate*
Schunk Kohlenstofftechnik GmbH	• *No response*
SiCeram GmbH [77] *Meeting*	• *Consistent with other manufacturers, SiCeram would propose the adoption of SSiC to take advantage of superior mechanical and corrosion properties* • *The technology already exists to produce a small VHLW canister, although the attainment of acceptable density at 50mm thickness would need to be demonstrated* • *With appropriate development activity and equipment investment, a full size SSiC container could be feasible when strengthened by a potting infill.* • *Sealing would need to be by matching filler rather than by a glassy solder. Significant investment activity would be required.*
HC Starck Ceramics GmbH *Correspondence*	• *Can manufacture required sections in SiSiC, but lengths limited to 500mm* • *Multi-piece constructions could be a solution*
Technical Ceramics Haldenwanger (Morgan Advanced Materials) *Correspondence*	• *Did not see a high probability with SSiC* • *SiSiC could be possible with appropriate investment/ development (indicative costs provided [86])*

Table G7: Estimated Development/Investment Costs for SiSiC Nuclear Waste Disposal Canister

WORK PACKAGE	COST kCHF	TIME years
1 Process/technology development of required SiC material	750	1.5
2 Specification of kiln and construction of R&D kiln	900	1.0
3 First samples / validation of equipment	210	0.8
4.1 Production validation	90	0.8
4.2 Adjustment of design and technology *(as necessary, there may need to be more than one design and technology adjustment iteration step)*	(360)	(1.0)
5 Material and design freeze / engineering of production plant	1,200	1.0
6 Construction of production plant for 500 to 1000 units per year	42,000	1.5
7 Run-up production plant		0.5
Totals	≥ 45,150	≥7.1

WITHOUT COSTS FOR JOINING/SEALING DEVELOPMENT

Courtesy Technical Ceramics - Haldenwanger (Morgan Advanced Materials)

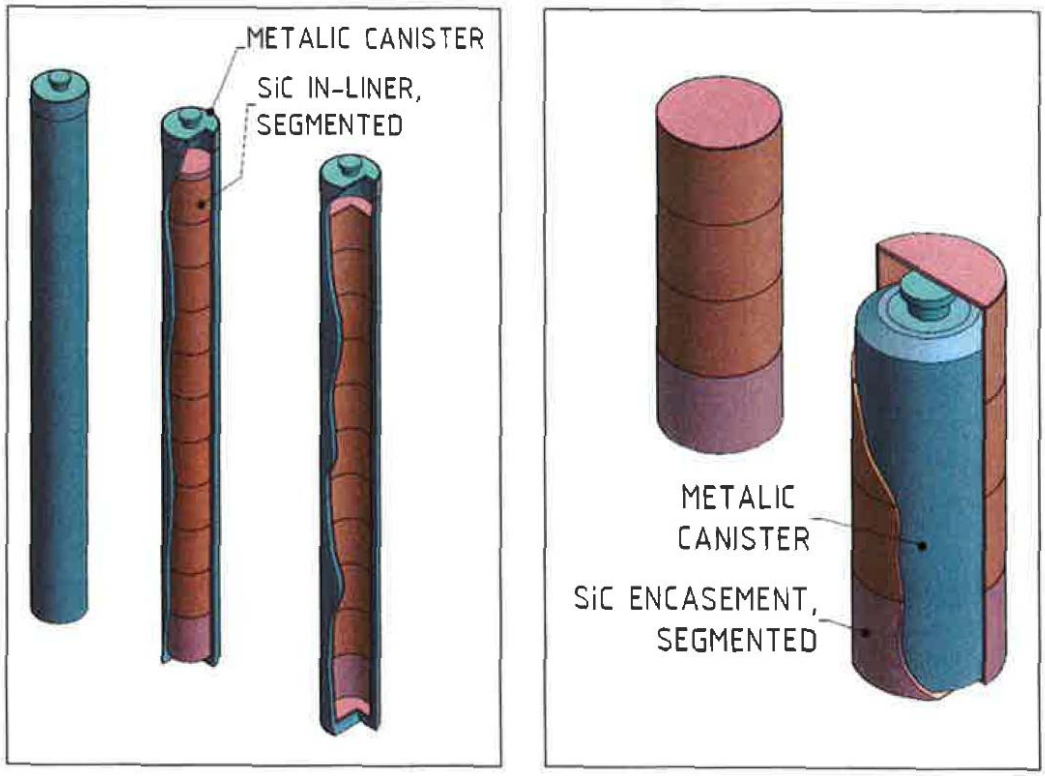

(a) (b)

Fig.G 1 Proposed SSiC encasement solutions for (a) SF rod disposal, with diameter 430mm and height 4980mm, and (b) VHLW disposal, with diameter 465mm and height 1,390mm [72]

(a) (b)

Fig.G 2 Andra half-scale model of Al_2O_3/SiO_2 VHLW canister [7], (a) complete model, (b) lid

APPENDIX H: COPPER SHELL WITH INTERNAL CAST IRON SUPPORT CANISTER (KBS-3) CONCEPT

H1 Background and Introduction

The copper shell with internal cast iron support canister concept was not specifically evaluated in the present study, but could not be ignored because of its international status and the available background knowledge to the concept. The so-called KBS-3 solution was initially developed in Sweden in the 1970s. The total concept involved a multi-barrier system, with the first barrier being the copper canister with cast iron insert, surrounded by a layer of bentonite clay (the second barrier), and then the emplacement bedrock (the third barrier).

The KBS-3 canister consisted of two main components, an outer corrosion barrier and a load bearing insert with channels for the spent fuel (Fig.H 1). The outer corrosion barrier was Cu-OFP (oxygen free copper doped with phosphorus, App. **D**). The insert was cast from SG iron such that the void space between the fuel channels was also filled (Fig.C 1). The design of the canister was such that a load bearing steel lid could be bolted to the internal structure during the encapsulation process, and the canister could be final sealed by joining the copper lid to the copper shell by electron beam or friction stir welding. The concept could be used for the containment of both BWR and PWR spent fuel assemblies.

H2 Materials

The copper used for the outer container was high conductivity, oxygen free, and micro alloyed with 30-100ppm phosphorus to improve the creep properties. The outer shells were mostly extruded, but could also be formed by pierce-and-draw or open forging processes, prior to final machining to a wall thickness of 50mm and to provide a clearance of ~1mm with the cast iron insert, App. **D**.

The inserts were cast from SG iron Grade GJS-400. App. **C**.

H3 Mechanical Integrity

A range of handling and disposal load cases had been extensively evaluated with a focus on the failure criteria which could be life limiting for both the copper shell and the insert [23]. In the case of the copper, the main failure criteria were fracture due to excessive plastic deformation and rupture due to creep deformation [31]. As a generality, the likelihood of such failures was unlikely as a consequence of the high tensile and rupture ductilities of copper, although there were concerns relating to exhaustion of the creep ductility of the material in long times under multi-axial loading conditions before it fully collapsed on to the insert. Creep crack growth was a concern, but tests appeared to indicate that this sub-critical crack growth mechanism was not possible at 20 and 75°C due to the high creep ductility of copper at these temperatures.

The main concerns with the insert had been plastic collapse (buckling), crack initiation (stable crack growth) and exceeding the tensile strength. The assessed safety margins had been judged to be more than acceptable, in particular for the BWR canister [23].

A comprehensive review of the KBS-3 canister design was given in [41].

H4 Environmental Damage

For the KBS-3 concept, environmental protection was provided by the thick walled copper canister. The corrosion properties of copper are reviewed in App. **D**. The treatment of corrosion in the safety assessment involved:

- ***thermodynamic*** considerations to determine which species in the canister environment had the potential to corrode the copper, with
- determination of the extent of corrosion processes by ***mass balance calculations***, if the source of corrodants could be bounded, or by
- ***transport calculations*** utilising the limited transport capacity in the repository, and bounds on concentrations of the transported species in e.g. the groundwater.

Importantly ***reaction rates were not used*** as a limiting factor in the safety assessment, with reactions between copper and corrodants being assumed to be instantaneous.

H5 Fabrication

H5.1 Manufacture

The copper canisters were made from cylindrical copper ingots which were then formed by extrusion, pierce-and-draw processing or forging [25]. Pierce-and-draw processing offered the advantage of canister manufacture with an integral bottom, as an alternative to the manufacture of cylinders requiring both bottoms and lids to be welded (App. **D**). The technology for copper canister manufacture for this application was now regarded as well developed.

Similarly, the feasibility of manufacturing nuclear waste disposal canister inserts from GJS-400 had specifically been well established by a number of Swedish foundaries (App. **C**).

H5.2 Welding

Electron beam welding was currently the first choice sealing weld procedure for the KBS-3 copper shell, with friction-stir welding as the back-up solution [26]. The full penetration welding of 50mm thick copper sections (greater in the case of the shell bottoms prior to final machining) was challenging, but high integrity welds by both techniques were now possible.

The GJS-400 insert was not welded, but sealed with a mechanically fitted steel lid.

H5.3 Inspection

Prior to the KBS-3 development, there was little non-destructive testing inspection experience for large thick section copper structures. Copper canister manufacturers such as Wyman Gordon and Vallourec & Mannesmann Tubes employed ultrasonic testing, but only for defect detection, and not sizing [25]. With development activities focussing on time of flight diffraction (TOFD) and phased array, it was now possible to also size defects to the required acceptance standard.

In contrast, for the KBS-3 development, focus had been on the use of ultrasonic testing and radiography, and in particular pulsed echo ultrasound for inspection of the GJS-400 insert [25]. The geometry of the cast iron insert was complex, and refinement to the adopted procedures was on-going.

H6 Costs

Investment/Development Costs. The costs involved in the manufacture of the KBS-3 canister had been well researched (e.g. [26,25]). It was estimated that the development costs accumulated to date for this concept now exceeded ~100MCHF.

Unit Costs. Depending on the method of copper canister manufacture (forging, pierce & draw, or extrusion), total BWR-type canister unit costs ranged between 200 and 250kCHF, but were sensitive to the price of copper. This was a big concern for the future.

H7. Summary

The KBS-3 canister concept was considered to be well advanced with long-time integrity sufficient to achieve long-term safety [35]. In particular, significant effort had been directed towards the design assessment of mechanical and long-term corrosion integrity. It was acknowledged that improved understanding was still necessary with respect to the long-term creep deformation response and corrosion behaviour of copper, but in-depth studies of these issues were continuing with high priority.

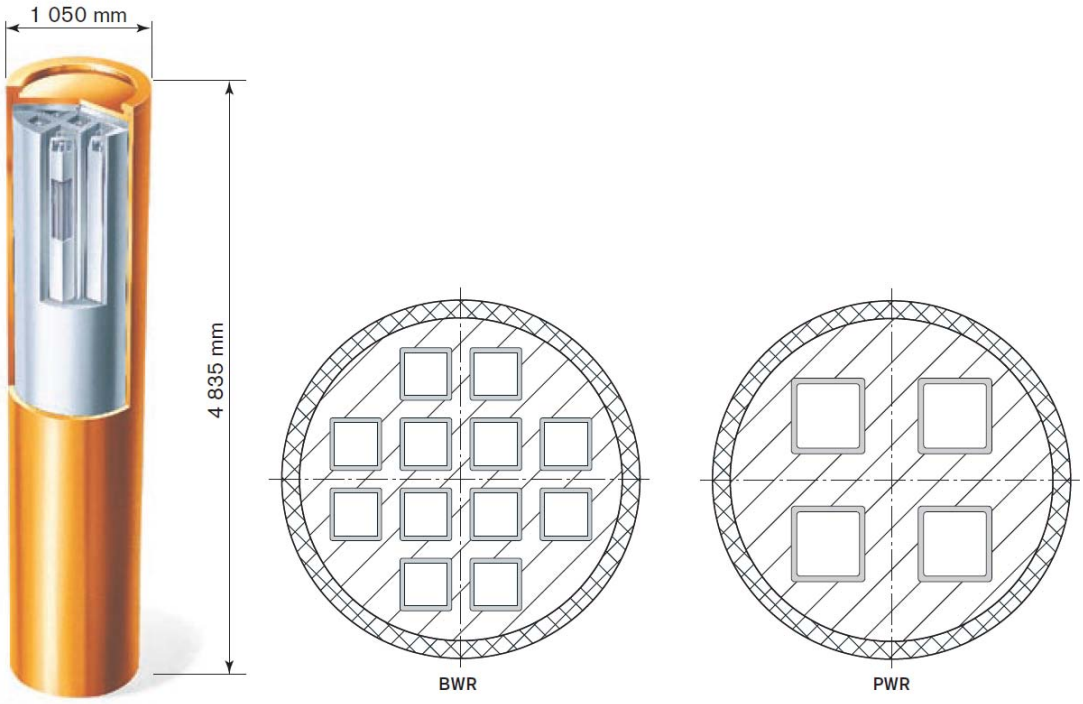

Fig.H 1 KBS-3 canister for disposal of spent nuclear fuel [23]

APPENDIX I: STRUCTURAL ANALYSES OF NAGRA DISPOSAL LOAD CASES

I1 Background and Introduction

NAGRA had commissioned a number of candidate canister structural analyses relating to load cases based on the repository scenario described in Sect. 3.1.3 and illustrated in Fig. 9 [10,94-98], i.e. for an emplacement depth of 900m. These considered a number of load cases covering either short time (Phases 1 to 3, in Fig. 3) or long time (Phase 4, in Fig. 3) emplacement for a number of SF and VHLW container configurations (Fig.I 1). The load cases were not intended to form the basis of formal design analyses, but to provide a platform for canister material comparison. The so-called TWI load cases are introduced in the following section.

In addition to these, disposal load case analyses relating to three ceramic VHLW container configurations had also been conducted [7]. The conditions for these are also reviewed.

I2 TWI Load Case Conditions

The TWI load cases covered short time and long time emplacement scenarios as described in the following sections.

I2.1 Short Time Scenarios

It was recognised that, in the short time, the external pressure on the disposal canister due to initial tunnel convergence and in particular due to buffer swelling (Fig. 9) was unlikely to be isotropic. The following three load cases aimed to represent what was likely to be the practical situation, with the distributions adopted in TWI-4 and TWI-5 being regarded as being closer to reality. The stress magnitudes adopted in TWI-4 and TWI-5 were proposed by NAGRA as conservative representations, in particular those of TWI-5.

Case TWI-3	Axial linear pressure variation between 3MPa at ends to 6MPa at centre (uniform around circumference), Fig.I 2c
Case TWI-4	Pressure variations, both around the circumference and along the axis, between 3MPa and 6MPa (Fig.I 3)
Case TWI-5	Pressure variations, both around the circumference and along the axis, between 1MPa and 6MPa (Fig.I 3)

The pressure distribution shown in Fig.I 3 was represented in a way to ensure that the net force was zero [97], using:

$$P = \frac{P_{end} + P_{mid}}{2} + \frac{P_{end} - P_{mid}}{2}.\cos\left(\frac{2\pi z}{L}\right) \qquad \text{(I1)}$$

where $P_{end} = P_{max} - (P_{max} - P_{min}).\sin\left(\frac{\alpha}{2}\right)$

and $P_{mid} = P_{min} + (P_{max} - P_{min}).\sin\left(\frac{\alpha}{2}\right)$

The stress analysis results reported by TWI for the short time load case scenarios [10,94-96] are summarised in Table I1, e.g. Fig.I 4. The nominal effect of wall thickness on von-Mises, axial, hoop and radial stresses for the short time load case TWI-5 is shown in Fig.I 5, although it must be recognised that the stresses compared are not always for the same canister configurations (i.e. different internal diameters and end-cap arrangements, Tables I1, I2, cf. Fig.I 1a and c).

Reference is also made to [10]:

Case TWI-1a Isotropic pressure, 4MPa (Fig.I 2a).

The results in Table I1b and Fig.I 5 indicated that the maximum stresses arising due to the short time TWI-5 loading of an SF disposal canister are axial at the outside diameter (horizontal).

Evidence to demonstrate the relatively small effect of elastic modulus on the stress calculations is also contained in Table I1b and Fig.I 5.

The TWI-4 and TWI-5 case stress analysis results for a VHLW canister are summarised in Table I2 and referred to in Fig.I 5.

In Fig.I 5, σ_{VM} and σ_a for the 770mm ID (4600mm long) SF canister are shown to be comfortably below $R_{p0.2}$(150°C) for carbon steel for thicknesses greater than 50mm. σ_{VM} and σ_a for the 440mm ID (1710mm long) VHLW canister are ~41MPa.

A simple analytical expression was proposed to relate axial stress to canister wall thickness under these conditions [99], i.e.

$$\sigma_{a,max} = \frac{\left(P_{e,max} - P_{e,min}\right).0.103523.\left(OD/2\right)^2.L^2}{0.049087.\left(OD^4 - ID^4\right)} \qquad (I2)$$

The effectiveness of this relationship is demonstrated in Fig.I 5.

I2.2 Long Time Scenarios

With the development of full hydration, axial pressure distributions on containers emplaced in Opalinus clay were likely to become more homogeneous, and to be more reasonably represented by the following load cases, in particular that of TWI-2 [10].

Case TWI-1 Isotropic pressure, 22MPa (Fig.I 2a)

Case TWI-2 Sinusoidal pressure variation around the circumference between 22MPa vertical and 29MPa horizontal (Fig.I 2b)

The stress analysis results reported by TWI for the long time load case scenarios [10,94-96] are summarised in Tables I3 and I4. The nominal effect of wall thickness on von-Mises, axial, hoop and radial stresses for the long time load case TWI-2 is shown in Fig.I 6 although, as above, it must be recognised that the stresses compared are for different canister configurations (i.e. different internal diameters and end-cap arrangements, Tables I3, I4, cf. Fig.I 1b and c). Examples of TWI-2 load case stress contour plots are given in Fig.I 7.

The results in Table I3 and Fig.I 6 indicated that the maximum tensile stresses arising due to the long time TWI-2 loading of an SF disposal canister are hoop at the internal diameter (horizontal).

The TWI-2 case stress analysis results for a VHLW canister are summarised in Table I2 and referred to in Fig.I 6.

In Fig.I 6, σ_{VM} for the 770mm ID (4600mm long) SF canister is shown to be above $R_{p0.2}$(22°C) for carbon steel for thicknesses below 120mm. σ_h for the SF canister is less than $R_{p0.2}$(22°C) for carbon steel for wall thicknesses greater than ~60mm. Similarly, for the 440mm ID (1710mm long) HLW canister with a wall thickness of 50mm, the magnitude of σ_{VM} is well in excess of $R_{p0.2}$(22°C) for carbon steel, while σ_h is ~50MPa.

I2.3 Practical Implications

The conducted finite element stress analyses were fully elastic. In this respect, not least due to the insensitivity to elastic modulus demonstrated in Table I1b and Fig.I 5, the stresses determined are applicable to all considered canister material solutions.

I3 Andra Load Case Conditions

There were only three Andra load case scenarios, all of which aimed to represent long time conditions at emplacement depths of ~500/630m [7].

Case Andra-C1 Isotropic pressure, 12MPa (5MPa water pressure plus 7MPa earth pressure at 500m)

Case Andra-C2 Isotropic pressure, 16.3MPa (6.3MPa water pressure plus 10MPa earth pressure at 630m)

Case Andra C3 Non uniform external pressure variation around the circumference, with a 7MPa zone (earth pressure and pressure from the swelling clay plug) and a 5MPa zone (water pressure), Fig.I 8

The results of the hemispherical ended Andra VHLW container C3 load case maximum principal stress analyses (Table I5) are compared in Fig.I 9 with the equivalent TWI-2 assessed container data. The magnitude of the maximum stresses associated with the smaller diameter containers are significantly lower than the full-size SF containers, in particular those for the VHLW containers. Notably, maximum stresses for the VHLW containers do not appear to be very sensitive to applied pressures associated with emplacement depths of 500m (7/5MPa) and 900m (29/22MPa), Fig.I 9.

I4 Plastic Collapse

The avoidance of plastic collapse (unstable gross plastic yielding) is an important fitness-for-purpose criterion for pressure vessels. The stress analyses conducted for this study were purely elastic [94-98], but even in such circumstances, an indication of the risk of plastic collapse may be obtained by comparing maximum σ_{VM} with 1.5.$R_{p0.2}$ (e.g. [100]), where for carbon steel, R_{pX} (typically ($R_{p0.2}$ + R_M)/2 [89,91]) is close to 1.5.$R_{p0.2}$. Such a comparison for carbon steel is illustrated as a function of thickness for different canister concept/scenarios in Fig.I 10.

In terms of this assessment criterion, the long-time TWI-2 (type) load case criterion is far more demanding than the short time TWI-5 (type) load case criterion (Fig.I 10a). This type of analysis suggests that carbon steel full size SF (x9) rod canisters with a wall thickness of greater than ~90mm would be acceptable. Similarly, for a VHLW configuration, a wall thickness of 50mm appeared to be acceptable.

It is acknowledged that there is scope for selecting higher strength carbon steels, e.g. as in [98], in particular when the canister is clad and not so sensitive to the effects of strength on environmental damage resistance.

$\sigma_{VM,max}/R_{p0.2,min}$ ratios for a number of canister material possibilities (as well as the equivalent $\sigma_{1,max}/R_{p0.2,min}$ ratios) are summarised in Tables I6 and I7.

A more appropriate approach for this type of pressure vessel is that considering ductility exhaustion but, for this, the determination of von Mises strain is required using an inelastic FEA approach (e.g. [10,98]).

It may also be concluded from Fig.I 10 that carbon steel SF (x3) rod canisters with a minimum wall thickness of ~50mm would be acceptable in terms of this plastic collapse criterion. Interestingly, for this canister configuration, the conclusion may be drawn equally on the basis of the evidence from both the short-time and long-time load case analyses.

I5 Summary

A significant outcome from the disposal load case stress analyses was that the maximum stresses arising from the short time (TWI-5) loading of both SF and VHLW canisters are axial at the external surface, whereas those arising from long time (TWI-2) loading are hoop at the internal surface. This meant that FAD constructions considering short time container loading had to assess a circumferential defect condition on the external surface, whereas those considering long time canister loading had to assess an axial defect condition on the internal surface.

A simple von Mises limit stress analysis using the results of elastic FEA indicates that carbon steel full size SF rod canisters with a wall thickness of greater than ~90mm would be acceptable. For a VHLW configuration, a wall thickness of 50mm appeared to be acceptable. Adopting such a simple approach was considered to be inappropriate for this type of pressure vessel, and for this reason an FAD approach was also adopted (App. **J**).

Table I1a: Summary of Short Time Disposal Load Case Stress Analysis Results for SF Canisters

l	ID	t_o	*t*	*E*	Ends	Load Case	*d*	σ_{VM}, MPa				σ_a, MPa				σ_h, MPa				Ref
								vertical		*horizontal*		*vertical*		*horizontal*		*vertical*		*horizontal*		
mm	mm	mm	mm	GPa			mm	OD	ID	OD	ID	OD	ID	OD	ID	OD	ID	OD	ID	
4600	770	140	140	207	Flat	TWI-1a		8	**16**	8	**16**									[10]
4600	770	140	140	207	Flat	TWI-3	0	14	**23**	14	**23**	-7	-5	-7	-5	-20	-25	-20	-25	[94]
							2000	4	9	4	9	-6	-6	-6	-6	-8	-10	-8	-10	
							2150	5	29	5	29	3	-22	3	-22	-2	-13	-2	-13	
4600	770	100	100	207	Flat	TWI-3	0	19	**29**	19	**29**	-7	-9	-7	-9	-26	-32	-26	-32	[95]
							2000	6	10	6	10	-8	-8	-8	-8	-11	-12	-11	-12	
							2150	9	40	9	40	7	-30	7	-30	0	-23	0	-23	
4300	476.3	41.25	41.25	207	Hemis	TWI-3	0	30	**39**	30	**39**	-12	-10	-12	-10	-38	-43	-38	-43	[96]
							2000	15	21	15	21	-12	-11	-12	-11	-21	-25	-21	-25	
							2150	12	15	12	15	-12	0	-12	0	-16	-15	-16	-15	
4425	463	47.63	47.63	207	Hemis	TWI-3	0	25	**35**	25	**35**	-10	-9	-10	-9	-32	-38	-32	-38	[98]
							2000	13	19	13	19	-10	-10	-10	-10	-18	-22	-18	-32	
							2210	10	13	10	13	-10	0	-10	0	-14	-13	-14	-13	
4600	770	140	140	207	Flat	TWI-4	0	14	15	**30**	**30**	-10	-5	**26**	10	-20	-16	-5	-25	[94]
							2000	6	12	9	12	-4	-7	-5	-2	9	-7	-6	-8	
							2150	7	36	9	33	2	-30	4	-28	-3	-12	0	-18	
4600	770	100	100	207	Flat	TWI-4	0	21	16	42	**44**	-11	-7	**38**	18	-29	-18	-5	-33	[95]
							2000	10	15	15	15	-10	-6	-10	0	-12	-16	-9	-10	
							2150	10	36	13	57	7	-36	9	-40	-3	3	-6	0	
4300	476.3	41.25	41.25	207	Hemis	TWI-4	0	42	20	**205**	175	-10	-5	**205**	155	-50	-15	**2**	-56	[96]
							2000	52	55	42	39	-5	-7	0	10	-22	-37	-28	-21	
							2150	50	30	38	35	-5	0	-5	0	-18	-22	-14	0	
4425	463	47.63	47.63	207	Hemis	TWI-4	0	25	15	**124**	116	-17	-5	**122**	85	-40	-16	-2	-45	[98]
							2000	15	33	33	20	-2	-10	-18	0	-15	-35	-42	-13	
							2210	10	24	20	14	-10	0	-15	2	-14	-20	-29	-5	

NOTE: Figures in bold are maximum values at centre span of canister (i.e.at d = 0)

Table I1b: Summary of Short Time Disposal Load Case Stress Analysis Results for SF Canisters

l	ID	t_o	t	E	Ends	Load Case	d	σ_{VM}, MPa				σ_a, MPa				σ_h, MPa				Ref
								vertical		*horizontal*		*vertical*		*horizontal*		*vertical*		*horizontal*		
mm	mm	mm	mm	GPa			mm	OD	ID	OD	ID	OD	ID	OD	ID	OD	ID	OD	ID	
4600	770	140	140	105	Flat	TWI-5	0	15	10	**51**	42	-5	0	**52**	25	-20	-9.5	4.5	-24	[97]
							2000	9	15	12	15	-2	-1	-5	7	-6	-10	-2	-10	
							2150	6	21	10	25	0	-11	3	-15	4	-0.5	2.5	-8	
4600	770	140	140	207	Flat	TWI-5	0	15	10	**51**	42	-5	0	**52**	25	-21	-10	5	-24	[94]
							2000	9	15	15	15	-2	0	4	6	-6	-10	-1	-2	
							2150	6	10	10	20	0	-10	2	12	-3	-10	3	-10	
4600	770	100	100	207	Flat	TWI-5	0	22	10	**70**	62	-10	0	**75**	40	-30	-9	9	-33	[95]
							2000	12	20	18	20	-2	0	-5	9	-9	-12	9	-33	
							2150	9	18	12	20	1	-10	4	-20	-5	-8	5	-10	
4600	770	50	50	207	Flat	TWI-5	0	57	2	138	**146**	-30	0	**150**	90	-70	-1	35	-76	[97]
							2000	26	35	40	37	-5	3	-20	15	-20	-20	-7	-8	
							2150	17	35	30	63	5	-20	0	-45	-4	-19	10	-15	
4300	476.3	41.25	41.25	207	Hemis	TWI-5	0	50	5	**350**	310	-5	0	**360**	280	-57	4	30	-63	[96]
							2000	65	50	78	50	0	0	10	25	-10	-30	-44	-3	
							2150	75	40	20	28	0	0	0	0	-8	-20	-38	20	
4425	463	47.63	47.63	207	Hemis	TWI-5	0	37	3	**207**	184	-10	0	**215**	155	-45	-1	19	-50	[98]
							2000	20	35	20	16	3	0	-15	15	-3	-33	-14	4	
							2210	5	20	22	5	0	0	-5	0	-5	-20	-18	5	

NOTE: Figures in bold are maximum values at centre span of canister (i.e.at d = 0)

Table I2: Summary of Short Time Disposal Load Case Stress Analysis Results for VHLW Canisters

l	ID	t_o	t	E	Ends	Load Case	d	σ_{VM}, MPa				σ_a, MPa				σ_h, MPa				Ref
								vertical		*horizontal*		*vertical*		*horizontal*		*vertical*		*horizontal*		
mm	mm	mm	mm	GPa			mm	OD	ID	OD	ID	OD	ID	OD	ID	OD	ID	OD	ID	
1710	440	50	50	207	Flat	TWI-4	0	22.7	20	23	**35**	-14	-7	**17.5**	1	-31	-22	-7.5	-34	[97]
							648	10	16	8	16	0	-11	-4	-5	-9	-11	-4.5	-15	
							671	11.5	41	8	45	5	-39	4	-30	-3.5	-20	0	-25	
1710	440	50	50	207	Flat	TWI-5	0	24	13.5	39	**41.5**	-10	0	**41**	12	-31	-14	7.5	-33	[97]
							648	15.5	18	12.5	20	2	-4	0	8	-7	-8	-19	-5.5	
							671	2	35	10.5	15	8	-21	5	-9	-2.5	-5	-14	-14	

NOTE: Figures in bold are maximum values at centre span of canister (i.e.at d = 0)

Table I3: Summary of Long Time Disposal Load Case Stress Analysis Results for SF Canisters

l	ID	t_o	*t*	*E*	Ends	Load Case	σ_{VM}, MPa				σ_a, MPa				σ_h, MPa				Ref
							vertical		*horizontal*		*vertical*		*horizontal*		*vertical*		*horizontal*		
mm	mm	mm	mm	GPa			OD	ID	OD	ID	OD	ID	OD	ID	OD	ID	OD	ID	
4600	770	140	120	207	Flat	TWI-1	55	**90**	55	**90**									[10]
4600	770	140	120	207	Flat	TWI-1	58	**93**	58	**93**	-32	-32	-32	-32	-83	-105	-83	-105	[94]
4600	770	100	100	207	Flat	TWI-1	70	**106**	70	**106**	-36	-36	-36	-36	-97	-119	-97	-119	[95]
4300	476.3	41.25	41.25	207	Hemis	TWI-1	107	**142**	107	**142**	-48	-48	-48	-48	-139	-161	-139	-161	[96]
4425	463	47.63	47.63	207	Hemis	TWI-1	89	**125**	89	**125**	-42	-42	-42	-42	-119	-141	-119	-141	[98]
4600	770	140	120	207	Flat	TWI-2	25	**240**	150	40									[10]
4600	770	140	120	207	Flat	TWI-2	20	**220**	150	0	-8	-75	-66	0	0	-75	-195	**0**	[94]
4600	770	100	100	207	Flat	TWI-2	40	**270**	200	25	0	-90	-80	8	20	-300	-250	**25**	[95]
4600	770	50	50	207	Flat	TWI-2	250	**680**	560	270	65	-235	-210	90	250	-760	-680	**280**	[97]
4300	476.3	41.25	41.25	207	Hemis	TWI-2	110	**450**	360	110	28	-150	-150	40	110	-505	-430	**120**	[96]
4425	463	47.63	47.63	207	Hemis	TWI-2	74	**355**	278	66	13	-120	-115	23	60	-405	-345	**78**	[98]

NOTE: Figures in bold are maximum values at centre span of canister (i.e.at d = 0)

Table I4: Summary of Long Time Disposal Load Case Stress Analysis Results for VHLW Canisters

l	ID	t_o	*t*	*E*	Ends	Load Case	σ_{VM}, MPa				σ_a, MPa				σ_h, MPa				Ref
							vertical		*horizontal*		*vertical*		*horizontal*		*vertical*		*horizontal*		
mm	mm	mm	mm	GPa			OD	ID	OD	ID	OD	ID	OD	ID	OD	ID	OD	ID	
1630	440	50	50	207	Flat	TWI-2	55	**315**	242	47	5	-107	-97	16	45	-350	-300	**50**	[97]

NOTE: Figures in bold are maximum values at centre span of canister (i.e.at d = 0)

Table I5: Summary of Long Time Disposal Load Case Stress Analysis Results for Ceramic VHLW Canisters

l	ID	t_o	t	E	Ends	Load Case	σ_{VM}, MPa				σ_a, MPa				σ_h, MPa				Ref
							vertical		*horizontal*		*vertical*		*horizontal*		*vertical*		*horizontal*		
mm	mm	mm	mm	GPa			OD	ID	OD	ID	OD	ID	OD	ID	OD	ID	OD	ID	
1340	470	50	50	150	Hemis	Andra-C1	-	-	-	-	-	-	-	-	-	-	-	2.1	[7]
1340	470	40	40	150	Hemis	Andra-C1	-	-	-	-	-	-	-	-	-	-	-	3.4	[7]
1340	470	50	50	150	Hemis	Andra-C2	-	-	-	-	-	-	-	-	-	-	-	0.7	[7]
1340	470	40	40	150	Hemis	Andra-C2	-	-	-	-	-	-	-	-	-	-	-	1.75	[7]
1340	470	50	50	150	Hemis	Andra-C3	-	-	-	-	-	-	-	-	-	-	-	32.8	[7]
1340	470	40	40	150	Hemis	Andra-C3	-	-	-	-	-	-	-	-	-	-	-	53.7	[7]

Onlylimited stress analysis results were available for this case [7]

Table I6: Summary of $\sigma_{VM,max}/R_{p0.2,min}$ and $\sigma_{1,max}/R_{p0.2,min}$ Ratios for Candidate 4.6m Long SF Canister Solutions

SF Canister Load Case Scenario	Short Time (TWI-5)		Long Time (TWI-2)		Short Time (TWI-5)		Long Time (TWI-2)	
	$\sigma_{VM,max}$	$\sigma_{VM,max}/R_{p0.2,min}$	$\sigma_{VM,max}$	$\sigma_{VM,max}/R_{p0.2,min}$	$\sigma_{1,max}$	$\sigma_{1,max}/R_{p0.2,min}$	$\sigma_{1,max}$	$\sigma_{1,max}/R_{p0.2,min}$
Carbon steel (770mm ID, 140/120mm thick)	51	0.29	220	0.98	52	0.30	0	0.00
Carbon steel (770mm ID, 100mm thick): - Copper coated - Ti Gr.7 clad - Ni Alloy C22 clad	70	0.40	270	1.20	75	0.43	25	0.11
Carbon steel (770mm ID, 80mm thick): - Copper coated - Ti Gr.7 clad - Ni Alloy C22 clad	95	0.54	**380**	**1.69**	97	0.55	95	0.42
Carbon steel (770mm ID, 50mm thick):	146	0.83	**680**	**3.02**	150	0.86	**280**	**1.25**
Ti Gr.2 (770mm ID, 100mm thick)	70	0.32	220	0.80	75	0.34	25	0.09
Ti Gr.2 (770mm ID, 80mm thick)	95	0.43	380	1.38	97	0.44	95	0.35
Ni Alloy C22 (770mm ID, 100mm thick)	70	0.26	220	0.71	75	0.28	25	0.08
Ni Alloy C22 (770mm ID, 80mm thick)	95	0.35	380	1.23	97	0.36	95	0.31
Al_2O_3/SiO_2 (770mm ID, 100mm thick)	70	*n/a*	220	*n/a*	75	*n/a*	25	*n/a*
Al_2O_3/SiO_2 (770mm ID, 80mm thick)	95	*n/a*	380	*n/a*	97	*n/a*	95	*n/a*
SSiC (770mm ID, 100mm thick)	70	*n/a*	220	*n/a*	75	*n/a*	25	*n/a*
SSiC (770mm ID, 80mm thick)	95	*n/a*	380	*n/a*	97	*n/a*	95	*n/a*

$\sigma_{VM,max}/R_{p0.2,min}$ ratios exceeding 1.5, and $\sigma_{1,max}/R_{p0.2,min}$ ratios exceeding 1.0 are highlighted in bold. In these circumstances, the canister concept is highlighted in red

Table I7: Summary of $\sigma_{VM,max}/R_{p0.2,min}$ and $\sigma_{1,max}/R_{p0.2,min}$ Ratios for Candidate 1.6m Long VHLW Canister Solutions

VHLW Canister Load Case Scenario	Short Time (TWI-5)		Long Time (TWI-2)		Short Time (TWI-5)		Long Time (TWI-2)	
	$\sigma_{VM,max}$	$\sigma_{VM,max}/R_{p0.2,min}$	$\sigma_{VM,max}$	$\sigma_{VM,max}/R_{p0.2,min}$	$\sigma_{1,max}$	$\sigma_{1,max}/R_{p0.2,min}$	$\sigma_{1,max}$	$\sigma_{1,max}/R_{p0.2,min}$
Carbon steel(440mm ID, 50mm thick): - Copper coated - Ti Gr.7 clad - Ni Alloy C22 clad	41.5	0.24	315	1.40	41	0.23	50	0.22
Ti Gr.2 (440mm ID, 50mm thick)	41.5	0.19	315	1.15	41	0.19	50	0.18
Ni Alloy C22 (440mm ID, 50mm thick)	41.5	0.15	315	1.02	41	0.15	50	0.16
Al_2O_3/SiO_2 (440mm ID, 50mm thick)	41.5	*n/a*	315	*n/a*	41	*n/a*	50	*n/a*
SSiC (440mm ID, 50mm thick)	41.5	*n/a*	315	*n/a*	41	*n/a*	50	*n/a*

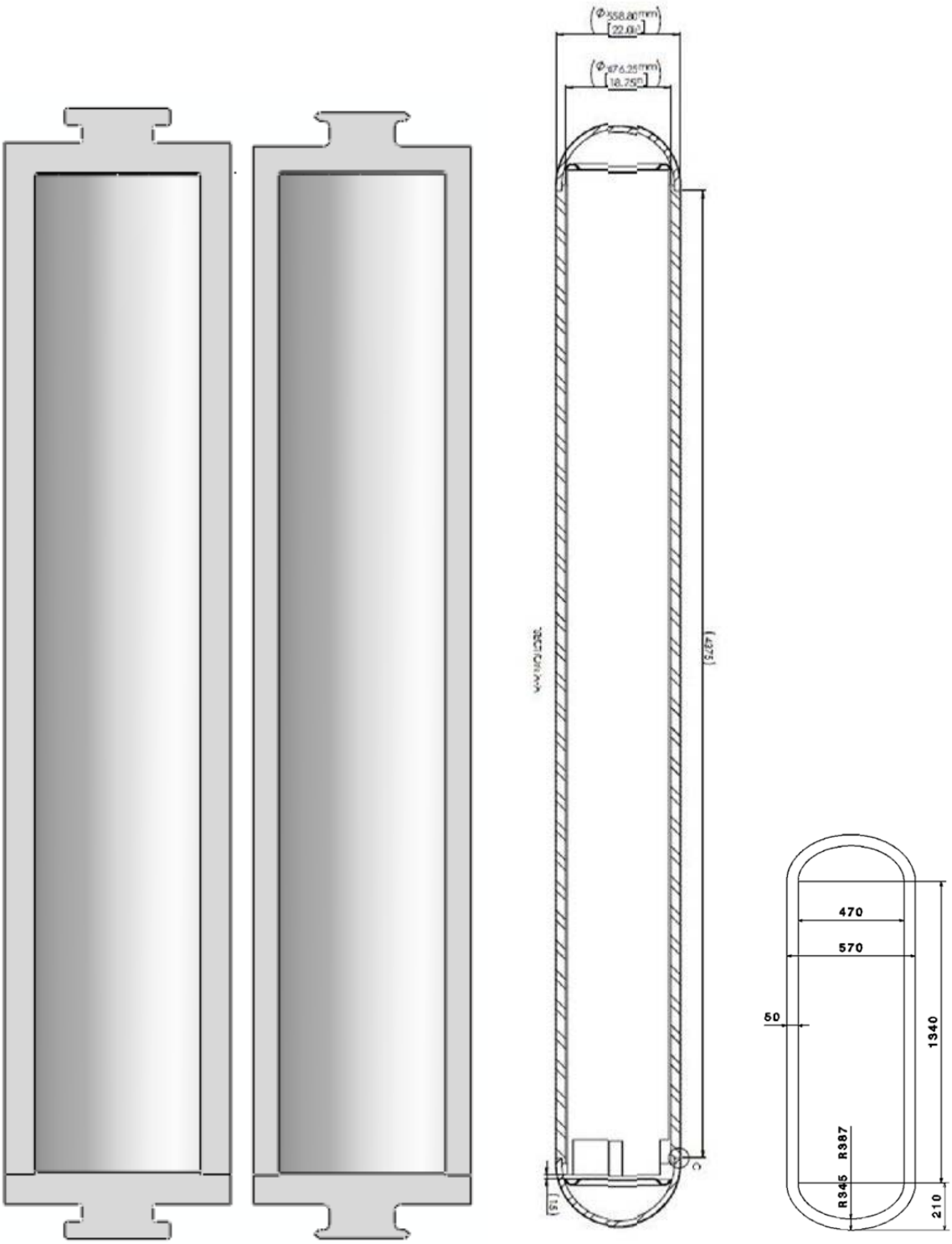

(a) (b) (c) (d)

Fig.I 1 Container configurations considered in NAGRA structural analyses of disposal load cases, i.e. (a) Design 2 (with an SF assembly containment length of 4600mm, an internal diameter of 770m and an original thickness of 140mm) [10,94], (b) Design 2 after removal of a 20mm corrosion allowance from the body and lid thickness [10,94], (c) a smaller diameter copper coated container variant with hemispherical ends for the disposal of 3 BWR SF assemblies (with a containment length of 4300mm, and internal diameter of 476mm and a thickness of 41mm) [96], and (d) a VHLW container (with a containment length of 1340mm, an internal diameter of 570mm and a wall thickness of 50mm [7,97]

A version of Design 2 for copper coating with a wall thickness of 100mm was also considered [96]

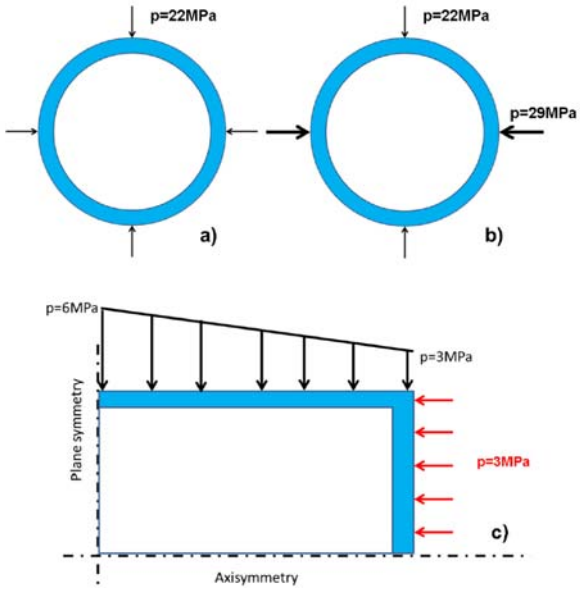

Fig.I 2 Pressure distributions for the TWI load cases a) TWI-1, b) TWI-2, and c) TWI-3 [94]

The pressure distribution for Load Case TWI-1a was similar to that depicted in a), but for an isotropic pressure of 4MPa [10]

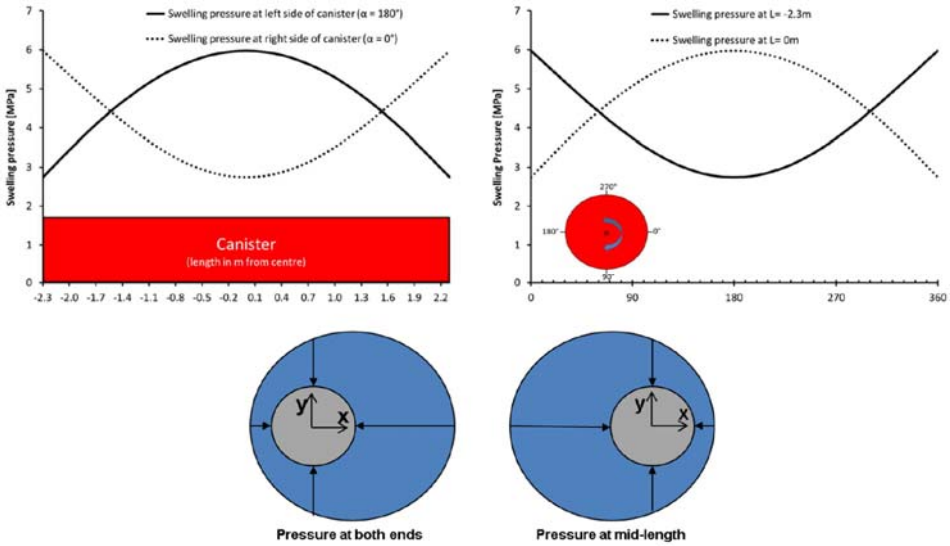

Fig.I 3 External pressure distribution for Load Case TWI-4 [94]

The pressure distribution for Load Case TWI-5 was similar, but with the pressure varying from 1MPa to 6MPa instead of from 3MPa to 6MPa

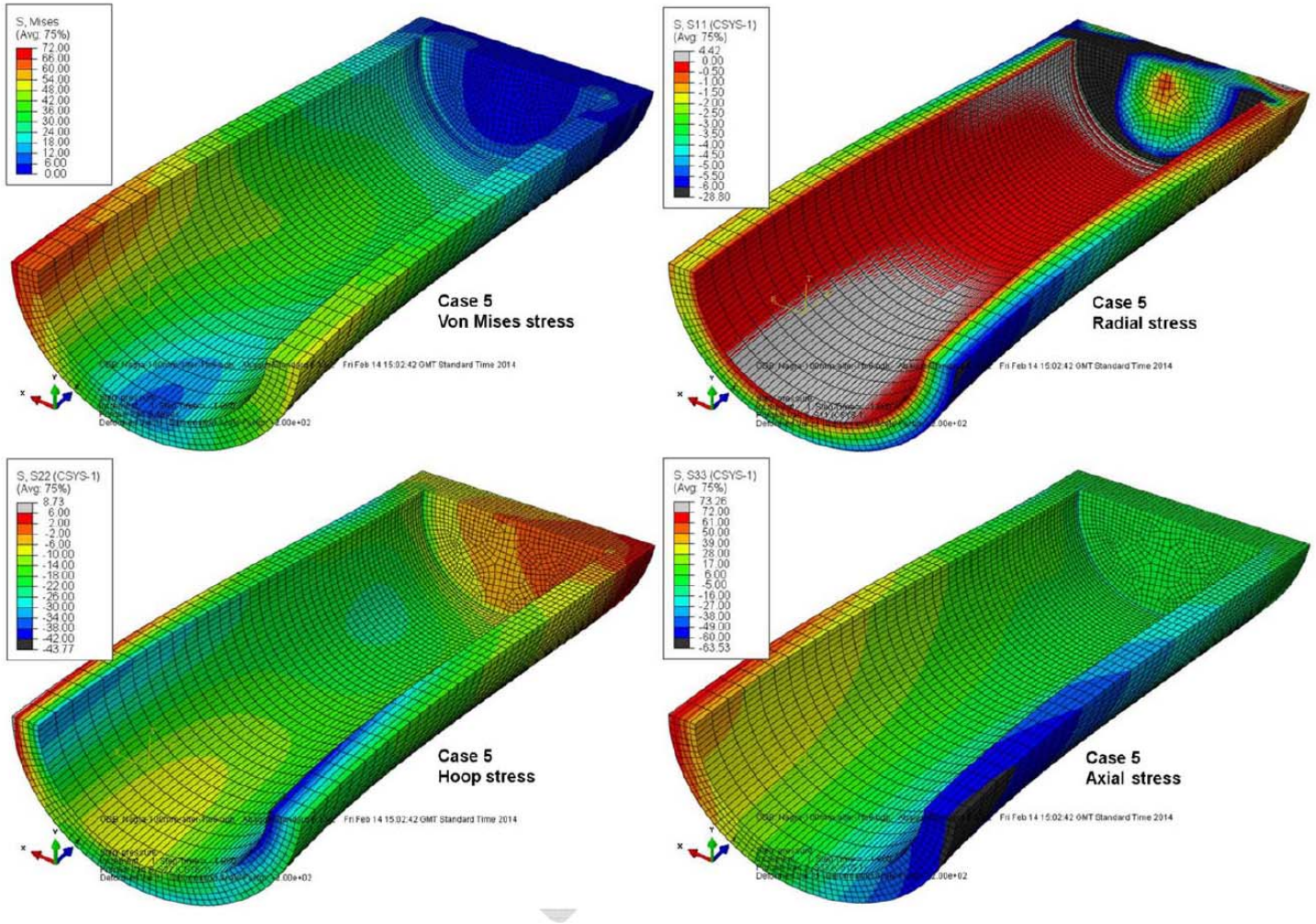

Fig.I 4 Examples of stress contour plots obtained from TWI-5 load case analyses [95]

(with displacement magnification factor of 200)

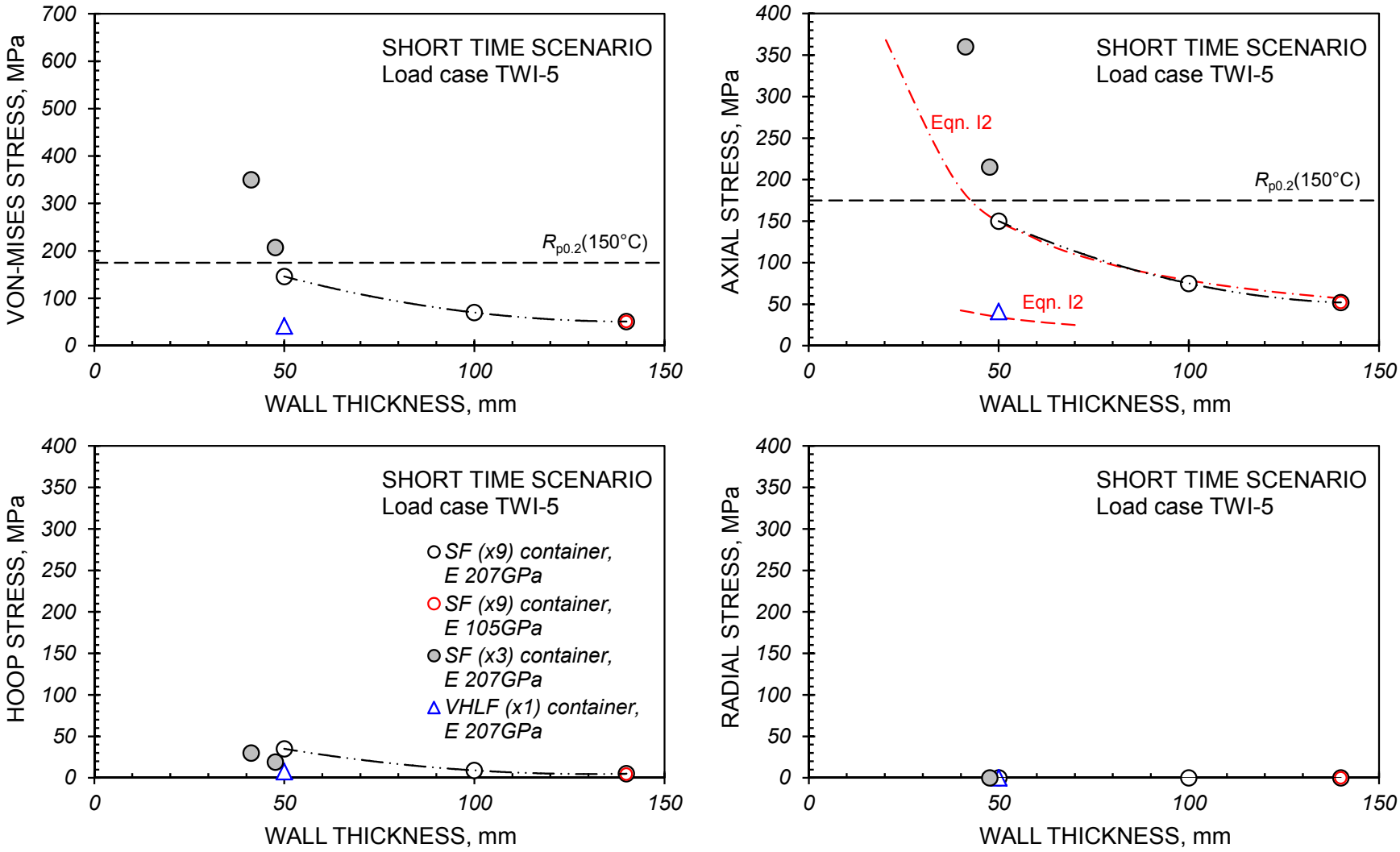

Fig.I 5 Stress analysis results for TWI-5 short time disposal scenario (compared with $R_{p0.2}$(150°C) for carbon steel container material)

The chain lines represent the effect of thickness on maximum stresses for the container configuration shown in Fig.I 1a, while the shaded points represent analysis results for the container configuration shown in Fig.I 1c (with hemispherical ends). The VHLW configuration is that shown in Fig.I 1d, but with flat ends

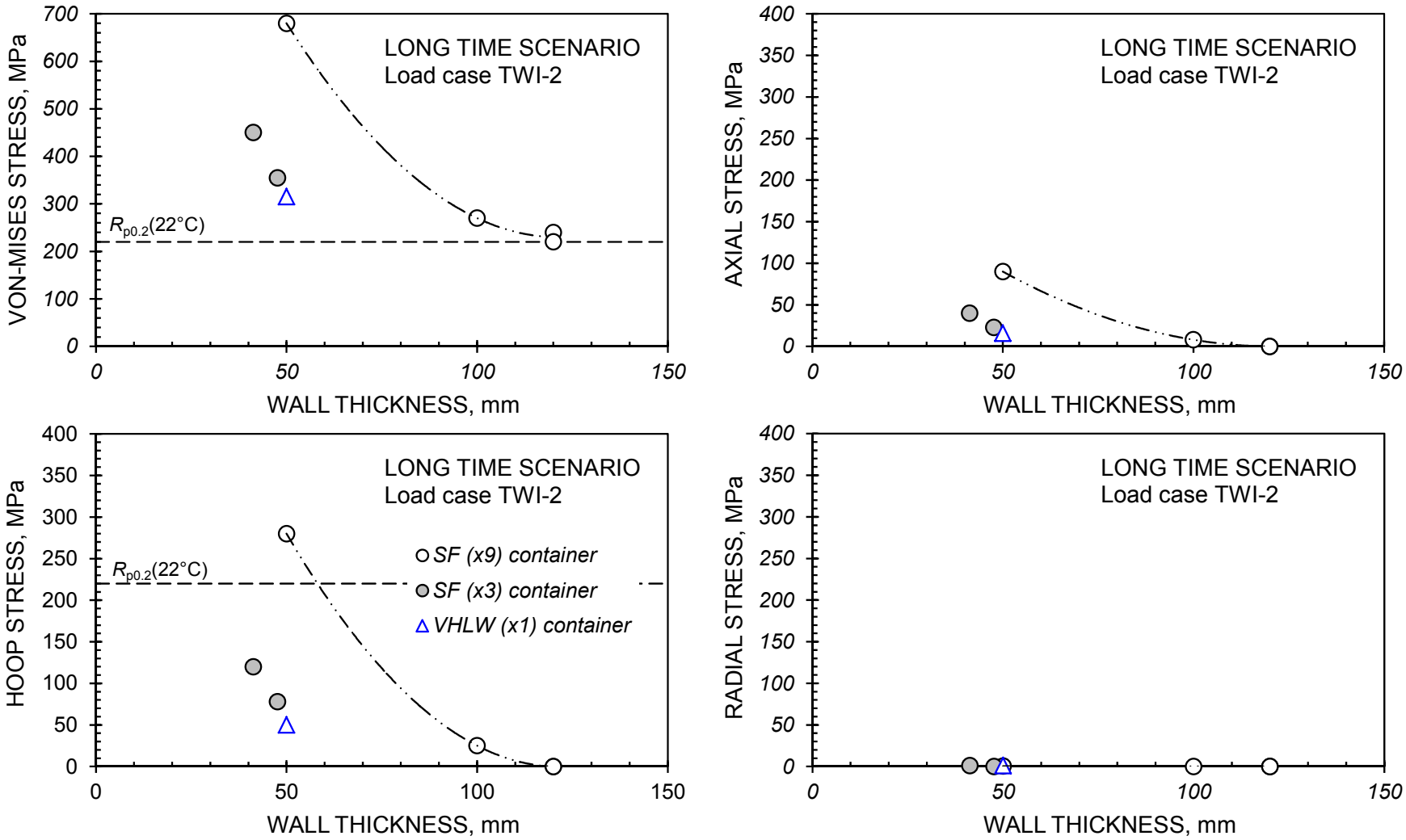

Fig.I 6 Stress analysis results for TWI-2 long time disposal scenario (compared with $R_{p0.2}$(22°C) for carbon steel container material)

The chain lines represent the effect of thickness on maximum stresses for the container configuration shown in Fig.I 1b, while the shaded points represent analysis results for the container configuration shown in Fig.I 1c (with hemispherical ends). The VHLW configuration is that shown in Fig.I 1d, but with flat ends

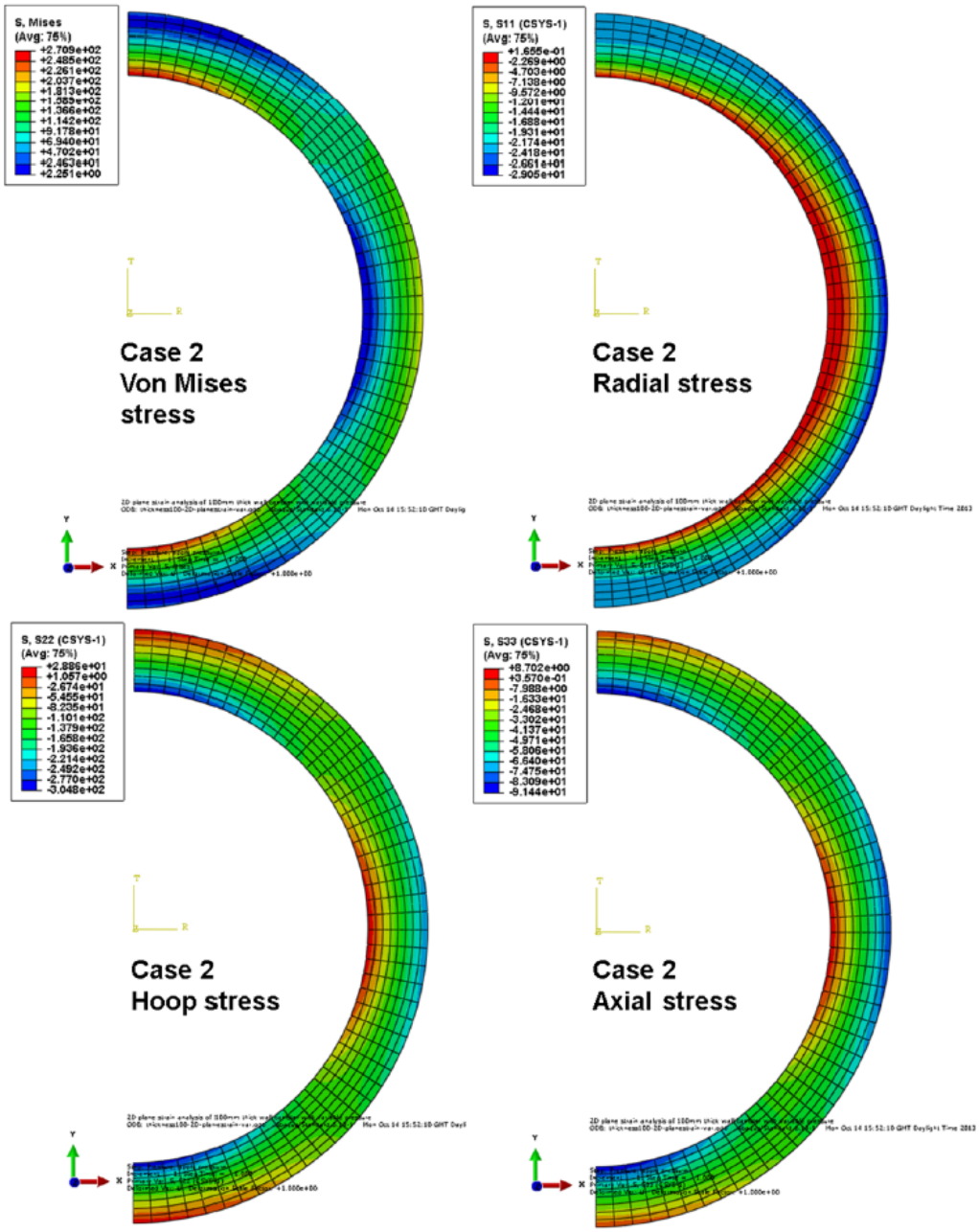

Fig.I 7 Examples of stress contour plots obtained from TWI-2 load case analyses [95]
(with displacement magnification factor of 10)

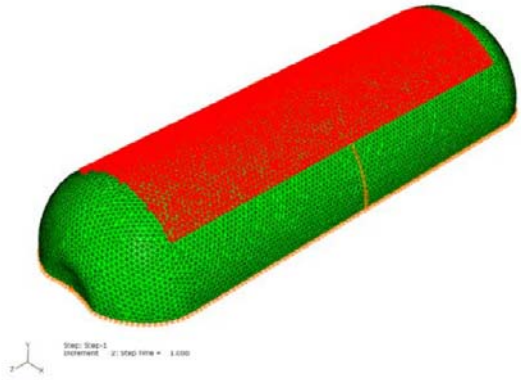

C3 load combination (the areas with a pressure of 5MPa are shown in red and those with a pressure of 7MPa in green).

Fig.I 8 Illustration of external pressure distribution to VHLW canister due to application of Andra C3 load case [7]

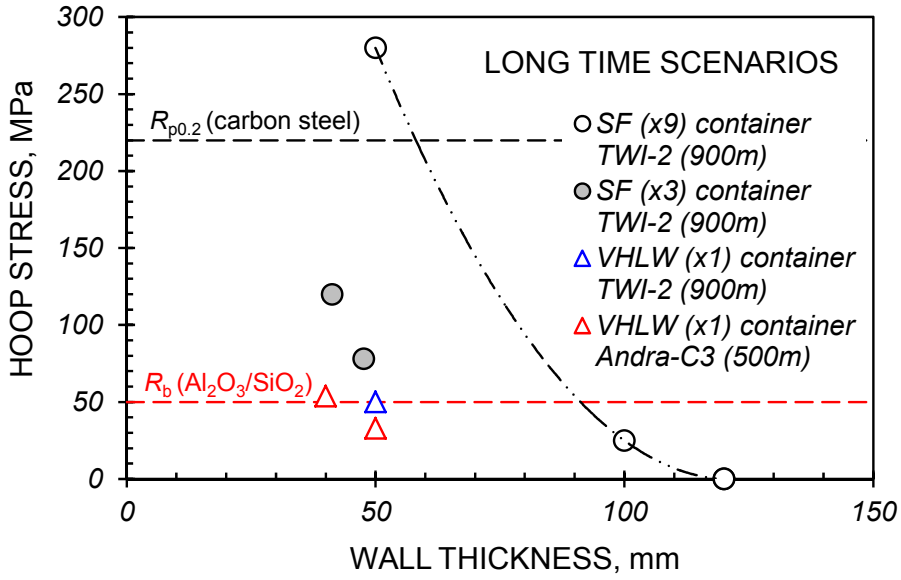

Fig.I 9 Comparison of maximum hoop stress values for different SF and VHLW canister configurations subjected to TWI-2 (type) long time load case scenarios

Red data points and line represent Andra Al_2O_3/SiO_2 VHLW canister conditions [7]. Remainder are for carbon steel [94-97]

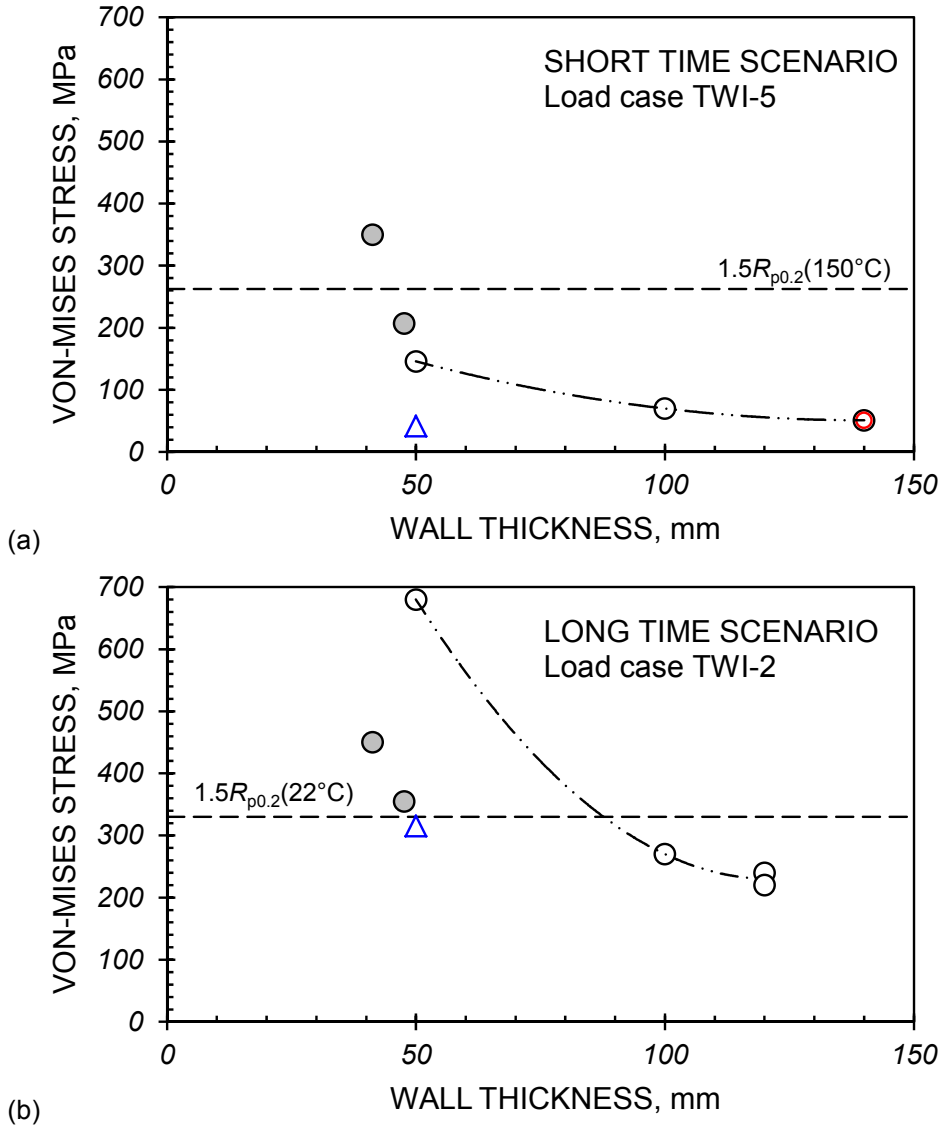

Fig.I 10 Comparison of maximum σ_{VM} values with 1.5.$R_{p0.2}$ for different SF and VHLW carbon steel canister options, (a) for short time scenario TWI-5 (type) load case and (b) for long time scenario TWI-2 (type) load case

Open circles represent x9 BWR SF canisters; Shaded circles represent x3 BWR SF canisters, Open triangles represent x1 VHLW canister

APPENDIX J: FAD ANALYSES OF NAGRA DISPOSAL LOAD CASES

J1 Background and Introduction

One important outcome of the disposal load case structural analyses (App. **I**) was that maximum tensile stresses arising from the short time (TWI-5 case) loading of both SF and HLW containers are axial at the external surface, whereas those arising from long time (TWI-2 case) loading are hoop at the internal surface (App. **I**). This meant that FAD constructions considering short time canister loading needed to assess a circumferential defect condition on the external surface, whereas those considering long time canister loading needed to assess an axial defect condition on the internal surface. The CO/CO^{FAE} ratios (Fig. 8) contained in the feasibility evaluation summary tables (Table 6, Table 7) are based on the assessment of semi-circular surface defects with load case appropriate orientations and locations (i.e. Fig.J 1). The thick walled cylinder K_1 and σ_{ref} solutions defined in [89] were adopted with the appropriate material properties reviewed in Apps. **B** to **G** to determine the $K_r(L_r)$ co-ordinates in the failure assessment diagrams constructed, and presented in the following appendix.

Failure assessment diagrams were constructed for a number of SF and VHLW container concepts, and the derived CO/CO^{FAE} ratios are respectively summarised in Tables J1 and J2. Assessments were conducted for two surface semi-circular defect sizes, namely 2mm and 0.25t, the latter being considered because of the common practice in the nuclear industry to assume a quarter wall thickness reference flaw.

J2 SF Disposal Containers

J2.1 Carbon Steel

A candidate solution for the disposal of spent fuel assemblies was a carbon steel container with an internal diameter of 770mm, a cylinder length of 4.6m, and a wall thickness of 140mm (including a 20mm corrosion allowance). FADs representing the short and long-time stress state conditions (App. **I**) are given in Fig.J 2. The associated CO/CO^{FAE} ratios are given in Table J1.

The determination of K_r values for the long time load case acknowledges that the fracture toughness of carbon steel reduces significantly (i.e. from 220 to 85MPa$\sqrt{m}$) as a consequence of hydrogen embrittlement (e.g. Fig.B 1). It also acknowledges that the temperature of the container can increase to as much as 140°C in the short term, but then reduces to ~40°C after long time. The analysis material property input data have been selected accordingly.

In practice, CO/CO^{FAE} ratios at critical locations such as the closure weld could be much higher, in particular if complete PWHT is not possible [10]. Such circumstances will have to be considered in a formal design assessment

J2.2 Copper Coated (3-5mm thick) Carbon Steel

An alternative to the Scandinavian solution of adopting a 50mm thick outer copper container as the corrosion barrier to an internal cast iron structure (App. **H**) is the adoption of a 3-5mm thick copper coating directly onto a carbon steel container. Two scenarios were considered, one involving a 770mm ID container with a length of 4.6m and a wall thickness of 100mm (Fig.J 3), and one involving a 770mm ID container with a length of 4.6m and a wall thickness of 80mm (Fig.J 4). The CO/CO^{FAE} ratios associated with the carbon steel structure are relatively low (Table J1). While the flow strength of the copper is low, the integrity of the evaluated coated structures appeared to be sufficient.

Only short-time FADs were constructed for 2mm deep pre-existing defects for the coated/clad conditions. For the considered long-time load case conditions, the critical defect location was at the internal surface, and therefore unaffected by the mechanical characteristics of the cladding.

J2.3 Titanium Clad Carbon Steel

As an alternative to coating with copper, carbon steel containers could be clad with Ti-Gr.2(~5mm thickness), or better Ti-Gr.7. The FADs for the 100mm thick and 80mm thick carbon steel canisters are respectively given in Fig.J 5 and Fig.J 6. On the basis of the evidence presented, the mechanical integrity of a titanium clad carbon steel 770mm ID SF disposal container with an 80mm wall thickness appeared to be acceptable (Table J1).

J2.4 Nickel Alloy Clad Carbon Steel

Similar assessments conducted for carbon steel containers clad with Nickel Alloy C22 indicated that the mechanical integrity of this solution may be even better (Fig.J 8 and Table J1).

J2.5 Solid Titanium

While the cost of a solid titanium SF rod disposal canister was regarded as high, the results of FAD defect assessments of 100mm and 80mm thick containers are respectively given in Fig.J 9 and Fig.J 10, and are summarised in Table J1.

J2.6 Solid Nickel Alloy

Similarly, while the cost of a solid nickel alloy SF rod disposal canister was also regarded as high, the results of FAD defect assessments of 100mm and 80mm thick containers are respectively given in Fig.J 11 and Fig.J 12, and are summarised in Table J1.

J2.7 Ceramics

The manufacture of either Al_2O_3/SiO_2 or SSiC SF rod disposal canisters was regarded as being well beyond the current state of the art [70]. Nevertheless, FAD defect assessments were respectively performed to demonstrate the high mechanical integrity risks associated with these two material solutions for 80mm thick canisters, e.g. Fig.J 13 and Fig.J 14. Assessment results for 100mm and 80mm thick canisters are summarised in Table J1.

Special considerations were required for the assessment of ceramic canisters and these are described in detail below in Sect.J3.7.

J3 VHLW Disposal Containers

J3.1 Carbon Steel

While recognising that this thickness may not be sufficient to limit the radiation level at the external surface to below that which would not influence corrosion rates (≤ 1Gy/h [104]), the defect assessment of VHLW canister solutions was based on the stress analysis results for a 50mm thick container with an ID of 440mm and a cylinder length of 1.6m. Uncoated (or unclad) carbon steel was not considered as a specific solution because of the inevitable and unacceptable wall thinning due to corrosion during canister lifetime.

J3.2 Copper Coated (3-5mm thick) Carbon Steel

The assessment results for a copper coated carbon steel VHLW container are summarised in Fig.J 15. On the basis of this evidence, the mechanical integrity of a copper coated 50mm thick VHLW canister was regarded as acceptable. The CO/CO^{FEA} ratios are summarised in Table J2.

J3.3 Titanium Clad Carbon Steel

Short and long-time disposal failure assessment diagrams for Gr.2/7 clad carbon steel VHLW canisters are shown in Fig.J 16. These indicate that the mechanical integrity of this solution was acceptable. The CO/CO^{FEA} ratios are summarised in Table J2.

J3.4 Nickel Alloy Clad Carbon Steel

Short and long-time disposal failure assessment diagrams for Alloy C22 clad carbon steel VHLW canisters are shown in Fig.J 17. These indicate that the mechanical integrity of this solution was acceptable. The CO/CO^{FEA} ratios are summarised in Table J2.

J3.5 Solid Titanium

Short and long-time disposal failure assessment diagrams for a 50mm thick solid Gr.2/7 VHLW canister are shown in Fig.J 18. These indicate that the mechanical integrity of this solution was acceptable. The CO/CO^{FEA} ratios are summarised in Table J2.

J3.6 Solid Nickel Alloy

Short and long-time disposal failure assessment diagrams for a 50mm thick solid Alloy C22 VHLW canister are shown in Fig.J 19. These indicate that the mechanical integrity of this solution was acceptable. The CO/CO^{FEA} ratios are summarised in Table J2.

J3.7 Ceramics

More than for metallic solutions, there are higher uncertainties associated with the assessment of ceramic VHLW canister solutions. Inherently, ceramics contain fine distributions of micro-pores. This

can lead to a significant variability in strength and fracture toughness properties requiring special treatment when considered for mechanical integrity calculations, e.g. exploiting a knowledge of the appropriate Weibull modulus and employing Eqn. (G1), App. **G**. While indicative strength values are available for the ceramic grades of interest, they are rarely accompanied by information relating to the specimen used to determine the material property (e.g. V_{spec}) and the associated Weibull modulus.

Al_2O_3/SiO_2. In fact, the difficulty just introduced was not a problem for the mechanical integrity assessment of a 50mm thick Al_2O_3/SiO_2 VHLW canister, i.e. Fig.J 20. Comprehensive information concerning V_{spec} and V_{part}, and a complete R_F^{spec} distribution (with associated m) were available from [7]. This enabled the construction of short and long-time failure assessment diagrams with a breaking stress for a failure probability of 1:21,000 (as used by Andra for their normal reference calculations involving vitrified waste packages).

The V_{spec}/V_{part} effective volume (in tension) ratio employed by Andra in their long-time load case scenario assessment was ~0.015 [7]. This compared with the short and long-time load case scenario V_{spec}/V_{part} values determined for the analyses in the present study of ~5.1×10^{-6} and ~0.038 respectively, assuming the same V_{spec} value as that for the Andra test specimen.

For both short and long-time load cases, a 50mm thick Al_2O_3/SiO_2 VHLW disposal canister was judged to be unsafe, for an initial semi-circular surface defect size of 2mm and 0.25.t, Table J2, Fig.J 20.

SSiC. For the SSiC assessment, only indicative information was available from the literature (e.g. [72,71]), with no indication of the specimen details or the statistical distribution used to determine the information. In these circumstances, the Andra specimen details and statistical strength distribution characteristics (but with m = 12 [71]) were assumed. With these assumptions, short and long-time breaking stresses of ~90MPa and ~250MPa were respectively derived, leading to the failure assessment diagram constructions shown in Fig.J 21. These indicate that a 50mm thick SSiC VHLW canister could be considered acceptable, assuming a permissible semi-circular surface defect size of 2mm (but not if the permissible defect size is 25% of the wall thickness).

It should not be forgotten that this indicative assessment does not acknowledge the presence of a final sealing joint, and the reduced properties associated with such a feature.

J4 Summary

The results of the stress analyses summarised in App. **I**, and the properties reviewed in Apps. **B** to **G** have been used to examine the mechanical integrity of different SF and VHLW disposal canister scenarios using an FAD approach. For pre-existing semi-circular surface defects with depths of 2mm and 0.25.t, all the considered metallic solutions were shown to be acceptable.

Both ceramic SF canister solutions were shown to be unsafe for the assumed load cases. For VHLW disposal, Al_2O_3/SiO_2 canisters were unacceptable, irrespective of the assumed pre-existing defect size. For a permissible 2mm deep defect, an SSiC canister appeared to be safe. However, for an assumed intial defect size of 0.25.t, such a canister was unacceptable.

It is important to acknowledge that the conducted FAD analyses simply examined the mechanical integrity of the cylindrical bodies of the candidate canister material solutions. No account was taken of the inevitable presence of joints, their geometrical construction and material properties, which will have to be considered as part of any formal design analysis.

Table J1: Summary of FAD CO/CO^{FAE} Ratios for Candidate 4.6m Long SF Canister Solutions

SF Canister Load Case Scenario	Short Time (TWI-5)	Long Time (TWI-2)	Short Time (TWI-5)	Long Time (TWI-2)
Crack depth, *a*	2mm	2mm	0.25*t*	0.25*t*
Carbon steel (770mm ID, 140/120mm thick)	**0.21**	0.00	**0.26**	0.01
Carbon steel (770mm ID, 100mm thick):	**0.31**	0.11	**0.36**	0.13
- Copper coated	0.14	**0.28**	**0.36**	0.13
- Ti Gr.7 clad	**0.30**	0.10	**0.36**	0.13
- Ni Alloy C22 clad	**0.16**	0.06	**0.36**	0.13
Carbon steel (770mm ID, 80mm thick):	0.40	**0.41**	0.46	**0.48**
- Copper coated	0.14	**0.44**	0.46	**0.48**
- Ti Gr.7 clad	**0.39**	0.37	0.46	**0.48**
- Ni Alloy C22 clad	0.21	**0.23**	0.46	**0.48**
Carbon steel (770mm ID, 5ck0mm thick)	0.62	**1.21**	0.69	**1.16**
Ti Gr.2 (770mm ID, 100mm thick)	**0.30**	0.10	**0.35**	0.11
Ti Gr.2 (770mm ID, 80mm thick)	**0.39**	0.37	**0.44**	0.41
Ni Alloy C22 (770mm ID, 100mm thick)	**0.10**	0.06	**0.17**	0.08
Ni Alloy C22 (770mm ID, 80mm thick)	0.21	**0.23**	0.21	**0.29**
Al_2O_3/SiO_2 (770mm ID, 100mm thick)	**3.00**	0.80	**7.13**	2.30
Al_2O_3/SiO_2 (770mm ID, 80mm thick)	**3.50**	3.03	**8.26**	7.87
SSiC (770mm ID, 100mm thick)	**1.70**	0.38	**4.07**	1.30
SSiC (770mm ID, 80mm thick)	**2.00**	1.69	**4.72**	4.42

The maximum CO/CO^{FAE} values for each condition are highlighted in bold. Those exceeding unity are highlighted in red

Table J2: Summary of FAD CO/CO^{FAE} Ratios for Candidate 1.6m Long VHLW Canister Solutions

VHLW Canister Load Case Scenario	Short Time (TWI-5)	Long Time (TWI-2)	Short Time (TWI-5)	Long Time (TWI-2
Crack depth, *a*	2mm	2mm	0.25*t*	0.25*t*
Carbon steel (440mm ID, 50mm thick):	0.17	**0.22**	0.19	**0.24**
- Copper coated	0.14	**0.44**	0.19	**0.24**
- Ti Gr.7 clad	0.16	**0.20**	0.19	**0.24**
- Ni Alloy C22 clad	0.09	**0.12**	0.19	**0.24**
Ti Gr.2 (440mm ID, 50mm thick)	0.16	**0.20**	0.18	**0.21**
Ni Alloy C22 (440mm ID, 50mm thick)	0.09	**0.12**	0.09	**0.15**
Al_2O_3/SiO_2 (440mm ID, 50mm thick)	**1.23**	1.20	2.78	**3.31**
SSiC (440mm ID, 50mm thick)	0.70	**0.77**	1.59	**1.84**

The maximum CO/CO^{FAE} values for each condition are highlighted in bold. Those exceeding unity are highlighted in red

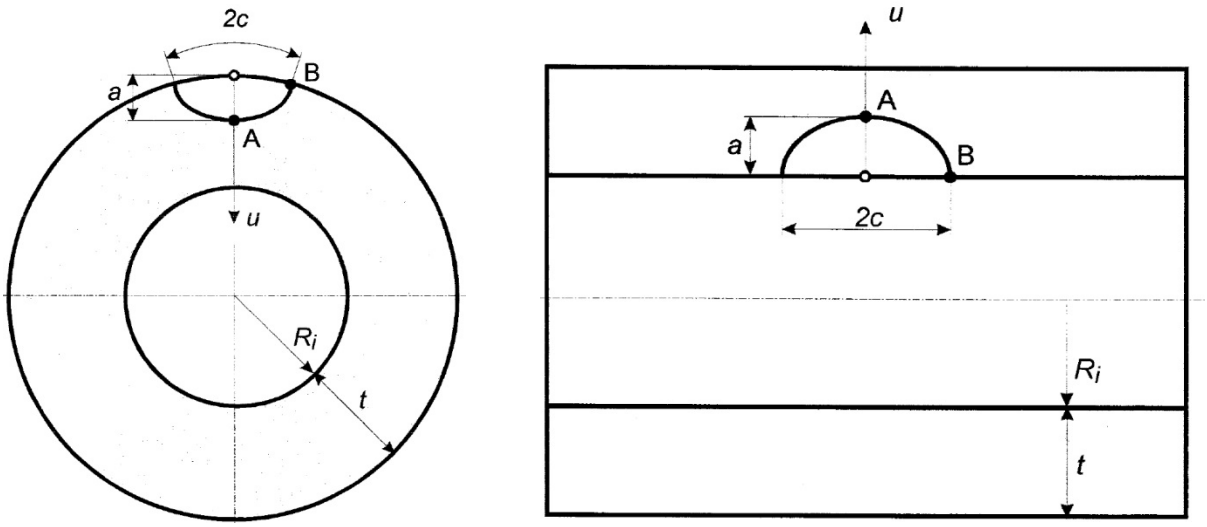

(a). (b)

Fig.J 1 Semi-circular defects in a thick walled cylinder: (a) external-circumferential defect condition relating to maximum short-time (TWI-5) load case stresses, and (b) internal-axial defect condition relating to maximum long-time (TWI-2) load case stresses

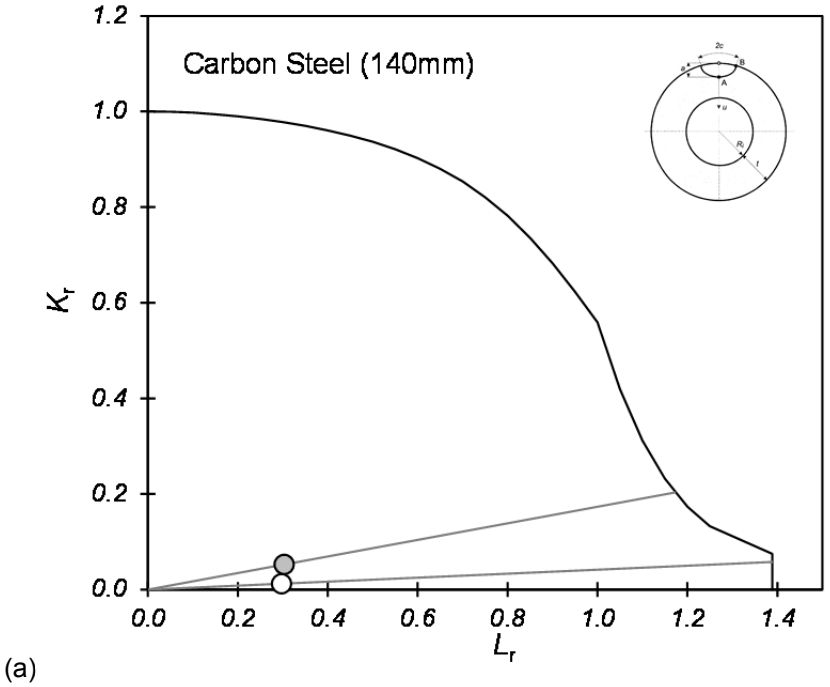

(a)

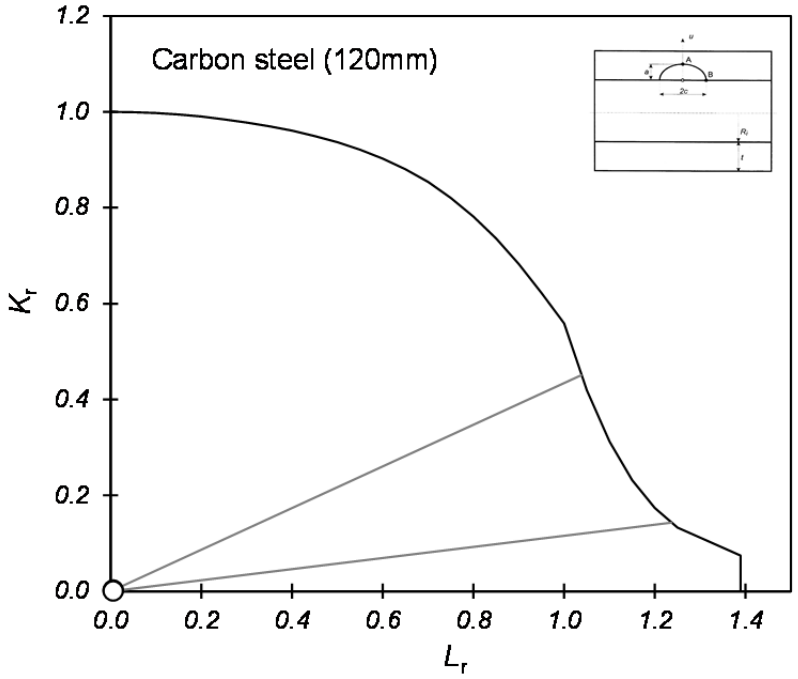

(b)

Fig.J 2 Failure assessment diagrams for 770mm ID carbon steel SF container with corrosion allowance, (a) short time (TWI-5) disposal load case at 150°C, and (b) long-time (TWI-2) disposal load case at ambient temperature

(open point: a=2mm, shaded point: a=0.25.t)

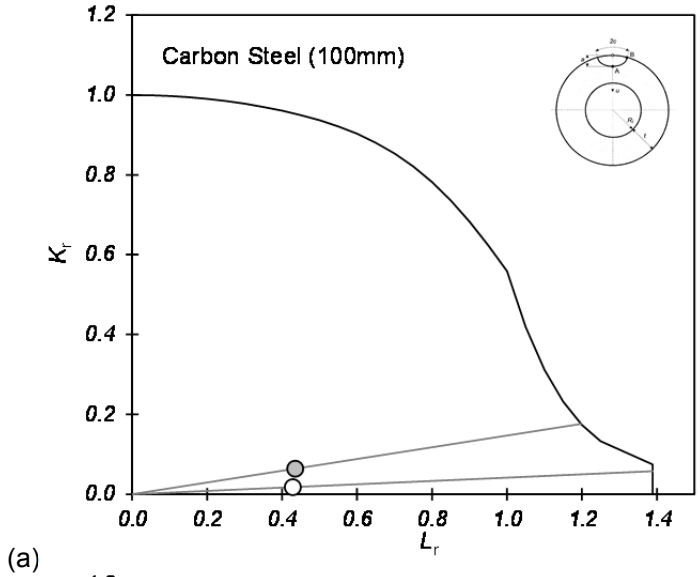

(a)

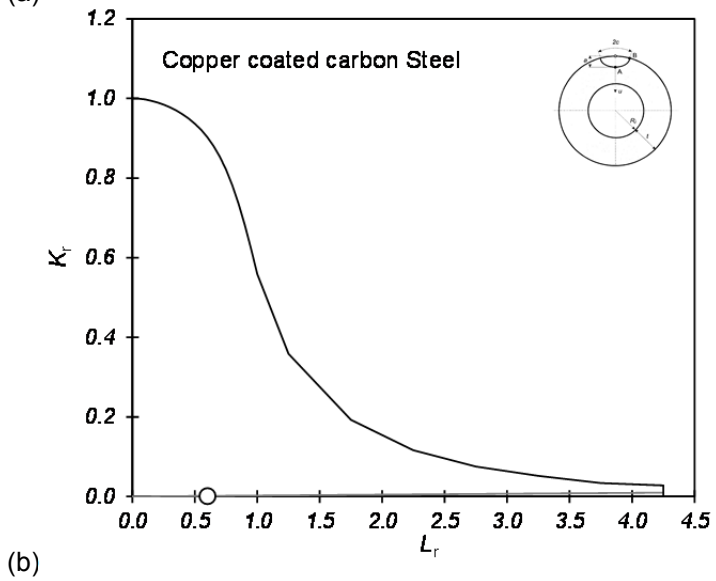

(b)

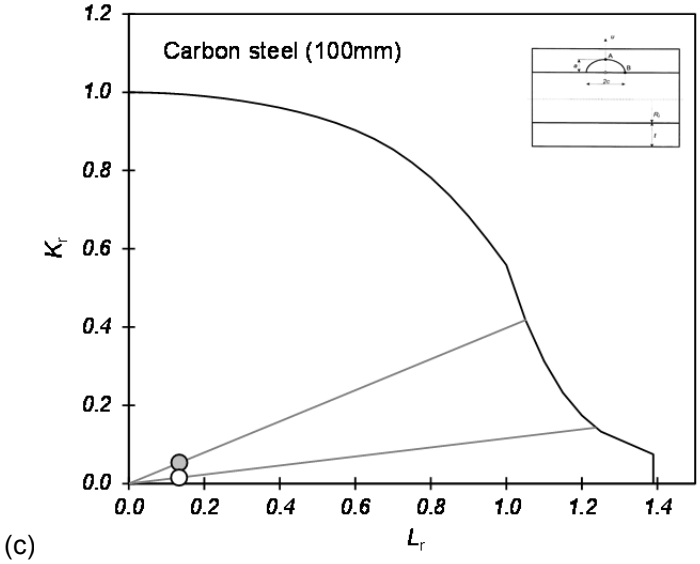

(c)

Fig.J 3 Failure assessment diagrams for 770mm ID, 100mm thick carbon steel SF container with copper corrosion barrier, (a,b) short-time (TWI-5) disposal load case at 150°C, and (c) long-time (TWI-2) disposal load case at ambient temperature

(open point: a = 2mm, shaded point: a = 0.25.t)

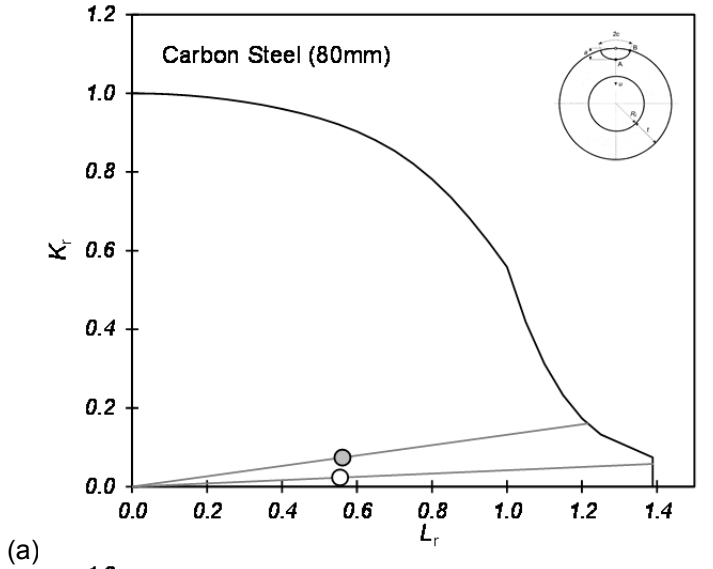

(a)

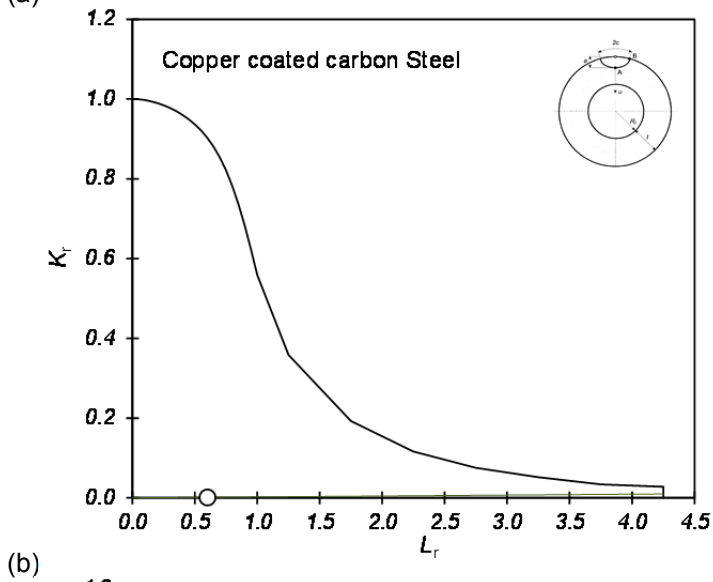

(b)

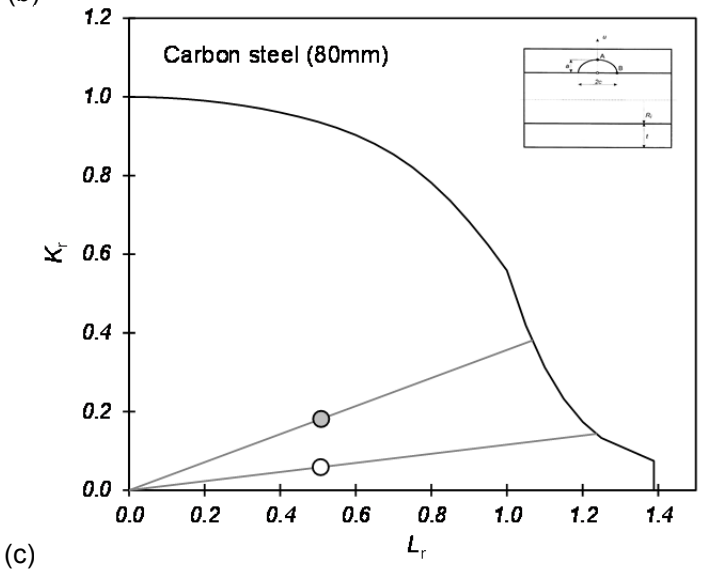

(c)

Fig.J 4 Failure assessment diagrams for 770mm ID, 80mm thick carbon steel SF container with copper corrosion barrier, (a,b) short-time (TWI-5) disposal load case at 150°C, and (c) long-time (TWI-2) disposal load case at ambient temperature

(open point: a = 2mm, shaded point: a = 0.25.t)

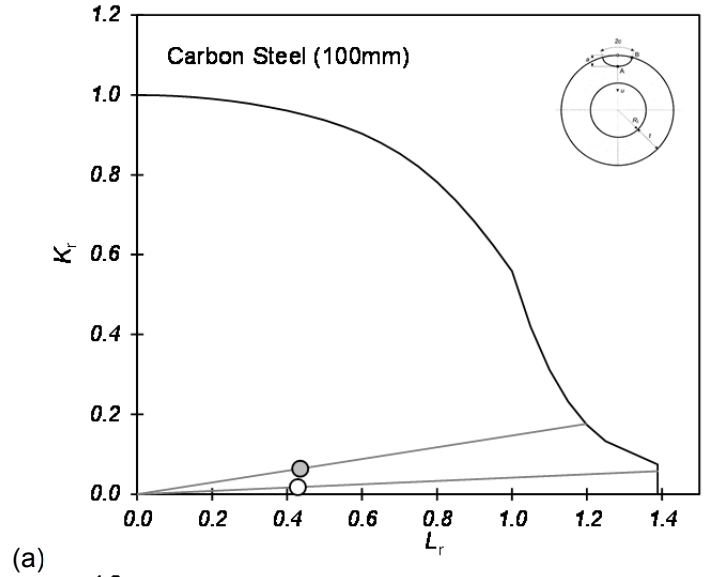

(a)

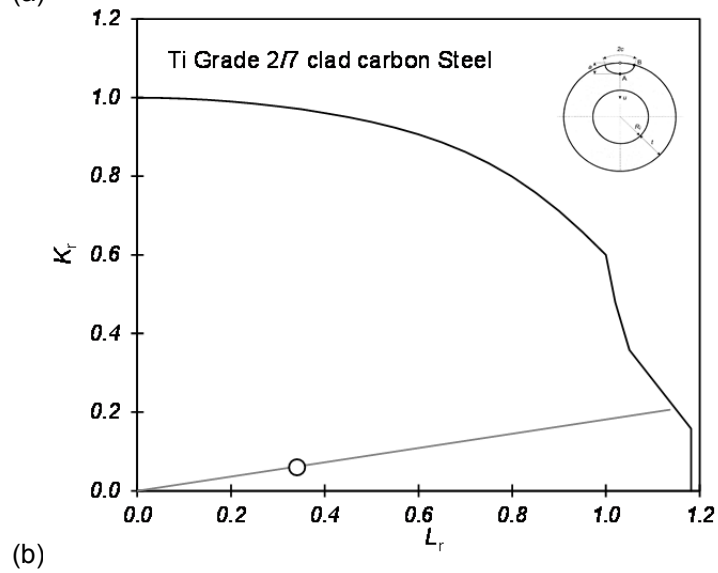

(b)

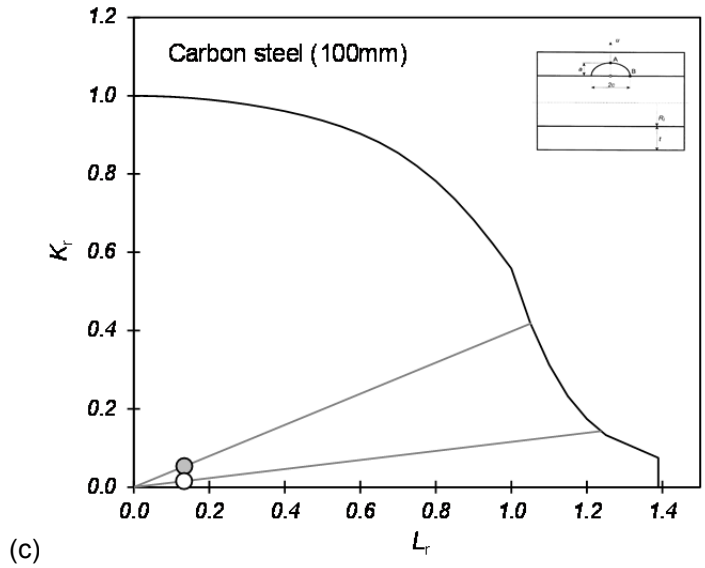

(c)

Fig.J 5 Failure assessment diagrams for 770mm ID, 100mm thick carbon steel SF container with titanium Gr.2/7 corrosion barrier, (a,b) short-time (TWI-5) disposal load case at 150°C, and (c) long-time (TWI-2) disposal load case at ambient temperature

(open point: a = 2mm, shaded point: a = 0.25.t)

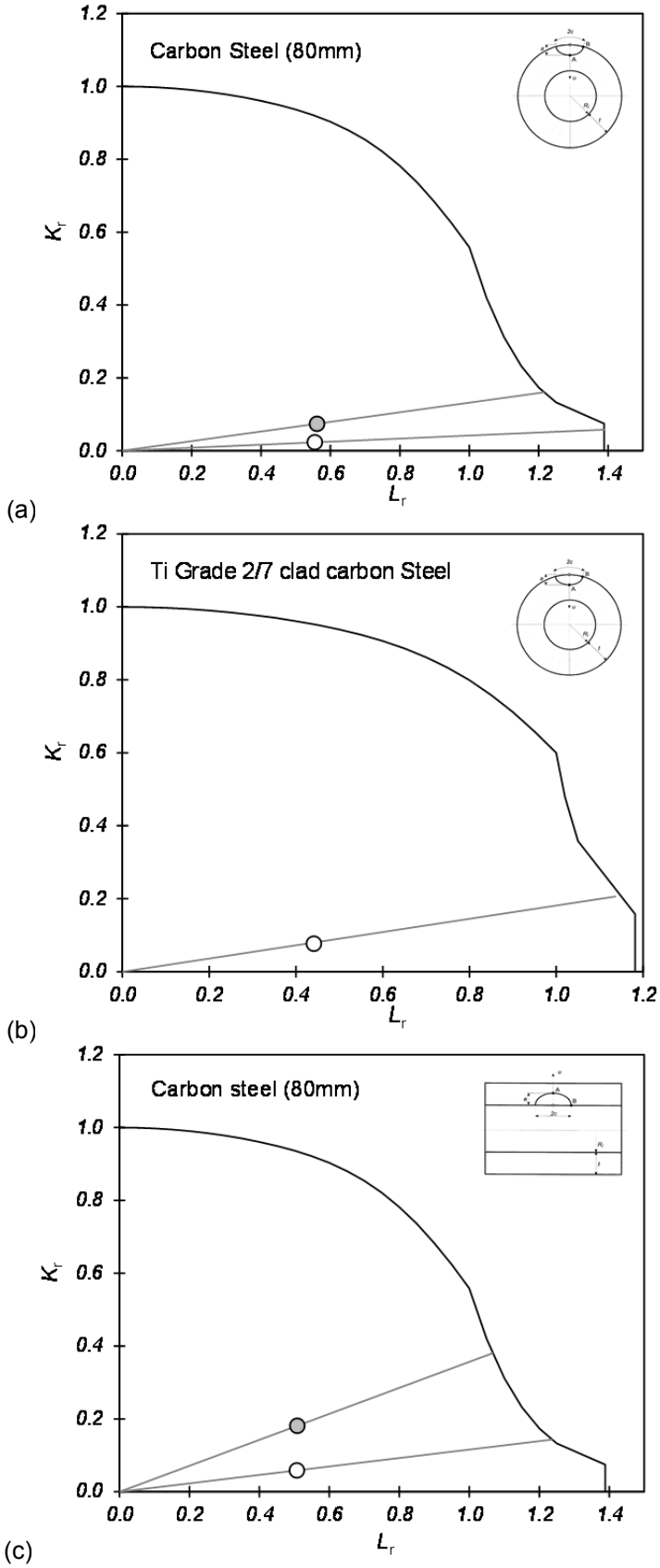

Fig.J 6 Failure assessment diagrams for 770mm ID, 80mm thick carbon steel SF container with titanium Gr.2/7 corrosion barrier, (a,b) short-time (TWI-5) disposal load case at 150°C, and (c) long-time (TWI-2) disposal load case at ambient temperature

(open point: a = 2mm, shaded point: a = 0.25.t)

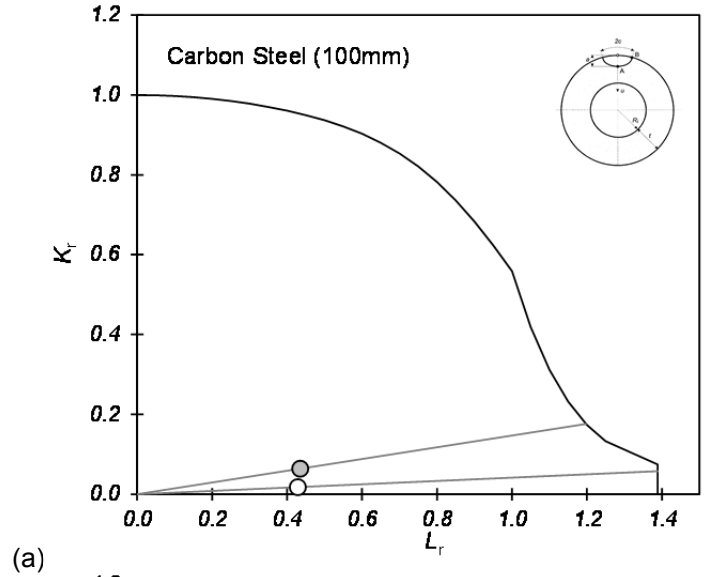

(a)

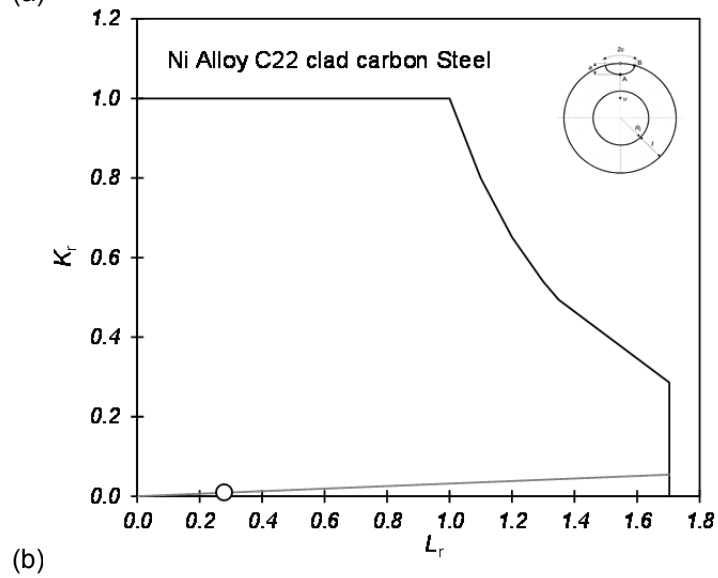

(b)

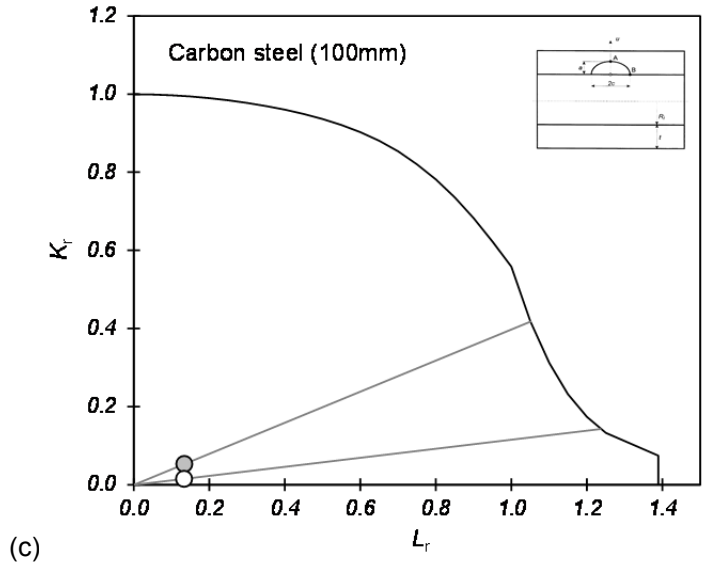

(c)

Fig.J 7 Failure assessment diagrams for 770mm ID, 100mm thick carbon steel SF container with nickel alloy C22 corrosion barrier, (a,b) short-time (TWI-5) disposal load case at 150°C, and (c) long-time (TWI-2) disposal load case at ambient temperature

(open point: a = 2mm, shaded point: a = 0.25.t)

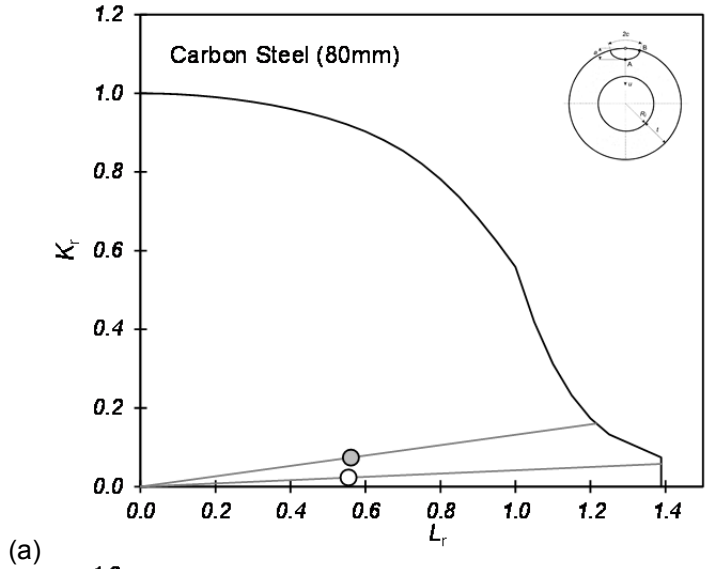

(a)

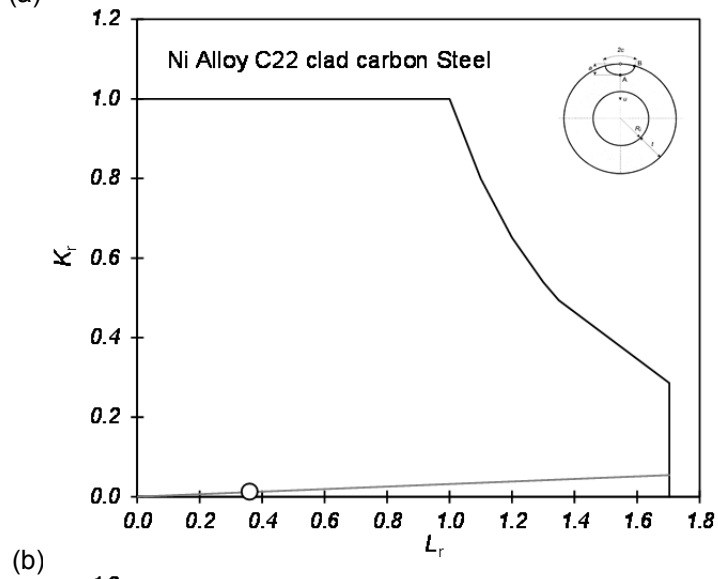

(b)

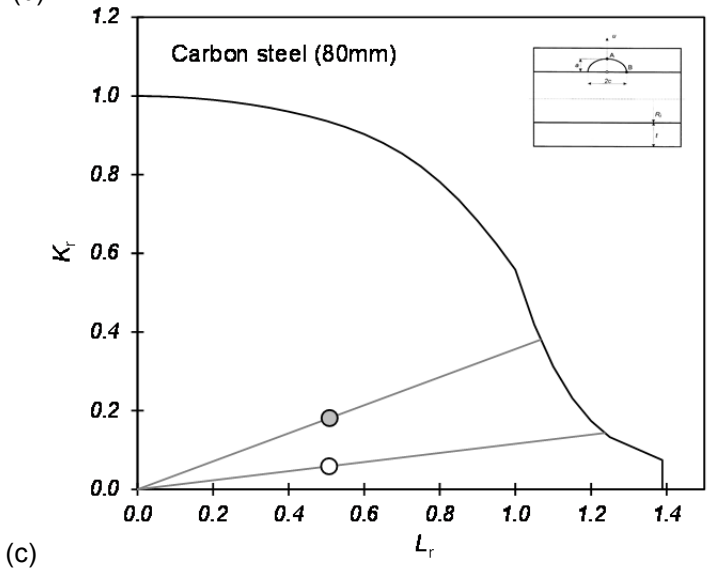

(c)

Fig.J 8 Failure assessment diagrams for 770mm ID, 80mm thick carbon steel SF container with nickel alloy C22 corrosion barrier, (a,b) short-time (TWI-5) disposal load case at 150°C, and (c) long-time (TWI-2) disposal load case at ambient temperature

(open point: a = 2mm, shaded point: a = 0.25.t)

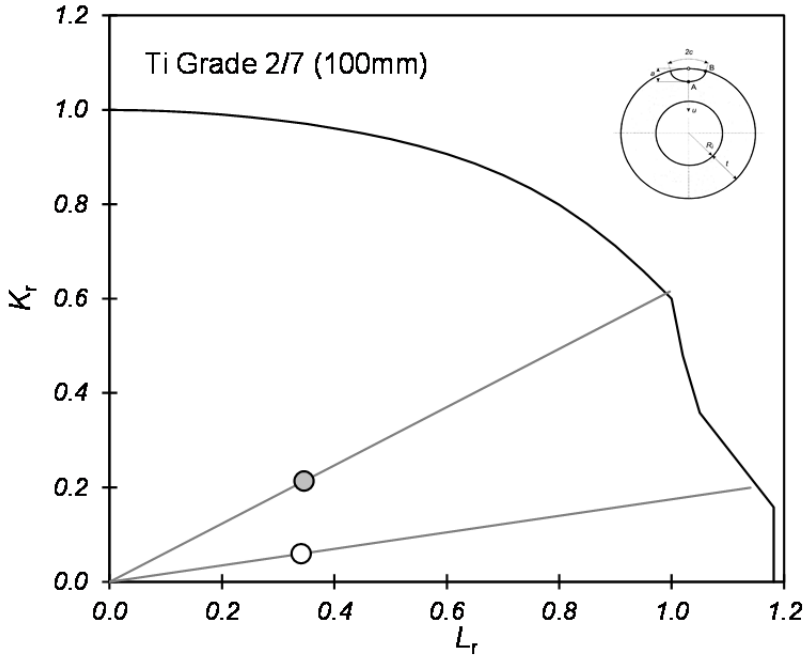

(a)

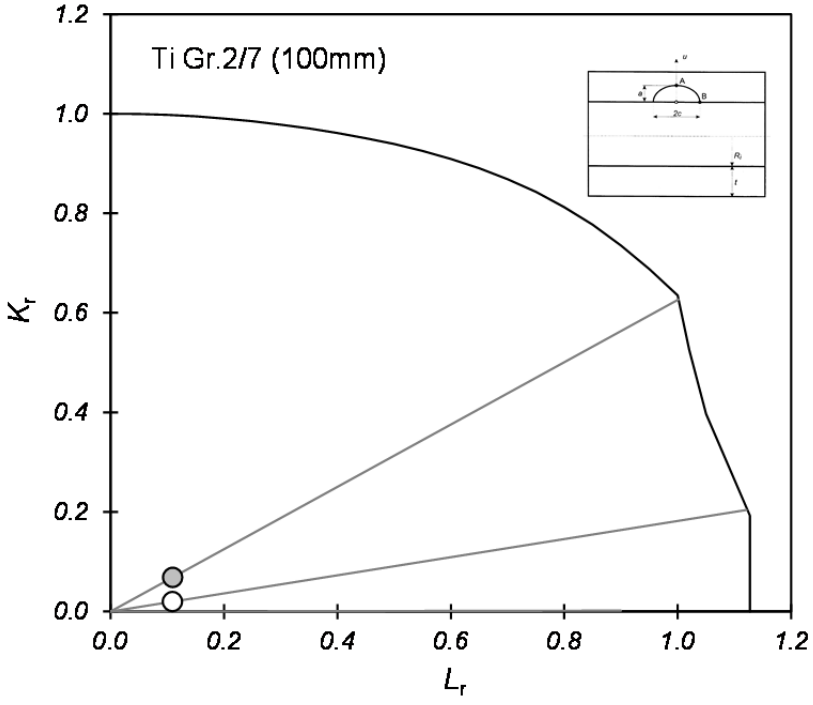

(b)

Fig.J 9 Failure assessment diagrams for 770mm ID, 100mm thick titanium SF container, (a) short-time (TWI-5) disposal load-case at 150°C, and (b) long-time (TWI-2) disposal load case at ambient temperature

(open point: a=2mm, shaded point: a=0.25.t)

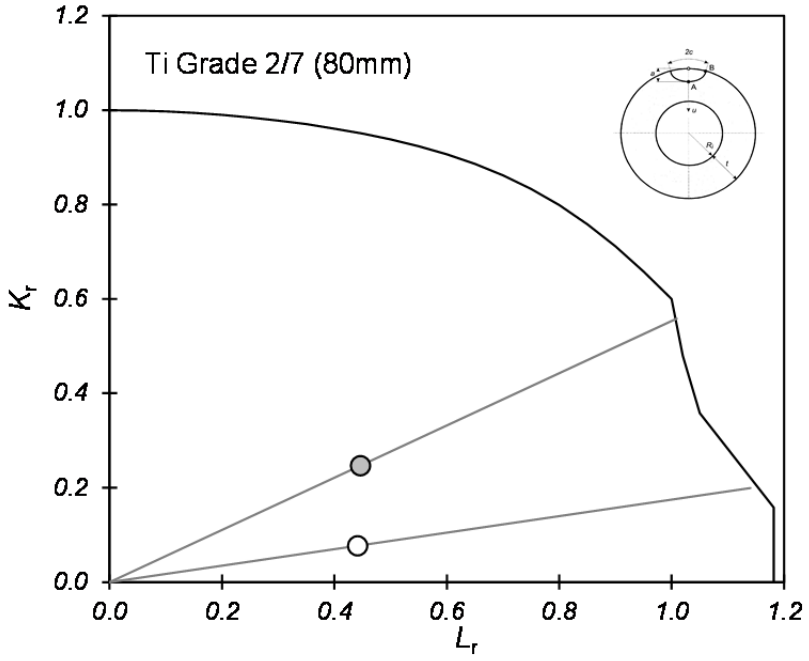

(a)

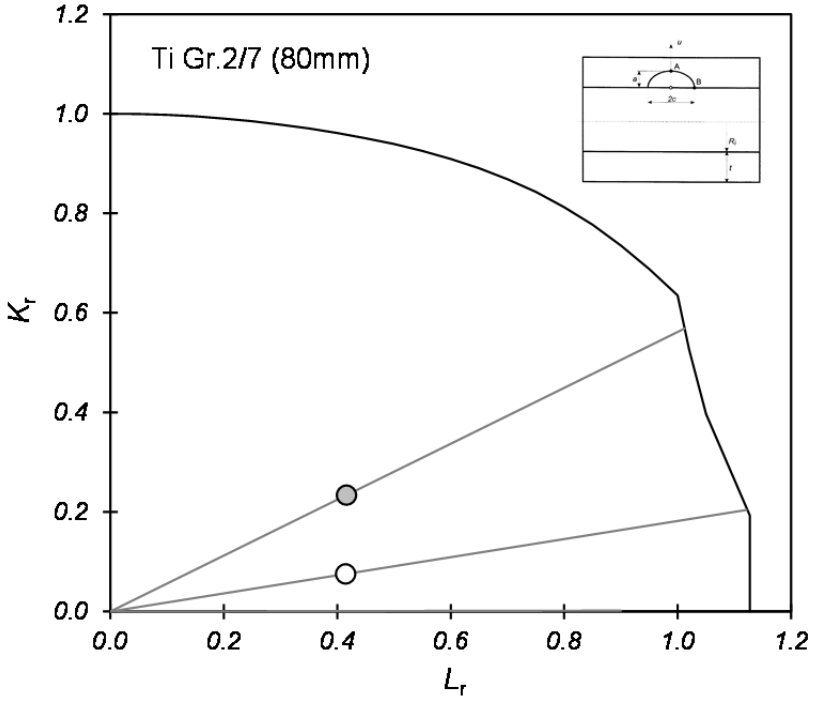

(b)

Fig.J 10 Failure assessment diagrams for 770mm ID, 80mm thick titanium SF container, (a) short-time (TWI-5) disposal load case at 150°C, and (b) long-time (TWI-2) disposal load case at ambient temperature

(open point: a=2mm, shaded point: a=0.25.t)

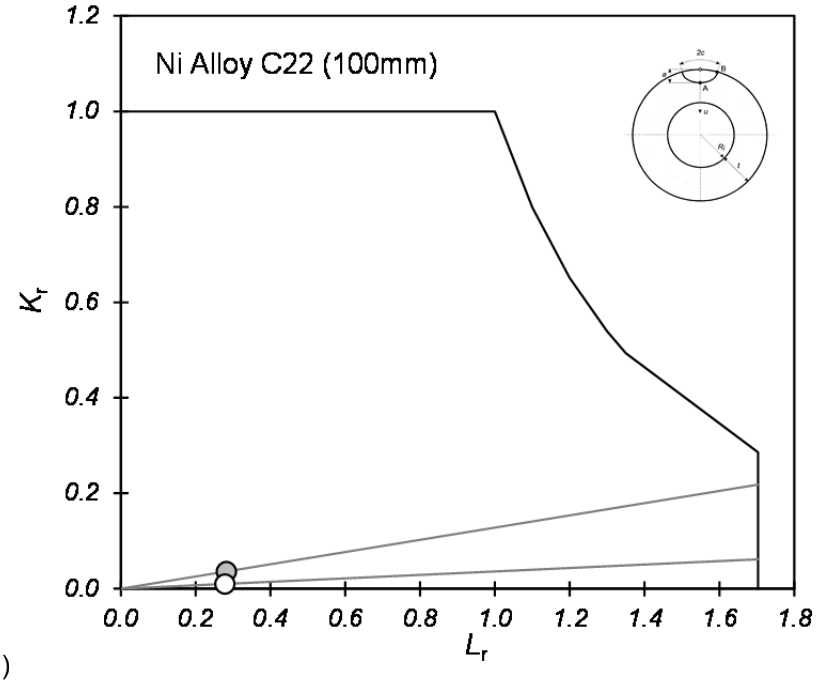

(a)

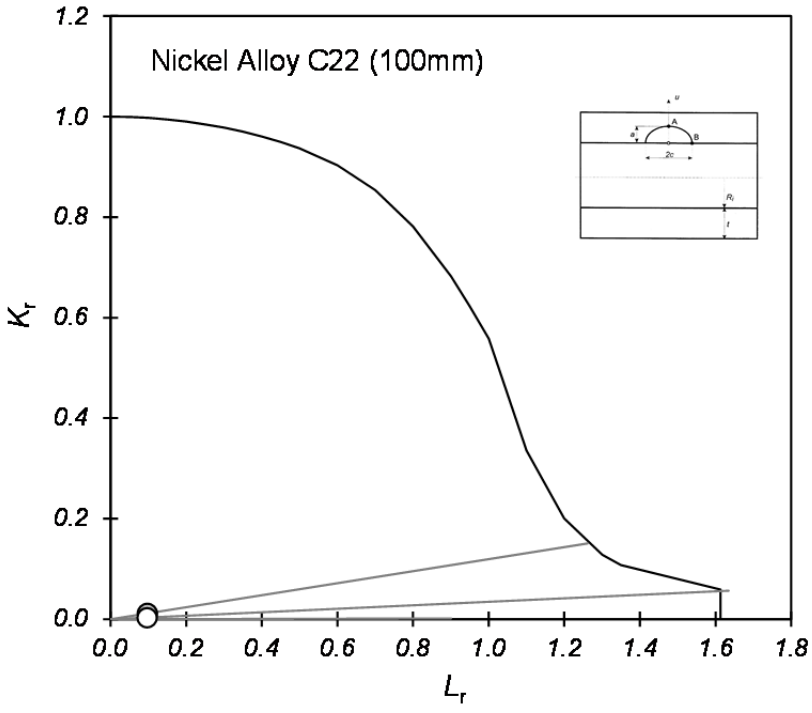

(b)

Fig.J 11 Failure assessment diagrams for 770mm ID, 100mm thick nickel alloy C22 SF container, (a) short-time (TWI-5) disposal load-case at 150°C, and (b) long-time (TWI-2) disposal load case at ambient temperature

(open point: a=2mm, shaded point: a=0.25.t)

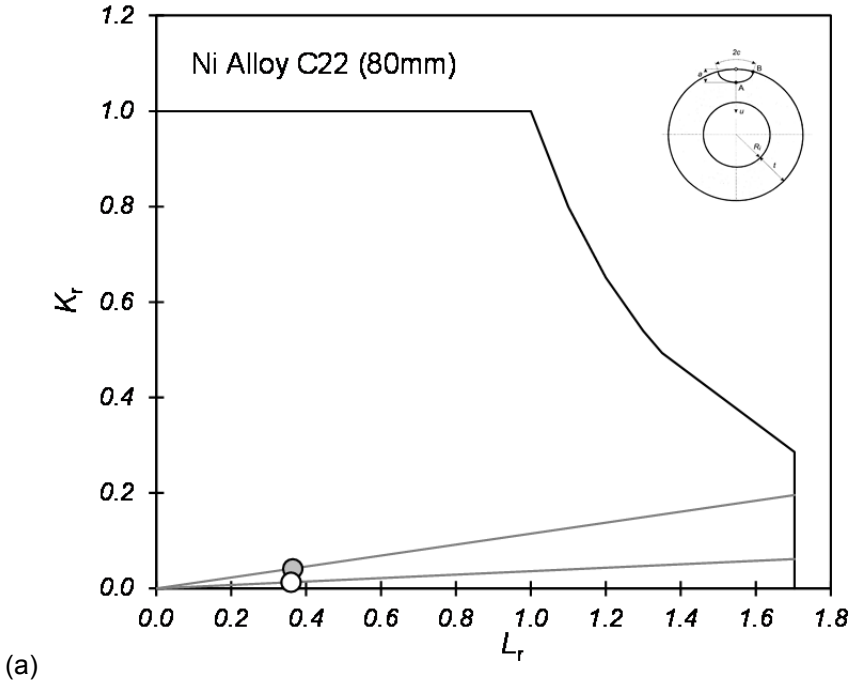

(a)

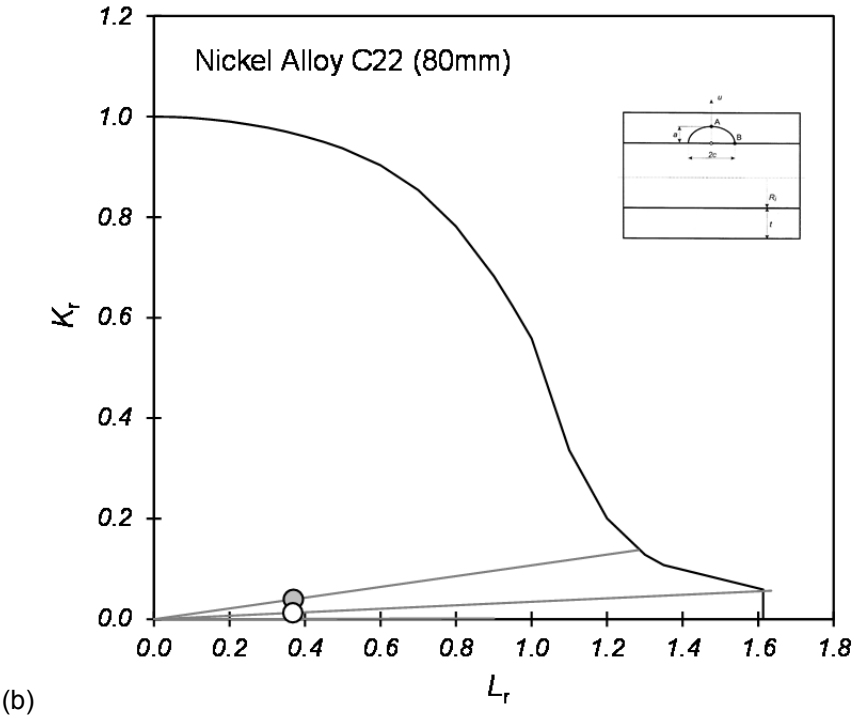

(b)

Fig.J 12 Failure assessment diagrams for 770mm ID, 80mm thick nickel alloy C22 SF container, (a) short-time (TWI-5) disposal load case at 150°C, and (b) long-time (TWI-2) disposal load case at ambient temperature

(open point: a=2mm, shaded point: a=0.25.t)

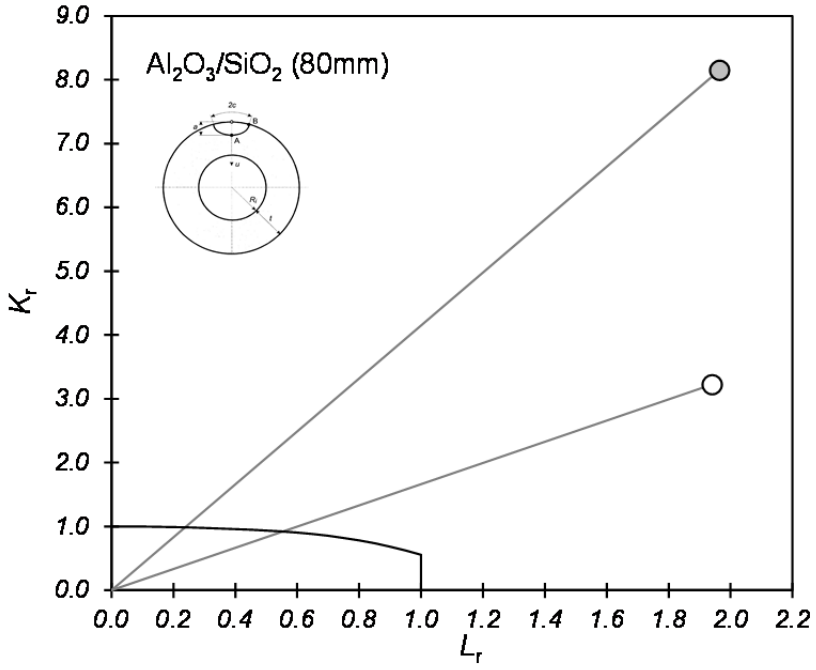

(a)

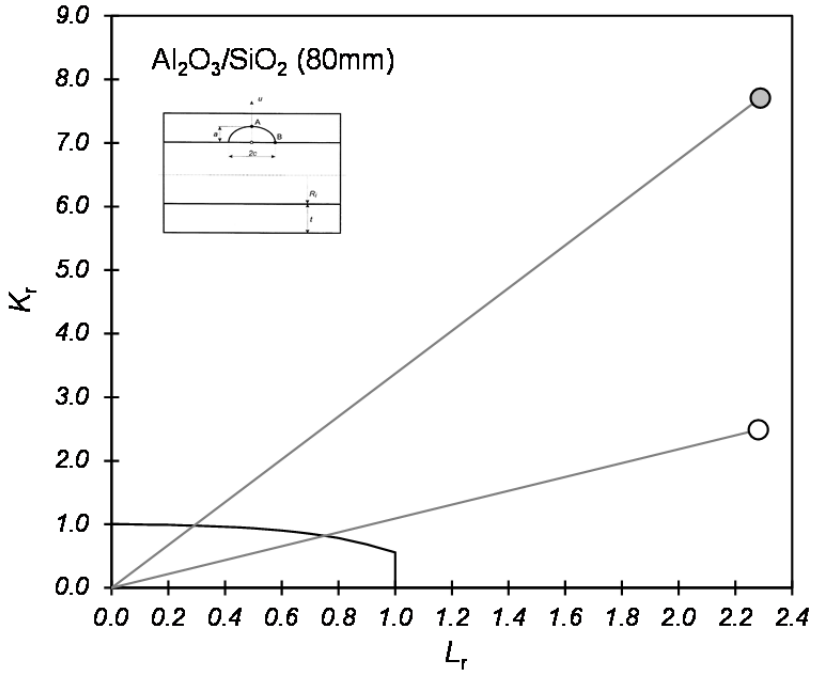

(b)

Fig.J 13 Failure assessment diagrams for 770mm ID, 80mm thick Al_2O_3/SiO_2 SF container, (a) short-time (TWI-5) disposal load case at 150°C, and (b) long-time (TWI-2) disposal load case at ambient temperature

(open point: a = 2mm, shaded point: a = 0.25.t)

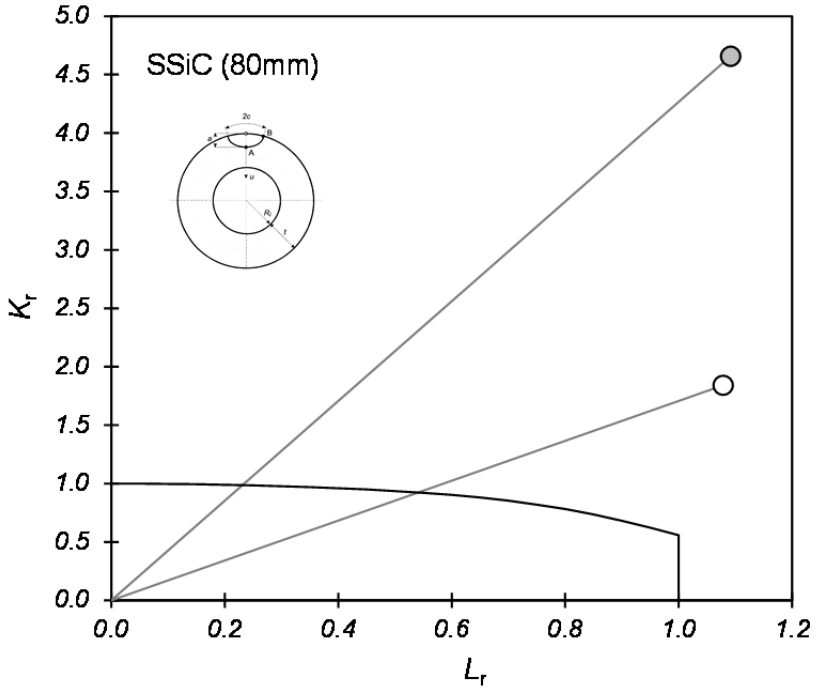

(a)

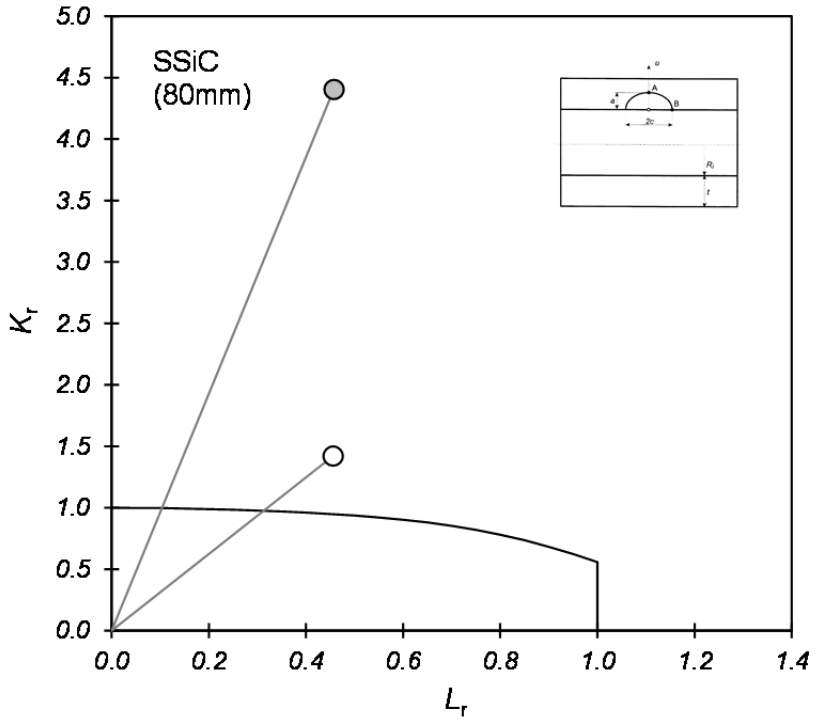

(b)

Fig.J 14 Failure assessment diagrams for 770mm ID, 80mm thick SSiC SF container, (a) short-time (TWI-5) disposal load case at 150°C, and (b) long time (TWI-2) disposal load case at ambient temperature

(open point: a = 2mm, shaded point: a = 0.25.t)

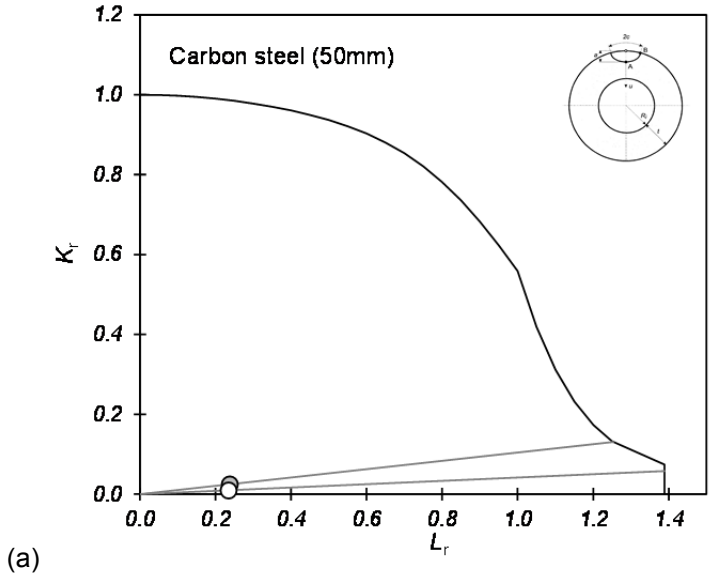

(a)

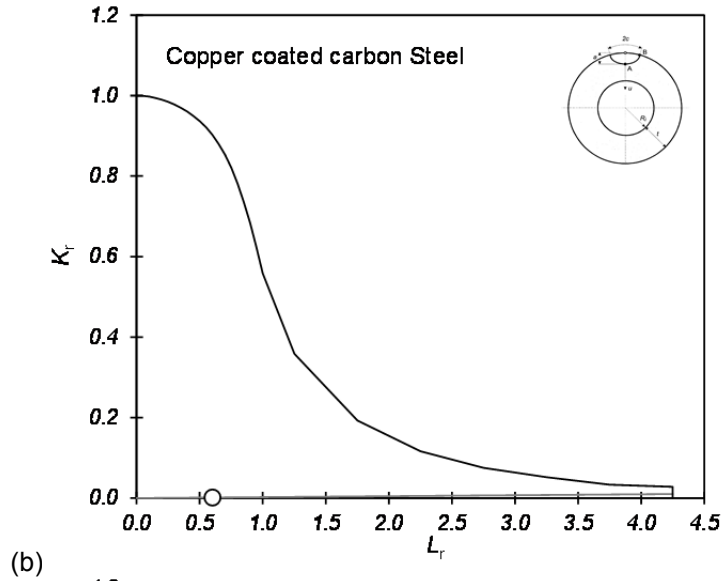

(b)

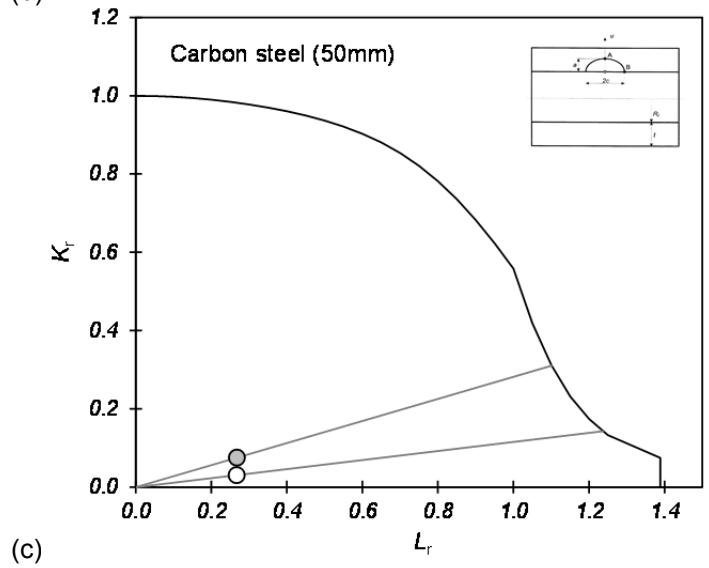

(c)

Fig.J 15 Failure assessment diagrams for 440mm ID, 50mm thick carbon steel VHLW container with copper corrosion barrier, (a,b) short-time (TWI-5) disposal load case at 150°C, and (c) long-time (TWI-2) load case at ambient temperature (open point: a = 2mm, shaded point: a = 0.25.t)

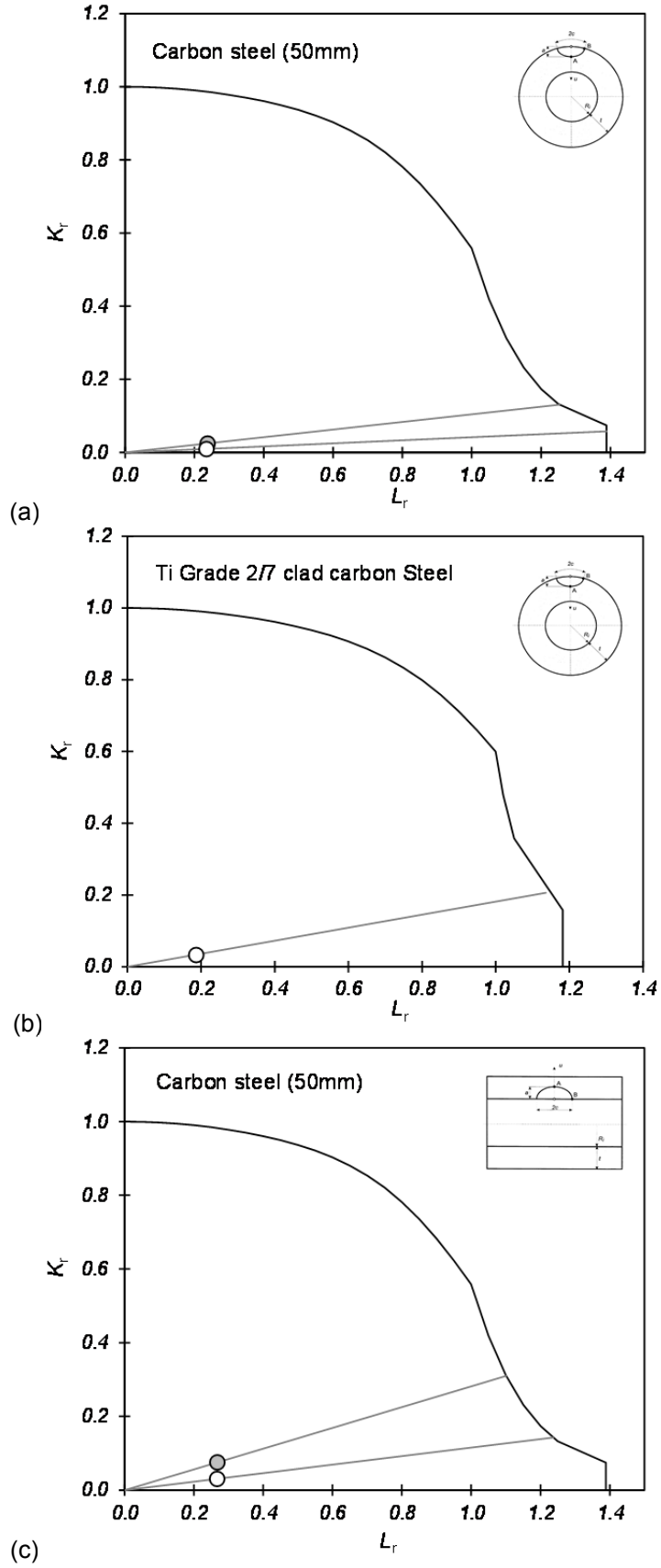

Fig.J 16 Failure assessment diagrams for 440mm ID, 50mm thick carbon steel VHLW container with Grade 2/7 titanium corrosion barrier, (a,b) short time (TWI-5) disposal load case at 150°C, and (c) long time (TWI-2) load case at ambient temperature

(open point: a = 2mm, shaded point: a = 0.25.t)

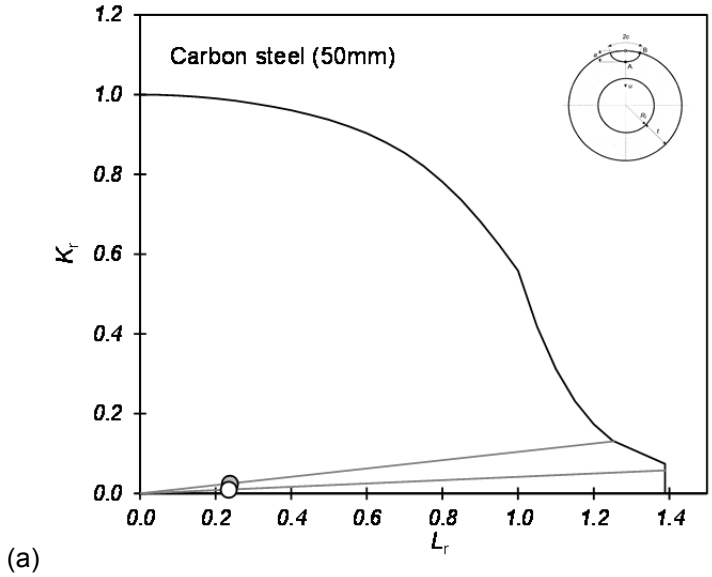

(a)

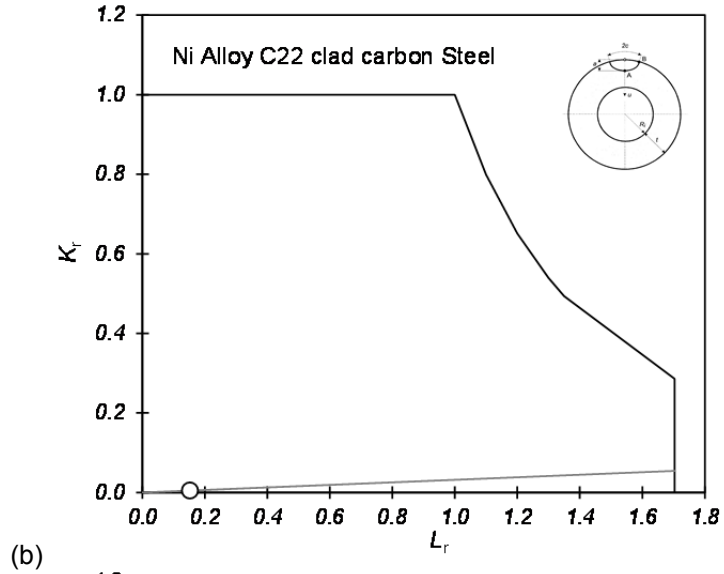

(b)

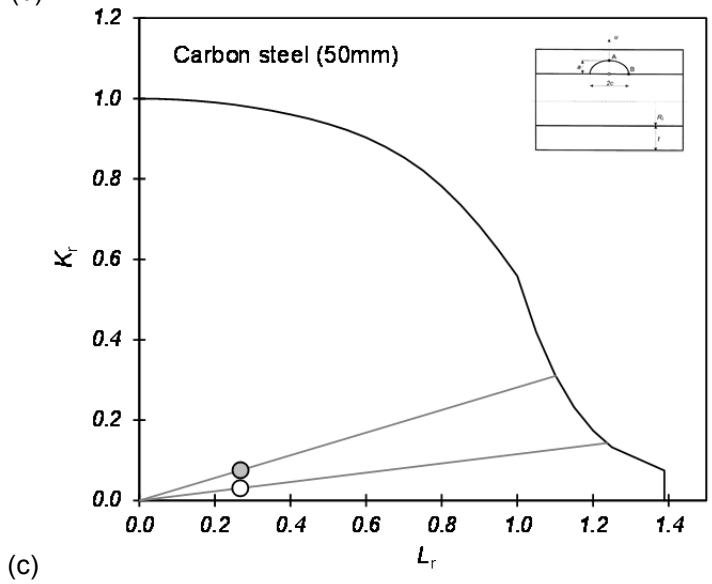

(c)

Fig.J 17 Failure assessment diagrams for 440mm ID, 50mm thick carbon steel VHLW container with nickel Alloy C22 corrosion barrier, (a,b) short time (TWI-5) disposal load case at 150°C, and (c) long time (TWI-2) load case at ambient (open point: a = 2mm, shaded point: a = 0.25t)

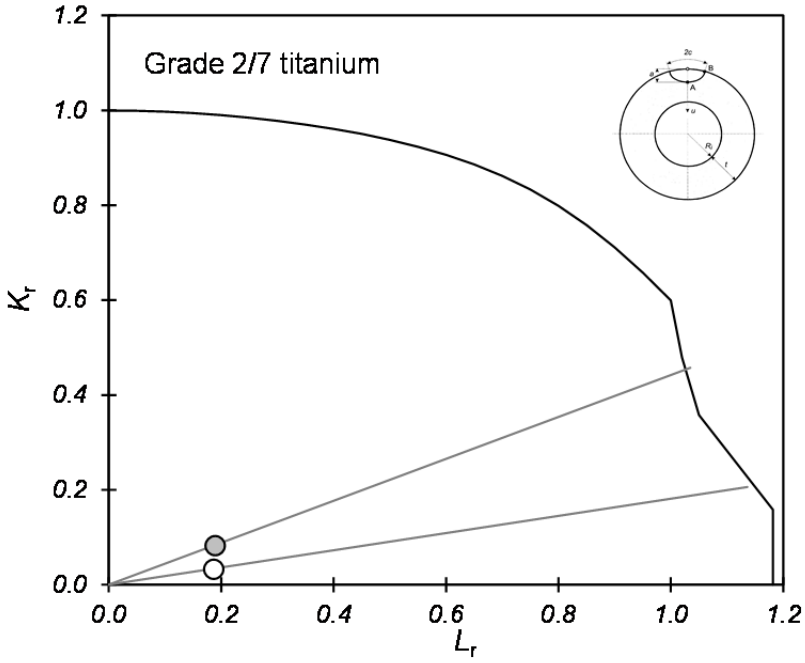

(a)

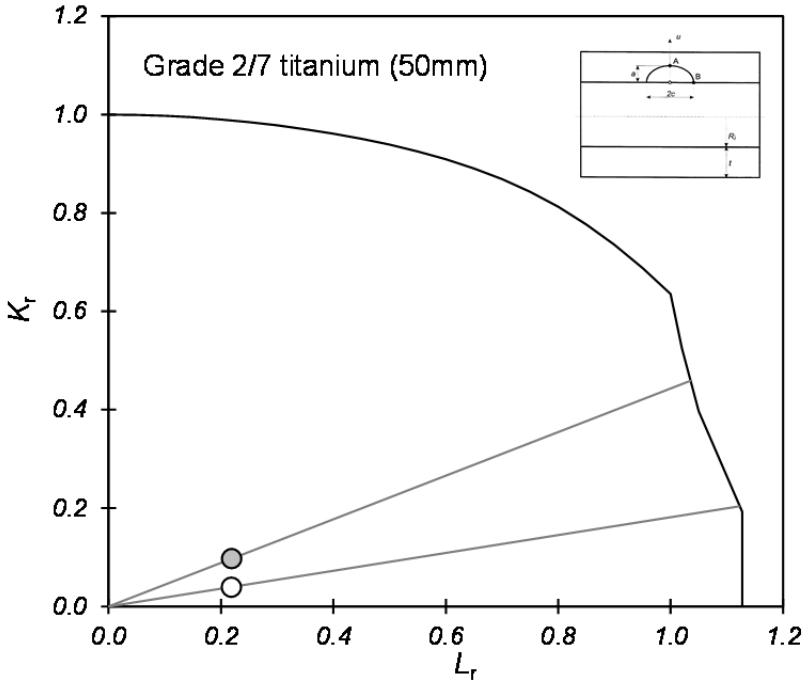

(b)

Fig.J 18 Failure assessment diagrams for 440mm ID, 50mm thick Gr.2/7 titanium VHLW container, (a) short-time (TWI-5) disposal load case at 150°C, and (b) long time (TWI-2) load-case at ambient temperature

(open point: a = 2mm, shaded point: a = 0.25.t)

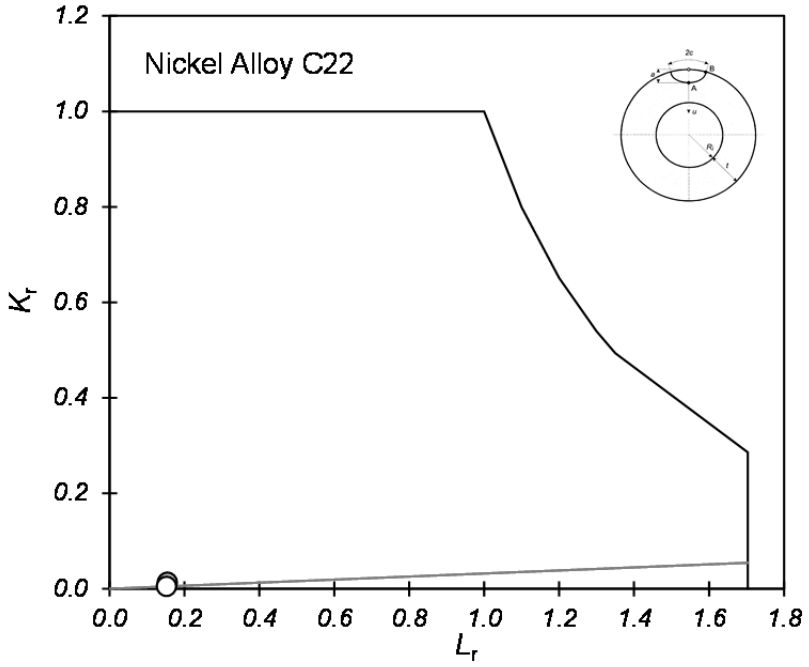

(a)

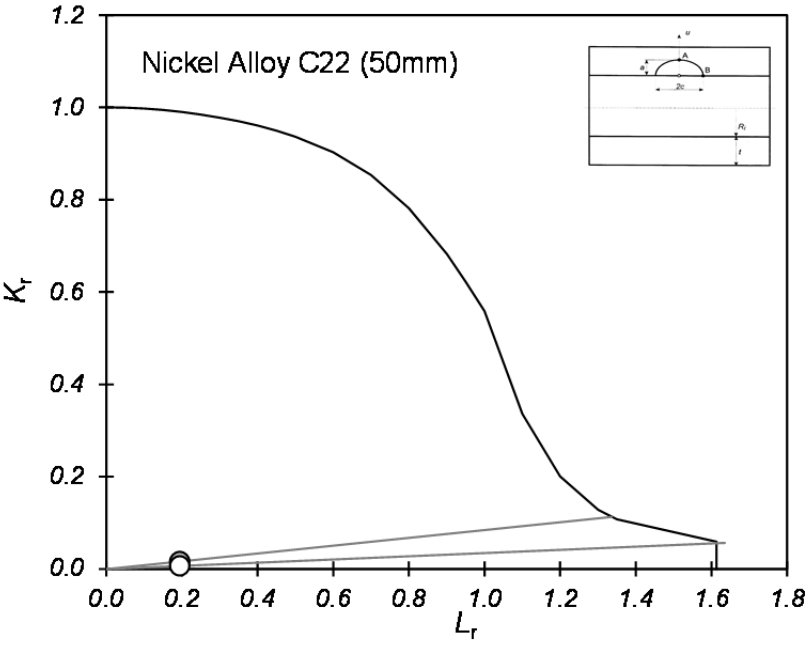

(b)

Fig.J 19 Failure assessment diagrams for 440mm ID, 50mm thick nickel Alloy 22 VHLW container, (a) short time (TWI-5) disposal load case at 150°C, and (b) long time (TWI-2) load case at ambient temperature

(open point: a = 2mm, shaded point: a = 0.25.t)

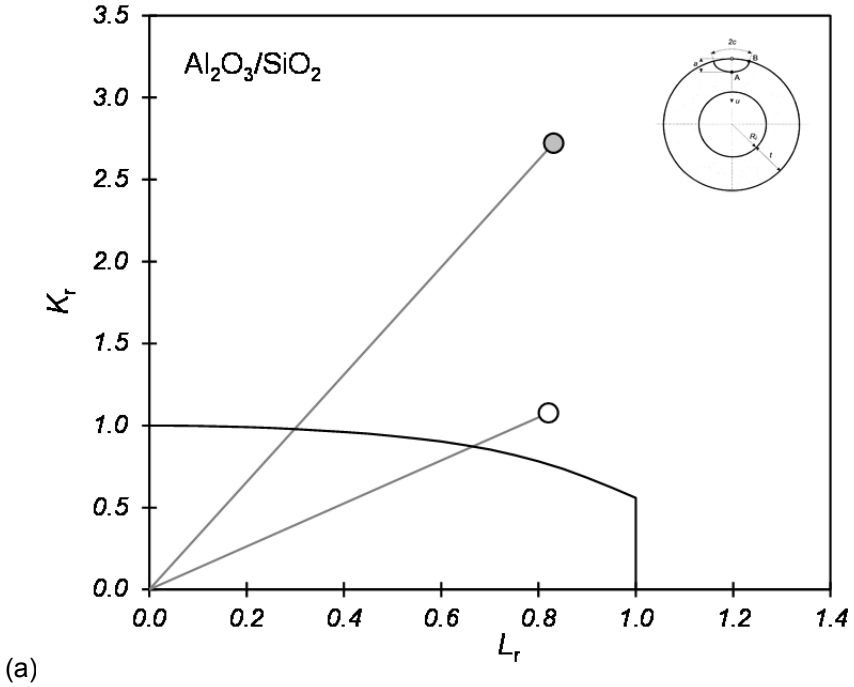

(a)

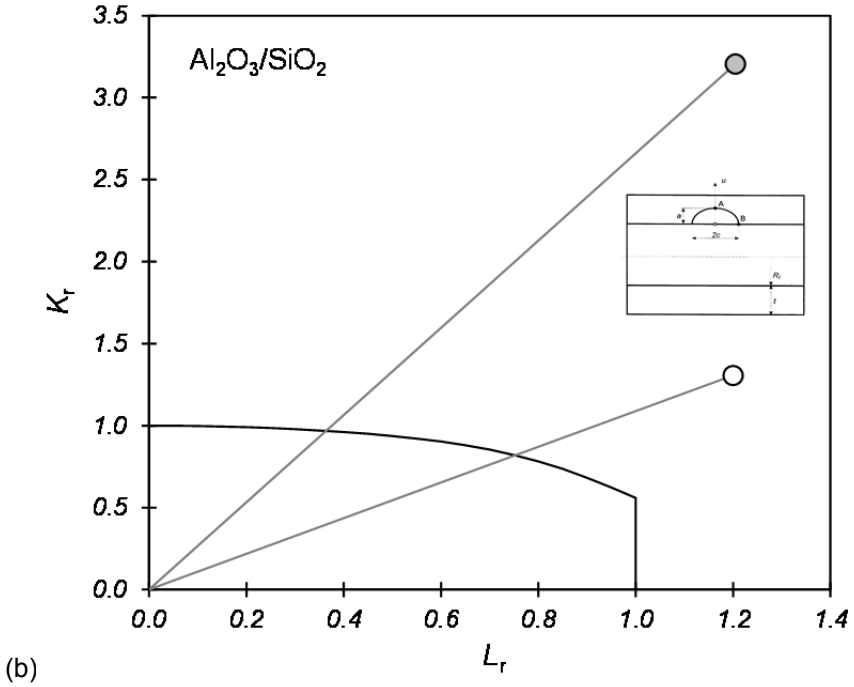

(b)

Fig.J 20 Failure assessment diagrams for 440mm ID, 50mm thick Al_2O_3/SiO_2 VHLW container, (a) short time (TWI-5) disposal load case at 150°C, and (b) long time (TWI-2) load case at ambient temperature

(open point: a = 2mm, shaded point: a = 0.25.t)

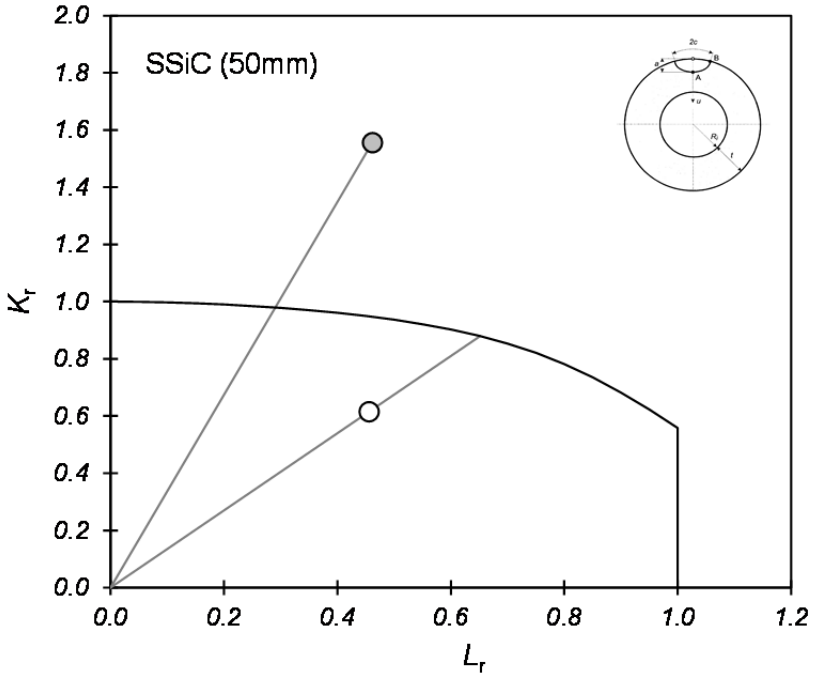

(a)

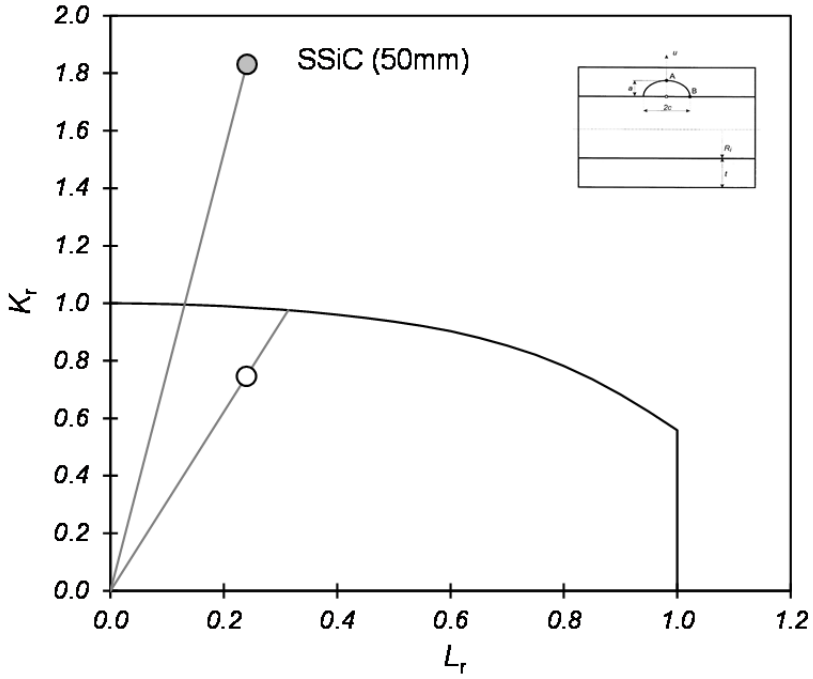

(b)

Fig.J 21 Failure assessment diagrams for 440mm ID, 50mm thick SSiC VHLW container, (a) short time (TWI-5) disposal load case at 150°C, and (b) long time (TWI-2) load case at ambient temperature

(open point: a = 2mm, shaded point: a = 0.25.t)